INFORMATION TO USERS

This manuscript has been reproduced from the microfilm master. UMI films the text directly from the original or copy submitted. Thus, some thesis and dissertation copies are in typewriter face, while others may be from any type of computer printer.

The quality of this reproduction is dependent upon the quality of the copy submitted. Broken or indistinct print, colored or poor quality illustrations and photographs, print bleedthrough, substandard margins, and improper alignment can adversely affect reproduction.

In the unlikely event that the author did not send UMI a complete manuscript and there are missing pages, these will be noted. Also, if unauthorized copyright material had to be removed, a note will indicate the deletion.

Oversize materials (e.g., maps, drawings, charts) are reproduced by sectioning the original, beginning at the upper left-hand corner and continuing from left to right in equal sections with small overlaps.

Photographs included in the original manuscript have been reproduced xerographically in this copy. Higher quality 6" x 9" black and white photographic prints are available for any photographs or illustrations appearing in this copy for an additional charge. Contact UMI directly to order.

ProQuest Information and Learning
300 North Zeeb Road, Ann Arbor, MI 48106-1346 USA
800-521-0600

Computer modeling of the energy performance of screw chillers

Babak Solati

A Thesis

in

The Department

of

Building, Civil and Environmental Engineering

Presented in Partial Fulfillment of the Requirements
For the Degree of Master of Applied Science at
Concordia University
Montreal, Quebec, Canada

February 2002

ABSTRACT

Computer modeling of the energy performance of screw chillers

Babak Solati

The energy crisis and mandatory energy conservation standards together with the advancement in computer technology led to rapid development of the energy calculation procedures for the prediction of the performance and energy requirements of buildings. DOE-2 is one of the major public domain programs, which is used throughout North America, however this program does not contain computer models for screw compressor chillers.

The main objective of this study is to evaluate the energy performance of screw-compressor chillers, based on thermodynamic principles and parameter identification from the manufacturers' data. The thermodynamic model used in this study was based on the ASHRAE Toolkit-I for primary HVAC system energy calculations.

Results showed that the screw compressor chillers perform almost similar to centrifugal chillers at off-design conditions under full load; however at part load regime, screw chillers perform completely different from centrifugal chillers. It was observed that unlike the centrifugal chillers, the screw chillers have the best performance at part load ratio about 0.7, and at low part load ratio the COP is significantly low.

After the energy performance correlation for screw compressor chillers were derived, they were used in the DOE-2 program to compare the energy performance of an office building in Montreal with that of centrifugal chillers. Results showed that the electric demand of screw chiller is significantly higher. Meanwhile the monthly peak electric demand is almost constant throughout the year, while that of centrifugal chillers shows a significant variation from month to month.

Beside the correlations for energy performance of screw compressor chiller based on the DOE-2 generic format, some other type of correlations were developed using the identified parameters, which can be used in the Fault Detection and Diagnostic (FDD) systems to check continuously the performance of chillers during the operation.

Acknowledgements

I wish to express my deepest gratitude to my supervisors, Professor R. Zmeureanu and Professor F. Haghighat for their unfaltering commitment, valuable guidance and encouragement.

Greatest respects go to Professor J. Paris for his coordinative efforts in the overall project and his aid and support whenever I required it.

For their financial support in form of grants that have made this study possible, I thank the NSERC – Collaborative Research Opportunities and the NSERC – Research program.

I also wish to thank Ms. V. Neuhann whose contribution to this study is greatly appreciated.

To Mr. S. Bélanger special thanks for offering his valuable expertise on computer facilities.

Last but not least, I wish to express my profound gratitude to my family for their love, patience and unconditional giving.

Table of contents

List of Figures

Figure **Page**

List of Tables

Table **Page**

NOMENCLATURE

Symbol	Meaning	Units
adp	apparatus dew point	-
$A_{c,i}$	total inside surface area of condenser tubes	m^2
A_{cl}	first coefficient in the Clausius-Clapayron equation	-
A_{eff}	estimated effective or wetted area of one turn of the coil	m^2
A_i	inside surface area of one turn of the coil	m^2
A_l	leakage area	m^2
ANCR	ratio of available capacity to nominal capacity	-
B	isentropic slope in a Duhring chart	-
B_{cl}	second coefficient in the Clausius-Clapayron equation	-
BF	bypass factor	-
c	transfer function	-
C	effective clearance volume ratio	-
C.V.	coefficient of variance	-
CAP	capacity	W
CAP_d	design capacity	W
CAP_x	capacity at any working point	W
CDD	cooling degree-days	°C
COP	coefficient of performance	-
COP_{actual}	actual coefficient of performance	-
COP_{carnot}	Carnot coefficient of performance	-
COP_{comp}	compressor coefficient of performance	-
COP_d	coefficient of performance at design condition	-

COP_{ideal}	ideal coefficient of performance	-
$COP_{overall}$	overall coefficient of performance	-
COP_{PL}	Part load coefficient of performance	-
COPx	coefficient of performance at any working point	-
Cp_{liq}	specific heat of liquid	J/kgK
CPR	compressor power ratio	-
Cp_{vap}	specific heat of vapor	J/kgK
Cp_{w}	specific heat of water	J/kgK
d_i	inner diameter of coil	m
$dp_{pumping}$	pressure jump encountered by the refrigerant bypassed	Pa
D_{AB}	mass diffusivity	m^2/s
D_{cd}	inside condenser tube diameter	m
EER	energy efficiency ratio	-
EIR	nominal electric input ratio	-
ELEC	electric input	W
f_{HX}	dimensionless term	-
FLPR	full load power ratio	-
FRAC	ratio of required capacity over the minimum operation capacity	-
g	gravitational acceleration	m/s^2
gpm	Gallon per minute	gpm
G	characteristic parameter	-
G_1	ratio of COP to design COP	-
G_2	ratio of chilled water leaving temperature to condenser entering water temperature	-

G_3	ratio of the available capacity to the design capacity	-
h_{adp}	enthalpy of the air at apparatus dew point	kJ/kg
h_c	coolant side heat transfer coefficient	W/m^2K
$h_{c,i}$	heat transfer coefficient of water flow inside condenser tubes	W/m^2K
$h_{c,o}$	heat transfer coefficient for refrigerant	W/m^2K
hfg	heat of vaporization of refrigerant	J/kg
hfgo	enthalpy of vaporization at reference temperature	J/kg
hfo	enthalpy of saturated liquid at reference temperature	J/kg
h_{ra}	enthalpy of the return air	J/kg
h_s	heat transfer coefficient at solution side	J/kg
h_1	enthalpy of the refrigerant before entering the compressor	kJ/kg
h_2	enthalpy of the refrigerant entering the condenser	kJ/kg
h_3	enthalpy of the refrigerant entering the expansion device	kJ/kg
h_4	enthalpy of the refrigerant entering the evaporator	kJ/kg
HDD	heating degree-days	°C
HRF	heat rejected factor	-
IPLV	integrated part load ratio	-
k	specific heat ratio	-
k_c	coolant thermal conductivity	W/mK
k_{cooper}	thermal conductivity of copper (tubing)	W/mK
k_f	mass transfer coefficient for falling film	m^2/s
k_l	thermal conductivity of the liquid refrigerant	W/mK
k_w	thermal conductivity of water	W/mK
le	air leaving the cooling coil	-

$LMTD_{cd}$	condenser logarithmic mean temperature difference	K
$LMTD_{ev}$	evaporator logarithmic mean temperature difference	K
MAE	mean absolute error	-
$\dot{M}_R$	mass flow rate of the refrigerant	Kg/s
$\dot{M}_{R_N}$	refrigerant mass flow rate at part load	Kg/s
$\dot{M}_{w,cd}$	condenser water mass flow rate	Kg/s
$\overline{\dot{M}}_{w,cd}$	average condenser water mass flow rate	Kg/s
$\dot{M}_{w,ev}$	evaporator water mass flow rate	Kg/s
$\overline{\dot{M}}_{w,ev}$	average evaporator water mass flow rate	Kg/s
n	polytropic coefficient	-
N	number of working points	-
NFLPR	nominal full load power ratio	-
N_t	number of horizontal tubes	-
Nu_c	Nusselt number at coolant side	-
oa	outdoor air	-
p_{cd}	condensing pressure	Pa
p_{ev}	evaporating pressure	Pa
p_i	actual compressor discharge pressure	Pa
P_{cd}	first guess of condenser load	W
$P_{discharge}$	absolute discharge pressure	Pa
P_{ev}	first guess of evaporator load	W
PLR	part load ratio	-
Pr_c	Prandtl number at coolant side	-
Pr_w	Prandtl number of water	-

P_{sat}	saturation pressure	Pa
$P_{suction}$	absolute suction pressure	Pa
q	net heat transfer in a process	J/kg
$\dot{q}_{cd}$	rate of internal losses in condenser	W
q_{cd}	condenser heat transfer	J/kg
$\dot{q}_{ev}$	rate of internal losses in evaporator	W
q_{ev}	evaporator specific heat transfer	J/kg
q_t	instantaneous heat gain at time t	W
$\dot{Q}_{base}$	rated condenser capacity	W
$\dot{Q}_{cc}$	cooling coil load	W
$\dot{Q}_{cd}$	condenser heat rejection	W
$\overline{\dot{Q}}_{cd}$	average condenser load	W
$\dot{Q}_{ev}$	evaporator capacity	W
$\overline{\dot{Q}}_{ev}$	average evaporator load	W
$\dot{Q}_g$	generator heat flux	W
Q_t	cooling load at time t	W
r	gas constant =81.4899	J/kgK
ra	return air	-
r_c	the ratio of effective outside condenser tube area to inside area	-
r_i	inner radius of coil	m
rm	room air	-
r_o	outer radius of coil	m
R	radius of coil	m
R^2	coefficient of determination	-

R_c	conductive thermal resistance of the tube material	W/m^2K
RCAP	rated cooling capacity	W
Re	Raynolds number at solution side	-
Re_c	Raynolds number at coolant side	-
Re_{cd}	Raynolds number associated with water flow in an individual condenser tube	-
RH	relative humidity	-
RPM	revolution per minute	rpm
s	characteristic parameter	-
s_1	entropy of the refrigerant entering the compressor	J/kgK
s_4	entropy of the refrigerant entering the evaporator	J/kgK
Sc_s	Schmidt number for solution	-
SE	standard error	-
SEER	seasonal energy efficiency ratio	-
T_{CA}	arithmetic mean of cooling water temperature	K
T_{cd}	condensing temperature	K
$T_{w_{ev1}}$	entering chilled water temperature	K
$T_{w_{ev2}}$	leaving chilled water temperature	K
$T_{w_{cd1}}$	condenser entering water temperature	K
$T_{w_{cd2}}$	condenser leaving water temperature	K
T_{cwOut}	chiller cooling water leaving temperature	K
T_{cwIn}	chiller cooling water entering temperature	K
$T_{c,s}$	average outside surface temperature of tube	K
T_{env}	condenser air (environmental temperature)	K

T_{ev}	evaporating temperature	K
$T_{ev'}$	refrigerant temperature after heating up	K
T_{in}	inside surface temperature	K
T_o	reference temperature	K
T_{out}	outside surface temperature	K
T_{sat}	saturation temperature	K
TR	tons of refrigeration (1TR = 3.52 kW)	TR
T_1	temperature of refrigerant entering the compressor	K
T_2	temperature of refrigerant entering the condenser	K
T^*	ratio of chilled water leaving temperature to condenser entering water temperature	-
U	overall heat transfer coefficient	W/m^2K
$\overline{UA}_{cd}$	average condenser overall heat transfer coefficient	W/K
UA_{cd}	condenser overall heat transfer coefficient	W/K
$\overline{UA}_{ev}$	evaporator overall heat transfer coefficient	W/K
UA_{ev}	evaporator overall heat transfer coefficient	W/K
V	volume of cylinders	m^3
$\dot{V}_a$	Air volumetric flow rate	m^3/s
$\dot{V}_{pumping}$	bypassed refrigerant volumetric flow rate	m^3/s
$\dot{V}_r$	volumetric flow rate of refrigerant	m^3/s
$\dot{W}$	electric demand of compressor	W
w	work done in a process	J/kg
$\dot{W}_{actual}$	compressor actual power	W
w_{comp}	work done by compressor	J/kg

$\dot{W}_{ideal}$	compressor ideal power	W
$\dot{W}_{in}$	compressor internal power	W
$\dot{W}_{in_{PL}}$	part load internal power	W
$\dot{W}_{in_{red}}$	reduction of internal power of compressor	W
$\dot{W}_{lo}$	compressor constant losses	W
w_{net}	net work done by compressor	J/kg
$\dot{W}_{PL}$	electric demand at part load	W
$\dot{W}_{pump}$	power required to bypass the refrigerant at part load	W
$\dot{W}_{total-losses}$	total electromechanical losses	W
X_i	transfer function	-
Y_i	transfer function	-

Greek Symbols

α	coefficient of variable electromechanical losses	-
δ	falling film thickness	m
δp	pressure drop	Pa
ΔT_{min}	minimum total temperature difference	K
ΔT_o	arithmetic mean temperature of external heat exchanger fluids	K
$\overline{\varepsilon_{cd}}$	average effectiveness of the condenser	-
ε_{cd}	effectiveness of the condenser	-
$\overline{\varepsilon_{ev}}$	average effectiveness of the evaporator	-
ε_{ev}	effectiveness of the evaporator	-
γ	isentropic coefficient	-
η_{comb}	combined efficiency	-
η_{is}	isentropic efficiency	-

η_m	efficiency of electric motor	-
η_v	volumetric efficiency	-
μ_f	viscosity of saturated liquid refrigerant	Pa.s
ν_s	solution kinematic viscosity	m^2/s
π	external pressure ratio	-
π'	internal pressure ratio	-
ρ_a	air density	kg/m^3
ρ_f	density of saturated liquid refrigerant	kg/m^3
ρ_v	density of saturated vapor refrigerant	kg/m^3
υ_{ev}	refrigerant specific volume after heating up	m^3/kg
υ_i	weighting factors	-
$\upsilon_{suction}$	refrigerant suction specific volume	m^3/kg
ω_i	weighting factors	-
ψ	characteristic parameter	-
ζ	mean compressibility factor	-

Chapter 1

Introduction

1.1 Introduction

Mechanical systems are one of the essential components in buildings. As an indication they occupy almost 10 percent of the gross area and account for about 30 percent of the total initial cost of the commercial buildings. Primary equipment such as chillers and boilers are generally the major energy-consuming equipment of Heating, Ventilating and Air-Conditioning (HVAC) systems in a building. Accurate evaluation of energy performance by means of computer simulation requires detailed information that includes design parameters, environmental conditions, control techniques and load variation in secondary systems.

Refrigeration equipments are one of the most important equipment in primary systems and play a great role in HVAC systems to provide comfort condition in occupied spaces. Their energy performance directly affects the operating and maintenance cost of mechanical systems.

Throughout the years due to the great demand of refrigeration equipment, many different technologies have been introduced and consequently remarkable competition in refrigeration equipment manufacturers can be seen. This wide variety sometimes makes it difficult for the users to select the optimum system which best suits their needs because there are many parameters that can be considered in comparing different refrigeration units. Since the first thing that mostly draws the engineers' attention is the efficiency, the engineers need some tools to evaluate the energy performance of refrigeration equipment.

Therefore various mathematical models for refrigeration systems have been developed; some of these models can be applied to all types of refrigeration systems and some are system specific.

The most used refrigeration systems are the electricity-driven vapor-compression systems due to the high efficiency; they use Chlorofluorocarbons (CFC) or Hydro-chlorofluorocarbons (HCFC) as refrigerant, which are harmful for the environment. After the ozone layer problem reached a serious stage, regulations were legislated that prohibit the use of certain refrigerants such as CFC-11, which is no longer produced since 1995, and also limit the use of some others such as HCFC-123 up to a certain date (e.g. year 2020) [1]. This problem makes the manufacturers find other refrigerants to replace the original one in the existing refrigeration equipment. This short-term solution somehow leads to less energy-efficiency and remarkable expenses for replacing the refrigerant. Facing this problem, some end-users found turning to another technology such as absorption chiller as the only long-term option.

Because of their lower efficiency, the absorption chillers were less attractive during the past years. Regarding the latest environmental regulations however, the option of exchanging the traditional vapour-compression chillers with the absorption chillers seems to be a tangible solution to the environmental problems. The considerable rise in the number of absorption chillers shows this trend. In 1990, the double effect absorption chillers in the United States represented the capacity of 600,000 tons [1], since they have been introduced by Brooklin Union Gas in 1979.

There are two main categories of refrigeration systems:

- Vapor Compression Systems
- Absorption Systems

Each of these categories is classified to some other sub-groups (Figure 1-1), which are explained in the next chapter.

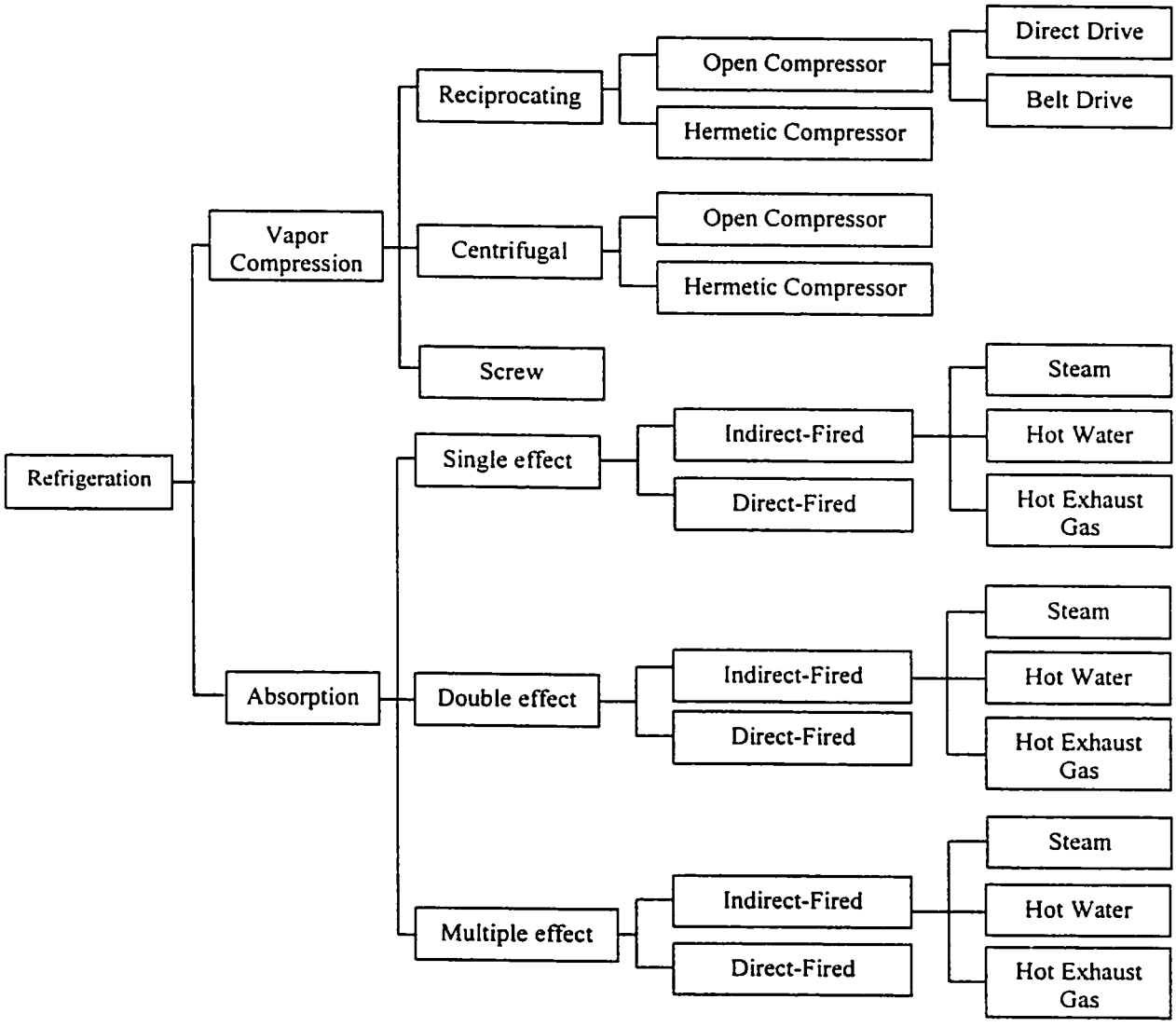

Figure 1-1 Classification of Refrigeration Equipment

1.2 Performance Comparison

Some samples of working conditions of chillers are presented in Table 1-1. The COP of a refrigeration machine is defined as the amount of cooling delivered by a refrigeration machine divided by the amount of energy input required to produce cooling. This is a rating ratio of energy transferred to energy input. The COP does not include auxiliary electricity to operate the pumps and fans [2].

Table 1-1 Working specification of different type of chillers [2]

	Absorption			Vapor-compression
	Lithium Bromide/Water		Water/Ammonia	
	single-effect	double-effect		
COP	0.6-0.7	0.9-1.2	0.1-0.8	2-6.75
Steam consumption kg/hr per TR	8	5	-	-
Steam or gas temp. °C	105-120	175-185	100-195	-
Steam pressure kPa	135-205	550-1100	100-1480	-
Hot water temp. °C	115-150	155-205	100-195	-
Cooling output °C	4-38	4-27	-40-15	-
Condenser flow rate gpm per TR	3.6	4	-	3
Electric demand kW/TR	0.02	0.018	-	0.75

The COP of a single-effect absorption system is typically two-thirds that of a double-effect absorption system. For a single-effect system, COP range is from 0.6 to 0.7 while for a double-effect system range from 0.9 to 1.2. A double-effect machine makes more efficient use of the input energy. For low-pressure absorption systems, COP range is from 0.1 to 0.8. For vapor–compression systems, the COP range is from 2 to 6.75. While the COP of vapor-compression systems is higher than that of absorption systems, vapor-compression systems typically require a higher grade of energy to power them (electricity versus gas or recovered heat). Therefore, when comparing the COP of an absorption cycle to that of a vapor-compression cycle, it is important to account for the differences in the costs of the energy required by each. In the vapor-compression cycle,

the COP is determined by the amount of mechanical work required to pressurize the vapor, while in an absorption system, the COP is determined by the amount of heat required to operate the cycle.

The energy required for operating condenser fans, cooling towers, circulation pumps, and other equipment is not included in the COP of chillers. However these energy costs must be included in the full economic analysis of the system. Also the controls required to achieve acceptable part-load and off-design conditions must be accounted for in the life cycle cost analysis.

Since the cost to produce the mechanical work needed to provide one ton of refrigeration in a vapor-compression cycle is typically greater than the cost of heat required by an absorption system to produce one ton of refrigeration, the absorption systems can often compete economically with vapor-compression systems. Differences in local utility rates and specific site information can affect the economic analysis.

Another factor to be considered when comparing the COP is the conditions under which the COP was obtained. Generally, the COP of chillers is introduced at standard conditions as published by the Air Conditioning and Refrigeration Institute (ARI).

On the other hand, the use of absorption chillers driven by steam or hot water as the heat source, requires greater capital and maintenance costs.

1.3 Layout of the study

This thesis consists of eight chapters. At the beginning different types of refrigeration systems were introduced. In Chapter two a literature review is presented containing different methods of evaluation of energy performance of refrigeration systems. The literature survey revealed that a number of mathematical models for different chiller types already exist. However, there are no models for screw chillers, which are used by the energy analysis program such as DOE-2. Based on the literature survey, the study is directed forward the screw chillers.

A mathematical model for the ideal standard vapor-compression cycle is developed and corrected with the manufacturer's data in Chapter three.

In Chapter four the mathematical modeling of ASHRAE Toolkit-I for screw-compressor chillers is presented and the required modification is followed in Chapter five.

In Chapter six, the correlation-based models of the energy performance of screw chillers are derived using the ASHRAE Toolkit-I models, the manufacturer's data and the regression techniques.

The newly developed correlation-based models are used in the DOE-2 energy simulation program, which does not contain corresponding correlations for screw-compressor chillers. Then, in Chapter seven, the energy performance of screw chiller is compared with that of centrifugal chillers for a base case building.

Finally, conclusions and recommendations for further studies are discussed in Chapter eight.

Chapter 2

Literature review of mathematical models of chillers

This chapter consists of three main parts. In the first part, the operation of refrigeration systems is explained briefly. In the second part, the literature survey of the mathematical models available is presented and finally, in the third part the objective of the study is introduced.

2.1 Refrigerating operation

Based on the classification of refrigeration systems mentioned in section 1.1, the operation of different types of chillers is presented here, but before introducing the refrigeration systems it is worth mentioning some definitions mostly used in this section.

2.1.1 Definitions

Coefficient of Performance (COP) – cooling [3]

The ratio of the rate of heat removal to the rate of energy input in consistent units, for a complete cooling system or factory assembled equipment, as tested under a nationally recognized standard or the designated operating conditions.

Tons of Refrigeration (TR) [4]

The amount of heat per time unit which is required to melt one ton of ice (2000 Lb) at 32°F in 24 hours; the latent heat of melting ice at 32°F is 144 Btu/hr;

1 Ton of Refrigeration = 2000 × 144 Btu/Lb in 24 hours

= 288,000 Btu in 24 hours

= 12,000 Btu/hr

= 3.517 kW

Part Load Ratio (PLR)

The ratio of the actual load at a certain time to the nominal load of a refrigeration machine.

2.1.2 Vapor-compression systems

The vapor compression cycle is the cycle most often used for air conditioning and refrigeration applications. The basic cycle is essentially the same regardless of the compressor type or refrigerant used. Figure 1-2 shows a schematic of the equipment layout for a typical vapor compression cycle. It consists of four main components, the compressor, condenser, evaporator and expansion valve, which are connected by piping systems [2].

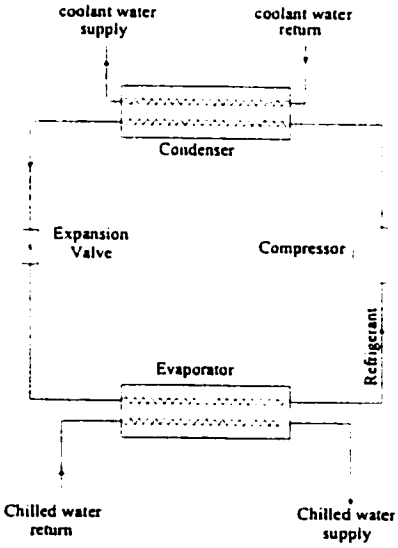

Figure 2-1 Schematic of equipment layout of typical vapor-compression refrigeration cycle

Superheated vapor leaves the compressor and is liquefied in a condenser by the heat exchange with cooling fluid (water or air). The liquid refrigerant then passes through an expansion valve and the low-pressure liquid enters the evaporator. It absorbs heat from

the medium to be cooled and is vaporized. The vapor enters the compressor and is raised to a higher pressure [4]. The vapor compression systems are also categorized based on the type of their compressors:

1) Reciprocating

2) Centrifugal

3) Screw

Compressors have many types of drive: electrical motors, gas and diesel engines and gas and steam turbines.

A reciprocating compressor is a single acting piston driven by a pin and a connecting rod from its crankshaft. It is a positive displacement compressor in which an increase in the pressure of the refrigerant gas is achieved by reducing the volume of the compression chamber through work applied to the mechanism. This type of compressor is applied to the refrigerants having low specific volumes and relatively high-pressure characteristics. The compressor sizes range between 1/16 to 150 kW, and can be classified as either open or hermetic compressors. Reciprocating chillers are generally used up to 210 kW (60 TR). But in some special cases they may be used up to 700 kW (200 TR) [5,6].

Centrifugal compressors are built for heavy-duty continuous operation and have a reputation for reliability in all types of commercial and industrial applications. Their reliability is high and their maintenance is low, because centrifugal compression involves the purely rotary motion of only a few mechanical parts. The compressor uses the centrifugal force to raise the pressure of continuous flow of refrigerant gas from the

evaporator pressure to the condenser pressure. It handles high volume of gas, and can use refrigerants having high specific volumes. There are two types of centrifugal chillers: (i) those with open compressors and, (ii) with hermetic compressors. Centrifugal refrigeration machines were developed to fill the need for single refrigeration units of large capacity. A single centrifugal machine can be used in place of many reciprocating units. The capacities of these machines range from 350 kW to 35MW (100-10,000 TR) of refrigeration and most of them have water-cooled condensers [5,6].

The advantages of centrifugal chillers can be summarized as follows:

1. Reliability
2. Compactness
3. Low maintenance cost
4. Long life
5. Ease of operation
6. Quietness

The screw compressor is a positive displacement compressor that uses a rotor driving another rotor (twin) or gaterotors (single) to provide the compression cycle. The compression process starts with the rotors meshed at the inlet point of the compressor. As the rotor turns, the lobes are separated, causing a reduction in pressure and drawing in the refrigerant. The intake cycle is completed when the lobe has turned far enough to be between the meshing points of the rotors, the discharge housing, and the stator and rotors. is continuously decreased. When the rotor turns far enough, the lobe opens to the discharge port, allowing the gas to leave the compressor (Figure 2-2).

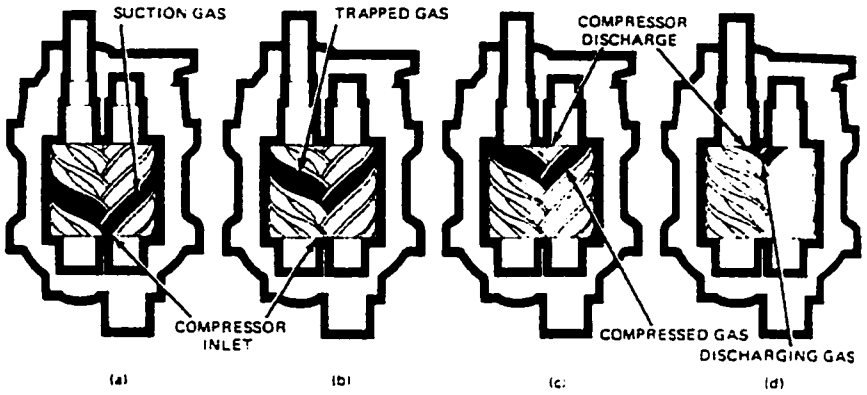

Figure 2-2 Twin Screw Compression cycle [6]

The gas is continuously compressed until the lobes are totally meshed. This eliminates undesirable condition in reciprocating compressors where the gas, in the clearance volume between the piston and the top of the cylinder, reexpands within the cylinder, resulting in reduced volumetric efficiency and increase in required input power. The screw compressors using R-22, have the capacities ranging from 176 to 5626 kW (50 to 1600 TR) [6].

2.1.3 Absorption systems

Absorption chillers are machines that utilize the heat to cool down the circulating medium. The absorption cycle utilizes an absorbent (usually a salt solution) and a refrigerant. Low-pressure refrigerant is dissolved in absorbant in a generator, and vapor at high pressure is driven out of the solution by heat. The vapor is liquefied in a condenser and expanded through an expansion valve, as in a compression system. The low-pressure liquid enters the evaporator and absorbs heat from the medium to be cooled. It vaporizes and returns to the generator [6]. Figure 2-3 shows an absorption cycle.

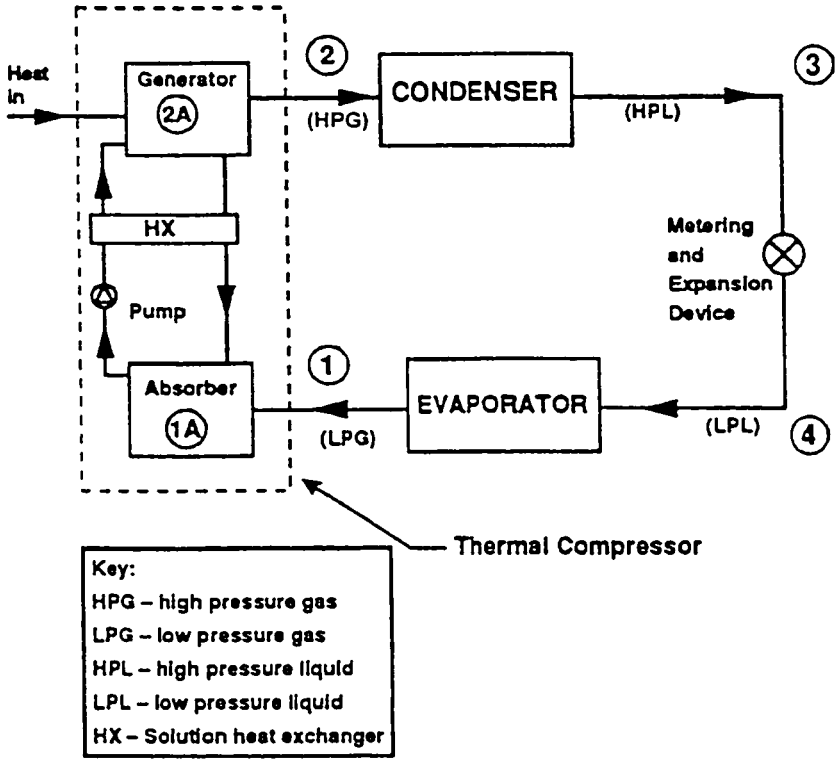

Figure 2-3 Absorption Refrigeration Cycle [2]

The key difference between the absorption cycle and the vapor-compression cycle is the process by which the low-pressure refrigerant is transformed to a high-pressure vapor. In the absorption cycle the low-pressure vapor is absorbed into a solution at low pressure, pumped to a high pressure and then heated to produce a high-pressure vapor [2].

Absorption chillers are usually classified according to the type of heat used as the input, and whether it has a single-stage or two-stage generator. Absorption machines using steam, hot water or hot gas as the heat energy source are referred to as *indirect-fired* machines, while those, which have their own flame source, are called *direct-fired* machines. Machines having one generator are called *single –stage* absorption chiller, and those with two generators are called *two-stage* absorption chiller.

The capacity of large absorption chillers ranges from 352 to 5280 kW (100 to 1500 TR). Small-tonnage absorption machines are produced for residential and small commercial applications ranging from 17 to 35 kW (5 to 10 TR).

2.2 Literature survey

The need for the prediction of energy performance of the chillers, has led to the development of different simulation techniques. In a simple refrigeration cycle, the simple models seem to be a fast and satisfactory solution to evaluate the performance of refrigeration equipment, however, in complex systems offered by different manufacturers, the calculations are lengthy and the researchers are faced with complicated thermodynamic and mathematical models to be solved. Meanwhile general thermodynamic models alone do not cover the whole area of refrigeration equipment because they require the manufacturers' data. On the other hand, making an accurate thermodynamic model requires a detailed knowledge of the arrangement of the equipment components and properties. All of these parameters make the models different and the degree of accuracy of the models is influenced by the assumptions made and the data used. The models, which present the refrigeration equipment in a modular form making it flexible to use them in different cycle arrangements, and conditions that can be modified with the manufacturers' data, are more attractive and have survived over the years. Some of them have become the base of today so called energy analysis codes that are so popular such as BLAST [7] and DOE-2 [8].

According to the studies already done on refrigeration equipment, two types of modeling can be recognized: (i) First principle models, and (ii) Correlation-based models.

First-Principle models are based on thermodynamic equations governing different components of a chiller (e.g. compressor, condenser, evaporator) that are coupled to evaluate the whole chiller performance. The accuracy of this kind of model is based on the assumptions made. To use some unknown data the researchers refer to parameters specified by manufacturers. These parameters somehow are different among various manufacturers or even vary with different sizes of the same type of chiller. The complicated nature of chillers has discouraged the use of this type of modeling, however, these models allow confident application outside the range of available data.

Correlation-based models relate the energy performance of chiller with different operating or constructive parameters using regression analyses of the manufacturers' published data. Since the operating data published by manufacturers are generally for full-load design conditions, additional correction functions are used to derive part-load data. This method might be appropriate when the user has a large set of measurements of the plant. The part-load corrections often represent the greatest uncertainty in this type of models, which causes the greatest effect on annual energy prediction. It should be noted that the correlation-based models are valid within the range of parameters used in their development, and extrapolation out of this range may cause remarkable errors. In this section the most important models of chillers are presented in two parts:

- Absorption systems
- Vapor-compression systems

2.2.1 Absorption chillers

The computer code BLAST (the Building Load Analysis and System Thermodynamics program) was introduced by Hittle [7]. In this code the heat consumed by the absorption chiller is determined in terms of design capacity of the chiller CAP_d and part load ratio PLR.

$$\left(\frac{Heat\ input}{CAP_d}\right) = \frac{1}{PLR}\left(A_1 + A_2 PLR + A_3 PLR^2\right) \tag{2-1}$$

The ratio of the heat input over the cooling capacity represents the inverse of COP. The coefficients A_1, A_2 and A_3 are determined by curve fitting data from manufacturers.

The Department of Energy of the United States supported the development of the DOE-2 program [8] for energy simulation of buildings. In this computer code, the heat input of the absorption chiller is modeled by a binomial equation as follows:

$$Heat\ input = CAP_d \times HIR_d \times F_1 \times F_2 \times F_3 \times FRAC \tag{2-2}$$

where:

HIR_d : The design heat input ratio; the ratio of the heat input to the cooling capacity at design conditions (7°C evaporator leaving water temperature and 30°C condenser entering water temperature)

F_1 : Correction factor for the COP at full-load regime at off-design conditions

$$F_1 = \left(\frac{COP_d}{COP_x} \right)_{FL} \tag{2-3}$$

F_2 : Correction factor for the COP at part load regime at off-design conditions

$$F_2 = \frac{(COP_x)_{FL}}{(COP_x)_{PL}} \tag{2-4}$$

F_3 : Correction factor for the cooling capacity at off-design conditions

$$F_3 = \frac{CAP_x}{CAP_d} \tag{2-5}$$

FRAC: The fraction of hour when the chiller is cycled on; the required capacity is below the minimum operating capacity of the chiller and is calculated as follows:

$$\text{FRAC} = \frac{\text{Required capacity}}{\text{Minimum operating capacity}} \tag{2-6}$$

The correction factors are determined by binomial correlations as follows:

$$F_1 = a_1 + b_1 T_{w_{ev2}} + c_1 T_{w_{ev2}}^2 + d_1 T_{w_{cd1}} + e_1 T_{w_{cd1}}^2 + f_1 T_{w_{ev2}} T_{w_{cd1}} \tag{2-7}$$

$$F_2 = a_2 + b_2 PLR + c_2 PLR^2 \tag{2-8}$$

$$F_3 = a_3 + b_3 T_{w_{ev2}} + c_3 T_{w_{ev2}}^2 + d_3 T_{w_{cd1}} + e_3 T_{w_{cd1}}^2 + f_3 T_{w_{ev2}} T_{w_{cd1}} \tag{2-9}$$

where:

$T_{w_{out}}$: leaving chilled water temperature

$T_{w_{in}}$: entering condenser water temperature

All types of absorption chillers are modeled with the same approach but with different coefficients regardless of the solution type.

A computer code has been developed by Grossman and Michelson [9], and Grossman et al. [10]. It is a modular computer code, which makes it flexible to simulate different absorption systems in varying cycle configurations with different working fluids. The components in the absorption cycle (evaporator, absorber, generator and condenser) are modeled by subroutines, which contain the fundamental equations applicable to that unit, such as energy and mass balance. Once all the governing equations are defined based on the input and thermodynamic properties of the absorption fluid pair, a set of non-linear equations is formed. These equations are solved simultaneously, using appropriate constraints. The subroutines are linked together by the main program according to the user's specifications to form the complete system. This code was used by Gommed and Grossman [11] to investigate the performance of a single stage and three double stage absorption chillers with different configurations using a lithium-bromide/water fluid pair.

Later this model was tried by G. Grossman et al. [12] to evaluate the performance of a triple-effect absorption cycle with different configurations including three condenser-three generator (3C3D), double condenser coupled (DCC) and dual loop configurations.

They concluded that in each case parallel flow system results in a better COP than series flow and the risk of crystallization is lower but the capacity is slightly lower too. Also they found out that DCC creates an increase in the COP of the corresponding 3C3D cycle with no additional piping cost due to different piping arrangement.

Seewald and Perez-Blanco [13] introduced a simple model for calculating the performance of a lithium-bromide/water absorber. They developed this model on a particular absorber and presented the effect of various parameters on the performance of the absorber, which is an essential part of an absorption cycle; the overall performance of the absorption chiller depends on this component. The application of this model is limited to one type of absorber in which the coolant water flows inside the coil, and the solution falls from one turn of coil to the other in the form of droplets. The heat and mass transfer processes are considered separately in this model. Heat transfer occurs when the solution is in contact with the coil. Mass transfer is of greatest consideration when the solution is leaving one turn of coil dropping on the other turn as a droplet, and comes to an equilibrium with water vapor in the absorber. The overall heat transfer coefficient between the solution and the coolant water is determined as follows:

$$U = \left[\frac{1}{h_c} + r_i \frac{\ln(\frac{r_o}{r_i})}{k_{copper}} + \frac{A_i}{h_s A_{eff}} \right]^{-1} \qquad (2\text{-}10)$$

$$A_i = 4\pi^2 r_i R$$

$$H_c = \frac{Nu_c k_c}{d_i} \tag{2-11}$$

$$Nu_c = 0.023 Re_c^{0.85} \left[\frac{r_i}{R}\right]^{0.1} Pr_c^{0.4} \tag{2-12}$$

where

h_c : coolant side heat transfer coefficient (W/m^2K)

h_s : solution side heat transfer coefficient (W/m^2K)

A_i : inside surface area of one turn of the coil (m^2)

A_{eff} : estimated effective or wetted area of one turn of the coil (m^2)

R : radius of coil (m)

r_i : inner radius of tube (m)

r_o : outer radius of tube (m)

d_i : inner diameter of tube (m)

k_c : coolant thermal conductivity (W/mK)

k_{copper}: thermal conductivity of copper (tubing) (W/mK)

Nu_c : coolant side Nusselt number

Pr_c : coolant side Prandtl number

Re_c : coolant side Reynolds number

Once the overall heat transfer coefficient is evaluated, the heat transferred from the solution to the coolant water is estimated for given temperatures of solution and coolant water. Assuming that a mass of solution descending from one turn to the next comes to equilibrium according to its state and surrounding, it will absorb an appropriate amount

of water vapor [13]. The mass transfer coefficient k_f is determined by the following formula:

$$\frac{k_f \delta}{D_{AB}} = 1.38\left[\frac{z}{\delta}\cdot\frac{1}{\mathrm{Re}_s}\cdot\frac{1}{Sc_s}\right]^{1/2} \tag{2-13}$$

$$z = \frac{\pi r_o}{2}$$

$$\mathrm{Sc}_s = \frac{\nu_s}{D_{AB}} \tag{2-14}$$

where:

k_f : mass transfer coefficient for falling film (m^2/s)

δ : falling film thickness (m)

D_{AB} mass diffusivity (m^2/s)

Re_s : solution side Raynolds number

Sc_s : Schmidt number for solution

ν_s : solution kinematic viscosity (m^2/s)

Knowing the mass flow rate and specific heat of solution, and the saturation temperature of water vapor, then the amount of water vapor absorbed by the solution is determined.

Using this model, we can examine the effect of variation of each parameter holding the others constant. These variables are: the solution and coolant water flow rate, the

number of sites at which the droplets form, the absorber vapor pressure, and the solution initial concentration. The results show:

- Variation in solution flow rate produces an optimum point of absorber performance.
- Increasing the coolant flow rate resulted in a limited increase in absorber performance.
- Improving the solution distribution, by increasing the number of sites at which droplets form on the coil surface, improves the performance of the absorber.
- Increasing the vapor pressure increases the absorber performance.
- The higher the initial concentration of the solution, the better the performance of the absorber.

Hellmann and Ziegler [14] introduced a simple model for absorption chiller and heat pumps that reduces the characteristics of the machine to only two algebraic equations, one for COP and the other for cooling capacity. These equations contain the complete thermodynamic information in a simplified way and the results are acceptable if the range of operation is not too large. This is a very fast and stable energy performance model that can be used in other energy simulation codes. It is also an appropriate tool to derive correlations, based on manufacturer's data of commercial absorption chiller, to make those information available for different computer programs. One parameter called total temperature difference is introduced in this study:

$$\Delta T_o = (T_G - T_A) - B\,(T_C - T_E) \qquad (2\text{-}15)$$

The temperatures "T" designate the arithmetic mean temperature, in degree Kelvin of fluids in four major heat exchangers. Indices G, A, C, and E corresponds to generator, absorber, condenser, and evaporator respectively. The coefficient B is about 1.0 for lithium/bromide/water system. The evaporator capacity $\dot{Q}_{ev}$ is expressed as a linear function of ΔT_o if the characteristic parameters are constant within the operating range (equation (2-15)). The slope of this function "s" can be considered as the overall heat transfer coefficient of the four major heat exchangers, which depends on the design of the absorption machine. Using this total temperature difference ΔT_o seems to be inconvenient due to the fact that typically the temperatures of the cooling water entering and leaving the chiller are known rather than entering and leaving the condenser and absorber. So after the modification the model estimates the COP and cooling capacities as follows:

$$\dot{Q}_{ev} = s\,(\Delta T - \Delta T_{min}) \tag{2-16}$$

$$COP = \frac{\dot{Q}_{ev}}{\dot{Q}_g} = \frac{\Delta T - \Delta T_{min}}{G.\Delta T + \left(\frac{1}{\psi} - G\right)\Delta T_{min}} \tag{2-17}$$

$$\Delta T = (T_G - T_{CA}) - B(T_{cwOut} - T_E) \quad \text{(for serial cooling water)} \tag{2-18}$$

$$\Delta T = (T_G - T_{cwOut}) - B(T_{cwIn} - T_E) \quad \text{(for parallel cooling water)} \tag{2-19}$$

$$T_{CA} = \frac{1}{2}(T_{cwin} + T_{cwout}) \tag{2-20}$$

where:

ΔT_{min} : minimum total temperature difference that is required to overcome the solution heat exchanger loss before the chiller can start producing cold.

$\dot{Q}_g$: generator heat flux (W)

T_{cwin} : chiller leaving cooling water temperature (K)

T_{cwout} : chiller entering cooling water temperature (K)

B : a constant obtained from Dühring chart (equal to one for lithium/Bromide)

G, ψ and s are characteristic parameters and contain complete information about the design of chiller. If the coefficients B, s and ΔT_{min} are constant, the cooling capacity of a single effect absorption chiller can be expressed by a linear function of temperatures of the external heat exchanger fluids (equation (2-16)). Also if the parameters ψ and G are constant, the COP can be calculated from (equation (2-17)), which is a ratio of two linear functions of total temperature difference ΔT. The average value of characteristic parameters used in this model can be approximated based on the design data or fitting performance data published by the manufacturer.

The design process of Generator-Absorber-Heat exchanger GAX absorption cycle was presented by Priedeman and Christensen [15]. This design process relies on computer simulations that are validated by experimental data. The original code used is called ABSIM, which was written by Grossman et al. [16] that allows the designer to

incorporate standard absorption cycle component in various arrangements. The authors and others subsequently modified ABSIM to include more component types and working fluids and allow for modeling of pressure losses and ambient heat losses.

2.2.2 Vapor-compression chillers

The computer code BLAST [7] calculates the off-design capacity for vapor compression chillers by the following binomial correlation:

$$ANCR = B_1 + B_2\Delta T + B_3\Delta T^2 \tag{2-21}$$

where:

$$\Delta T = \left(\frac{T_{w,cl} - 95}{1.19}\right) - \left(T_{w,ch} - 44\right) \tag{2-22}$$

$ANCR$: the ratio of available capacity to nominal capacity

$T_{w,cl}$: condenser leaving water temperature (°F)

$T_{w,ch}$: chilled water leaving temperature (°F)

The program uses a binomial correlation to calculate the full load power ratio FLPR (the ratio of electric input to the cooling capacity) in terms of ANCR.

$$FLPR = NFLPR\,[C_1 + C_2\,(ANCR) + C_3\,(ANCR)^2] \tag{2-23}$$

where:

NFLPR: nominal full load power ratio.

The coefficients C_1, C_2 and C_3 are determined by curve fitting the manufacturer's data. All reciprocating and centrifugal chillers are modeled in the same way.

The computer code DOE-2 [8] uses a model to evaluate the electric input of open and hermetic reciprocating, and centrifugal chillers, which has the following form:

$$\text{Electric input} = CAP_d \times EIR_d \times F_1 \times F_2 \times F_3 \times FRAC \qquad (2\text{-}24)$$

where:

EIR_d: The design electric input ratio; the ratio of the compressor power input to the cooling capacity at design conditions.

CAP_d , F_1, F_2, F_3 and FRAC are similar to the model presented by this code for absorption chillers (section 2.2.1).

Cecchini and Marchal [17] developed a model using the thermodynamic cycle and experimental data from the equipment testing for simulating refrigerating and air-conditioning equipment. The model characterizes the performance of chillers using a small number of parameters, which are determined from the results of a few testing points. In this model the following assumptions are made:

-Steady state operation

-Pressure drop neglected, except at the expansion valve

-Constant sub-cooling at the condenser outlet

-Constant superheating at the evaporator outlet.

Five parameters (polytropic exponent, swept volume, built-in volume ratio, evaporator and condenser heat transfer area) are identified from two testing points at steady state conditions. The refrigeration cycle is described by eleven equations with eleven unknowns, which are: the saturation pressures and temperatures at the evaporator and condenser, the enthalpies before and after each component, the refrigerant mass flow rate, the refrigerant density, and the evaporator and condenser thermal conductances. The model was tested for two different air-cooled chillers with the cooling capacities of 25 kW and 35 kW respectively, and the accuracy of the model was found satisfactory (an uncertainty of about $\pm$ 5%).

Bourdouxhe et al. [18] presented a reciprocating chiller model using an approach with a minimum sufficient number of parameters for annual energy calculations. In this model a quasi-static state has been considered, allowing the user to apply for operation at part load conditions.

In this model two alternatives are available: 1) modeling the compressor alone, and 2) modeling the chiller composed of compressor, evaporator and condenser. These models are integrated in the ASHRAE toolkit-I [19], which contains models of boilers, chillers, cooling towers, engines and turbines. The model for screw chillers will be explained in chapter four. In modeling the compressors, the following assumptions are considered:

-Isobaric aspiration of refrigerant into the cylinders

-Isentropic compression

-Isobaric expulsion of refrigerant from the cylinder

-Isentropic re-expansion of the refrigerant that remains in the clearance volume at the end of the expulsion process.

Only five parameters are used to model the compressors: the geometric displacement of the compressor, the clearance factor, the exhaust area of the compressor cylinders, the constant part of electromechanical losses, and the loss factor for the proportional losses. These parameters have to be identified prior to simulation. If the whole chiller is under consideration, the overall heat transfer coefficient of the condenser and the evaporator has to be identified too. The parameters are identified from manufacturer data. In the evaporator and condenser, no pressure drop is considered on the refrigerant side. All parameters are assumed to remain constant during the simulation. The heat transfer coefficients are also assumed to be independent of water flow rate. Refrigerant is presumed to be perfect liquid or gas.

The model needs, as input data, the type of refrigerant, the evaporator water flow rate, the chilled water leaving temperature, the condenser water flow rate, the condenser water entering temperature and chilled water set point temperature. The model gives, as output, the input power of the compressor, the COP, the evaporator and condenser water temperature at the other side. For example, if the evaporator leaving water temperature is given in the input, the model gives the evaporator entering water temperature. For identification step, experimental data is required. At each working point the following data is needed:

-the condensing and evaporating temperatures,

-the possible sub-cooling and superheating,

-the refrigerating capacity, and the power consumed by the compressor.

Because of the assumptions and simplifications mentioned earlier, this model tends to overestimate the condenser load and overall heat transfer coefficients [18].

Strand et al. [20] developed models for direct and indirect ice-storage for energy analysis. These models were also implemented in the Building Loads Analysis and System Thermodynamics (BLAST) energy analysis program. In ice-storage, the common vapor compression system is used. In this study authors modeled evaporator, compressor and condenser and linked them in their simulation program. The advantage of these models is that they require less information about the system, and they are valid for all ice-storage systems. As an example, the model presented by Jacobson [21] prior to these models had the problem of availability of information required to model the system such as tube lengths and number of tubes, which are not always readily available. The most important assumption in the study by Strand et al. is that the evaporator load is set equal to the rated compressor capacity; the refrigeration system will always balance when it is operating at steady state. The evaporating temperature is presented as a function of percentage of storage capacity:

$$\left[\frac{T_{ev}}{T_a}\right] = A_1 + A_2(\%CAP) + A_3(\%CAP)^2 \qquad (2\text{-}25)$$

where:

$\%CAP$: Fraction of storage capacity (present storage capacity divided by the total tank capacity).

T_{ev} : Evaporator temperature (K)

T_o : Reference temperature (300K)

For an ice-harvester A_1 is the evaporator temperature divided by reference temperature while A_2 and A_3 are zero because the evaporator temperature is constant. For the compressor, instead of using the common adiabatic efficiency or polytropic expansion analysis, the authors developed correlation-based models by curve-fitting the manufacturers' data. The compressor capacity CAP is given by:

$$\left[\frac{\dot{Q}_{ev}}{RCAP}\right] = B_1 + B_2\left[\frac{T_{ev}}{T_o}\right] + B_3\left[\frac{T_{ev}}{T_o}\right] + B_4\left[\frac{p_c}{p_e}\right] + B_5\left[\frac{p_c}{p_e}\right]^2 + B_6\left[\frac{T_{cd}}{T_o}\right]^2 + B_7\left[\frac{T_{cd}}{T_o}\right]^2$$

(2-26)

where:

T_{cd} : Condensing temperature (K)

T_{ev} : Evaporating temperature (K)

p_c : Condensing pressure (Pa)

p_e : Evaporating pressure (Pa)

$\dot{Q}_{ev}$: Cooling capacity at the operating condition of interest (W)

$RCAP$: Rated (nominal) cooling capacity (W)

The electric demand of the compressor $\dot{W}$ at full load under the operating condition of interest is given by:

$$\left[\frac{\dot{W}}{RCAP}\right] = C_1 + C_2\left[\frac{T_{cd}}{T_a}\right] + C_3\left[\frac{T_{ev}}{T_a}\right] + C_4\left[\frac{p_c}{p_e}\right] + C_5\left[\frac{p_c}{p_e}\right]^2 + C_6\left[\frac{T_{cd}}{T_a}\right]^2 + C_7\left[\frac{T_{ev}}{T_a}\right]^2 \tag{2-27}$$

The performance of the compressor at part load regime was presented as:

$$CPR = D_1 + D_2\left[\frac{T_{ev}}{T_a}\right] + D_3\left[\frac{T_{ev}}{T_a}\right]^2 + D_4(PLR) + D_5(PLR)^2 + D_6(PLR)\left[\frac{T_{ev}}{T_a}\right] \tag{2-28}$$

where:

CPR : Compressor power ratio (ratio of electric demand at the operating condition to the nominal capacity of the compressor)

PLR : Fraction of the full load at the evaporator

The electric demand at part load is:

$$\dot{W}_{PL} = CPR \cdot \dot{W} \tag{2-29}$$

Using the compressor electric motor efficiency η_m, the compressor electric input $ELEC$ is calculated as:

$$ELEC = \frac{\dot{W}_{PL}}{\eta_m} \tag{2-30}$$

The compressor was modeled based on the evaporating and condensing temperatures and pressures. The temperatures are determined from the condenser and evaporator models, which are explained later, and the corresponding pressures are calculated as follows:

$$P_{sat} = EXP[E_1 + E_2.T_{sat} + \frac{E_3}{T_{sat}} + \ln(T_{sat})] \tag{2-31}$$

where T_{sat} is the saturation temperature in K, and P_{sat} is in Pa.

For the condenser, the model uses the heat rejected factor HRF, which is the ratio of the heat rejected by the condenser $\dot{Q}_{cd}$ to rated condenser capacity $\dot{Q}_{base}$. The rated condenser capacity is the sum of compressor power and rated evaporator load. They introduced a correlation that relates the condenser temperature with HRF.

$$\left[\frac{T_{cd}}{T_a}\right] = F_1 + F_2\left[\frac{T_{env}}{T_a}\right] + F_3\ HRF \tag{2-32}$$

T_{env} : Condenser air (environmental) temperature (K)

Integrating the components models mentioned, the simulation was developed using iteration method with successive substitution technique. First the condensing and

evaporating temperatures are estimated. Knowing condensing and evaporating temperatures, the cooling capacity and the compressor power input are calculated. After the compressor and storage tank are analyzed, the condensing and evaporating temperatures are reevaluated and the whole calculation is repeated until it converges. Almost the same approach has been used for indirect ice-storage. In indirect ice-storage the authors used the heat transfer balance in the evaporator and condenser as a heat exchanger and instead of using many unknown variables like outside and inside radius of the tubes in the heat exchangers, they developed some binomial functions to relate the heat transmission in terms of logarithmic mean temperature difference. The correlations are calculated from manufacturer's data. The advantage of this model is its ability to handle various system configurations. The user only needs to use a simple curve-fitting program with manufacturer's data to adjust the model for other cases.

A simple thermodynamic model for chillers was developed by Gorden and Ng [22], which uses a linear relationship between 1/COP and $1/\dot{Q}_{ev}$, in terms of the condenser and evaporator internal losses, the chilled water leaving temperature, and condenser water entering temperature:

$$\frac{1}{COP} = -1 + \left(\frac{T_{w_{cd1}}}{T_{w_{ev2}}}\right) + \frac{1}{\dot{Q}_{ev}}\left(\frac{\dot{q}_{ev} T_{w_{cd1}}}{T_{w_{ev2}}} - \dot{q}_{cd}\right) + f_{HX} \qquad (2\text{-}33)$$

where:

$T_{w_{cd1}}$: entering condenser water temperature (K)

$T_{w_{ev2}}$: leaving evaporator water temperature (K)

$\dot{Q}_{ev}$: evaporator load (W)

$\dot{q}_{ev}$: rate of internal losses in evaporator (W)

$\dot{q}_{cd}$: rate of internal losses in condenser (W)

f_{HX} : dimensionless term (usually negligible)

Equation (2-33) was also presented in a simple form as follows:

$$\frac{1}{COP} = C_1\left(\frac{1}{\dot{Q}_{ev}}\right) + C_0 \qquad (2\text{-}34)$$

where C_1 represents the chiller internal losses. C_1 and C_0 are linear regression coefficients which are determined from the manufacturer's data, or through measurements of the chilled water leaving and entering temperatures and flow rate. In this model the impact of the variation of condenser and evaporator water temperature is assumed to be small in comparison with the effects of load variation. The model is applicable to chillers with constant-temperature control of the evaporator and condenser temperatures, and to chillers in which the evaporator and condenser temperatures are a direct function of chiller load. The temperature dependent model has also been introduced that includes the effect of chilled water supply and condenser water return

temperatures. The first simple model is a special limiting case of the temperature-dependent model, which develops an expression for $\frac{1}{COP}$ as a function of cooling capacity $\dot{Q}_{ev}$, leaving chilled water temperature $T_{w_{ev2}}$ and condenser entering water temperatures $T_{w_{cd1}}$ (equation (2-35)). These parameters are usually available in manufacturers' technical data.

$$\frac{1}{COP} = -1 + \left(\frac{T_{w_{cd1}}}{T_{w_{ev2}}}\right) + \frac{-A_0 + A_1(T_{w_{cd1}}) - A_2(T_{w_{cd1}}/T_{w_{ev2}})}{\dot{Q}_{ev}} \qquad (2\text{-}35)$$

The values of A_0, A_1 and A_2 are determined from measuring the leaving and entering chilled water temperatures, the chilled water flow rate, and the condenser entering temperature for different working points. Plotting $\left(\frac{1}{COP} + 1 - \left(\frac{T_{w_{cd1}}}{T_{w_{ev2}}}\right)\right)\dot{Q}_{ev}$ versus the temperature ratio $\frac{T_{w_{cd1}}}{T_{w_{ev2}}}$ for different condenser leaving water temperature results a series of parallel lines the slope of which determines the value of A_2. Then using this value of A_2 and plotting $\left(\frac{1}{COP} + 1 - \left(\frac{T_{w_{cd1}}}{T_{w_{ev2}}}\right)\right)\dot{Q}_{ev} + A_2\left(\frac{T_{w_{cd1}}}{T_{w_{ev2}}}\right)$ versus the condenser leaving water temperature results a single straight line the slope of which represents the value of A_1. The intercept of this line determines the value of A_0. Once the coefficients A_0, A_1 and A_2 are known, the performance curve of the chiller (COP versus $\dot{Q}_{ev}$) is defined. This model is applicable to all vapor–compression chillers.

Later, these models were used by Phelan et al. [23] for in-situ performance testing of chillers for energy analysis together with uncertainty analysis. The chiller part load ratio has been found as the most significant factor affecting chiller efficiency, with the evaporator and condenser water temperatures having a secondary effect. The simple chiller model appeared to be practical and accurate for many applications, specially when evaporator and condenser water temperatures are relatively constant. Meanwhile the ease of calculations and implementation of the simple model makes it attractive. The temperature-dependent chiller model also appears accurate to use for calculation of annual energy consumption specially when there are significant changes in evaporator and condenser temperatures during operation.

Figueroa et al. [24] used the Gordon and Ng model [22] for water-cooled centrifugal chillers. They determined the coefficient A_2 from one straight line instead of a series of parallel lines, and they described the discrepancy by the limited range of condenser supply temperature in water cooled chillers.

Jähing et al. [25] presented a semi-empirical method for representing domestic refrigerator/freezer compressor. Usually the performance of the small hermetic compressor of refrigerators or freezers are modeled with a polynomial correlation with ten coefficients based on ARI standard 540-91 [26]. Generally these coefficients fit the testing data, however, do not necessarily provide reliable interpolations and extrapolations for other conditions, which are outside the testing range. The objective of

the study by Jähing et al. was to find a model that can be applied for a wide range of operating conditions. The model was constructed based on volumetric efficiency and polytropic compression process. There are five parameters that are determined through the curve fitting of experimental data. The volumetric efficiency η_v of reciprocating compressor is calculated as:

$$\eta_v = 1 - C\left[\left(\frac{P_{discharge}}{P_{suction}}\right)^{\frac{1}{n}} - 1\right] \tag{2-36}$$

where:

C :effective clearance volume ratio

$P_{discharge}$: absolute discharge pressure (Pa)

$P_{suction}$: absolute suction pressure (Pa)

n : polytropic exponent

The values of n and C are determined by non-linear regression between the refrigerant mass flow rate, and the suction and discharge pressures. It was found that the values of C and n determined in this way are not independent of each other. The mass flow rate of the refrigerant $\dot{M}_R$ is calculated by equation (2-37):

$$\dot{M}_R = \left\{1 - C\left[\left(\frac{p_{cd}}{p_{ev}(1-\delta p)}\right)^{\frac{1}{k}} - 1\right]\right\} \cdot \frac{V \cdot RPM}{\upsilon_{suction} \cdot 60} \tag{2-37}$$

where:

k :specific heat ratio

δp :pressure drop on the low-pressure side of the compressor (Pa)

V :volume of the cylinders (m^3)

$\upsilon_{suction}$:refrigerant suction specific volume (m^3/kg)

RPM :compressor revolution per minute (rpm)

The corresponding pressures at the evaporator and condenser are determined using the evaporating and condensing temperatures, and the thermodynamic properties of the refrigerant. Compressor work is calculated as:

$$\dot{W} \cdot \eta_{comb} = \dot{m} \cdot \frac{k}{k-1} \cdot P_{suction} \cdot \upsilon_{suction} \left[\left(\frac{P_{discharge}}{P_{suction}} \right)^{\frac{k-1}{k}} - 1 \right] \qquad (2\text{-}38)$$

where:

$P_{suction} = (1 - \delta p) p_{ev}$

$P_{discharge} = p_{cd}$

η_{comb} : combined efficiency of electric motor and compressor.

The only unknown in equation (2-38) is the combined efficiency, which is not constant. The variation of the combined efficiency is derived as an exponential function based on curve-fitting the experimental data. Equation (2-39) was found to be the best curve that fits the data.

$$\eta_{comb} = d + e \cdot \exp(f \cdot p_{ev}) \tag{2-39}$$

where d, e and f are regression parameters.

The model is called semi-empirical because it uses the experimental data to determine the unknown variables through curve-fitting method while using thermodynamic base equations for the reciprocating compressor. Interpolating and extrapolating in this model can be done up to ± 10°C about the evaporating and condensing temperatures. Corresponding relative errors for mass flow rate and compressor power is 5%.

McIntosh et al. [27] developed two models for vapor compression chillers, using a simple refrigeration cycle as the framework for compressor and heat exchangers. The objective of their study was to develop a model that can be used in the fault detection and diagnosis of vapor compression chillers. The first model is based on the simple vapor-compression cycle considering isentropic efficiency η_{is} (Figure 2-4). The following relation between the actual and ideal process in the compressor is used:

$$h_2 - h_1 = \frac{h_{2s} - h_1}{\eta_{is}} \tag{2-40}$$

and the compressor COP_{comp} is determined as:

$$COP_{comp} = \frac{h_1 - h_4}{h_2 - h_1} \tag{2-41}$$

h_1, h_2, h_{2s}, h_3, h_4 are the enthalpies of corresponding points on the cycle shown in Figure 2-4.

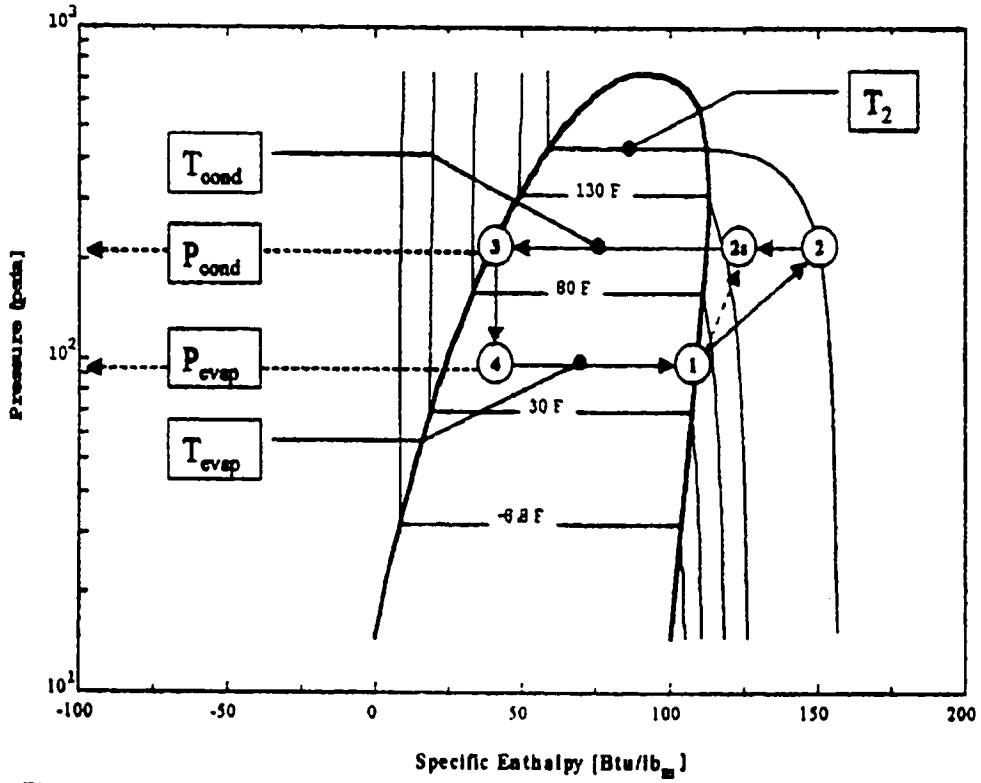

Figure 2-4 Pressure-Enthalpy diagram for R-22 showing the thermodynamics states[27]

The evaporator and condenser model were constructed based on the fundamental equations of heat exchanger:

$$\dot{Q}_{cd} = \dot{M}_{w_{cd}} C_{p_w} (T_{w_{cd2}} - T_{w_{cd1}}) \tag{2-42}$$

$$\dot{Q}_{ev} = \dot{M}_{w_{ev}} C_{p_w} (T_{w_{ev1}} - T_{w_{ev2}}) \tag{2-43}$$

$$\dot{Q}_{cd} = \dot{M}_R (h_2 - h_3) \tag{2-44}$$

$$\dot{Q}_{cd} = UA_{cd} \cdot LMTD_{cd} \tag{2-45}$$

$$LMTD_{cd} = \frac{(T_{cd} - T_{w_{cd1}}) - (T_{cd} - T_{w_{cd2}})}{\ln\left(\frac{T_{cd} - T_{w_{cd1}}}{T_{cd} - T_{w_{cd2}}}\right)} \tag{2-46}$$

$$\dot{Q}_{ev} = UA_{ev} \cdot LMTD_{ev} \tag{2-47}$$

$$LMTD_{ev} = \frac{(T_{w_{ev1}} - T_{ev}) - (T_{w_{ev2}} - T_{ev})}{\ln\left(\frac{T_{w_{ev1}} - T_{ev}}{T_{w_{ev2}} - T_{ev}}\right)} \tag{2-48}$$

where:

$\dot{Q}_{cd}$: condenser heat rejection (W)

$\dot{Q}_{ev}$: evaporator heat gain (W)

$T_{w_{cd1}}$: condenser entering water temperature (K)

$T_{w_{cd2}}$: condenser leaving water temperature (K)

T_{cd} : condenser saturation temperature (K)

$T_{w_{ev1}}$: chilled water entering temperature (K)

$T_{w_{ev2}}$: chilled water leaving temperature (K)

T_{ev} : evaporator saturation temperature (K)

$\dot{M}_{w_{cd}}$: condenser water mass flow rate (kg/s)

$\dot{M}_{w_e}$:evaporator water mass flow rate (kg/s)

$\dot{M}_R$: refrigerant mass flow rate (kg/s)

C_{p_w} :specific heat of water (J/kgK)

UA_{cd} : condenser overall heat transfer coefficient (W/K)

UA_{ev} : evaporator overall heat transfer coefficient (W/K)

The set of equations is solved using the measurements of the temperatures and flow rates. The overall heat transfer coefficient is a function of fluid velocity and would change due to fouling effects. The compressor power $\dot{W}$, which links the condenser and evaporator loads by equation (2-49), can also be measured.

$$\dot{Q}_{cd} = \dot{Q}_{ev} + \dot{W} \tag{2-49}$$

The overall coefficient of performance can be calculated as:

$$COP_{overall} = \frac{\dot{Q}_{ev}}{\dot{W}} = \frac{\dot{Q}_{ev}}{\dot{Q}_{cd} - \dot{Q}_{ev}} \tag{2-50}$$

The ratio between COP_{comp} (equation 2-41) and $COP_{overall}$ gives the combined motor and transmission efficiency:

$$\eta_{comb} = \frac{COP_{comp}}{COP_{overall}} \tag{2-51}$$

Using this model, the characteristic parameters such as UA_{cd} and UA_{ev} can be continuously calculated during the operation, and the faults can be diagnosed. For instance, change in the values of UA_{cd} and UA_{ev} can be due to the fouling and the reduction of flow rates condenser and evaporator.

The second model that the authors introduced was a detailed thermodynamic model using empirical correlations for modeling the physical mechanisms in different components of a centrifugal chiller. For example the overall heat transfer coefficient of the condenser is calculated by:

$$UA_{cd} = \frac{A_{c,i}}{\frac{1}{h_{c,i}} + \frac{1}{r_c h_{c,o}} + R_c} \tag{2-52}$$

where:

$A_{c,i}$:total inside surface area of the condenser tubes (m^2)

$h_{c,i}$:the heat transfer coefficient for water flow inside condenser tubes (W/m^2K)

$h_{c,o}$:the heat transfer coefficient for refrigerant (W/m^2K)

r_c : the ratio of effective outside condenser tube area (including fins) to inside area

R_c :resistance to heat transfer associated with the tube material (including fouling factor) (W/m^2K)

For the water side heat transfer, the McAdams correlation [28] is used:

$$h_{c,i} = 0.023\left(\frac{k_w}{D_{cd}}\right)\mathrm{Re}_{cd}^{0.8}\cdot \mathrm{Pr}_w^{\,0.4} \tag{2-53}$$

where:

k_w :thermal conductivity of water (W/mK)

D_{cd} :inside condenser tube diameter (m)

Re_{cd} :Reynolds number associated with water flow in an individual condenser tube

Pr_w :Prandtl number of water

The average heat transfer coefficient for vapor condensation on horizontal tubes (refrigerant side), the classical Nusselt correlation for laminar film condensation is used:

$$h_{c,o} = 0.725\left[\frac{k_l^3(\rho_f - \rho_v)^2 g h_{fg}}{N_t D_{cd}\mu_f (T_{cd} - T_{c,s})}\right]^{0.25} \tag{2-54}$$

where:

k_l : conductivity of the liquid refrigerant (W/mK)

h_{fg} : heat of vaporization of the refrigerant (J/kg)

g : gravitational acceleration (m/s^2)

ρ_f :density of saturated liquid refrigerant (kg/m^3)

ρ_v : density of saturated vapor refrigerant (kg/m^3)

μ_f : viscosity of saturated liquid refrigerant (Pa.s)

$T_{c,s}$: average outside surface temperature of tube (K)

N_t : number of horizontal tubes

Using equations (2-53) and (2-54) in equation (2-52), combined with the measurements, the fouling resistance R_c is found. The advantage of this model is that it uses less input variables than the first model (reduced model) and is capable to model the refrigeration cycle using only temperatures and flow rates on water side which are more readily available in manufacturer's technical catalogues.

Stoecker [29] developed correlation-based models for the cooling capacity $\dot{Q}_{ev}$ and for the required compressor electric input $\dot{W}$ (equations (2-55) and (2-56)). The corresponding coefficients "c" and "d" are determined for reciprocating compressors using manufacturer's technical catalogues and least square method.

$$\dot{Q}_{ev} = c_1 + c_2 T_{ev} + c_3 T_{ev}^2 + c_4 T_{cd} + c_5 T_{cd}^3 + c_6 T_{ev} T_{cd} + c_7 T_{ev}^2 T_{cd} + c_8 T_{ev} T_{cd}^2 + c_9 T_{ev}^2 T_{cd}^2 \quad (2\text{-}55)$$

$$\dot{W} = d_1 + d_2 T_{ev} + d_3 T_{ev}^2 + d_4 T_{cd} + d_5 T_{cd}^3 + d_6 T_{ev} T_{cd} + d_7 T_{ev}^2 T_{cd} + d_8 T_{ev} T_{cd}^2 + d_9 T_{ev}^2 T_{cd}^2 \quad (2\text{-}56)$$

where:

T_{ev} : evaporating temperature, °C

The energy crisis and mandatory energy conservation standards together with the advancement of computer technology led to rapid development of the energy calculation procedures for the prediction of the performance and energy requirements of buildings. It is important to know that almost all of the fundamental developments in energy calculation procedures resulted from governmental support [30]. Consequently two major public domain programs BLAST [7] and DOE-2 [8] have been introduced. Beside these, there are some other programs widely used and supported by companies, organizations or associations such as TRACE developed by the TRANE company; HAP developed by CARRIER; and HCC (loads) and ESP (energy) developed by Automated Procedures for Energy Consultants (APEC); these programs use simpler calculations for energy consumption of chillers.

2.3 Conclusion of the literature survey

Several models have been developed for different type of chillers. The precise thermodynamic-base models require detailed information from manufacturers' data and are usually system specific. The correlation models rely on manufacturers' data and they are valid within the range of working points that they were developed for and extrapolation may cause significant errors.

Base on the literature review, only one thermodynamic-base model (ASHRAE Toolkit-I) and no correlation-base model for screw compressor chiller was found. Although the ASHRAE Toolkit-I is a thermodynamic-base model but at part load regime it uses some imperial correlation for determining the compressor input power. Therefore

there is no complete thermodynamic-base model for screw compressor chiller at part load regime.

2.4 Objective of the study

The literature review has revealed that the most used energy analysis programs do not have the capability to estimate the energy performance of screw chillers.

The main objective of this study is to evaluate the energy performance of screw compressor chillers through deriving correlations, based on thermodynamic principles and regression analysis.

Using the energy performance of screw chiller in the DOE-2 program to simulate the energy consumption of an office building in Montreal in comparison with that of centrifugal chiller is another objective of this study.

Chapter 3

Mathematical model for standard vapor-compression chiller

In this chapter a mathematical model is developed to evaluate the performance of vapor-compression chillers using thermodynamic relationships of the ideal standard cycle, modified based on real performance of chillers, using the manufacturers' data.

In this chapter the study is conducted through the following steps; first the mathematical model based on thermodynamic ideal cycle is developed to evaluate the performance of the standard vapor-compression chiller. The performance of the real vapor-compression chiller is compared with the standard cycle afterwards, and the isentropic efficiency and its variation with the capacity, and the condenser and evaporator temperature is discussed. Later the correlations of the isentropic efficiency of chillers as a function of the capacity, and the condensing and evaporating temperatures for the water-cooled and air-cooled condenser of the corresponding manufacturer are developed.

3.1 Vapor-compression cycle

The vapor compression cycle, already discussed in chapter one, has four main components; the evaporator, the condenser, the expansion device, and the compressor. They are directly connected to each other in the order that is shown in Figure 3-1.

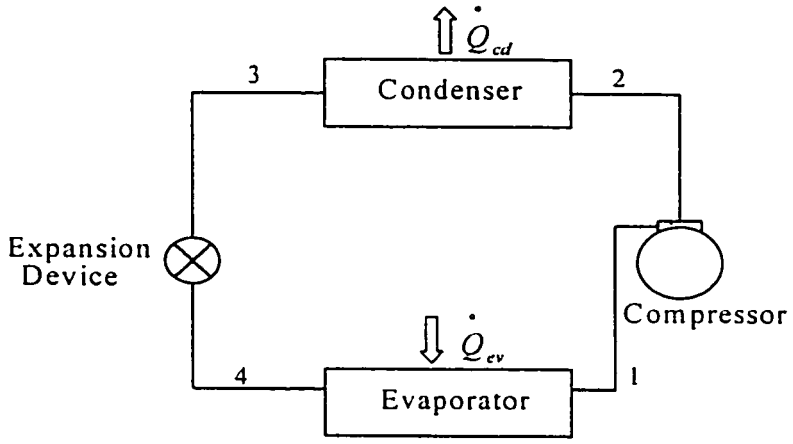

Figure 3-1 Vapor-compression refrigeration cycle

This cycle is essentially the classical Carnot cycle with some modifications dictated by practical considerations. In the following section first the basic Carnot cycle is introduced then the necessary modifications are applied to obtain the common vapor-compression cycle.

3.2 Carnot cycle

Basically the Carnot cycle is the one in which a heat engine receives heat from a high temperature reservoir, converts a portion of this heat to work and rejects the rest of the heat to the low temperature reservoir. If this cycle is reversed, the heat engine becomes a refrigerator and the cycle is called the Carnot refrigeration cycle. In this cycle heat is transferred from a low-level temperature reservoir to a high-level temperature reservoir [29]. This requires external work, which is done by the compressor. The T-S (temperature-entropy) diagram of the Carnot refrigeration cycle is shown in Figure 3-2.

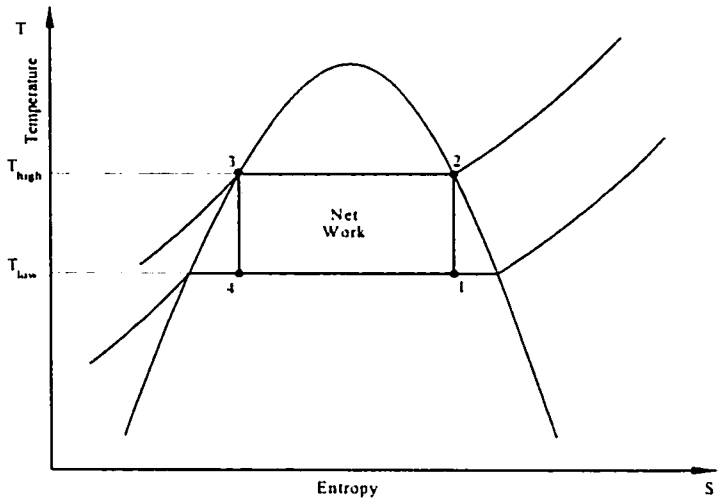

Figure 3-2 Carnot refrigeration cycle on temperature-entropy diagram

There are four processes that compose this cycle. These processes are:

1-2 Adiabatic reversible compression in which pressure and temperature of the working fluid increase while the entropy remains constant.

2-3 Heat is rejected from the working fluid at constant temperature (isothermal process).

3-4 Working fluid is expanded adiabatically from high pressure to low pressure (throttling process in which enthalpy remains constant).

4-1 Heat is gained by the working fluid at constant temperature (isothermal process).

The processes in the Carnot refrigeration cycle are reversible; hence it has the highest efficiency of any cycle operating between the same T_{low} and T_{high}. The importance of this ideal cycle is that the efficiency of real cycles can be compared with the efficiency of the Carnot cycle.

The heat gain extracted by the evaporator from low temperature reservoir, in the process 4-1 is the useful part of this cycle.

3.3 Vapor-compression refrigeration cycle parameters

Coefficient of performance

The performance of a refrigeration cycle is expressed by the coefficient of performance (COP), defined as the ratio of useful heat extracted by the evaporator $\dot{Q}_{ev}$, called cooling load, to the net work done by the compressor $\dot{W}_{net}$ in consistent units.

$$\text{COP} = \frac{\dot{Q}_{ev}}{\dot{W}_{net}} \tag{3-1}$$

If $\dot{Q}_{ev}$ is in Btu/hr and $\dot{W}_{net}$ is in watts, their ratio is called Energy Efficiency Ratio **EER**. There are some other terms used to evaluate the performance of vapor-compression equipment such as:

Seasonal Energy Efficiency Ratio **SEER**: The total cooling output of an air conditioner during its normal annual usage period for cooling in Btu, divided by the total electric input during the same period in watts-hour [3].

Integrated Part Load Value **IPLV**: A single number figure of merit based on part load EER or COP expressing part load efficiency for air conditioning and pump equipment on the bases of weighted operation at various load capacities for the equipment [3].

KiloWatt per Ton of Refrigeration **kW/TR**: The ratio of total electrical demand of a refrigeration machine in kW to the total cooling load delivered, in tons of refrigeration.

Higher COP indicates that lower amount of work is required for a given amount of cooling load. The isothermal heat transfer in a reversible process is determined as:

$$Q_{rev} = \int T\, ds \tag{3-2}$$

which graphically is represented by is the area under the isothermal reversible process; heat extraction in the evaporator and heat rejection in the condenser on temperature-entropy diagram are shown in Figure 3-3. Thus the useful heat gain in the evaporator (process 4-1) is the area 4-1-a-b-4, and the heat rejected by the condenser is the area a-2-3-b-a. Therefore the net work done on the compressor is the difference between the two areas, that is the area 1-2-3-4-1. Based on the above, the coefficient of performance can be rewritten as:

$$\text{COP} = \frac{T_1(s_1 - s_4)}{(T_2 - T_1)(s_1 - s_4)} = \frac{T_1}{T_2 - T_1} \tag{3-3}$$

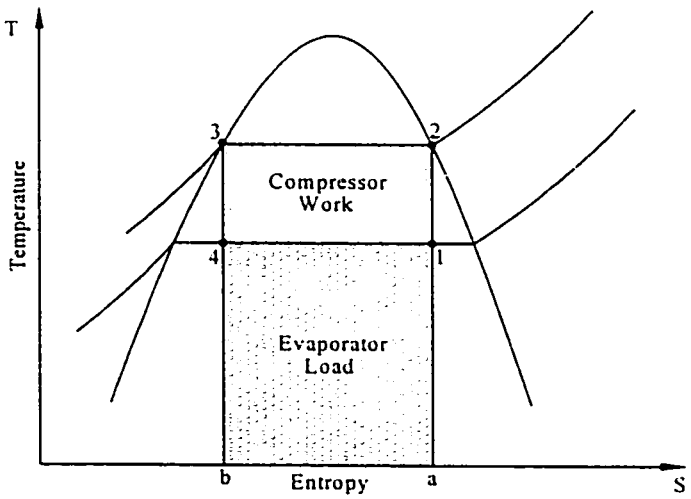

Figure 3-3 Evaporator refrigeration and net work of the Carnot cycle shown by the areas on the temperature-entropy diagram.

The coefficient of performance of the Carnot refrigeration cycle is therefore only a function of the condensing T_2 and the evaporating T_1 temperature. Looking at this expression, for a fixed T_2, the higher is the value of T_1, the higher is the resulting COP. The lower is the value of T_2, for the fixed T_1, the higher is the COP. It should be noted that the effect of increasing the evaporating temperature on COP would be more significant than the effect of decreasing the condensing temperature. Using the formulations derived from the first law of thermodynamics, the coefficient of performance can be presented in terms of enthalpies before and after the two components: compressor and evaporator. Figure 3-4 shows the pressure–enthalpy diagram of the same refrigeration cycle.

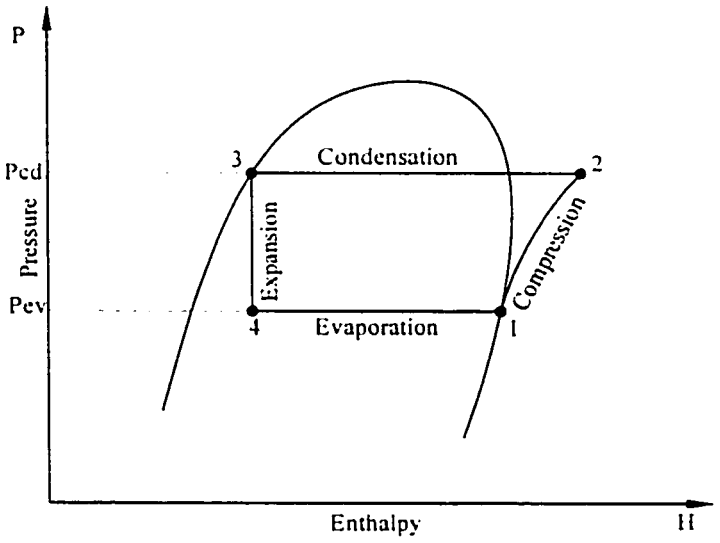

Figure 3-4 Standard vapor-compression cycle on the pressure-enthalpy diagram

Compressor work

The work done by the compressor w_{comp} (process 1-2) is equal to the change in enthalpy in this process. The energy equation between 1 and 2 in the Steady State Steady Flow process can be written as:

$$h_1 + q = h_2 + w \tag{3-4}$$

where: q is the net heat transfer in the process (J/kg)

w is the work done in the process (J/kg)

In analyzing the ideal cycle, generally it is reasonable to assume that the changes of kinetic and potential energies are negligible. Since it is assumed that the working fluid is compressed adiabatically, the value of q is equal to zero, therefore:

$$w_{comp} = h_1 - h_2 \tag{3-5}$$

The negative sign of the numerical value of w indicates that the work is done on the cycle.

Evaporator and condenser heat transfer

The energy equation for the steady state steady flow processes in the condenser and evaporator (2-3 and 4-1 respectively) can be written as:

$$q_{ev} = h_1 - h_4 \tag{3-6}$$

$$q_{cd} = h_3 - h_2 \tag{3-7}$$

(changes in kinetic and potential energy can be ignored)

The negative sign of the numerical value of q_{cd} indicates that the heat is transferred from the condenser; and q_{ev} is positive since the heat is transferred to the evaporator. Thus the coefficient of performance can be written in terms of enthalpies:

$$\text{COP} = \frac{h_1 - h_4}{h_2 - h_1} \tag{3-8}$$

3.4 Standard vapor-compression cycle

While the Carnot cycle mentioned so far is the ideal refrigeration cycle, some practical changes are required for a better representation of actual systems, which lead to the standard vapor-compression refrigeration cycle. The standard vapor-compression refrigeration cycle is shown in Figure 3-5.

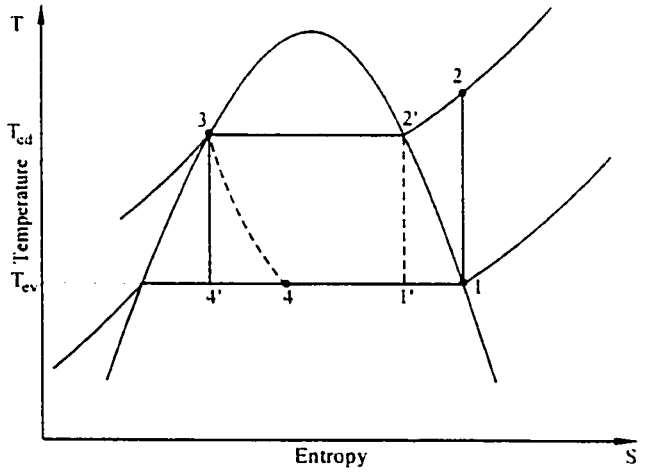

Figure 3-5 Standard vapor-compression refrigeration cycle

In the Carnot cycle the compression starts at 1', at which the working fluid consists of both vapor and fluid. If the compressor is of reciprocating type, the liquid is trapped in the head of the cylinder in the compression process; and this could possibly damage the valves and the piston head. Also the liquid droplets may wash out the lubricants on the cylinder wall that could damage the cylinder and the piston. Therefore the compression process 1-2 is preferable to the process 1'-2'; the compression process starts at 1, using only saturated vapor as the working fluid. In this case the refrigerant leaves the compressor superheated, having a temperature higher than the condensing temperature in the Carnot cycle.

Also it is not easy to have a reversible expansion such as the process 3-4'. It should be taken into consideration that the work resulting from the expansion process is too small in comparison with the work required for the compressor, and it is not economical to recover this energy. Meanwhile, since the fluid is in two phases (liquid and vapor), practical difficulties appear in a machine to be driven by this working fluid. Therefore the expansion process in a standard vapor-compression cycle is considered to be irreversible. Again the changes in the kinetic and potential energy are neglected and the process is considered to be adiabatic. Hence, based on the first law of thermodynamics since $q=0$ and $w=0$ then there is no change in enthalpy, therefore this process is considered to be a constant enthalpy throttling process.

3.5 Methodology

The thermodynamic model, which is the subject of this chapter, is based on the standard vapor-compression cycle shown in Figure 3-5. The four main points in this diagram for the ideal cycle are considered to be 1,2,3,4'. Four main processes in this cycle are 1-2 (compression), 2-3 (condensation), 3-4' (expansion), and 4'-1 (evaporation). Since we assume that this cycle is ideal, the evaporating and condensing temperatures are considered to be constant in the condenser and evaporator.

Once we know the evaporating and condensing temperatures, the enthalpies of the four main points in the cycle can be determined from the thermodynamic tables or charts. The enthalpy of point 1 is the enthalpy of saturated vapor of the refrigerant at evaporating temperature. The enthalpy of point 3 is the enthalpy of saturated liquid of the refrigerant at condensing temperature, which is equal to the enthalpy of point 4' due to throttling process in the expansion device. The entropy of point 2 is the entropy of superheated vapor at condensing pressure, and having the same entropy as point 1.

After the enthalpies of the main points on the cycle were determined, the mass flow rate $\dot{M}_R$ (kg/s) of the refrigerant is calculated for a given cooling load $\dot{Q}_{ev}$ (W) as follows:

$$\dot{M}_R = \frac{\dot{Q}_{ev}}{h_1 - h_4} \tag{3-9}$$

Consequently the condenser heat rejection $\dot{Q}_{cd}$ (W) and compressor power $\dot{W}_{ideal}$ (W) can be calculated as follows:

$$\dot{W}_{ideal} = \dot{M}_R \ (h_2 - h_1) \tag{3-10}$$

$$\dot{Q}_{cd} = \dot{M}_R \ (h_3 - h_2) \tag{3-11}$$

And finally the COP_{ideal} of the system is determined using equation (3-8).

For comparison purposes, the COP of the Carnot refrigeration cycle, which is the maximum COP that can be obtained for a cycle operating under the same condensing and evaporating temperature, is also determined. The COP of the Carnot cycle as discussed earlier is a function of only the condenser and evaporator temperatures, and it is calculated by equation (3-3). To facilitate the calculations based on the basic thermodynamic model, a computer program was written in C++ (Appendix A).

In the next step, the manufacturer performance data is used, along with the ideal standard vapor-compression cycle to calculate the compressor isentropic efficiency. The performance data used here are taken from two screw and one centrifugal chillers manufactured by CARRIER company. The screw chillers use R-134a and centrifugal chiller uses R11 as the refrigerant. The performance data of these three models are presented in Table B-1 for water-cooled screw chiller model 30HXC, Table B-2 for air-

cooled screw chiller model 3HXA and Table B-3 for centrifugal chiller model 19DK in Appendix B. The isentropic efficiency η_{is}, which is the ratio of the ideal work to the actual required compressor work (equation 3-12), can be determined from the manufacturer's catalogue in terms of:

-condensing and evaporating temperature.

-chiller capacity $\dot{Q}_{ev}$ and compressor power $\dot{W}_{actual}$

$$\eta_{is} = \frac{\dot{W}_{ideal}}{\dot{W}_{actual}} \tag{3-12}$$

where $\dot{W}_{ideal}$ is calculated from equation (3-10)

Figure 3-6 shows the information flow diagram of this thermodynamic model. The flow chart of the program is shown in Figure 3-7. On the following pages some sample results are shown.

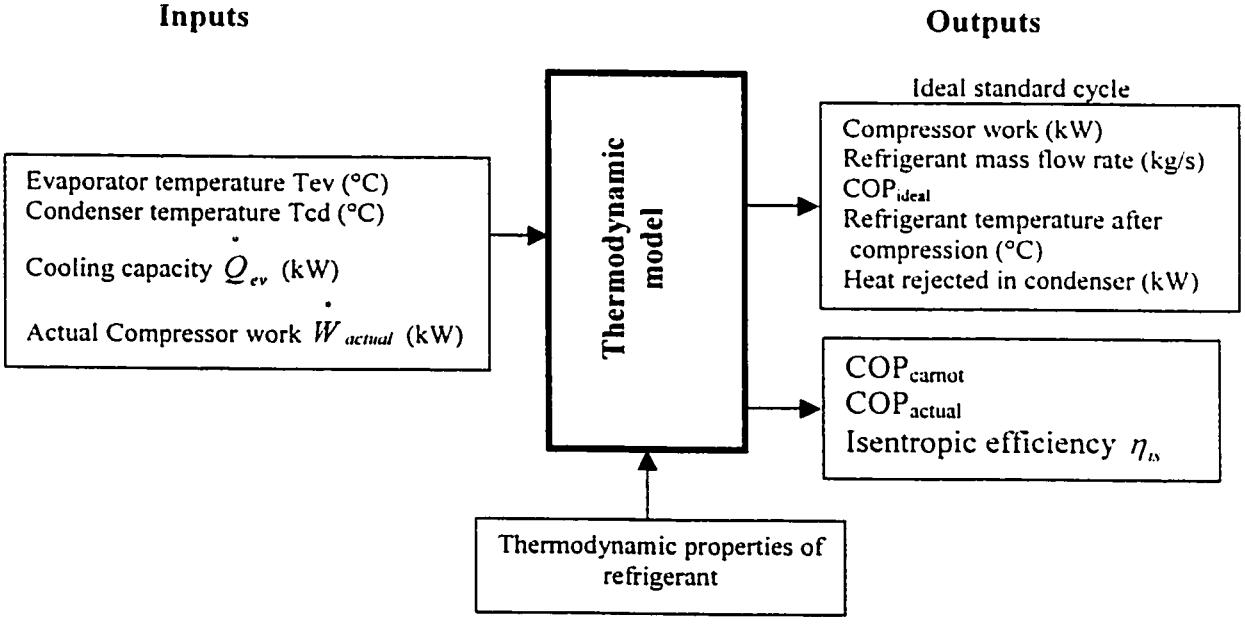

Figure 3-6 Information flow diagram of thermodynamic model

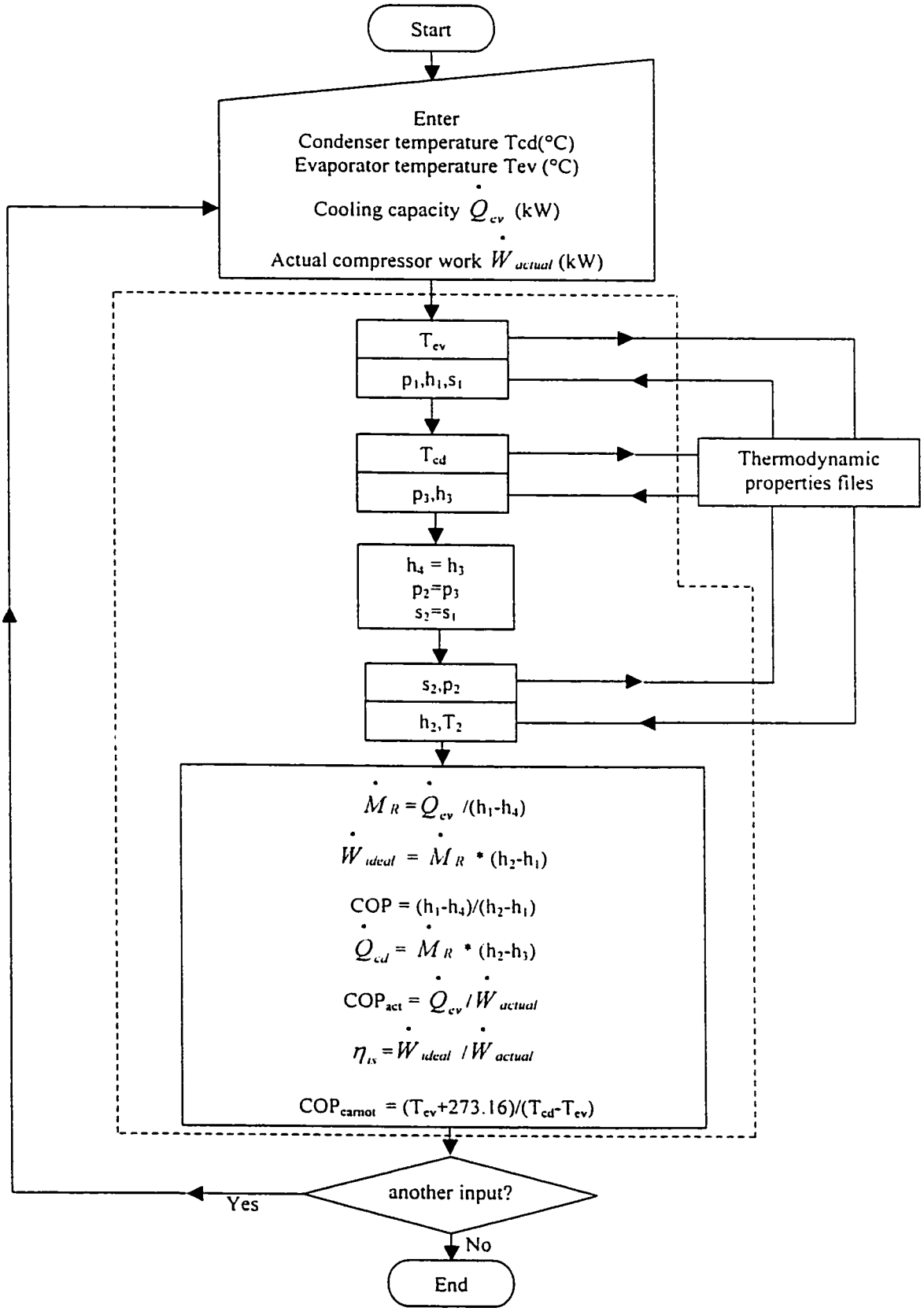

Figure 3-7 Computer model flow chart

Sample input (30HXC/R-134a)

T_{ev}= 4°C

T_{cd}= 30°C

$\dot{Q}_{ev}$ =253.3 kW

$\dot{W}_{actual}$ = 48.2 kW

Sample output

$\dot{W}_{ideal}$ =27. 6 kW

$\dot{Q}_{cd}$ =280.0 kW

$\dot{M}_R$ =1.52 kg/s

COP_{ideal}=9.2

COP_{actual}=5.3

COP_{carnot}=10.7

η_{ts}=57.2%

After the isentropic efficiency at different condition was determined based on the manufacturer's data and ideal standard cycle, the variation of compressor isentropic efficiency versus condenser temperature, evaporator temperature and cooling load are illustrated. On the next step the correlations, which best fit these data are developed.

3.6 Results

As an example of the results the performance of the water-cooled condenser 30HXC screw-compressor chiller at condenser temperature of 30°C and evaporator temperature of 6°C is presented in Table 3-1. The complete set of results for the other evaporator and condenser temperatures is presented in Tables C-1 to C-3 in Appendix C.

Table 3-1 Performance of water-cooled 30HXC screw compressor chiller/R-134a (CARRIER company) (The manufacturer's performance data is highlighted)

T_{cd}(°C)	T_{ev} (°C)	$\dot{Q}_{ev}$ (kW)	$\dot{W}_{actual}$ (kW)	$\dot{W}_{ideal}$ (kW)	η_{is}(%)	COP_{carnot}	COP_{ideal}	COP_{actual}
30	6	274.8	49.3	27.2	55.2	11.6	10.1	5.6
30	6	303.0	55.3	30.0	54.3	11.6	10.1	5.5
30	6	342.1	61.5	33.9	55.1	11.6	10.1	5.6
30	6	380.0	68.6	37.7	54.9	11.6	10.1	5.5
30	6	413.0	73.0	40.9	56.1	11.6	10.1	5.7
30	6	447.2	79.1	44.3	56.0	11.6	10.1	5.7
30	6	495.8	89.2	49.1	55.1	11.6	10.1	5.6
30	6	530.4	96.2	52.6	54.6	11.6	10.1	5.5
30	6	551.9	98.9	54.7	55.3	11.6	10.1	5.6
30	6	584.0	105.3	57.9	55.0	11.6	10.1	5.5
30	6	624.0	113.3	61.8	54.6	11.6	10.1	5.5
30	6	745.8	130.4	73.9	56.7	11.6	10.1	5.7
30	6	874.5	153.0	86.7	56.6	11.6	10.1	5.7
30	6	904.8	160.3	89.7	55.9	11.6	10.1	5.6
30	6	940.9	168.5	93.3	55.3	11.6	10.1	5.6

The evaporator load and the corresponding compressor work are taken from catalogue data, which are partially shown in Table 3-2. The same procedure was carried out for air-cooled condenser screw chiller model 30HXA and package hermetic centrifugal liquid chiller model 19DK.

Table 3-2 Performance data of chiller 30HXC water-cooled at 6°C evaporator temperature

LCWT (C)	UNIT SIZE 30HXC	CONDENSER ENTERING WATER TEMPERATURE (C)											
		25				30				35			
		Cap.	Input kW	Cooler Flow Rate (L/s)	Cond Flow Rate (L/s)	Cap.	Input kW	Cooler Flow Rate (L/s)	Cond Flow Rate (L/s)	Cap.	Input kW	Cooler Flow Rate (L/s)	Cond Flow Rate (L/s)
6.0	076	274.8	49.3	11.8	13.8	254.6	54.2	10.9	13.2	235.6	59.7	10.1	12.6
	086	303.0	55.3	13.0	15.3	281.0	60.9	12.1	14.6	261.1	67.2	11.2	14.0
	096	342.1	61.5	14.7	17.2	317.5	67.7	13.6	16.4	295.0	74.8	12.7	15.8
	106	380.0	68.6	16.3	19.1	352.4	76.2	15.1	18.3	326.9	86.5	14.0	17.6
	116	413.0	73.0	17.7	20.7	383.9	81.0	16.5	19.8	355.4	90.5	15.3	19.0
	126	447.2	79.1	19.2	22.4	415.9	88.0	17.9	21.5	385.7	98.2	16.6	20.6
	136	495.8	89.2	21.3	24.9	461.3	98.0	19.8	23.8	430.3	108.1	18.5	22.9
	146	530.4	96.2	22.8	26.7	493.0	106.3	21.2	25.5	460.1	117.8	19.8	24.6
	161	551.9	98.9	23.7	27.8	535.3	115.1	23.0	27.7	522.7	134.7	22.5	28 0
	171	584.0	105.3	25.1	29.4	568.2	121.7	24.4	29.4	556.5	141.7	23.9	29.7
	186	624.0	113.3	26.8	31.4	607.0	130.8	26.1	31.4	595.3	152.0	25.6	31.8
	206	745.8	130.4	32.0	37.4	723.5	150.2	31.1	37.3	703.4	174.7	30.2	37.4
	246	874.5	153.0	37.6	43.8	850.6	177.1	36.5	43.8	827.4	207.0	35.5	44.1
	261	904.8	160.3	38.9	45.4	880.4	184.9	37.8	45.4	860.1	215.0	36.9	45.8
	271	940.9	168.5	40.4	47.3	915.5	194.2	39.3	47.3	895.9	225.6	38.5	47.8

Cap. — Capacity kW
Cond — Condenser
kW — Compressor Motor Input Power at Rated Voltage
LCWT — Leaving Chilled-Water Temperature (C)

Figure 3-8 shows the variation of compressor isentropic efficiency and COP in terms of the evaporator temperature, at condenser temperature equal to 35°C, for two screw chillers (30HXC water cooled, 30HXA air-cooled) and one centrifugal chiller (19DK water cooled). The difference between the isentropic efficiency of air-cooled and water-cooled condenser is evident. Meanwhile it can be seen that the isentropic efficiency of the new screw chiller (30HXC water-cooled) of this manufacturer is improved in comparison with the old centrifugal chiller (19DK water-cooled). It is important to note that the increase of the evaporator temperature leads to the decrease of the isentropic efficiency, while the COP increases only slightly.

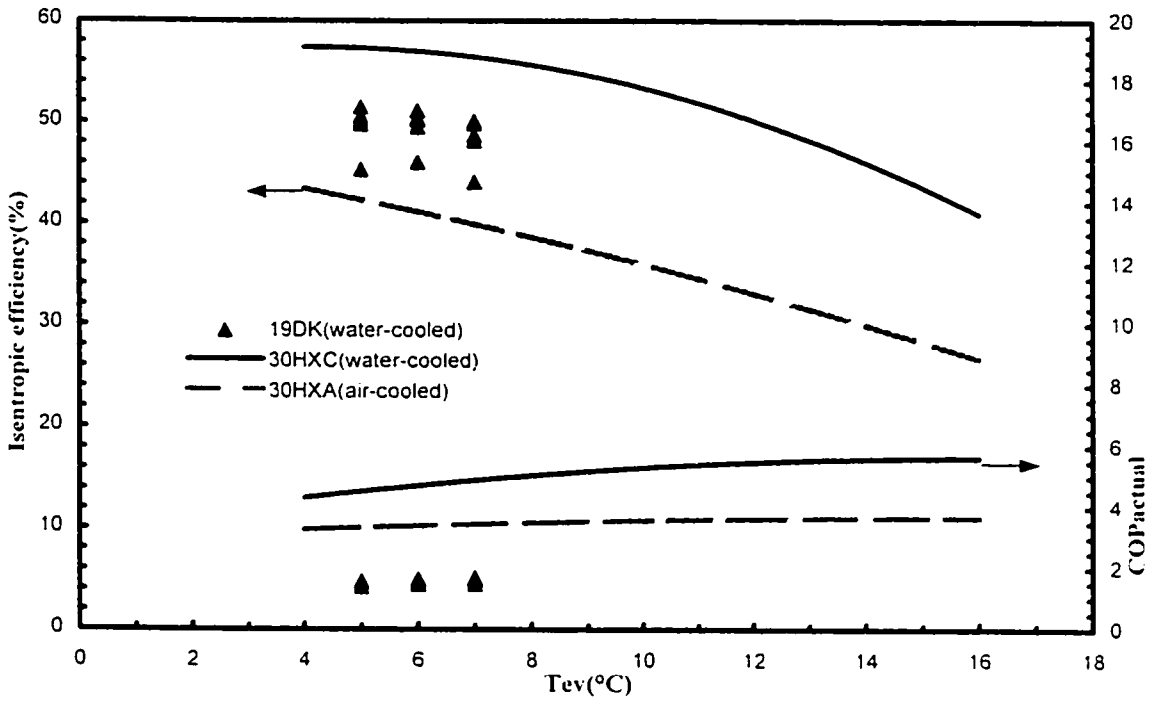

Figure 3-8 Compressor isentropic efficiency and COP variation versus evaporator temperature at condenser temperature equal to 35°C

Figure 3-9 shows the variation of compressor isentropic efficiency in terms of the condenser temperature, at evaporator temperature equal to 6°C. As discussed in section 3.3, the increase of the condensing temperature results in lower COP, and the results from manufacturer's data show the same trend. The COP in the air-cooled condenser is less affected by increasing the condensing temperature. It can be seen that there is almost no difference between the COP of the new water-cooled condenser and the old one.

It should be noted that the results presented in Figures 3-8 and 3-9 were obtained for all capacities indicated by the manufacturer for these chillers.

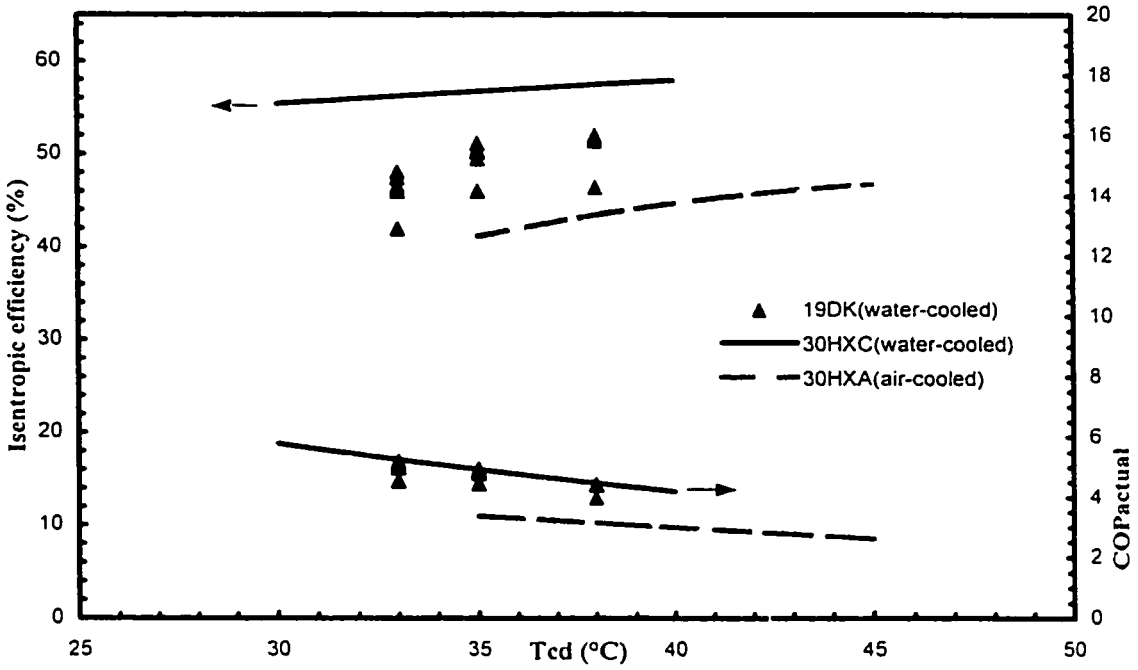

Figure 3-9 Compressor isentropic efficiency variation vs. condenser temperature at evaporator temperature equal to 6°C

There is another parameter, which also affects that performance, and its effect is not negligible: this is the cooling capacity of the evaporator. Figure 3-10 shows the variation of compressor isentropic efficiency with the capacity, at evaporator temperature equal to 6°C and condenser temperature equal to 35°C, for the three chillers. The three models show the same variation of isentropic efficiency with the evaporator cooling capacity: the increase of the cooling load results in a slight increase of the isentropic efficiency.

It should also be noted that the refrigerants, which are used in old and new chillers are different. Different thermodynamic properties of refrigerants can also affect the efficiency of chillers.

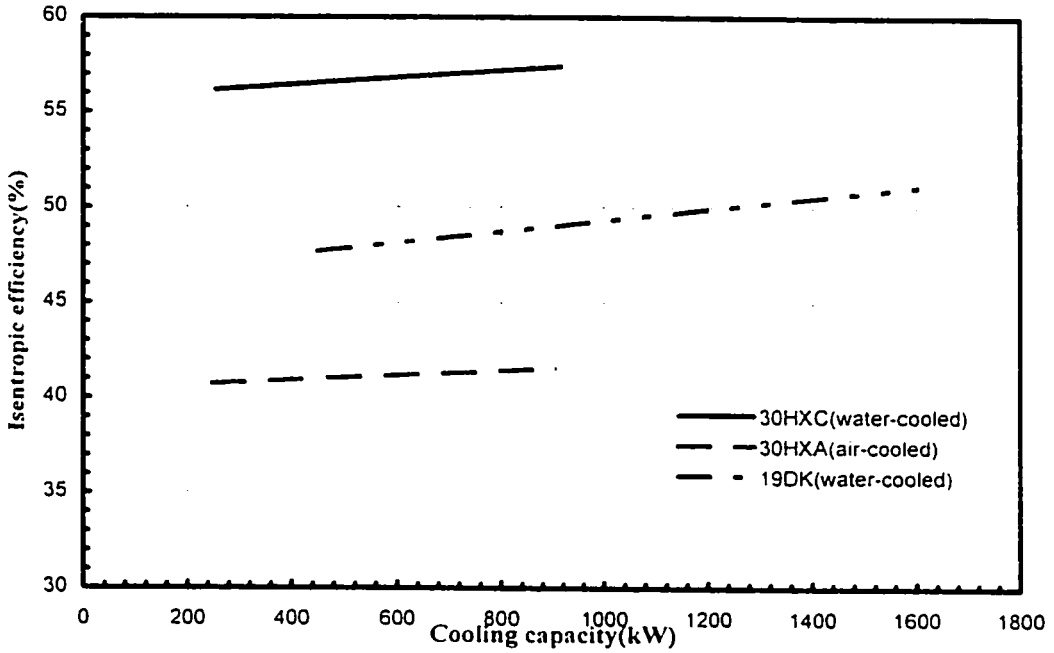

Figure 3-10 Compressor isentropic efficiency variation vs. capacity at evaporator temperature equal to 6°C and condenser temperature equal to 35°C

Based on what has been shown, it could be recognized that the isentropic efficiency is a function of the condenser temperature, the evaporator temperature and the evaporator capacity. The correlation between isentropic efficiency and these three parameters was derived, using Statgraphics software version 5 [31]. The function and the regression coefficients are summarized in Table 3-3 for the new water-cooled screw chillers (30HXC), air-cooled screw chillers (30HXA) and the old centrifugal chiller (19DK).

Table 3-3 Coefficients of the equation developed for compressor isentropic efficiency as a function of capacity, condenser and evaporator temperatures. Temperatures are in °C and Q_{ev} is in kW.

	$\eta_{is} = aT_{cd}^2+bT_{cd}+cT_{ev}^2+dT_{ev}+eT_{cd}^2T_{ev}+fT_{cd}T_{ev}+gQ_{ev}+h$							
	a	b	c	d	e	f	g	h
water-cooled(new)	0.00795681	-0.720042	-0.0990296	-4.35949	-0.00187854	0.206899	0.00204116	71.449
water-cooled(old)	0.00323769	-0.806621	-0.368173	-8.81889	0	0.3604	0.0247924	50.8743
air-cooled(new)	-0.0316958	2.90112	-0.0296849	-1.45279	0.000321176	0.00683086	0.00170575	-16.5018

Statistical information

	SE	MAE	C.V.(%)	R^2(%)
water-cooled(new)	0.769613	0.619601	1.44	98.27
water-cooled(old)	0.676721	0.475445	1.34	95.55
air-cooled(new)	1.44978	2.23495	3.55	93.06

where:

SE: standard error $= \sqrt{\frac{\sum (y-\hat{y})^2}{n}}$

(n = number of data, $\hat{y}$ = values calculated by the correlation)

MAE: mean absolute error = $\frac{\sum |y-\hat{y}|}{n}$

C.V.: Coefficient of Variance (%) $= \frac{SE}{\bar{y}} \times 100$

R^2: Coefficient of determination $= \frac{\sum (y-\bar{y})^2 - (y-\hat{y})^2}{(y-\bar{y})^2} \times 100$, $\bar{y} = \frac{\sum y}{n}$

As an example, the water-cooled screw chiller model 076 that operates with 35°C water temperature entering the condenser, and produces 5°C chilled water, has the cooling capacity of 227.2 kW. The isentropic efficiency based on Table 3-3 is determined as 57.92%, which has an error of 1.8% in comparison with the isentropic efficiency calculated by the equation (3-12). All the statistical information shows that the derived correlations cover the calculated isentropic efficiency with acceptable approximation.

Looking at the coefficients, it can be recognized that the performance of the air-cooled condenser chiller is more affected by the condenser temperature than the evaporator temperature and the cooling load. Also changes in evaporator temperature have less effect on the new water-cooled condenser chiller than on the old one. As was

observed in Figure 3-10, the effect of evaporator load slightly affects the performance of the chiller and its effect is approximately linear.

Chapter 4

Modeling of screw chillers using ASHRAE Toolkit-I

ASHRAE Toolkit-I [19] is a package of models developed as a response to the need for computational algorithms to evaluate the energy performance for different primary HVAC equipments.

The model is based on steady-state algorithm, however it can also be employed in dynamic simulation comprising multiple quasi-state progressive processes. The assumption of steady state process is justified because usually a time-step of one-hour is typically considered in the calculations.

Among the two different categories of chiller models (regression and first principle) presented in section 2.3 of the literature survey, the model of screw chiller presented in ASHRAE Toolkit-I can be considered as a combination of the two. The model is based on fundamentals of thermodynamics. Although the approach of using fundamental principles with exhaustive description of the phenomena is successful for secondary HVAC components like pipes, ducts and cooling coils, it cannot be applied alone to determine all the characteristics and the performance of primary equipments without employing experimental information. In part-load regime, the model combines the first principle model with the correlation for the compressor part-load electric demand, derived from manufacturer's data.

The model of the chiller is based on a conceptual schema, which simulate the complex equipment to an assembly of a few classical and elementary, actual and fictitious components. Again a deterministic approach can be employed here, however

with a limited number of parameters. The conceptual schema of a screw-compressor in full load regime is shown in Figure 4-1a and b.

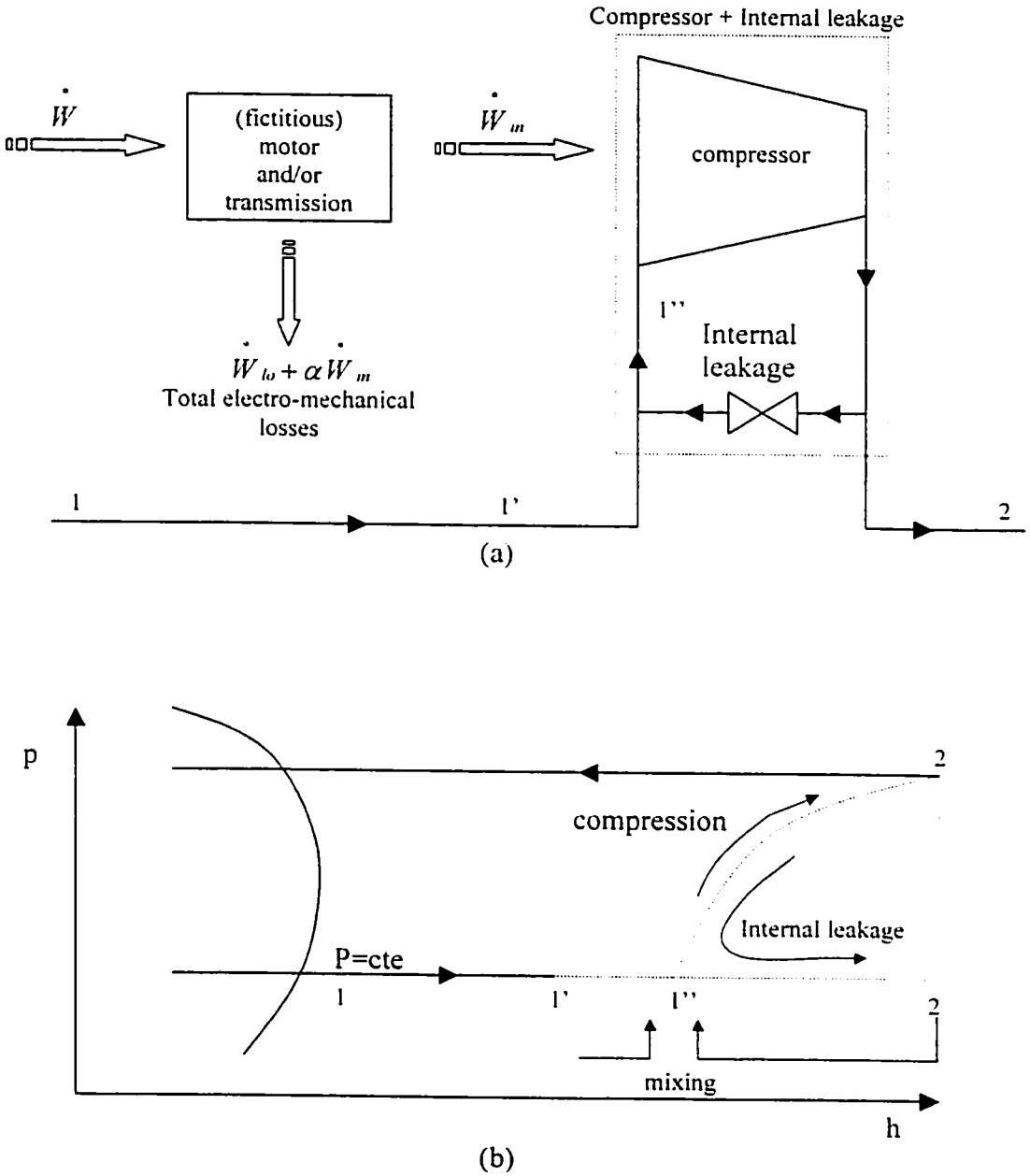

Figure 4-1 (a) Conceptual schema of a screw-compressor in full-load regime [19]
(b) p-h diagram of compression process [19]

A screw chiller is modeled in two regimes:

- Full load
- Part load

Each regime is modeled through two consecutive steps:

1) Identification
2) Simulation

In the identification step, important characteristics of the chiller are identified by using the first principle model and data from the manufacturer's catalogue.

In the simulation step, the first principle model is used along with the identified characteristics, and the operating conditions under which the performance of the chiller is evaluated.

4.1 Screw chiller parameter description

Compressor electric input or rate of work is composed of two parts: (1) the work required by the compression, internal power ($\dot{W}_{im}$) and (2) the energy losses due to irreversible losses which occur in the compressor; the losses are composed of two types: (a) constant losses ($\dot{W}_{lu}$) which are independent of input power and (b) variable losses ($\alpha \dot{W}_{im}$) which are a fraction of the work required by the compression. The total compressor electric input can be calculated as:

$$\dot{W} = \dot{W}_{lu} + \alpha \dot{W}_{im} + \dot{W}_{im} \qquad (4\text{-}1)$$

Internal pressure ratio (built-in ratio) is the ratio of the actual compressor discharge pressure p_i to the evaporating pressure $p_{ev}(\pi_i)$, while the external pressure ratio is the ratio of condensing pressure p_2 to the evaporating pressure (π). These two pressure ratios should be distinguished as different ratios. The compressor is called unadapted when these two ratios are not the same. In such a case the internal work will be higher than the work required in an isentropic compressor [19]. In this study, since there is no information about the pressures within the cycle, these two pressure ratios are considered to be the same.

Internal leakage is assimilated to a throttling process [19]. Internal mass flow rate, corresponds to the mass flow rate through a choked nozzle with the throat area (A_l) (leakage area).

4.2 Identification of chiller characteristic in full-load regime

4.2.1 Mathematical model for twin-screw chiller in full load regime

There are two main assumptions made in this mathematical model:

1) The fluid is considered to be perfect fluid and the equations of perfect gas, liquid and wet vapor are used.
2) The temperature difference between the chilled water leaving the evaporator $T_{w_{ev2}}$ and refrigerant evaporating temperature T_{ev} and also between the cooling water leaving the condenser $T_{w_{cd2}}$ and refrigerant condensing temperature T_{cd} are considered to be 5K.

$$T_{w_{ev2}} - T_{ev} = 5K$$

$$T_{cd} - T_{w_{cd2}} = 5K$$

The average value of overall heat transfer coefficient is calculated at a fictitious working point with the average parameters of all working points. Thus for N working points the following parameters can be calculated:

Average evaporator load

$$\overline{\dot{Q}}_{ev} = \sum \frac{\dot{Q}_{ev}}{N} \tag{4-2}$$

Average condenser load

$$\overline{\dot{Q}}_{cd} = \sum \frac{\dot{Q}_{cd}}{N} \tag{4-3}$$

Average evaporator water mass flow rate

$$\overline{\dot{M}}_{w_{ev}} = \sum \frac{\dot{M}_{w_{ev}}}{N} \tag{4-4}$$

Average condenser water mass flow rate

$$\overline{\dot{M}}_{w_{cd}} = \sum \frac{\dot{M}_{w_{cd}}}{N} \tag{4-5}$$

Average effectiveness of the evaporator (specific heat of water C'_{p_w} is given as 4187 J/kgK)

$$\varepsilon_{ev} = \frac{1}{1 + \frac{c_{p_w} . \dot{M}_{w_{ev}} . (T_{w_{ev,i}} - T_{ev})}{\dot{Q}_{ev}}} \tag{4-6}$$

Average effectiveness of the condenser

$$\varepsilon_{cd} = \frac{1}{1 + \frac{c_{p_w} \cdot \dot{M}_{w_{cd}} \cdot (T_{w_{cd2}} - T_{cd})}{\dot{Q}_{cd}}} \tag{4-7}$$

The overall heat transfer coefficient of the evaporator

$$AU_{ev} = -c_{p_w} \bar{\dot{M}}_{w_{ev}} \ln(1 - \bar{\varepsilon}_{ev}) \tag{4-8}$$

The overall heat transfer coefficient of the condenser

$$AU_{cd} = -c_{p_w} \bar{\dot{M}}_{w_{cd}} \ln(1 - \bar{\varepsilon}_{cd}) \tag{4-9}$$

Once the values of overall heat transfer coefficients AU_{ev} and AU_{cd} are determined, the effectiveness of the evaporator ε_{ev} and condenser ε_{cd} for each working point are calculated.

$$\varepsilon_{ev} = 1 - \exp\left[-\frac{AU_{ev}}{c_{p_w} \dot{M}_{w_{ev}}}\right] \tag{4-10}$$

$$\varepsilon_{cd} = 1 - \exp\left[-\frac{AU_{cd}}{c_{p_w} \dot{M}_{w_{cd}}}\right] \tag{4-11}$$

The evaporator and condenser water temperatures are presented in either of the four following combinations (choices):

1. Supply water temperature for both evaporator and condenser, $T_{w_{ev1}}, T_{w_{cd1}}$
2. Evaporator supply and condenser exhaust water temperature, $T_{w_{ev1}}, T_{w_{cd2}}$
3. Exhaust water temperature for both evaporator and condenser, $T_{w_{ev2}}, T_{w_{cd2}}$
4. Evaporator exhaust and condenser supply water temperature, $T_{w_{ev2}}, T_{w_{cd1}}$

Therefore the evaporating and condensing temperature can be calculated as:

Choice 1 or 2:

$$T_{ev} = T_{w_{ev1}} - \frac{\dot{Q}_{ev}}{\varepsilon_{ev} c_{p_w} \dot{M}_{w_{ev}}} \tag{4-12}$$

Choice 3 or 4:

$$T_{ev} = T_{w_{ev2}} + \frac{\dot{Q}_{ev}}{c_{p_w} \dot{M}_{w_{ev}}} (1 - \frac{1}{\varepsilon_{ev}}) \tag{4-13}$$

Choice 1 or 4:

$$T_{cd} = T_{w_{cd1}} - \frac{\dot{Q}_{cd}}{\varepsilon_{cd} c_{p_w} \dot{M}_{w_{cd}}} \tag{4-14}$$

Choice 2 or 3:

$$T_{cd} = T_{w_{cd2}} + \frac{\dot{Q}_{cd}}{c_{p_w} \dot{M}_{w_{cd}}} (1 - \frac{1}{\varepsilon_{cd}}) \tag{4-15}$$

The condenser and evaporator enthalpies and the saturation pressure of the refrigerant in condenser or evaporator is determined using:

The Clausius-Clapeyron equation $$p_{sat} = 1000\ e^{\left[A_{cl} + \frac{B_{cl}}{T_{sat}}\right]} \quad (4\text{-}16)$$

where A_{cl} and B_{cl} are the first and second coefficient in the Clausius-Clapeyron equation respectively.

The condenser and evaporator enthalpy are calculated as follows:

$$h_1 = h_{fo} + h_{fgo} + C_{p_{vap}} (T_{ev} - T_o) \quad (4\text{-}17)$$

$$h_3 = h_{fo} + C_{p_{liq}} (T_{cd} - T_o) \quad (4\text{-}18)$$

where:

h_{fo} : enthalpy of saturated liquid at reference temperature (J/kg)

h_{fgo}: enthalpy of vaporization at reference temperature (J/kg)

$C_{p_{vap}}$: specific heat of vapor (J/kgK)

$C_{p_{liq}}$: specific heat of liquid (J/kgK)

T_o : Reference temperature (273.15 K)

p_{sat} : Saturation pressure (Pa)

T_{sat} : Saturation temperature (K)

For instance for refrigerant R-134a:

A_{cl} = 15.489 , B_{cl} = -2681.99 , h_{fo} = 200000 (J/kg), h_{fgo} = 197900 (J/kg),

$C_{p_{sup}}$ =892.5 (J/kgK), $C_{p_{liq}}$ =1265 (J/kgK)

As an example, at T_{ev}=279.15 K , T_{cd}= 303.15K,

p_{sat} = 358274 Pa

h_1=403225 J/kg

h_3= 237950 J/kg

It should be noted that thermodynamic properties of the different refrigerants are available as a subroutine in the program.

The mass flow rate of refrigerant $\dot{M}_R$ can be calculated as:

$$\dot{M}_R = \frac{\dot{Q}_{ev}}{h_1 - h_3} \tag{4-19}$$

Assuming that temperature after heating up $T_{ev'}$ is equal to the evaporating temperature for the first trial, specific volume of the refrigerant is calculated as:

$$\upsilon_{ev'} = \frac{rT_{ev'}}{p_{ev}}\zeta \tag{4-20}$$

where :

r : gas constant (J/kgK)

ζ : mean compressibility factor

(for refrigerant R-134a: r = 81.4899 (J/kgK) and ζ =0.9411)

Taking leakage area A_l equals to $10^{-6}\ m^2$ for the first trial the volumetric flow rate of refrigerant $\dot{V}_s$ is calculated as:

$$\dot{V}_s = Y(i) + A_l \times X(i) \tag{4-21}$$

and initially is taken as:

$$Y(i) = aY(i) + b \tag{4-21a}$$

where:

$$Y(i) = \dot{M}_R \times \upsilon_{cv} \tag{4-22}$$

$$X(i) = p_1 \upsilon_{cv} \pi^{\frac{\gamma+1}{2\gamma}} \gamma \left(\frac{2}{\gamma+1} \right)^{\frac{\gamma+1}{\gamma-1}} \tag{4-23}$$

(γ is the isentropic coefficient; for refrigerant R-134a, $\gamma = 1.072$)

$a = -A_l$, the slope and $b = \dot{V}_s$, the intercept.(Figure 4-2).

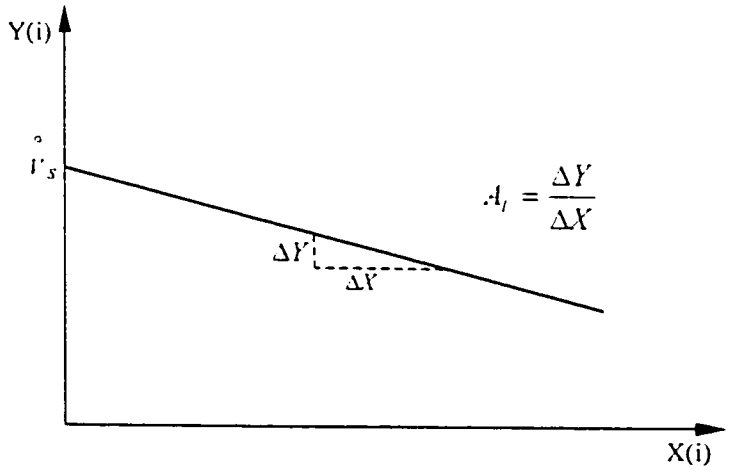

Figure 4-2 Graphical illustration of equation (4-21)

The internal power of the compressor is calculated as:

$$\dot{W}_m = \frac{\gamma}{\gamma - 1} . p_{ev} . \dot{V}_s \left[\pi^{\frac{\gamma-1}{\gamma}} - 1 \right] \tag{4-24}$$

where π is the external pressure ratio which is the ratio of condensing pressure to the evaporating pressure. The refrigerant mass flow rate is calculated by equation (4-21) to (4-23) solving for $\dot{M}_R$. Now the temperature after heating up can be determined and compared with the first trial by the aid of equation (4-25).

$$T_{ev'} = T_{ev} + \frac{\dot{W}_{lo} + \alpha \dot{W}_m}{C_{p_{vap}} \dot{M}_R} \tag{4-25}$$

If the difference between the previous value of the temperature after heating up and the one calculated by equation (4-25) exceeds 10^{-4}, the program recalculates the parameters starting from specific volume of the refrigerant. The iteration goes on until the convergence reaches to a good approximation. In the next step using statistical analysis and equation (4-21), two coefficients in equation (4-21a) can be identified as:

$$A_1 = \frac{\sum X(i)Y(i) - \frac{1}{N}\sum X(i)\sum Y(i)}{\sum X(i)^2 - \frac{1}{N}(\sum X(i))^2} \tag{4-26}$$

$$\dot{V}_s = \frac{\sum Y(i) - A_l \sum X(i)}{N} \tag{4-27}$$

The same procedure is done for equation (4-1):

$$\dot{W} = \dot{W}_{lo} + \alpha \dot{W}_m + \dot{W}_m \tag{4-1}$$

This equation can be arranged so to get the general equation of a line:

$$\dot{W} = (1 + \alpha)\dot{W}_m + \dot{W}_{lo} \tag{4-1a}$$

so the coefficients can be identified as:

$$\alpha = \frac{\sum \dot{W} \sum \dot{W}_m - N \sum \dot{W} \cdot \dot{W}_m}{(\sum \dot{W}_m)^2 - N \sum \dot{W}_m^2} - 1 \tag{4-28}$$

$$W_{lo} = \frac{\sum \dot{W} - \alpha \sum \dot{W}_m}{N} \tag{4-29}$$

This new value of the leakage area A_l is compared with the previous value and if the difference exceeds 10^{-4}, the calculations start again from equation (4-21). The iteration calculation continues till it converges with a good approximation. The flow chart of this procedure is shown in Figure 4-3.

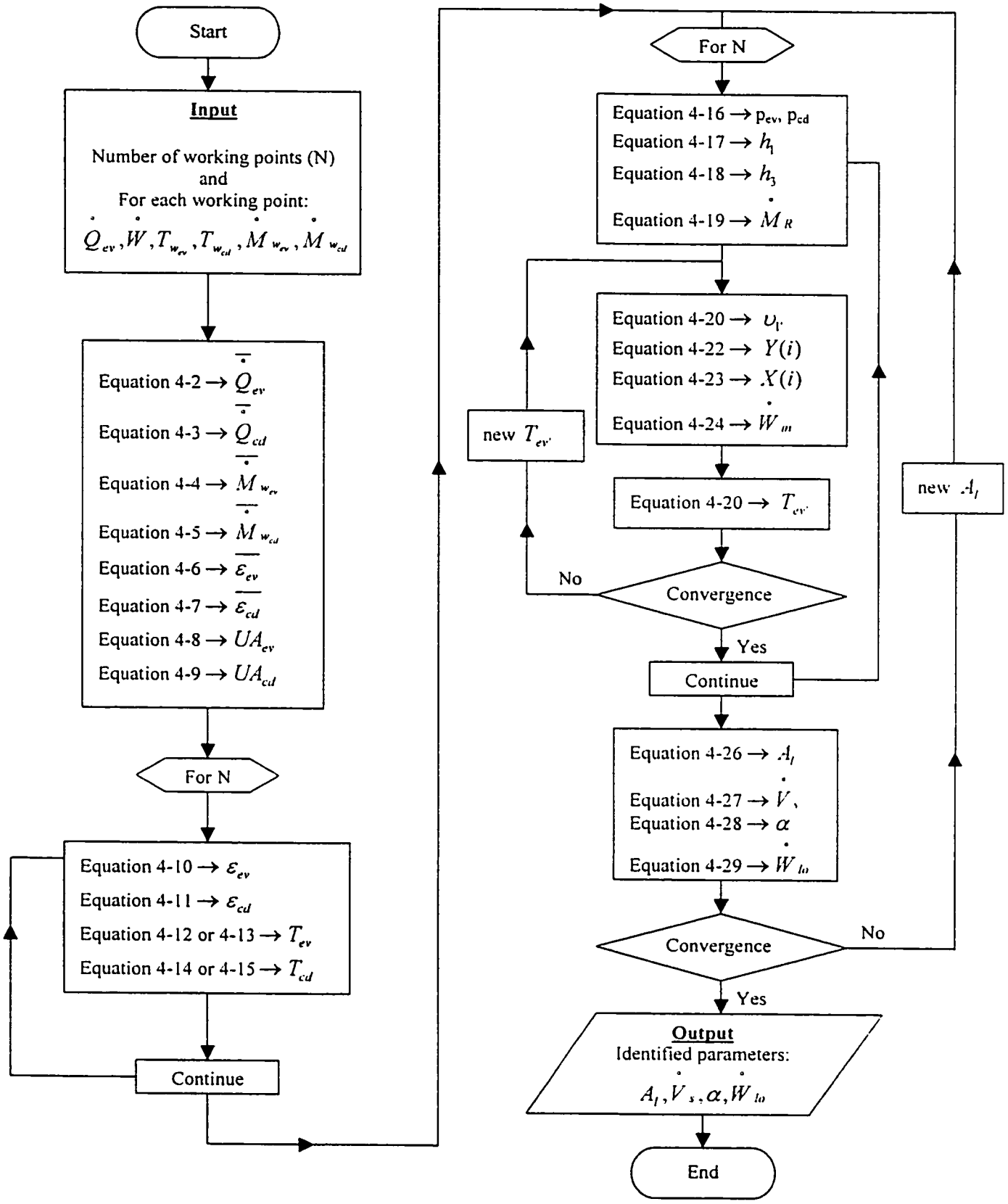

Figure 4-3 Full load identification procedure flow-chart

4.2.2 Input data

An input file has to be made with the following information:

- Refrigerant type

Six different refrigerant thermodynamic properties are available in this modeling.

1. Refrigerant 12
2. Refrigerant 134a
3. Refrigerant 114
4. Refrigerant 22
5. Refrigerant 502
6. Refrigerant 717

- Number of working points, N

For each working point:

- evaporator load (cooling capacity), $\dot{Q}_{ev}$ (W)
- compressor power input, $\dot{W}$ (W)
- evaporator and condenser water temperatures according the choice $T_{w_{ev}}$, $T_{w_{cd}}$ (K)
- water mass flow rate of condenser and evaporator, $\dot{M}_{w_{ev}}$, $\dot{M}_{w_{cd}}$ (kg/s)

At the end:

- initial guess of refrigerating capacity and heat rejected by the condenser, P_{ev}, P_{cd} (W)
- value of internal volume pressure ratio corresponding to each working point, if it is not equal to external pressure ratio.

4.2.3 Output data

After the required data were input in the program, the following parameters are identified:

-evaporator overall heat transfer coefficient, AU_{ev} (W/K)

-condenser overall heat transfer coefficient, AU_{cd} (W/K)

-constant part of electromechanical losses, $\dot{W}_m$ (W)

-coefficient for variable portion of electromechanical loss, α

-refrigerant volumetric flow rate at the beginning of compression, $\dot{V}$, (m^3/s)

-leakage area A_l (m^2)

The output also includes the values of internal power of the compressor $\dot{W}_m, X(i), Y(i)$ for each working point and the standard deviation of the linear regression over $Y(i)$ versus $X(i)$ and $\dot{W}$ versus $\dot{W}_m$.

A typical identification input and output data are shown in the next pages. The information flow diagram for full load identification program is also illustrated in Figure 4-4.

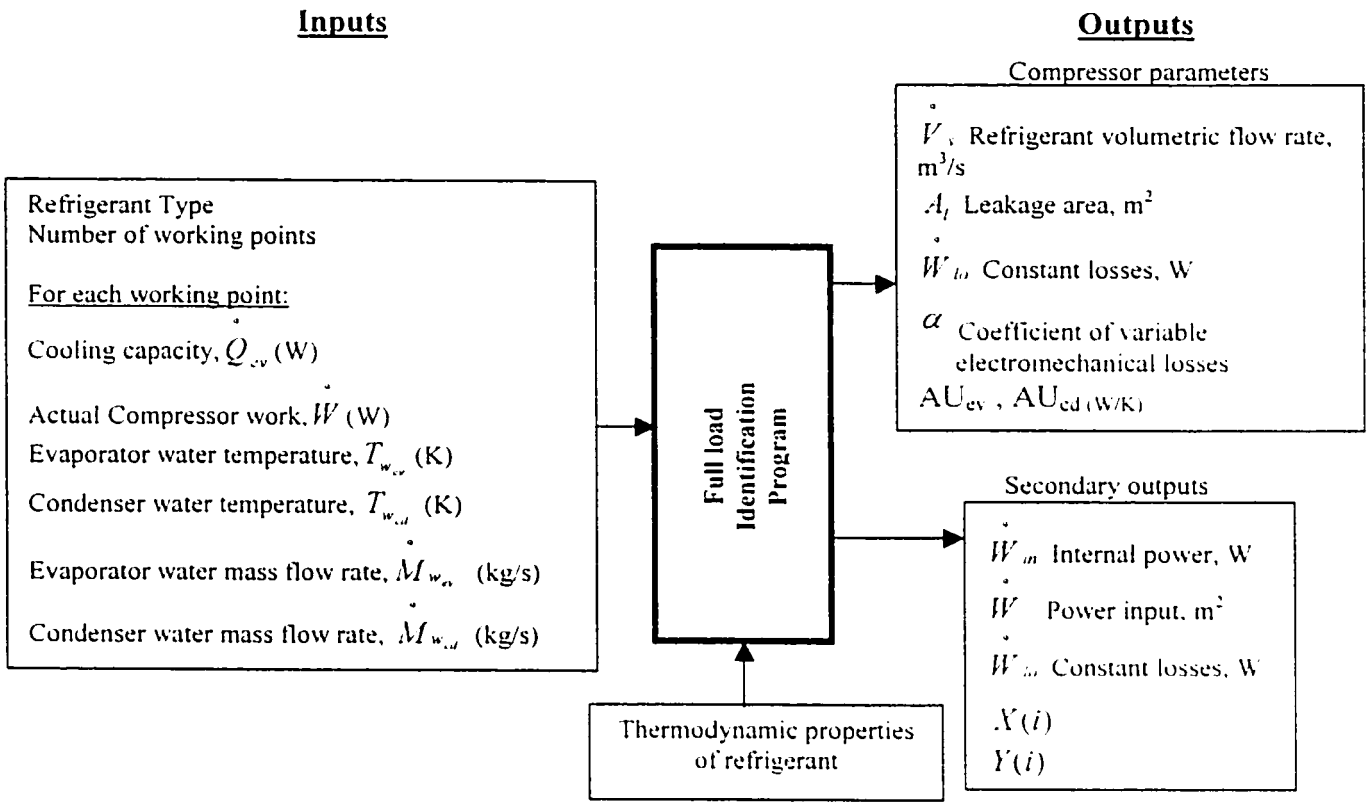

Figure 4-4 Information flow diagram of full load identification [19]

Full load identification typical input data

CARRIER screw compressor chiller Model 30HXC076, refrigerant R-134a

```
2      Ifluid
27     N
253300  48200      D(2*I-1),D(2*I)
264000  48600
274800  49300
285800  50000
297000  50500
307100  50900
316800  51200
333200  51500
330100  51400
234300  53200
244200  53700
254600  54200
265500  54700
276700  55100
288100  55600
299500  56300
318800  57500
315200  57300
219000  58900
227200  59300
235600  59700
244700  60100
254900  60700
265400  61300
276500  61800
295300  62700
291700  62600
4              choice
10.9    12.8       Mfrwev(I),Mfrwcd(I)
277.15  298.15     Twev(I),Twcd(I)
11.3    13.3
278.15  298.15
11.8    13.8
279.15  298.15
12.3    14.3
280.15  298.15
12.8    14.8
281.15  298.15
13.2    15.3
282.15  298.15
13.6    15.7
283.15  298.15
14.4    16.4
286.15  298.15
14.2    16.3
289.15  298.15
10.1    12.2
277.15  303.15
```

10.5 12.7
278.15 303.15
10.9 13.2
279.15 303.15
11.4 13.7
280.15 303.15
11.9 14.2
281.15 303.15
12.4 14.7
282.15 303.15
12.9 15.2
283.15 303.15
13.7 16.1
286.15 303.15
13.6 15.9
289.15 303.15
9.4 11.8
277.15 308.15
9.8 12.2
278.15 308.15
10.1 12.6
279.15 308.15
10.5 13
280.15 308.15
11.0 13.5
281.15 308.15
11.4 13.9
282.15 308.15
11.9 14.4
283.15 308.15
12.7 15.3
286.15 308.15
12.6 15.1
289.15 308.15
300000 300000 PevG.PcdG
0 Mismatch

Identification typical output data

"Win"	"Pcomp"	"X"	"Y"
48993.3	48200.0	270.247	.121728
49846.2	48600.0	265.373	.123505
50752.7	49300.0	260.989	.125362
51660.7	50000.0	256.798	.127188
52540.6	50500.0	252.704	.128932
53082.0	50900.0	248.216	.129910
53515.8	51200.0	243.833	.130582
51722.1	51500.0	227.652	.125957
45587.5	51400.0	207.546	.112829
53579.6	53200.0	301.822	.115052
54471.3	53700.0	295.995	.116640
55441.8	54200.0	290.547	.118358
56520.8	54700.0	285.619	.120276
57613.3	55100.0	280.898	.122187
58727.0	55600.0	276.440	.124093
59828.7	56300.0	272.206	.125921
59107.7	57500.0	255.077	.123228
52777.4	57300.0	232.707	.110165
59003.8	58900.0	337.562	.110474
59686.6	59300.0	330.438	.111340
60344.5	59700.0	323.422	.112126
61175.4	60100.0	317.085	.113244
62270.4	60700.0	311.437	.114910
63415.8	61300.0	306.084	.116541
64635.0	61800.0	301.027	.118363
64166.8	62700.0	281.651	.116027
57874.7	62600.0	257.201	.103689

AUevId= 36000.000 AUcdId= 44000.000
LossesId= 9124.7520
AlphaId=-.17678
VsFLId= .144040
AIId= .0000895
SEw= .03876 SEv= .05390

4.3 Simulation of chiller in full-load regime

The main purpose of this section is to evaluate the energy performance (COP) of a chiller based on working points data and identified parameters determined in the identification section.

4.3.1 Mathematical model

In the simulation program almost the same thermodynamic and heat transfer concepts have been considered and the same equations have been used. The program starts by calculating the evaporator and condenser effectiveness by equations (4-10) and (4-11), knowing the overall heat transfer coefficient as identified parameter and the mass flow rate of the water as working point parameters. Then the condensing and evaporating temperatures are determined using equations (4-12) to (4-15) based on the choice and first guess of the condenser and evaporator loads. Following the condensing and evaporating temperatures, the pressure and enthalpies of the refrigerant at the leaving point in the evaporator and condenser are calculated using the thermodynamic properties of the refrigerant and equations (4-16) to (4-18). Internal work can then be determined by equation (2-24)

Specific volume of the refrigerant in this step is calculated by equation (4-20) and assuming that the temperature after heating up is equal to the evaporator temperature as the first guess. After $\upsilon_{s,r}$ was determined, mass flow rate of the refrigerant is calculated using equation (4-21) to (4-23) solving for $\dot{M}_R$. By using the identification parameters the temperature after heating up is to be checked by the following equation:

$$T_{ev'} = T_{ev} + \frac{\dot{W}_{in} + \alpha \dot{W}_{m}}{c_{p_{vap}} \dot{M}_R} \tag{4-30}$$

The new value of $T_{ev'}$ is compared with the previous value. If the difference between the previous value of the temperature after heating up and the one calculated by equation (4-31) exceeds 10^{-4}, the program recalculates the parameters starting from specific volume of the refrigerant till it converges.

Now having the internal work from equation (4-30), A_i and α identified by the identification program, the compressor power $\dot{W}$ can be determined using equation (4-1). At this step the condenser load is checked by adding the compressor power and evaporator load (first guess)(equation 4-31).

$$\dot{Q}_{cd} = \dot{W} + \dot{Q}_{ev} \tag{4-31}$$

If the difference between the guessed value of the condenser load and the calculated value was not less than 10^{-4} , the last value of the condenser load replaces the previous value and the program recalculates the parameters starting with condensing pressure and temperature. This iteration goes on until it converges. On the next stage evaporator load is calculated by equation (4-19) solving for $\dot{Q}_{ev}$. Then the value is compared with the first guess. If the difference was less than 10^{-4} the program recalculates the parameters starting from evaporating pressure and temperature till the acceptable error is reached.

Now COP can easily be calculated using equation (3-1). To determine the temperature of water on the other side of the condenser and evaporator knowing the water temperature on one side, the following equations can be used:

Choice 1 and 2:

$$T_{w_{ev2}} = T_{w_{ev1}} - \frac{\dot{Q}_{ev}}{c_{p_w} \dot{M}_{w_{ev}}} \tag{4-32}$$

Choice 3 and 4:

$$T_{w_{ev1}} = T_{w_{ev2}} + \frac{\dot{Q}_{ev}}{c_{p_w} \dot{M}_{w_{ev}}} \tag{4-33}$$

Choice 1 and 4:

$$T_{w_{cd2}} = T_{w_{cd1}} + \frac{\dot{Q}_{cd}}{c_{p_w} \dot{M}_{w_{cd}}} \tag{4-34}$$

Choice 2 and 3:

$$T_{w_{cd1}} = T_{w_{cd2}} - \frac{\dot{Q}_{cd}}{c_{p_w} \dot{M}_{w_{cd}}} \tag{4-35}$$

The whole simulation procedure is illustrated in a flow-chart shown in Figure 4-5.

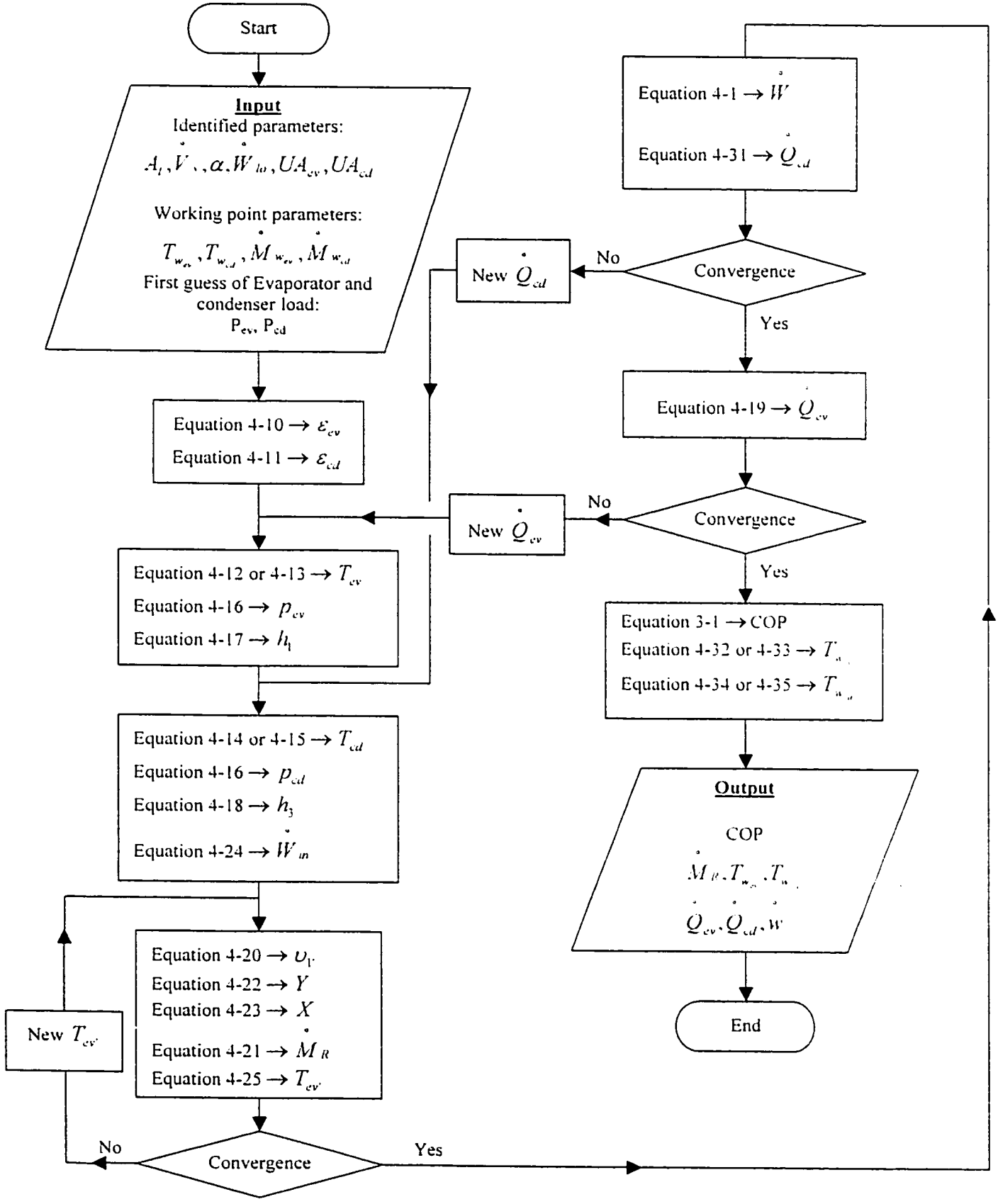

Figure 4-5 Full load simulation procedure flow-chart

4.3.2 Input data

As input data, the program requires:

- refrigerant type (as discussed in 4.2.2)
- six identified parameters $A_l, \dot{V}_{,}, \alpha, \dot{W}_{lo}, UA_{ev}, UA_{cd}$
- evaporator and condenser water temperatures,(K) (One of the four choices explained in 4.2.1), $T_{w_{ev}}, T_{w_{cd}}$
- water mass flow rate of condenser and evaporator, $\dot{M}_{w_{ev}}, \dot{M}_{w_{cd}}$ (kg/s)
- initial guess of refrigerating capacity and heat rejected in the condenser, W
- value of internal volume pressure ratio corresponding to each working point, if it is not equal to external pressure ratio, π

It should be noted that for each of the working points mentioned in the identification part, one simulation input file has to be prepared, therefore the chiller performance in each working point is to be investigated.

4.3.3 Output data

Using these input data, the model will give the coefficient of performance together with other useful data including the mass flow rate of refrigerant, the water temperatures at the other side of evaporator and condenser (based on the choice), the compressor energy demand, and the evaporator cooling capacity. The last two parameters are calculated based on the identification parameters already determined in the identification part, which can be compared with the real values offered by the manufacturer in the technical catalogue. The information flow diagram for the

simulation program is shown in Figure 4-6. A typical input and output file for the simulation model is shown on the next page.

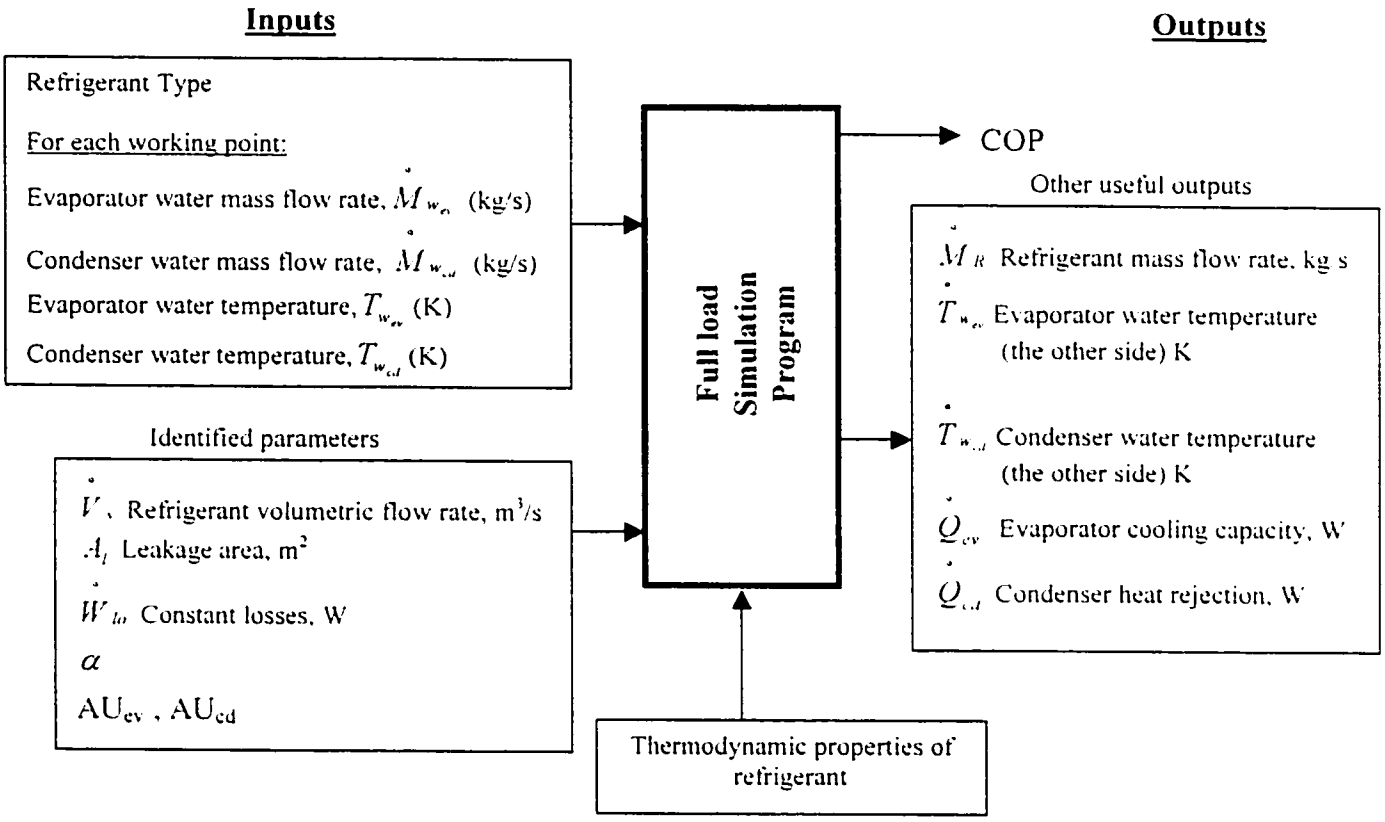

Figure 4-6 Information flow diagram of full load simulation [19]

CARRIER screw compressor chiller Model 30HXC076, refrigerant R-134a

Full load simulation typical input data

'AUev' 36000
'AUcd' 44000
'Losses' 9124.7520
'Alpha' -0.17678
'Al' 0.0000895
'VsFL' 0.144040
'Ifluid' 4
'Mfrwev' 10.9
'Mfrwcd' 12.8
'Choice' 1
'Twev1' 277.15
'Twcd1' 298.15
'PevG' 150000
'PcdG' 160000
'Mismatch' 0
'vratio' 0

Full load simulation typical output data

OUTPUTS	Component: SCHIFLSI		
MfrRef	= 1.62027	Pev	= 247489.
Pcomp	= 62610.4	Pcd	= 310099.
COP	= 3.95283	Twev2	= 282.573
Twcd2	= 303.936		

4.4 Identification of chiller characteristics in part-load regime

Part load characteristics are the most important and complicated issues of a chiller. There is not enough available information of chillers working at part load and the existing information that the manufacturers have for their products are usually obtained through some experiments. The part load model of ASHRAE Toolkit-I for twin-screw compressor chillers has the options of using either part load parameters if available or full load parameters for the same working points. In this study we use the full load data from the manufacturers' catalogue for the part load modeling.

4.4.1 Mathematical model

The program starts by calculating the effectiveness of the evaporator using equation (4-10). The evaporating temperature is the next parameter that is determined by equation (4-12) or (4-13) based on the choice. The same parameters are calculated for the condenser using equations (4-11) and (4-14) or (4-15) (the condenser load is calculated by equation (4-32). Pressures and enthalpies at the leaving points of evaporator and condenser are the next parameters that are determined by equations (4-15), (4-16) and (4-17).

To derive the compressor input power at partial load $\dot{W}_{pl}$ the model uses an empirical equation as follow:

$$\dot{W}_{PL} = \dot{W}\,(0.3 + 0.567PLR + 0.133PLR^2) \qquad (4\text{-}36)$$

where PLR (part load ratio) is the ratio of the evaporator actual load over its full load cooling capacity.

That would be the case when the information given in the input file is for the full load. Then using equation (4-1) knowing the identified parameters for the full load, the internal power at part load regime $\dot{W}_{in_{pl}}$ can be specified. The mass flow rate of the refrigerant, $\dot{M}_{R_{pl}}$, can be determined by the equation (4-19).

Now as a first guess for the volume flow rate of the refrigerant bypassed due to the partial load, $\dot{V}_{pumping}$, the model starts with $\dot{V}_{pumping} = 0.5\dot{V}_s$. $\dot{V}_s$ is known as an identified parameter for the full load. The amount of reduced internal power due to partial load is calculated by equation (4-37).

$$\dot{W}_{in_{red}} = \frac{\gamma}{\gamma - 1} p_{ev} (\dot{V}_s - \dot{V}_{pumping}) (\pi^{\frac{\gamma-1}{\gamma}} - 1) \qquad (4\text{-}37)$$

Temperature after heating up is determined by:

$$T_{ev'} = T_{ev} + \frac{\dot{W}_{pl} - \dot{W}_{in_{red}}}{\dot{M}_{R_{pl}} c_{p_{vap}}} \qquad (4\text{-}38)$$

Refrigerant specific volume and X are calculated by equation (4-20) and (4-23) respectively. The new value of $\dot{V}_{pumping}$ can be calculated by equation (4-39).

$$\dot{V}_{pumping} = \dot{V}_{s} + A_{l}X - \dot{M}_{R_{pl}}\upsilon_{ev} \tag{4-39}$$

The new value of $\dot{V}_{pumping}$ is compared with the first guess. If the difference was less than 10^{-4}, $\dot{V}_{pumping}$ is replaced by the new value and the program recalculates the parameters starting $\dot{W}_{in_{pl}}$ till the iteration reaches the acceptable error. On the next step, the compressor power required to by-pass the refrigerant in part load, $\dot{W}_{pump}$ is calculated by equation (4-40).

$$\dot{W}_{pump} = \dot{W}_{in_{pl}} - \dot{W}_{in_{ref}} \tag{4-40}$$

The last parameter to be calculated, is the pressure jump encountered by the fluid by passed due to part load and that is:

$$dp_{pumping} = \frac{\dot{W}_{pump}}{\dot{V}_{pumping}} \tag{4-41}$$

The flow chart of the whole procedure is shown in Figure 4-7.

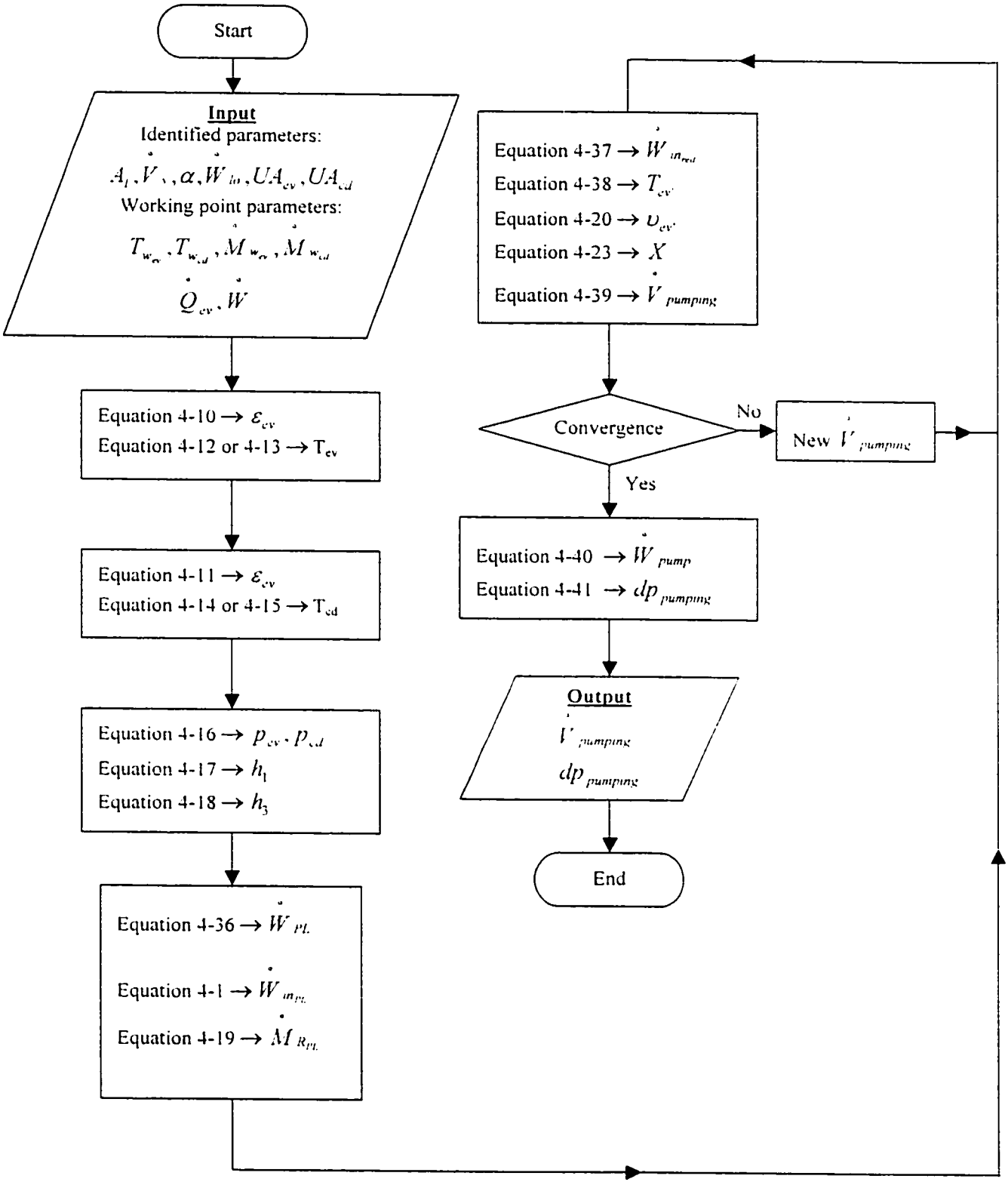

Figure 4-7 Part load identification procedure flow-chart

4.4.2 Input data

The input data includes:

- refrigerant type (as discussed in 4.2.2)
- six identified parameters at full load $A_l, \dot{V}_s, \alpha, \dot{W}_{lo}, UA_{ev}, UA_{cd}$
- evaporator and condenser water temperatures (One of the four choices explained in 4.2.1), $T_{w_{ev}}, T_{w_{cd}}$ (K)
- water mass flow rate of condenser and evaporator, $\dot{M}_{w_{cd}}, \dot{M}_{w_{ev}}$ (kg/s)
- evaporator and compressor loads, $\dot{Q}_{ev}, \dot{W}$ (W)
- part load ratio, PLR

As can be seen from the input data, one separate input file has to be made for each working point. In addition to the parameters above there is another code in the input data indicating that the data belongs to part load or full load regime.

4.4.3 Output data

As output, the identified parameters will only be the bypassed refrigerant volume flow rate and the pressure jump encountered by the by passed fluid in part load regime. The information flow diagram of the part load identification is shown in Figure 4-8.

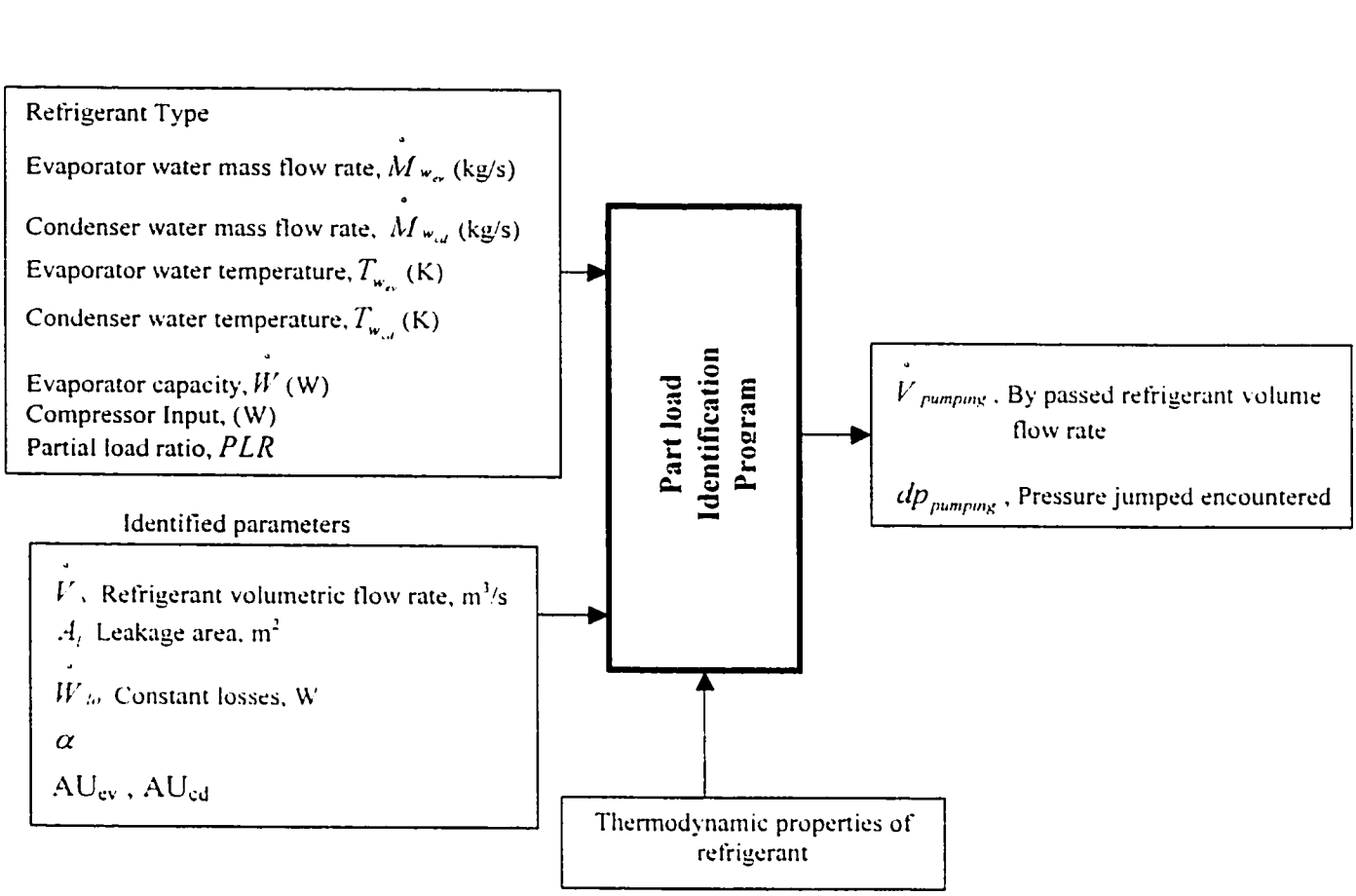

Figure 4-8 Information flow diagram of part load identification [19]

A typical input and output data file for part load identification model are shown on the next page.

CARRIER screw compressor chiller Model 30HXC076, refrigerant R-134a

Part load identification typical input data

'AUev' 36000
'AUcd' 44000
'Losses' 9124.752
'Alpha' –0.17678
'VsFL' 0.144040
'Al' 0.0000895
'Ifluid' 4
'PLorFL' 2
'Mfrwev' 10.9
'Mfrwcd' 12.8
'Choice' 1
'Twev1' 277.15
'Twcd1' 298.15
'Pev' 25300
'W' 48200
'PevRatio' 0.6
'Mismatch' 0
'vratio' 0

Part load identification typical output data

OUTPUTS Component: SCHIPLID
Vpumping = .802904E-01 dpPumpingId = 19753.5
ErrDetec = .000000

4.5 Simulation of chiller in part-load regime

The main objective of part load simulation is to evaluate the energy performance of the chiller (COP) in different part loads.

4.5.1 Mathematical description

The program starts by calculating the effectiveness of the condenser and evaporator using equations (4-10) and (4-11). The evaporating temperature is the next parameter to be calculated by equations (4-12) or (4-13) based on the choice. Then the evaporating pressure and enthalpy at the leaving point of the evaporator are determined by equations (4-16) and (4-17). Condensing pressure, temperature and enthalpy at the leaving point of the condenser are calculated in the same way as the evaporator by equations (4-14) or (4-15), (4-16) and (4-18). Internal compressor power input reduction $\dot{W}_{in_{red}}$ due to part load is calculated using identified values and equation (4-37). The compressor power to by-pass the refrigerant in part load $\dot{W}_{pump}$ is determined from equation (4-41) solving for $\dot{W}_{pump}$:

$$\dot{W}_{pump} = \dot{V}_{pumping} . dp_{pumping} \tag{4-42}$$

Consequently the internal power of the compressor is determined by:

$$\dot{W}_{in_{PL}} = \dot{W}_{in_{red}} + \dot{W}_{pump} \tag{4-43}$$

Refrigerant specific volume and X are calculated by equations (4-20) and (4-23), and the mass flow rate of the refrigerant $\dot{M}_{R_{HL}}$ is calculated as follows:

$$\dot{M}_{R_{HL}} = \frac{\dot{V}_s - \dot{V}_{pumping} - A_l X(i)}{\upsilon_{ev'}} \tag{4-44}$$

Then the new value of the temperature after heating up which was assumed to be equal to evaporating temperature is checked by equation (4-45).

$$T_{ev'} = T_{ev} + \frac{\dot{W}_{lo} + \alpha \dot{W}_m + \dot{W}_{pump}}{\dot{M}_{R_{HL}} C_{p_{sup}}} \tag{4-45}$$

If the difference between the new value and the first guess was not less than 10^{-4} the new value replaces the old one and equations (4-20) and (4-23) are used again till it reaches an acceptable error.

The next step is to calculate the compressor power input $\dot{W}$ based on the identified parameters and equation (4-1). Now the condenser heat rejection $\dot{Q}_{cd}$ is found by equation (4-32). This new value of condenser load is compared with the first guess from the input file. If the difference between the new value and the first guess is not less than 10^{-4} the new value replaces the old one and the program recalculates the parameters starting from condensing temperature till it reaches an acceptable error.

On the next step evaporator load is calculated by equation (4-19) solving for $\dot{Q}_{ev}$ and is compared with the first guess from the input file. If the difference between the new value and the first guess was not less than 10^{-4}, the new value replaces the old one and the program recalculates the parameters starting from evaporating temperature till it converges to an acceptable error.

Once we have the evaporator load and compressor input power, the COP can be determined using equation (3-1). Water temperatures at the other side of compressor and evaporator can be calculated by equations (4-32) to (4-35) based on the choice and the corresponding temperatures at one side. The whole procedure is illustrated in a flow chart shown in Figure 4-10.

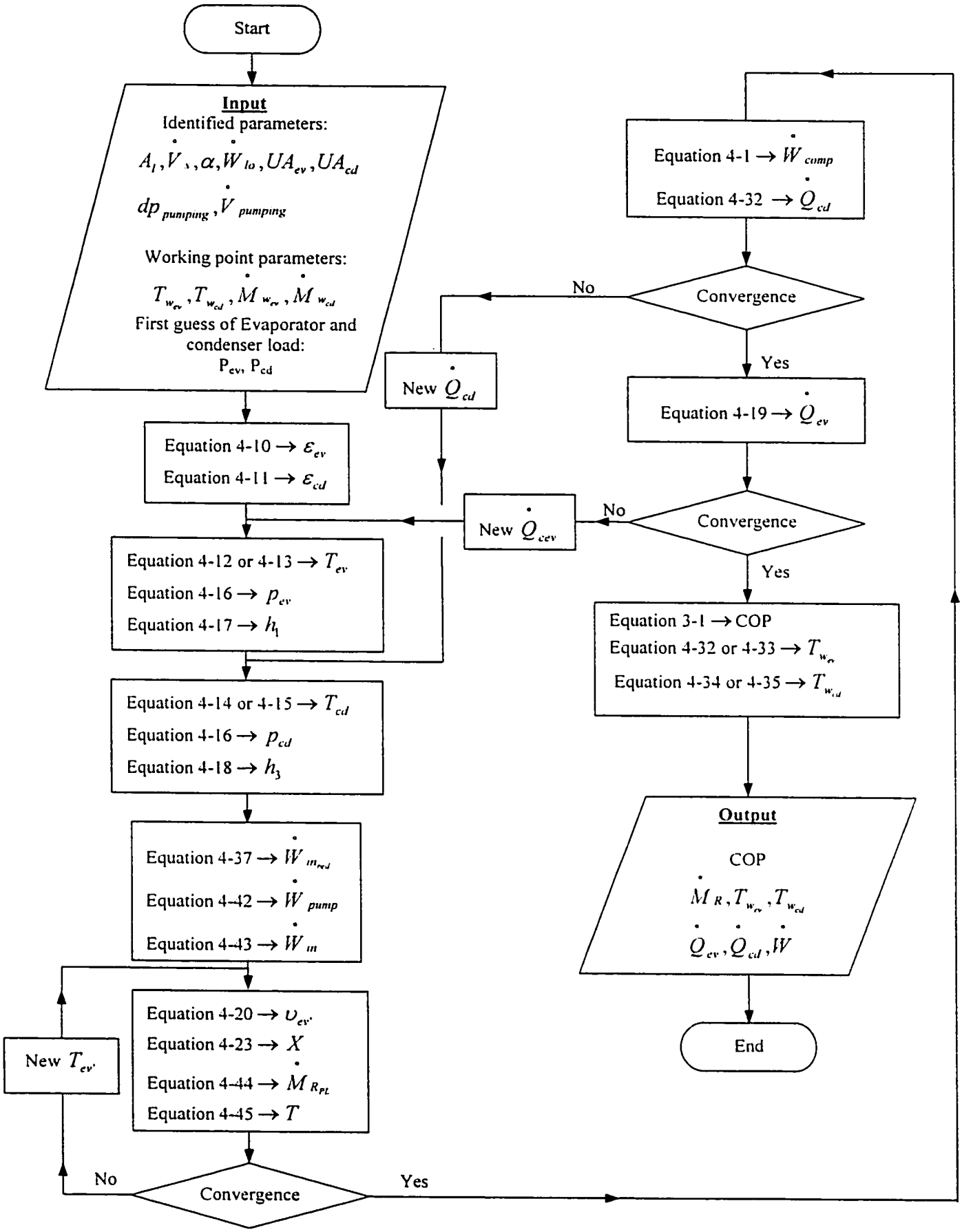

Figure 4-9 Part load simulation procedure flow-chart

4.5.2 Input data

The same parameters as for the full load simulation input file are required for part load simulation except that the part load identified parameters have to be added to them.

- refrigerant type (as discussed in 4.2.2)
- six identified parameters $A_f, \dot{V}_{,}, \alpha, \dot{W}_{lo}, UA_{ev}, UA_{cd}$ in full load regime
- the identified parameters $\dot{V}_{pumping}$, $dp_{pumping}$ in part load regime.
- evaporator and condenser water temperatures (One of the four choices explained in 4.2.1), $T_{w_{ev}}, T_{w_{cd}}$ (K)
- water mass flow rate of condenser and evaporator, $\dot{M}_{w_{ev}}, \dot{M}_{w_{cd}}$ (kg/s)
- initial uess of refrigerating capacity and heat rejected in the condenser, P_{ev}, P_{cd} (W)

4.5.3 Output data

As the result, the program gives the COP at specified part loads. The output file also consists of other useful data such as mass flow rate of refrigerant, condenser and evaporator load and compressor power input. The model also outputs the water temperatures at the other side of condenser and evaporator that could be some other useful information. Figure 4-9 shows the information flow diagram of the part load simulation.

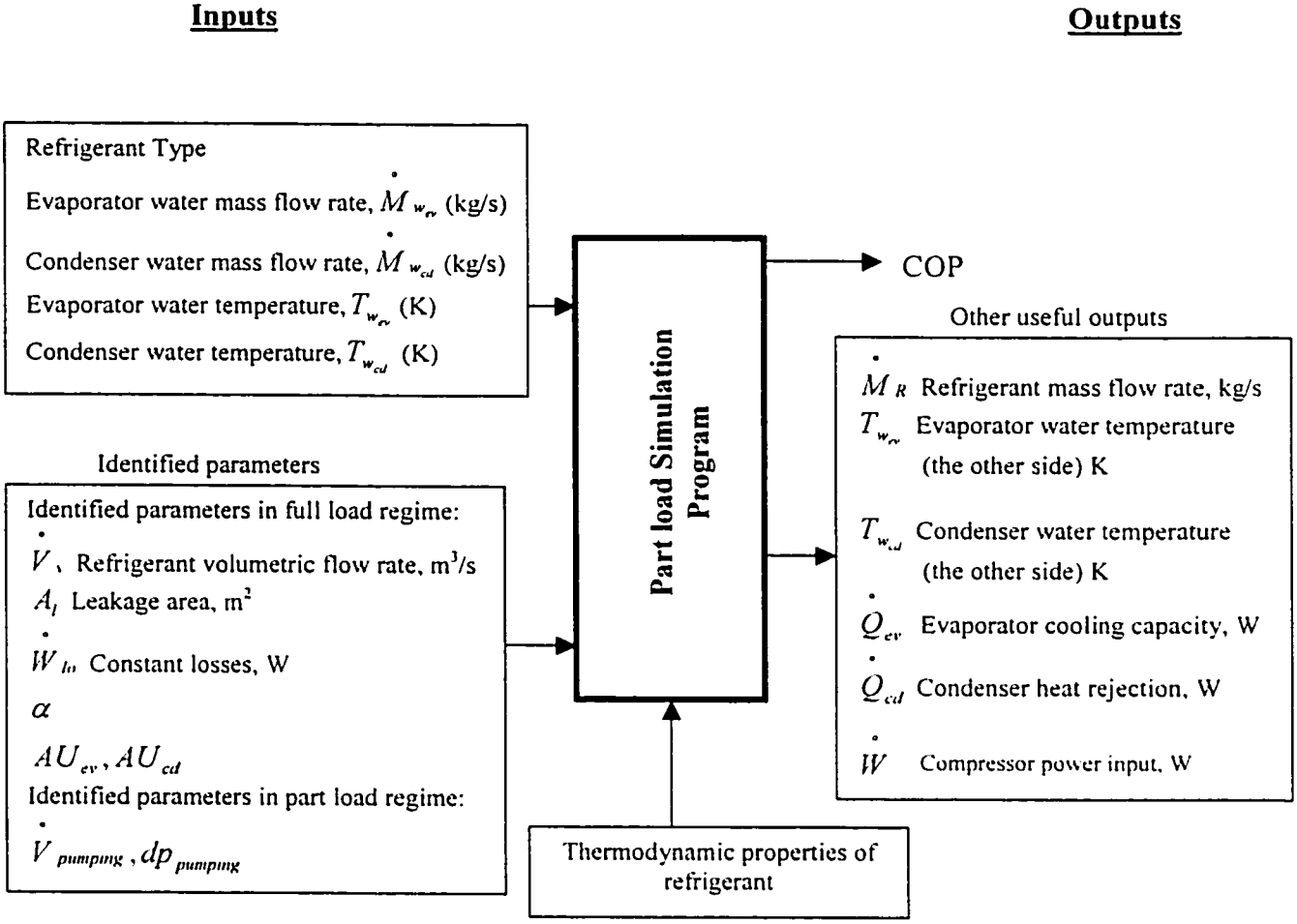

Figure 4-10 Information flow diagram of part load simulation [19]

CARRIER screw compressor chiller Model 30HXC076, refrigerant R-134a

Part load simulation typical input data

'AUev' 36000
'AUcd' 44000
'Losses' 9124.7520
'Alpha' -0.17678
'Al' 0.0000895
'VsFL' 0.144040
'dpPumping' 17402.4
'Ifluid' 4
'Mfrwev' 10.9
'Mfrwcd' 12.8
'Choice' 1
'Twev1' 277.15
'Twcd1' 298.15
'PevG' 150000
'PcdG' 160000
'Mismatch' 0
'vratio' 0
'Vpumping' 0.019335

Part load simulation typical output data

OUTPUTS	Component: SCHIPLSI		
MfrRef	= .318081	Pev	= 51585.6
Pcomp	= 25239.1	Pcd	= 76825.1
COP	= 2.04388	Twev2	= 281.231
Twcd2	= 304.489		

Chapter 5

Application of ASHRAE Toolkit-I with manufacturer's data

In the past the chiller manufacturers used to present in their catalogues, information about their products such as cooling capacity and electric input, for the most used chilled water and condenser water temperatures. However recently the information available in the manufacturers' catalogues include only the nominal capacity of different models of chillers at standard conditions (chilled water temperature of 6.7°C and condenser temperature of 29.4°C). Additional information at different off-design conditions or at part load regime is given to the clients only upon their request, and is obtained using the manufacturer's selection software, which is not easily available.

On the other hand, ASHRAE Toolkit-I requires as input, the chiller parameters for at least two working points for each model, however the more data is available, the more precise are the results. Meanwhile using the old catalogues and doing simulation on an old product is far behind the objective of this research. This made it hard to obtain a complete set of information and limits the variety of chillers with different manufacturers to be introduced into the model.

Due to the difficulties in collecting the relevant technical data for screw chillers, this study was performed using catalogue technical information published in year 2000 for the twin-screw compressor model 30HXC with water-cooled condenser, working with

refrigerant R-134a, manufactured by the CARRIER Company. In spite of repeated attempts, no other manufacturer made available similar catalogues or relevant data.

The 30HXC model includes in fact 15 different models starting from 264 kW nominal capacity up to 931 kW. For each model the following information is available at three different condenser water entering temperature $T_{w,c,i}$ (25, 30, 35°C) and nine different chilled water leaving temperatures $T_{w,e,i}$ (4, 5, 6, 7, 8, 9, 10, 13, 16 °C) (Table B-1, Appendix B):

- Cooling capacity (kW)
- Compressor input (kW)
- Condenser water mass flow rate (L/s)
- Evaporator water mass flow rate (L/s)

For each model there are 27 working points available.

5.1 Identification of parameters at full load for the 30HXC chiller

The input files (one for each model) were prepared for the full load identification method explained in section 4.2.3. The identified parameters are summarized in Table 5-1.

To see the variation of the identified parameters between different models, some graphs are presented. To start with, the variation of the overall heat transfer coefficient of condenser and evaporator with nominal capacity are shown in Figure 5-1. As expected, the value of these coefficients increases as the nominal capacity increases. The results fit very well the linear relationship between the UA and nominal capacity, with $R^2 \approx 0.999$. It can also be seen that the condenser heat transfer coefficient is always higher than that

of the evaporator, that is due to the fact that the heat rejection in the condenser is the sum of evaporator load and compressor work.

Table 5-1 Identification parameters of 30HXC/R-134a chiller at full load regime

Model	$\dot{Q}_{ev}$ Nom. (W)	$\dot{W}$ (W)	AU_{ev} (W/K)	AU_{cd} (W/K)	$\dot{W}_{lo}$ (W)	α	$\dot{V}_s$ (m^3/s)	A_l (m^2)	$\dot{W}_{in}$ (W)
076	264000	54700	36000	44000	9124.8	-0.1768	0.144040	0.0000895	56520.8
086	300000	61500	40000	48000	9500.4	-0.1648	0.161669	0.0001080	63494.3
096	335000	68300	45000	54000	9989.4	-0.1546	0.178912	0.0001082	70357.7
106	370000	76800	51000	61000	5967.7	-0.0755	0.198814	0.0001244	78055.0
116	405000	81500	55000	66000	7385.4	-0.1222	0.218846	0.0001445	85855.5
126	475000	88500	60000	72000	7721.3	-0.1152	0.236926	0.0001266	92768.8
136	510000	98800	67000	80000	17238.9	-0.1796	0.258762	0.0001576	101260.5
146	510000	107100	72000	86000	12847.6	-0.1318	0.282200	0.0001891	110248.1
161	545000	114900	76000	92000	-16523.3	0.7651	0.192250	-0.0002325	76738.5
171	580000	121700	81000	97000	-11862.2	0.7646	0.195680	-0.0002750	76824.6
186	615000	130500	80000	104000	-13501.2	0.8073	0.205986	-0.0003055	80936.3
206	743000	150100	103000	123000	-11741.7	0.6649	0.251646	-0.0003336	99229.6
246	866000	176500	121000	145000	-16960.6	0.7139	0.292139	-0.0004068	113510.7
261	896000	184800	125000	149000	-19400.7	0.8040	0.292407	-0.0004590	115594.1
271	931000	193800	130000	156000	-16448.3	0.7773	0.305521	-0.0004751	120413.7

* The values are for the standard condition. To see the values of internal power in other conditions refer to Table D-1 in Appendix D.

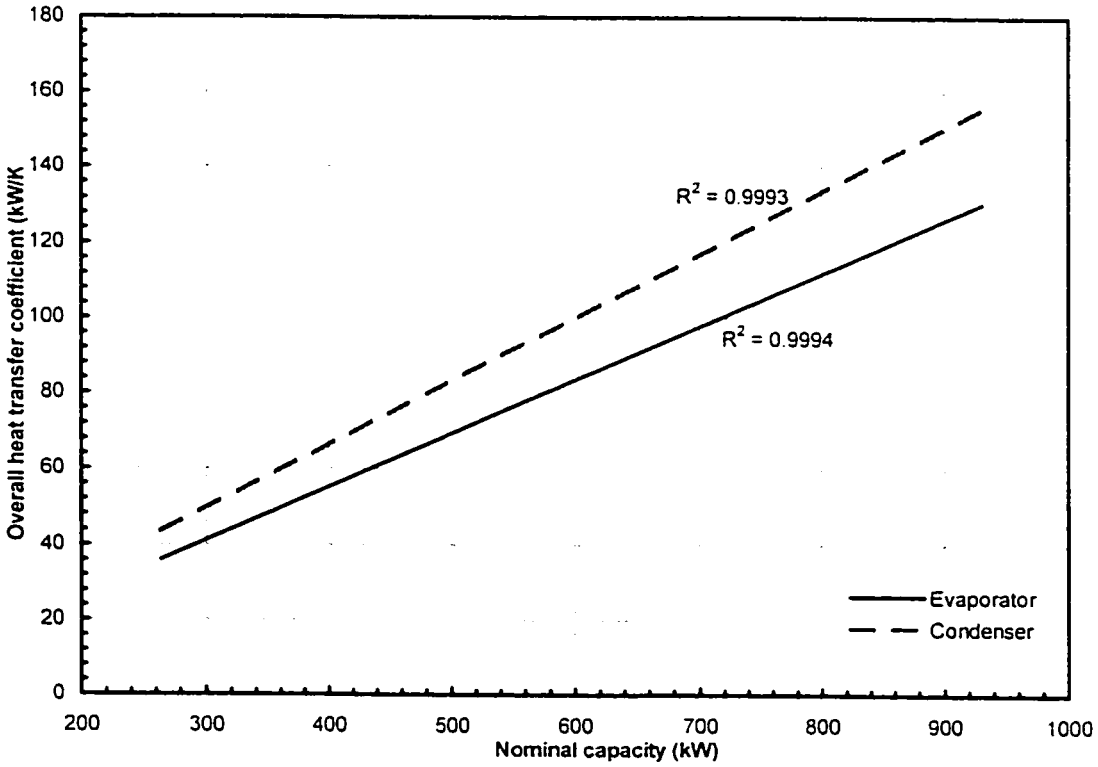

Figure 5-1 Variation of the overall heat transfer coefficients with nominal capacity

Figure 5-2 shows that by increasing the nominal capacity, the refrigerant volumetric flow rate increases, however there is a discontinuity between models 146 and 161 (510kW and 545 kW nominal capacities). By considering this discontinuity, the models can be grouped in two classes: less than 540kW and greater than 540 kW (Table 5-1).

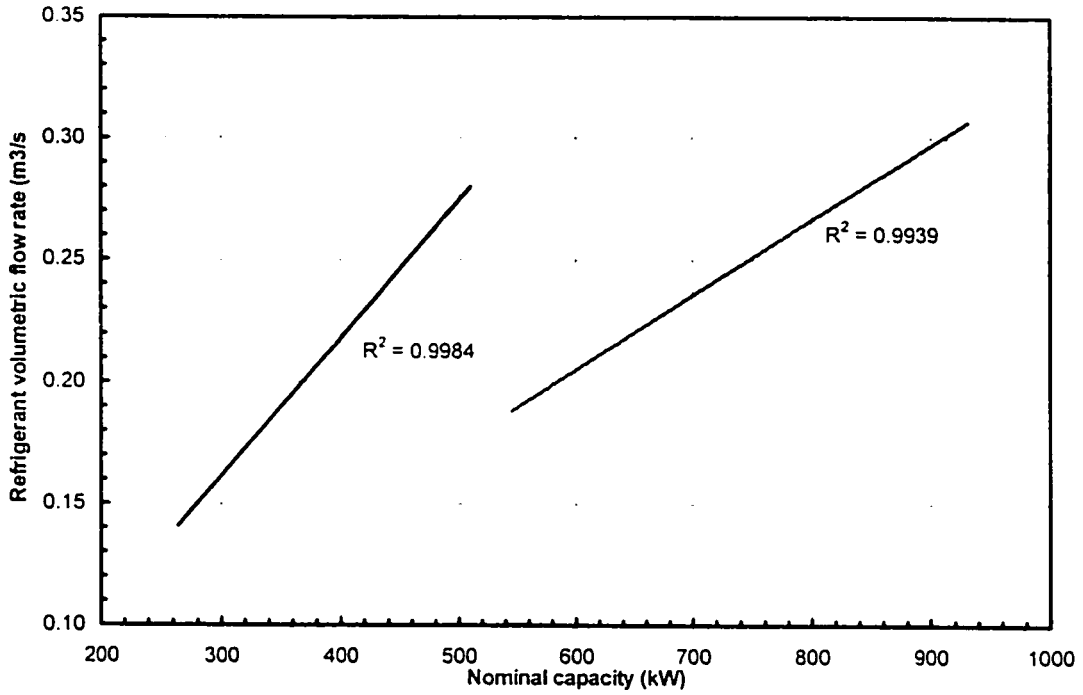

Figure 5-2 Variation of refrigerant volumetric flow rate with nominal capacity

This remarkable drop in refrigerant flow rate indicates a significant variation of the construction characteristics, which could possibly be because of some constraints or limitations in the design aspects (refrigerant velocity, pressure drop). This could be a deterministic factor deferring from one manufacturer to another.

Concerning the constant portion of losses, $\dot{W}_{lo}$ (Figure 5-3), the same discontinuity occurs between models 146 and 161. The variation of the coefficient α, which represents the variable electromechanical losses, shows the same discontinuity (Figure 5-4).

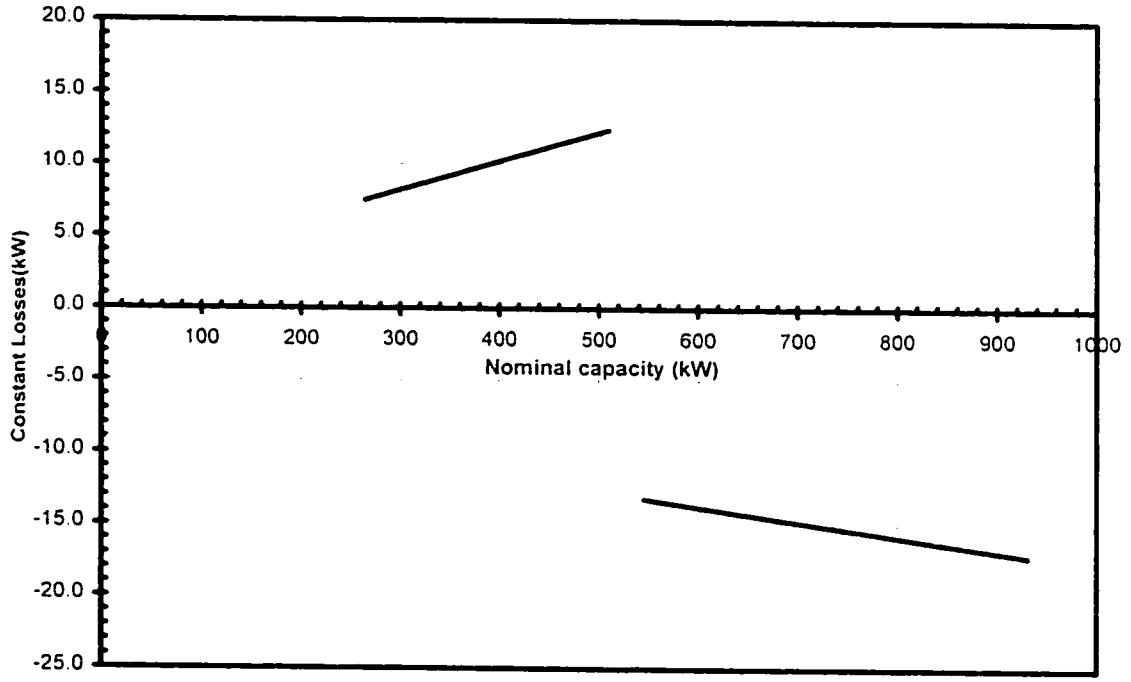

Figure 5-3 Variation of constant portion of losses ($\dot{W}_{lo}$) with nominal capacity

Figure 5-5 shows the variation of the total electromechanical losses ($\dot{W}_{lo} + \alpha \dot{W}_{in}$), at $T_{w,in1} = 30°C$ and $T_{w,in2} = 7°C$ with the nominal capacity. The same discontinuity is noticed. The total electromechanical losses have small negative values for small capacities, which might be due to the rounding errors or the sensitivity of the identification model to the input data (it will be discussed in section 5.3). The total electromechanical losses for small capacities can be considered as equal to zero.

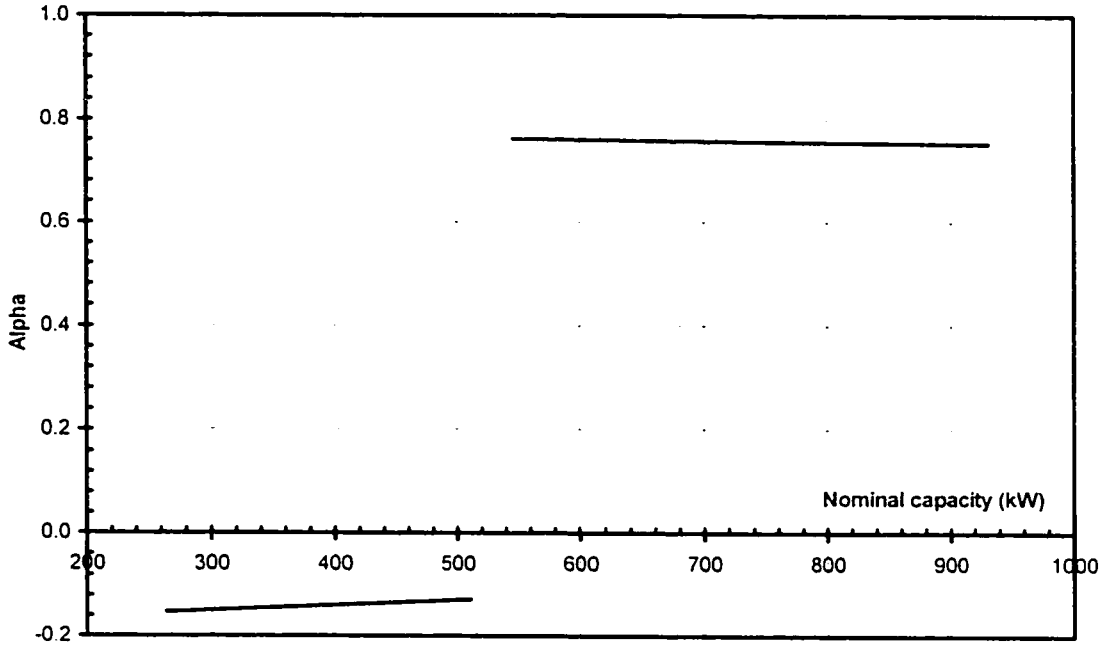

Figure 5-4 Variation of α with nominal capacity

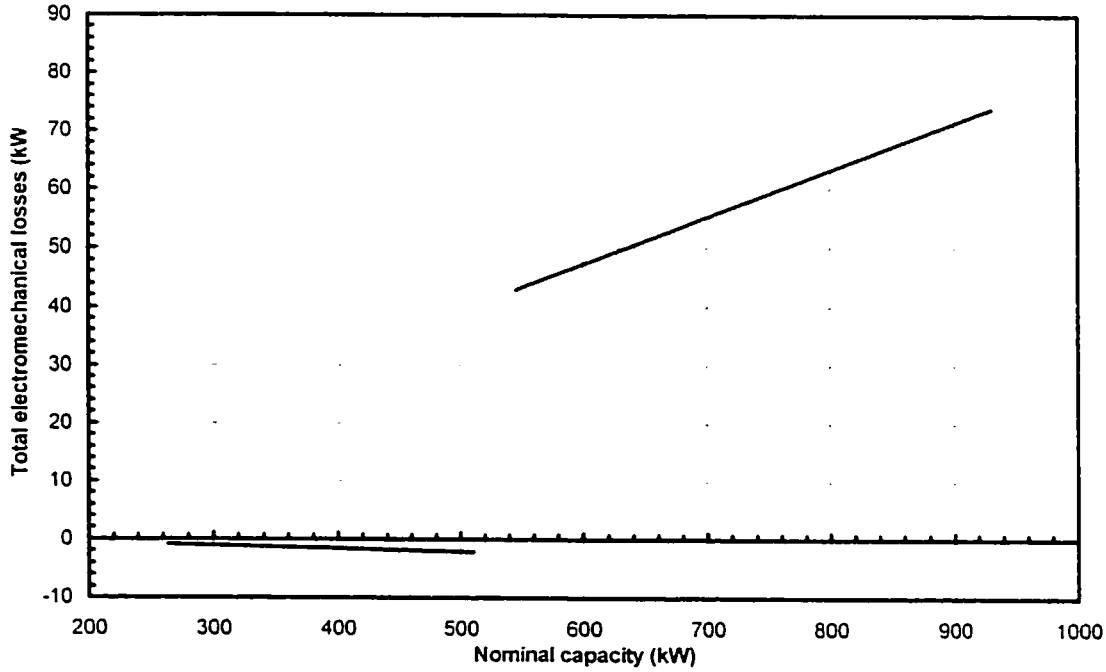

Figure 5-5 Variation of total electromechanical losses with nominal capacity

Another useful output coming out of identification model is the internal power $\dot{W}_{in}$. The variation of $\dot{W}_{in}$, at $T_{w,cd1} = 30°C$ and $T_{w,ev1} = 7°C$ with nominal capacity is illustrated in Figure 5-6. With the increase of capacity, the compressor internal load increases. The results fit very well the linear relationship between $\dot{W}_{in}$ and $\dot{Q}_{ev}$, with $R^2 \approx 0.99$. The same discontinuity is noticed around 540kW. The internal power $\dot{W}_{in}$ is almost equal to the power input $\dot{W}$ for the capacities less than 540kW (Figure 5-6), and is much less than the total power input for the capacities greater than 540 kW.

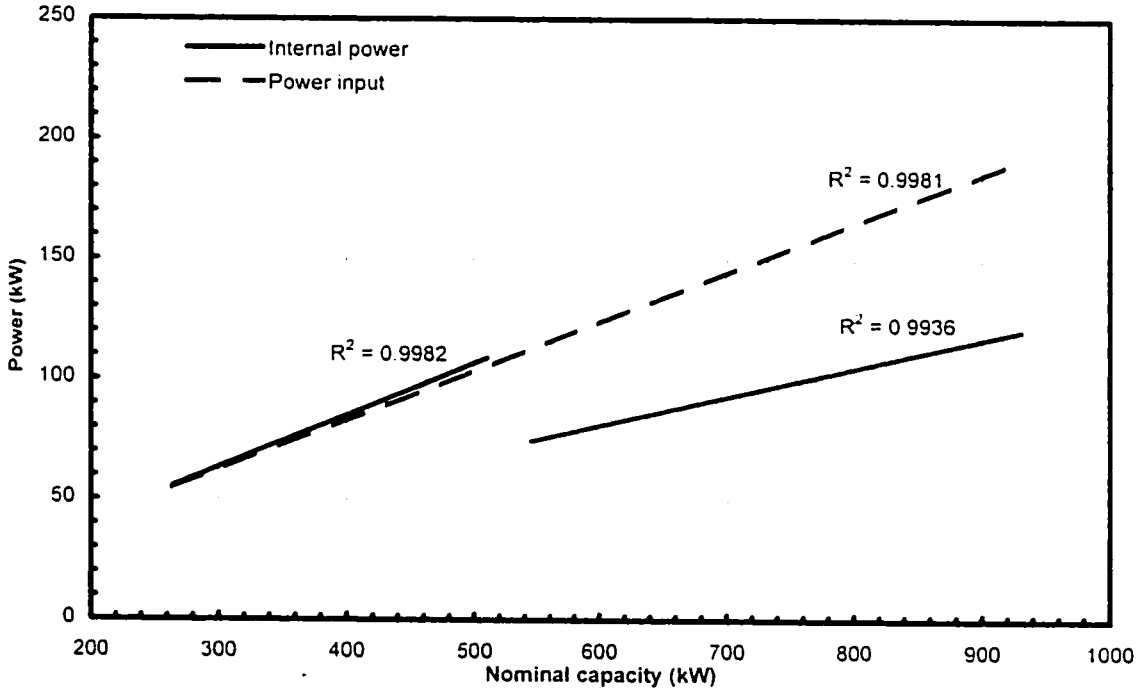

Figure 5-6 Variation of input power with nominal capacity

The last identified parameter is the leakage area, which shows two different variations for two groups of chillers (Figure 5-7). For the chillers with nominal capacities less than 540kW this value is positive and increasing with capacity while for the chillers with nominal capacities greater than 540kW, it is negative and decreasing.

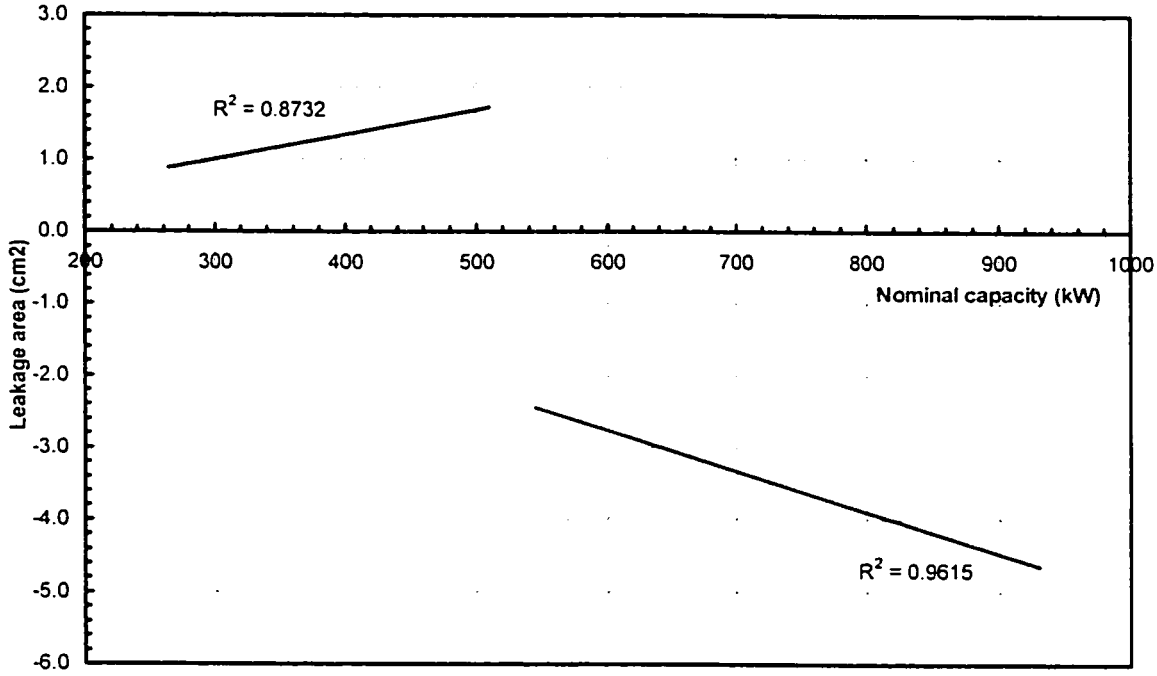

Figure 5-7 Variation of leakage area with nominal capacity

5.2 Modification of the identification program

The negative values of leakage area and total electromechanical losses, together with the values of $\dot{W}_m$ which are greater than $\dot{W}$, revealed some inconsistencies in the computer program included in the ASHRAE Toolkit-I for the modeling of the screw chiller.

First the iterative calculations were verified to ensure that the convergence is reached before the calculations stop. The convergence was reached after a maximum of seven iterations. Therefore the problem is hidden somewhere else.

As discussed in section 4.2.1, the main equations governing the whole procedure and iterations are equations (4-1) and (4-21) that can also be rewritten as in the form of equations (5-1) and (5-2).

$$\dot{W} = \dot{W}_{lo} + (1+\alpha)\dot{W}_{m} \tag{5-1}$$

$$Y(i) = \dot{V}_{s} + (-A_l)X(i) \tag{5-2}$$

Both the equations can be presented in a general form of:

$$Y = aX + b \tag{5-3}$$

where in equation (5-1) $Y = \dot{W}$, $X = \dot{W}_{m}$ and the coefficients are:

$$a = (1+\alpha) \tag{5-4}$$

$$b = \dot{W}_{lo} \tag{5-5}$$

and in equation (5-2) $Y = Y(i)$, $X = X(i)$ and the coefficients are:

$$a = -A_l \tag{5-6}$$

$$b = \dot{V}_{s} \tag{5-7}$$

Since a single value of each identified parameter is sought for all working points of one chiller model, the coefficients "a" and "b" are estimated using the least-squared statistical method:

(for n working points)
$$a = \frac{\sum_{i=1}^{n} X_i Y_i - \frac{1}{n}\sum_{i=1}^{n} X_i Y_i}{\sum_{i=1}^{n} X_i^2 - \frac{1}{n}(\sum_{i=1}^{n} X_i)^2} \tag{5-8}$$

$$b = \frac{1}{n}\sum_{i=1}^{n} Y_i - a\frac{1}{n}\sum_{i=1}^{n} X_i \tag{5-9}$$

Leakage area A_l as one of the coefficients in equation (5-2) appears to be the source of the inconsistencies mentioned before.

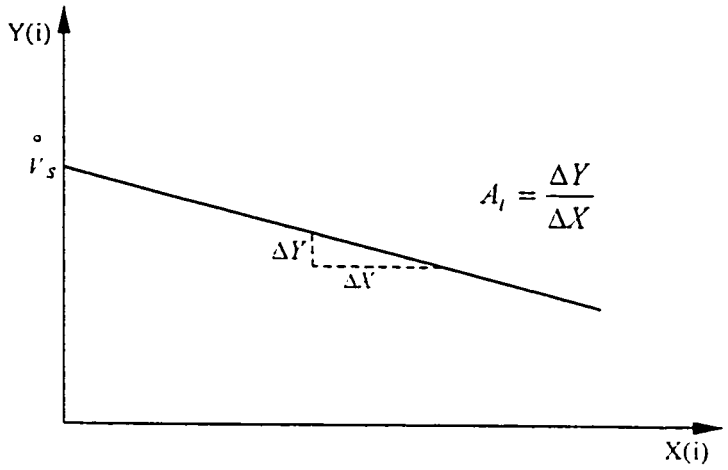

Figure 5-8 Graphical illustration of equation (5-2)

In the original identification program, the negative sign of "a" is introduced twice in the equations (5-2) and (5-8); in the latter, the denominator is $\sum_{i=1}^{n} X_i^2 - \frac{1}{n}(\sum_{i=1}^{n} X_i)^2$, instead of $\frac{1}{n}(\sum_{i=1}^{n} X_i)^2 - \sum_{i=1}^{n} X_i^2$, based on the least-squared method. As a result, the slope of equation (5-3) is positive, which contradicts equation (5-2). Moreover, A_l is modified in each iteration, and it plays a significant role in the estimation of volumetric flow rate. The original identification program was modified. To see the list of the modified program refer to appendix E.

The results obtained after the modification of the original identification program are tabulated in Table 5-2.

Table 5-2 Identification parameters of 30HXC R134a chiller at full load regime after modification of procedure

Model	$\dot{Q}_{ev}$ Nom. (W)	$\dot{W}$ (W)	AU_{ev} (W/K)	AU_{cd} (W/K)	$\dot{W}_{lo}$ (W)	α	$\dot{V}_r$ (m^3/s)	A_l (m^2)	$\dot{W}_m$ (W)
076	264000	54700	36000	44000	8253.8	0.1439	0.14043	0.000061	41346.0
086	300000	61500	40000	48000	6878.3	0.2286	0.15718	0.000073	45152.8
096	335000	68300	45000	54000	6873.6	0.2026	0.17452	0.000074	51926.8
106	370000	76800	51000	61000	3185.4	0.3109	0.19372	0.000085	57036.2
116	405000	81500	55000	66000	5392.2	0.2546	0.21284	0.000098	61484.9
126	475000	88500	60000	72000	4907.2	0.2740	0.23039	0.000106	66411.7
136	510000	98800	67000	80000	9562.4	0.2110	0.25230	0.000107	74714.5
146	510000	107100	72000	86000	7871.8	0.2769	0.27425	0.000128	78543.1
161	545000	114900	76000	92000	9088.3	-0.0776	0.19892	-0.000175	116550.0
171	580000	121700	81000	97000	18410.6	-0.1619	0.20344	-0.000208	125726.0
186	615000	130500	80000	104000	21425.4	-0.1777	0.21453	-0.000231	135337.0
206	743000	150100	103000	123000	21875.2	-0.1708	0.26104	-0.000252	158316.0
246	866000	176500	121000	145000	23087.8	-0.1620	0.30347	-0.000308	187367.0
261	896000	184800	125000	149000	30288.0	-0.1988	0.30507	-0.000348	197505.0
271	931000	193800	130000	156000	32694.9	-0.1977	0.31866	-0.000360	205084.0

* The values are for the standard condition. To see the values of internal power in other conditions refer to Table D-2 in Appendix D.

The overall heat transfer coefficients at the condenser and evaporator remain unchanged because they are calculated separately and have no interaction with the other identified parameters. Again the same two groups of chillers can be recognized from Table 5-2. In the group of chillers with the nominal capacity greater than 540kW the inconsistency can be seen and that is the values of $\dot{W}_m$ which is greater than $\dot{W}$.

Figure 5-9 shows the variation of $\dot{W}_m$ and $\dot{W}$ with nominal capacity, at $T_{w_{ev2}} = 7°C$ and $T_{w_{cd1}} = 30°C$. The variation of the refrigerant volumetric flow rate and the leakage area with nominal capacity are illustrated in Figure 5-10 and 5-11.

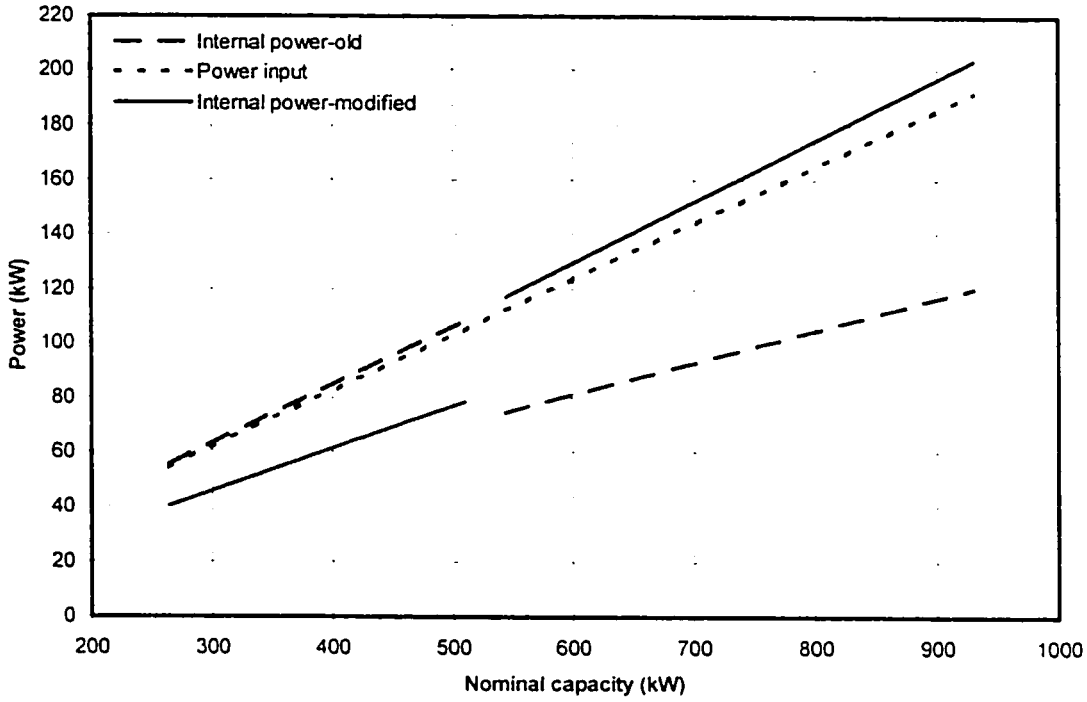

Figure 5-9 Variation of internal power with nominal capacity at $T_{w_{cw2}} = 7°C$ and $T_{w_{cw1}} = 30°C$ (after modification)

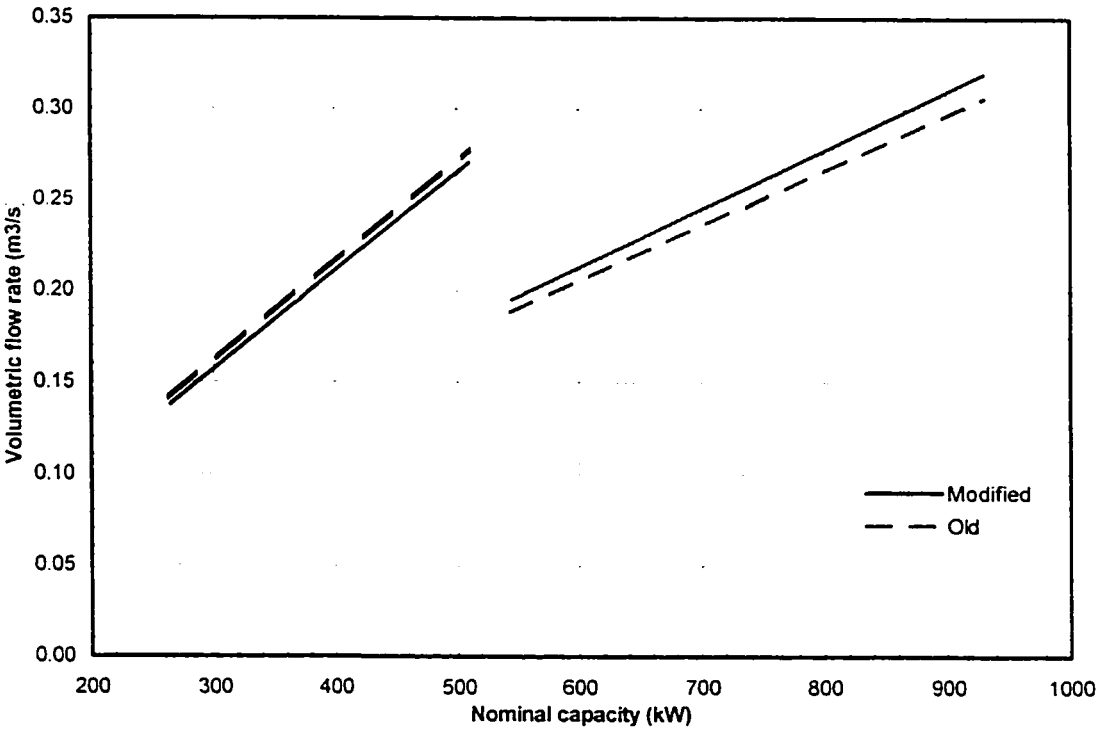

Figure 5-10 Variation of refrigerant volumetric flow rate with nominal capacity (after modification)

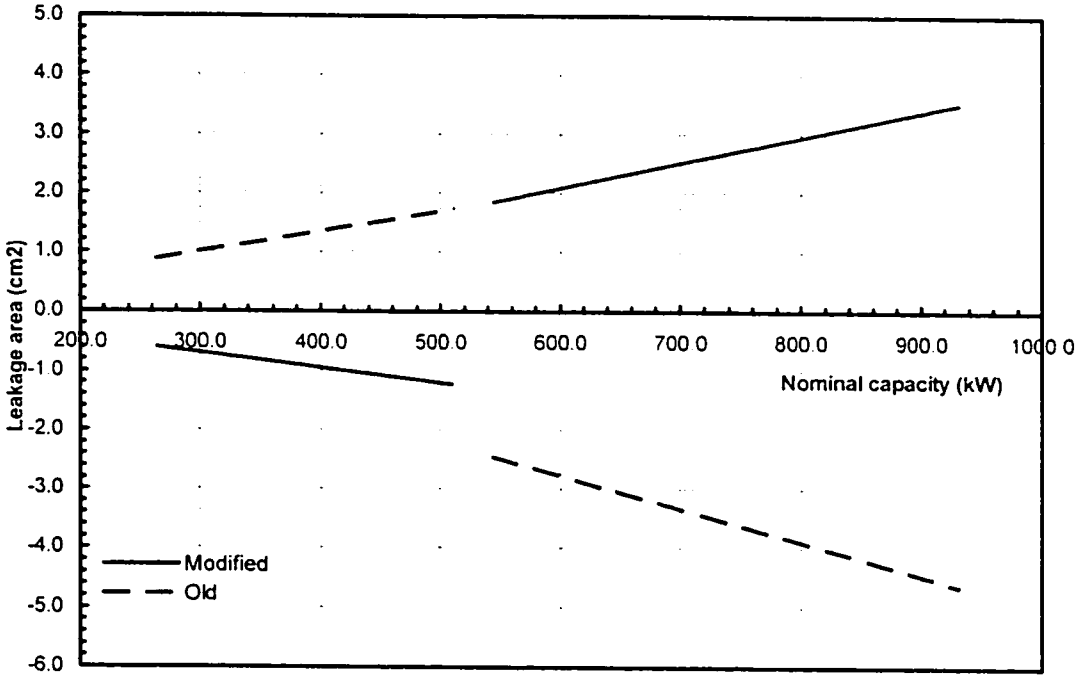

Figure 5-11 Variation of the leakage area with nominal capacity (after modification)

5.3 Sensitivity of the identification to input data

In the section 5.1 it was mentioned that some inconsistency might be due to sensitivity of the program to some input data. This issue is important in the way that it will give us the idea of how the errors in the manufacturer's data would affect the simulation. In this section the sensitivity of the program to input data including evaporator cooling capacity $\dot{Q}_{ev}$, compressor input power $\dot{W}$, evaporator water flow rate $\dot{M}_{w_{ev}}$ and condenser water flow rate $\dot{M}_{w_{cd}}$, is examined.

The evaporator cooling capacity at standard conditions ($T_{w_{ev1}} = 7°C, T_{w_{cd1}} = 30°C$) was changed while the other variables remained constant. The result is shown in Figure 5-12. As can be seen, the parameters α and $\dot{W}_{lo}$ are very sensitive to the variation of

$\dot{Q}_{ev}$, however their variations have different signs. The total losses are less sensitive than the two components α and $\dot{W}_{la}$. The other parameters, $\dot{V}_s$, A_f and $\dot{W}_{in}$ are not very sensitive to the evaporator load variation. Although accuracy of $\dot{Q}_{ev}$ does effect α and $\dot{W}_{la}$ which can be considered as internal variables, it does not affect the other identification parameters very much.

Figure 5-13 shows almost the same results for the compressor input power, $\dot{W}$. The difference is that the negative and positive changes of $\dot{W}$ have opposite effect on α and $\dot{W}_{la}$ while the changes of $\dot{Q}_{ev}$ in any direction have the same effect.

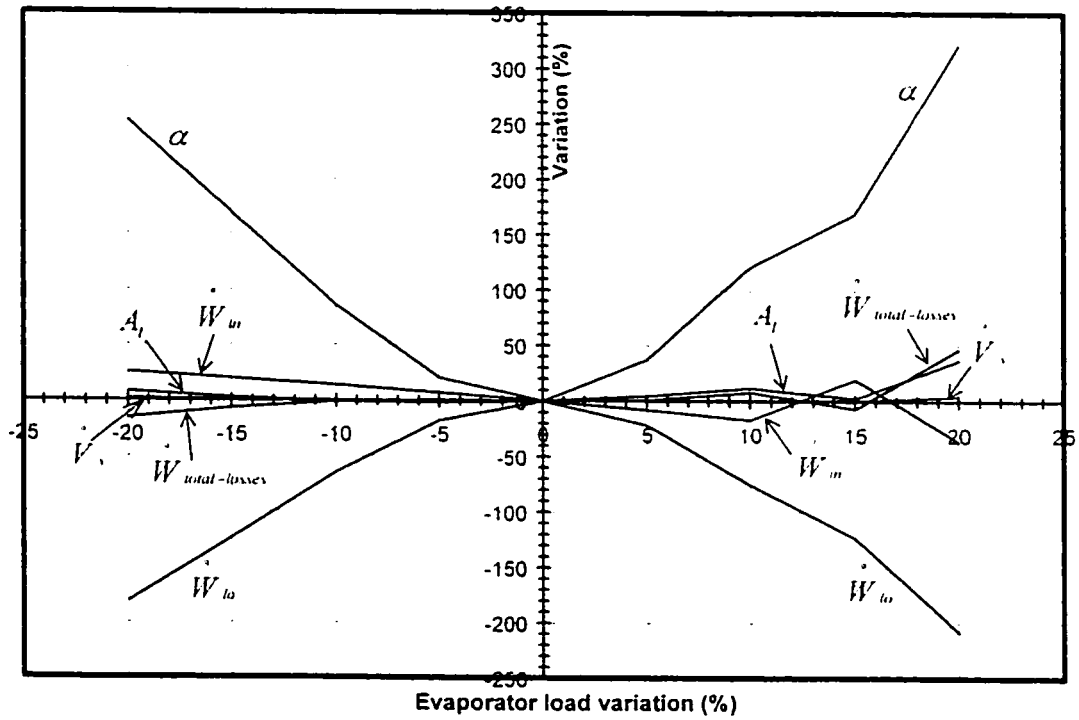

Figure 5-12 Sensitivity of the identification procedure to the evaporator cooling capacity

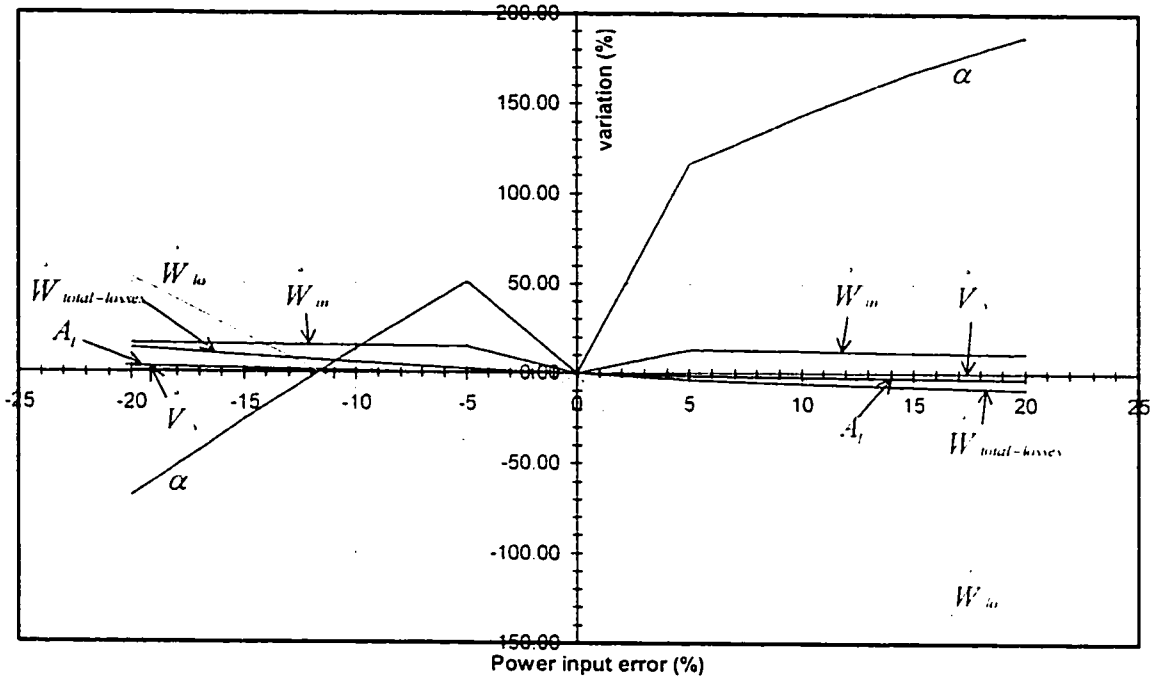

Figure 5-13 Sensitivity of the identification procedure to the compressor input power

Figures 5-14 and 5-15 show the effect of evaporator and condenser water flow rate on the identification parameters. The accuracy of data about the water flow rate at the evaporator and condenser have remarkable effect on α, $\dot{W}_{lo}$ and $\dot{W}_{in}$, and almost no effect on other identified parameters.

It can be concluded that the identified losses ($\dot{W}_{lo}$, $\alpha\dot{W}_{in}$) in the compressor are very sensitive to the input data ($\dot{Q}_{cv}$, $\dot{W}$, $\dot{M}_{w_{ev}}$, $\dot{M}_{w_{cd}}$), while the other identified parameters ($\dot{V}_s$, A_l, UA_{cd}, UA_{ev}) are not. It is worth mentioning again that the constant and variable parts of the electromechanical losses when considered together are not sensitive to the input data, while alone they are very sensitive. Therefore, the accuracy of manufacturer's data affects significantly the identification of individual losses.

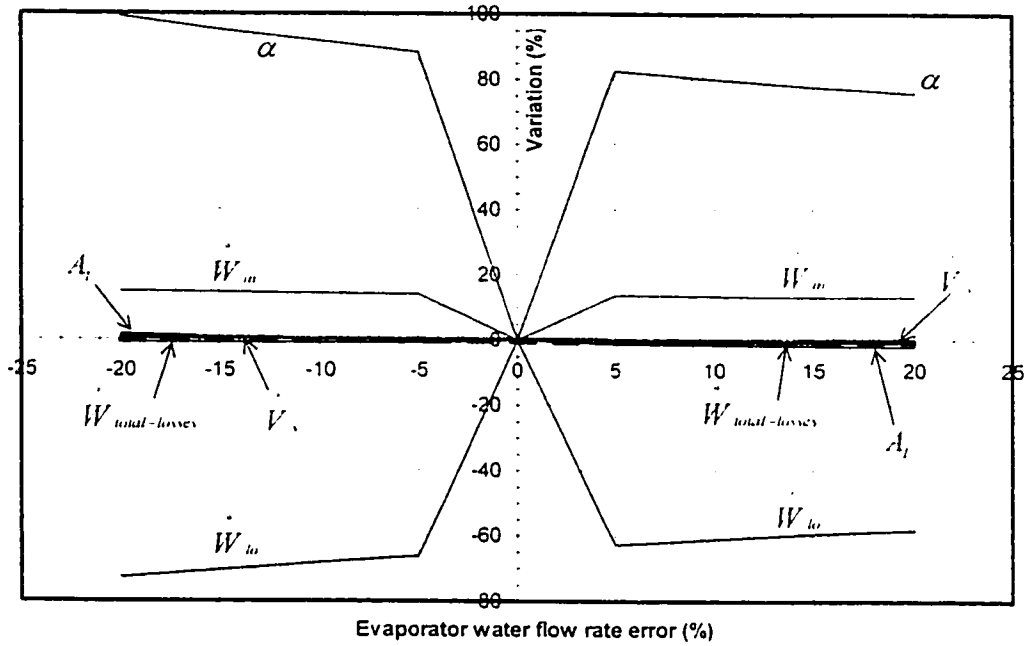

Figure 5-14 Sensitivity of the identification procedure to the evaporator water flow rate

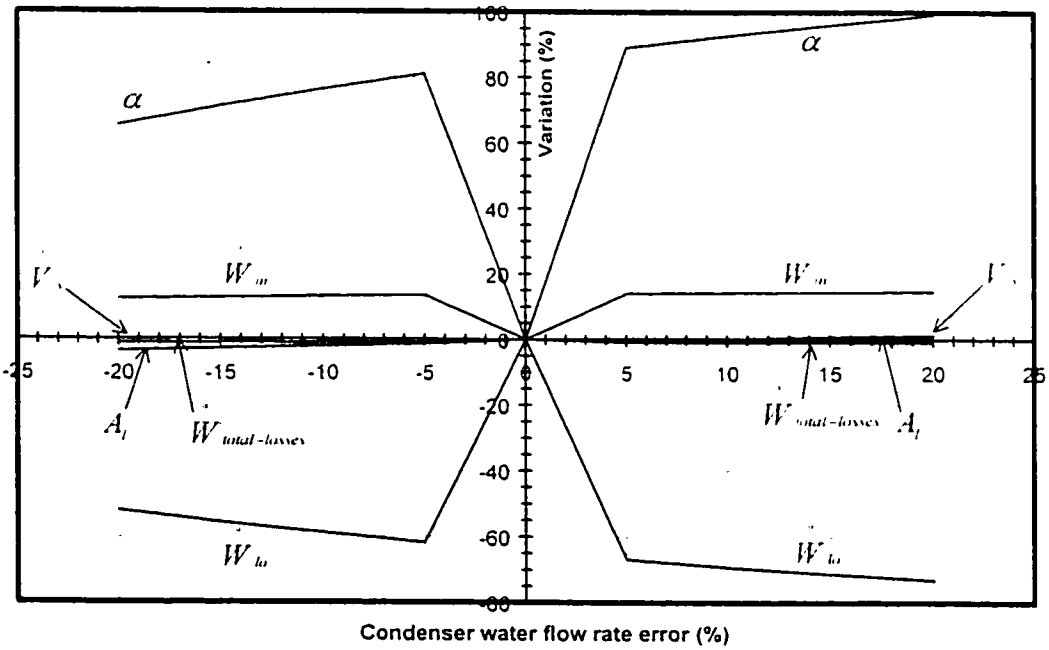

Figure 5-15 Sensitivity of the identification procedure to the condenser water flow rate

Chapter 6

Development of correlation-based models for screw compressor chillers

This chapter consists of three main parts. In the first part composed of sections 6.1 to 6.5, a correlation-based model is developed on a generic format that is used by the DOE-2 simulation program. It is important to note that the DOE-2 program does not contain correlations for this type of chillers.

On the second part, section 6-6, the correlations mentioned in section 6.1 to 6.5 are presented taking some other variables into account. Finally in the last part, section 6.7, new correlations are developed based on identified parameters, which are the chillers physical specification together with other relevant variables.

The sections 6.1-6.7 use data from the CARRIER company, screw chillers models 076 to 146 with the capacities less than 540 kW.

Section 6.8 presents the comparison between the correlation-based models developed by using data from two manufacturers.

6.1 Simulation of full load operation

Once all the identified parameters are known, the input file for the simulation program can be constructed, as explained in section 4.3.2.

For each working point, the program is run along with the identified parameters at full load to calculate the COP. The calculations are performed for eight models, using 27 working points per model, which give a total number of 216 values of the COP. Table 6-1 shows the estimated COP at full load compared with the measured values of the first

model (model 076), together with the corresponding identified variables. The results for other chiller models are presented in Table F-1 in appendix F.

Table 6-1 Typical results for the 30HXC/R-134a Carrier screw-compressor chiller at full load

Model	$\dot{Q}_{ev}$ (kW)	$T_{w_{ev2}}$ (°C)	$T_{w_{cd1}}$ (°C)	COP (toolkit)	COP (actual)	Identified Parameters						
						$\dot{Q}_{ev}$ Nom. (kW)	UA_{ev} (kW/K)	UA_{cd} (kW/K)	$\dot{W}_{lo}$ (kW)	α	$\dot{V}_{s}$ (m^3/s)	A_f (cm^2)
076	253.3	4	25	3.95	5.26	264	36	44	8.25	0.143929	0.14043	0. 611
	264.0	5	25	4 06	5.43							
	274.8	6	25	4.17	5.57							
	285.8	7	25	4.28	5.72							
	297.0	8	25	4.40	5.88							
	307.1	9	25	4.51	6.03							
	316.8	10	25	4.63	6.19							
	333.2	13	25	4.98	6.47							
	330.1	16	25	5.34	6.42							
	234.3	4	30	3.38	4.40							
	244.2	5	30	3.47	4.58							
	254.6	6	30	3.57	4.70							
	265.5	7	30	3.66	4.85							
	276.7	8	30	3.75	5.02							
	288.1	9	30	3.81	5.18							
	299.5	10	30	3 94	5.32							
	318.8	13	30	4.23	5.54							
	315.2	16	30	4.51	5.50							
	219.0	4	35	2.92	3 72							
	227.2	5	35	2.99	3 83							
	235.6	6	35	3.08	3.95							
	244.7	7	35	3.14	4.07							
	254.9	8	35	3.22	4.20							
	265.4	9	35	3.30	4.33							
	276.5	10	35	3.38	4.47							
	295.3	13	35	3.38	4.75							
	291.7	16	35	3.85	4.66							

Although there are some other useful outputs as discussed in section 4.3.3, COP is the most essential output that is required for this study.

The difference between the actual COP and the calculated COP gives an indication on the precision of the model; the standard error SE is equal to 1.31 and the coefficient of variance C.V. is 26.03%, which represents a significant difference between the values of calculated COP and the actual COP.

Figure 6-1 shows the variation of COP with the condenser entering water temperature and the chilled water leaving temperature based on the calculations.

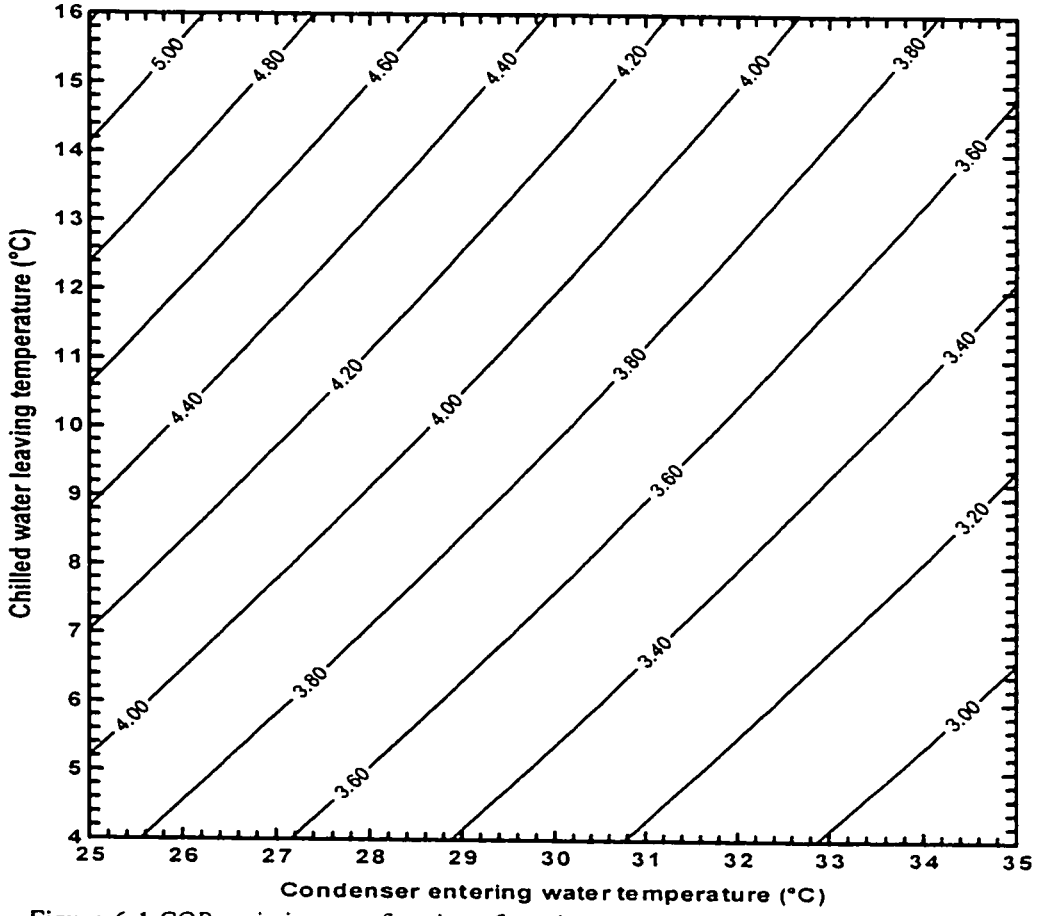

Figure 6-1 COP variation as a function of condenser entering water temperature and chilled water leaving temperature for all 30HXC models

Figure 6-1 shows that in different conditions the chiller performs at the same COP (for all 30HXC models). For instance at $T_{w_{cnd2}} = 5^{\circ}C$ and $T_{w_{evp1}} = 29.8^{\circ}C$ the COP is 3.4, while the same COP is expected at $T_{w_{cnd2}} = 7^{\circ}C$ and $T_{w_{evp1}} = 31.4^{\circ}C$. This determines the limits of condenser and evaporator temperatures when a minimum COP is required.

6.2 Identification of parameters at part load

Based on section 4.4.2, the input files for the part load identification were developed. For each working point (fixed condenser entering and evaporator leaving water temperature), six part load ratios were considered; 0.3,0.4,0.5,0.6,0.8,0.9. Therefore, the calculations were presented for 1728 different working points (8 models × 27 working points per model ×8 part load ratios per working point). For each working point, two parameters were identified, $\dot{V}_{pumping}$ and $dp_{pumping}$, which are required for part load simulation. It should be noted that based on the suggestion of the authors of the ASHRAE Toolkit-I, the part load ratios below 0.2 and above 0.9 were not used. Some results of part load identification for the chiller model 076 are shown in Table 6-2 as examples.

Table 6-2 Typical results of identification for the 30HXC/R-134a Carrier chiller at part load regime (model 076, with nominal capacity of 264 kW)

$T_{w_{ev2}}$ (°C)	$T_{w_{cd1}}$ (°C)	PLR	$\dot{V}_{pumping}$ (m^3/s)	$dp_{pumping}$ (W)
5	30	0.3	0.119586	62654.7
		0.4	0.107805	56654.0
		0.5	0.096124	50802.0
		0.6	0.084474	44921.3
		0.8	0.061167	32486.3
		0.9	0.049487	25456.0
6	30	0.3	0.118798	61685.0
		0.4	0.106865	54947.2
		0.5	0.095024	48152.4
		0.6	0.083212	41043.0
		0.8	0.059576	24612.9
		0.9	0.047730	14032.1
7	30	0.3	0.117976	60553.6
		0.4	0.105868	52960.1
		0.5	0.093846	45061.1
		0.6	0.081851	36494.0
		0.8	0.057844	15172.1
		0.9	0.045813	49.2

6.3 Simulation of part load operation

Using the results of partial load identification, the input files based on the format explained in section 4.5.2 have been formed. Hence, 1728 COP for all working points were obtained. Some results for the chiller model 076 are shown in table 6-3 as examples. The results obtained for other working points are available in Table F-2 in Appendix F.

Table 6-3 Typical results of simulation for the 30HXC/R-134a Carrier chiller at part load regime (model 076, with nominal capacity of 264 kW)

$T_{w_{cd1}}$ (°C)	$T_{w_{ev2}}$ (°C)	PLR	COP_{PL}
25	4	0.3	3.74
25	4	0.4	4.50
25	4	0.5	4.96
25	4	0.6	5.23
25	4	0.8	5.38
25	4	0.9	5.34
30	4	0.3	2.99
30	4	0.4	3.61
30	4	0.5	4.02
30	4	0.6	4.26
30	4	0.8	4.45
30	4	0.9	4.44
35	4	0.3	2.43
35	4	0.4	2.95
35	4	0.5	3.31
35	4	0.6	3.53
35	4	0.8	3.72
35	4	0.9	3.74

6.4 Correlation-based model based on DOE-2 format

The goal of the study is to develop correlation-based models for estimating the electric demand of the screw-compressor chiller, which can be used in the estimation of energy performance of HVAC systems. Generally, the manufacturer's technical

catalogue does provide the electric demand only at full load for some entering condenser water temperature and chilled water leaving temperatures.

A chiller has different cooling capacity and COP when it works at different condenser and evaporator water temperatures (off-design conditions). Also when it operates at part load regime, the chiller has a different COP.

The general formula to calculate the electric demand of a chiller, used by the DOE-2 program is [8]:

$$\text{Electric input} = CAP_d \times EIR_d \times F_1 \times F_2 \times F_3 \times FRAC \qquad (6\text{-}1)$$

where:

CAP_d: design capacity, the cooling capacity at design conditions (7°C chilled water leaving temperature, and 30°C condenser entering water temperature) according to ARI standards.

EIR_d: the design electric input ratio; the ratio of the compressor power input to the cooling capacity at design conditions.

F_1 : correction factor for the COP at full-load regime at off-design conditions

$$F_1 = \left(\frac{COP_d}{COP_c} \right)_{FL}$$

F_2 : correction factor for the COP at part load regime at off-design conditions

$$F_2 = \frac{(COP_c)_{FL}}{(COP_c)_{PL}}$$

F_3 : correction factor for the cooling capacity at off-design conditions

$$F_3 = \frac{CAP_x}{CAP_d}$$

the above coefficients must respect the following condition:

$F_1 = F_3 = 1$ at standard condition ($T_{w_{co}} = 7°C$ and $T_{w_{ci}} = 30°C$), and $F_2 = 1$ at full load regime (PLR=1).

FRAC: the fraction of hours that the required capacity is below the minimum operating capacity of the chiller.

$$FRAC = \frac{\text{required capacity}}{\text{Minimum operating capacity}}$$

F_1, F_2 and F_3 are correction factors, used to estimate the COP and capacity of chiller at off-design working conditions. The advantage of the above generic formula consists in its practical application; the user needs only to know the COP at full load and at design conditions. The correction factors have to be developed only once for each chiller type such as screw or centrifugal.

6.5 Calculation of correction factors based on DOE-2 format

6.5.1 Deriving required coefficients

The three numerical values of the correction factors F_1, F_2 and F_3 have been found based on the outputs obtained from the full and part load simulations. The correlation-based models of F_1, F_2 and F_3 in terms of $T_{w_{co}}$ and $T_{w_{ci}}$ were developed using the previously estimated COP values, and the regression techniques available in the Statgraphics program [31].

Special attention was given to the development of the correlation for F_2. Initially the correlation for $COP_{x_{PL}}$ was derived based on part load simulation mentioned in section 6.3. The form of correlation was kept as the DOE-2 format, that is, a function only of PLR ($COP_{x_{PL1}}$ in Table 6-4). However this format did not fit well the COP data (very low value of R^2 and high value of C.V.). Another type of function was then considered, in which the COP_{PL} is not only a function of PLR, but also of the evaporator and condenser water temperatures ($COP_{x_{PL2}}$ in Table 6-4). The results are shown in table 6-4. The statistical information shows that the functions of $COP_{x_{PL1}}$ and $COP_{x_{PL2}}$ fit well the actual data.

Table 6-4 Coefficients of the COP correlations at full load and part load regimes

	$a+b*T_{w_{ev1}}^2+c*T_{w_{ev1}}+d*T_{w_{ev2}}^2+e*T_{w_{ev2}}+f*T_{w_{ev1}}*T_{w_{ev2}}+g*PLR^2+h*PLR$							
	a	**b**	**c**	**d**	**e**	**f**	**g**	**h**
$COP_{x_{PL}}$	8.02711	0.0268889	-0.250483	0.000367989	0.203902	-0.00396354	0	0
$COP_{x_{PL1}}$	0.90111	0	0	0	0	0	-7.96202	11.8860
$COP_{x_{PL2}}$	7.81922	0.00530412	-0.455848	-0.00926693	0.450384	-0.0045712	-7.96205	11.8861

Statistical information

	SE	**MAE**	**C.V.(%)**	**R^2 (%)**
$COP_{x_{PL}}$	0.0833606	0.07446	2.22	98.22
$COP_{x_{PL1}}$	0.914104	0.763594	19.17	26.41
$COP_{x_{PL2}}$	0.253557	0.150992	5.32	94.36

Finally, the coefficient F_2 was considered as the ratio between $COP_{x_{PL}}$ and $COP_{x_{PL2}}$. It was verified that, while $COP_{x_{PL2}}$ depends on the $T_{w_{ev2}}$ and $T_{w_{cd1}}$, the correlation-based

model for F_2 is a function of PLR alone. Table 6-5 shows the correlations for F_1, F_2 and F_3.

Table 6-5 Coefficients F_1, F_2 and F_3 for the CARRIER 30HXC/R-134a screw compressor chillers

$$F_i = a + b*T_{w_{cdl}}^{\ 2} + c*T_{w_{cdl}} + d*T_{w_{evl}}^{\ 2} + e*T_{w_{evl}} + f*T_{w_{cdl}}*T_{w_{evl}} + g*PLR^2 + h*PLR$$

	a	b	c	d	e	f	g	h
F_1	0.420711	0.000340978	0.0160138	0.000444553	-0.0162125	-0.000507389	0	0
F_2	1.7921	0	0	0	0	0	1.8823	-2.6744
F_3	0.857144	-0.000199504	-0.0013426	-0.002059180	0.0723178	-0.000129739	0	0

Statistical information

	SE	MAE	C.V.(%)	R^2 (%)
F_1	0.0010772	0.0008423	0.11	99.99
F_2	0.0453489	0.0299612	5.65	85.35
F_3	0.133918	0.0104245	12.98	98.80

The statistical indicators show that the correlation of F_1 and F_2 represent well the actual data. In the case of F_3 the value of R^2 is acceptable, while the coefficient of variance is about 13%. However, since the input data came from the manufacturer's catalogue where the numbers are rounded up, the accuracy of results is acceptable.

As an example, the chiller model 076 with the design capacity of 265.5 kW produces 5°C leaving chilled water, and operates with a 35°C water temperature entering the condenser. Due to the off-design conditions, the available cooling capacity is reduced to 224.1 kW. The electric input to the compressor is calculated as follows:

$T_{w_{evl}} = 5°C$, $T_{w_{cdl}} = 35°C$, so using the correlations presented in from Table 6-5, the following coefficients are estimated:

At full load regime, F_1=1.24, F_3=0.849 and PLR =1, F_2=1

From Table 6-1, COP at design conditions ($T_{w_{ev2}} = 7°C$ and $T_{w_{cd1}} = 30°C$) is determined equal to 4.85. The design electric input ratio is calculated as:

$$EIR_d = \frac{1}{COP_d} = \frac{1}{4.85} = 0.206$$

Hence, the electric input at full load regime is determined from equation (6-1):

Electric input =$265.5 \times 0.206 \times 1.24 \times 1 \times 0.849 \times 1 = 57.6$

The electric input at full load regime is increased 2.9 kW in comparison with the electric input at design conditions (54.7 kW).

6.5.2 Comparison

The factors F_1, F_2 and F3 estimated in this study were compared with the factors used by the DOE-2 program for centrifugal chiller. It was not possible to make comparison for the screw chillers because presently the DOE-2 program does not contain the data for the energy demand estimation of screw chillers.

Variation of F_1 with condenser entering temperature and chilled water leaving temperature equal to 7°C has been illustrated in Figure 6-2 for both screw-compressor and centrifugal chiller whose coefficients were found in this study and DOE-2 respectively.

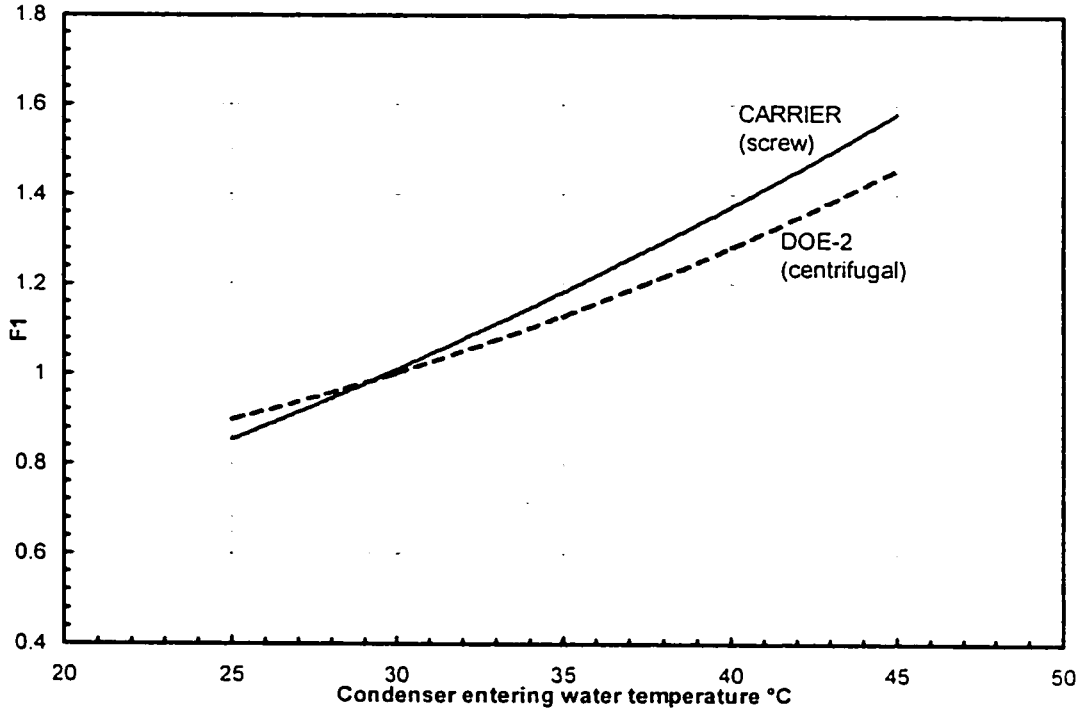

Figure 6-2 Variation of F_1 with the condenser entering water temperature, at chilled water leaving temperature=7°C

The results show almost the same variation and there is not a remarkable difference except at higher condenser water temperatures.

Figure 6-3 shows the variation of F_2 with the part load ratio PLR. This correction factor varies completely different in screw and centrifugal compressor chillers, which indicates the two types of chillers have a completely different performance in part loads. The centrifugal chillers require less electric input when operating in part load, while the electric input in screw chillers increases when the part load is less than 0.7. It is even higher than the full load electric input when the chiller is working in part load ratios less than 0.45.

Figure 6-4 shows that there is no remarkable difference between the two chillers with respect to F_3, except at higher condenser water temperatures.

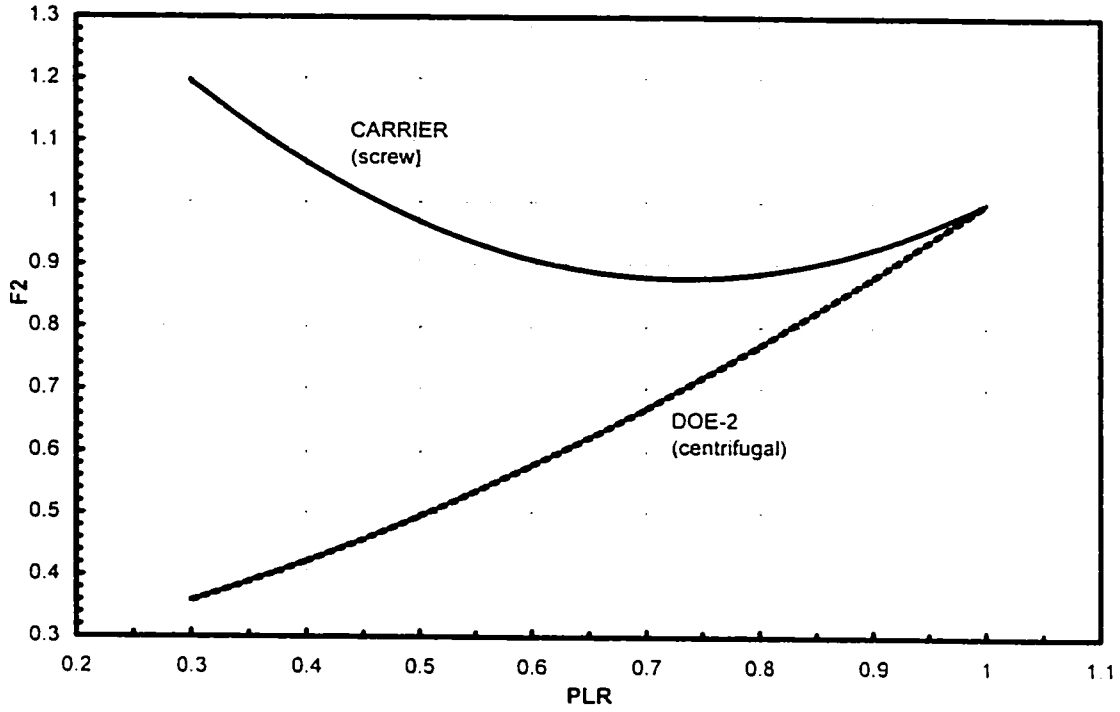

Figure 6-3 Variation of F_2 with part load ratio PLR

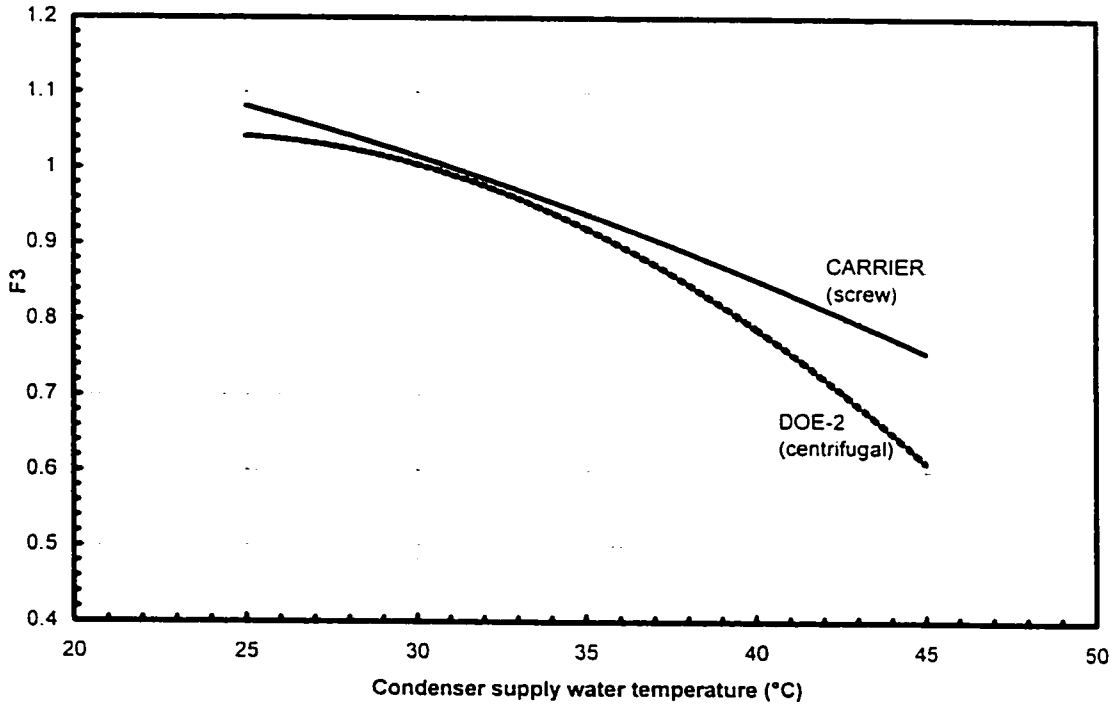

Figure 6-4 Variation of F_3 with the condenser entering water temperature, at chilled water leaving temperature=7°C

6.6 Correlations based on dimensionless groups at full load regime

According to the objective of this study, the required correlation for energy performance of screw compressor chiller is to be based on the DOE-2 generic format. However using dimensionless analysis could be another alternative to develop the correlation-based model for energy performance of chillers. It should be noted that applying dimensionless analysis using Buckingham Π theorem requires a complete understanding of all parameters affecting the performance of screw compressor chillers. In this section some dimensionless groups, which were observed so far, are introduced and correlated.

6.6.1 Approach one

As it was seen before, the COP is a function of evaporator and condenser water temperatures. Figure 6-5 shows the variation of the COP at full load with chilled water leaving temperature at different condenser entering water temperatures for three models (076, 106 and 146). One can notice that different condenser water temperatures and different capacities (models) develop different groups of curves, which tend to have lower slopes for larger units. The COP varies slightly with evaporator temperature for large models.

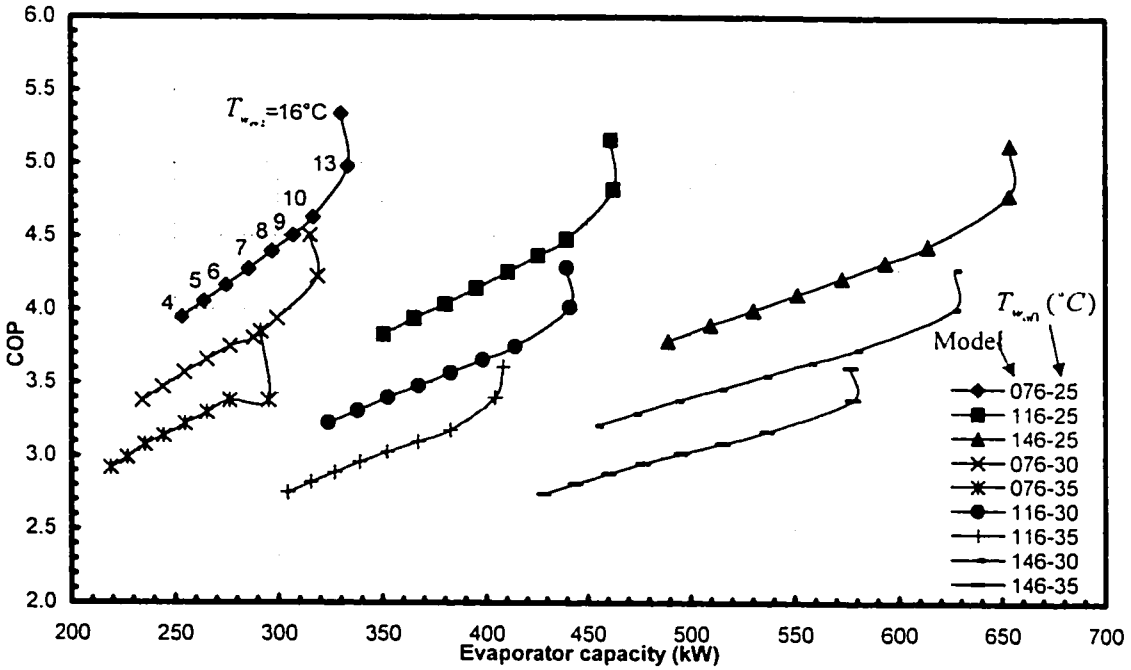

Figure 6-5 Variation of COP with condenser water entering temperature and chilled water leaving temperature for three different chiller models (076,106 and 146)

All such curves as those presented in Figure 6-5, can be compressed in one single curve, if the dimensionless criterion $T^* = T_{w,e2} / T_{w,e1}$ is used (Figure 6-6).

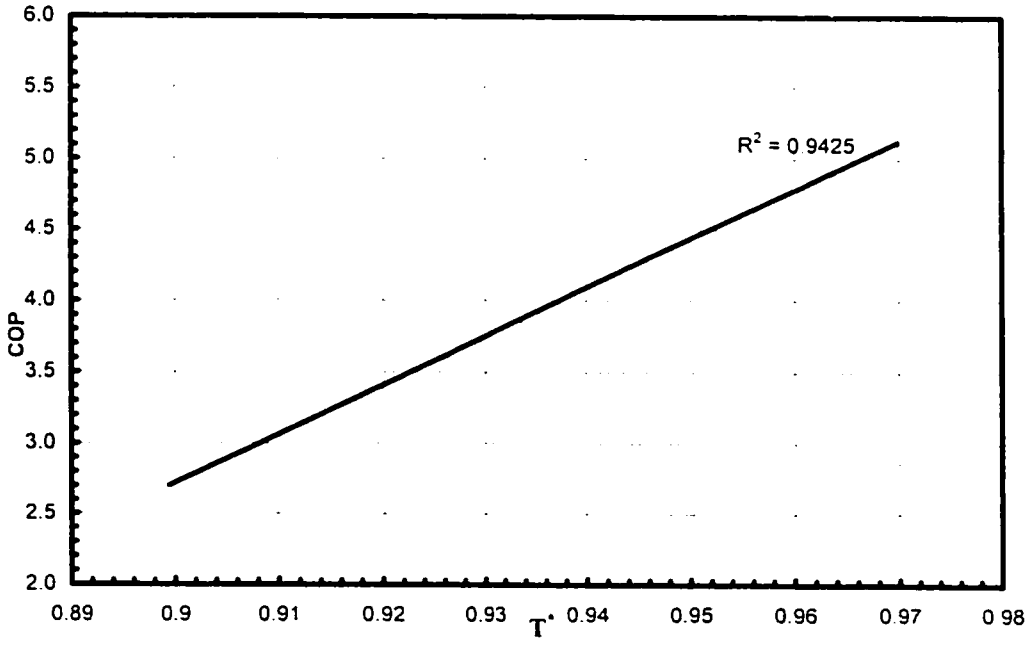

Figure 6-6 variation of COP with temperature ratio T^*

The dimensionless criterion T^* is the ratio of chilled water leaving temperature over condenser entering water temperature, both temperatures being expressed in K, and regardless of nominal capacity. Figure 6-6 shows a linear variation of COP with temperature ratio.

$$COP_{\tau_{FL}} = 34.397T^* - 28.235 \quad (6\text{-}2)$$

Statistical information				
	SE	MAE	C.V.(%)	R^2(%)
$COP_{\tau_{FL}}$	0.148268	0.116058	3.95	94.25

Equation (6-2) was derived based on the $COP_{toolkit}$ and the values of standard error, mean absolute error, coefficient of variance and R^2 are acceptable. Therefore the long correlation presented in Table 6-4 for COP at full load, can be replaced by equation (6-2) using only the temperature ratio as an independent variable. For example at $T_{w_{cnd}} = 7°C$ and $T_{w_{cnd}} = 30°C$ the temperature ratio is determined as $\frac{7+273.15}{30+273.15} = 0.92413$, so from equation (6-2), COP=3.55. This value of COP in comparison with $COP_{toolkit}$ in table 6-1 shows 3% error, however if compared with COP_{actual}, there is an error of 27%. It is worth mentioning that deriving such a correlation, based on the COP_{actual}, will create a significant error (SE=0.747559, MAE=0.644222, C.V.=14.89, R^2=14.90); due to the effect of nominal capacity.

6.6.2 Approach two

The correlations presented in the previous sections related the COP, its correction factors (F_1 and F_2), and the cooling capacity correction factor (F_3) in terms of the

evaporator and condenser water temperatures and part load ratios through separate correlations. In this section another performance curve is introduced for full load, using three dimensionless groups. This approach relates the six parameters for all models of chiller through a single curve. Once five parameters are known the sixth one can be determined directly.

Three dimensionless groups are proposed and denoted as G_1, G_2 and G_3. For the purpose of consistency in this section, the term G_2 is used; however it should be noted that $G_2=T^*$ presented in section 6.6.1, and the term $G_1 = \frac{1}{F_1}$ (section 6.4).

$$G_1 = \frac{COP_r}{COP_d} \tag{6-3}$$

$$G_2 = \frac{T_{w_{ev2}}}{T_{w_{ev1}}} \tag{6-4}$$

$$G_3 = \frac{\dot{Q}_{ev}}{CAP_d} \tag{6-5}$$

where:

$\dot{Q}_{ev}$: off-design capacity at full load regime (kW)

CAP_d : design capacity (kW)

The relation between the three dimensionless groups can be presented as in Figure 6-7.

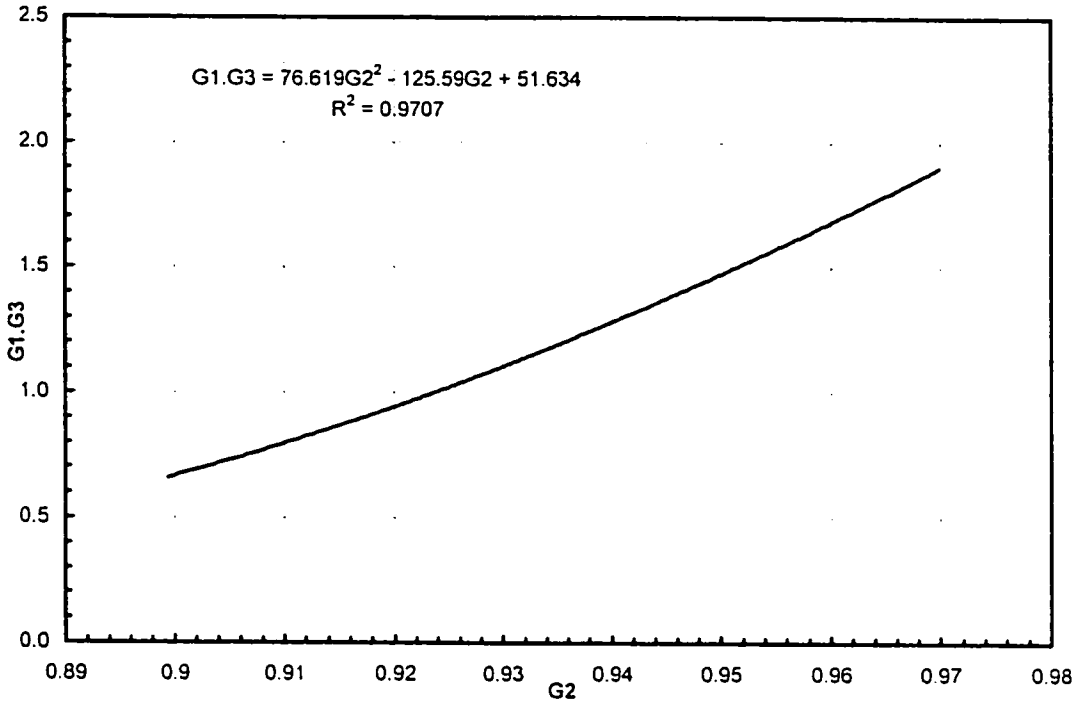

Figure 6-7 Variation of $G_1 G_3$ with G_2

Another correlation that was derived, presents G_1 as a function of the other two dimensionless groups in a nonlinear form ($G_1 = f(G_2, G_3)$). The statistical information shows that the correlation is satisfactory. The equation is shown as follows:

$$G_1 = a + bG_2^2 + cG_2 + dG_3^2 + eG_3 + fG_2G_3 \tag{6-6}$$

where:

$a = -50.4083$ $\quad$ $d = -1.70639$

$b = -72.8586$ $\quad$ $e = -20.4382$

$c = 121.602$ $\quad$ $f = 25.3262$

Statistical information

	SE	MAE	C.V.(%)	R^2 (%)
G_1	0.0404586	0.028911	4.67	94.81

The statistical information shows that the equation (6-6) correlates the dimensionless groups within the acceptable approximation.

As an example, at $T_{w_{ev2}} = 5°C$ and $T_{w_{cd1}} = 35°C$ from table 6-1 $\dot{Q}_{ev} = 227.2\,\text{kW}$, also at design conditions ($T_{w_{ev2}} = 7°C$ and $T_{w_{cd1}} = 30°C$) $\dot{Q}_{ev} = 265.5$ kW, and COP_d=4.85, therefore the dimensionless groups G_2 and G_3 are determined as follows:

$$G_2 = \frac{273.16+5}{273.16+35} = 0.90265 \;,\; G_3 = \frac{227.2}{265.5} = 0.856$$

Using equation (6-6), G_1 is calculated as equal to 0.816. Hence COP_x can be calculated from G_1 expression:

$G_1 = 0.816 = \frac{COP_x}{4.85}$, so COP_x=3.96, which in comparison with table 6-1 there is an error of 3.4%.

6.7 Correlations using the identified parameters

In addition to the DOE-2 generic correlation or those using the dimensionless criteria as a function of evaporator and condenser water temperatures, one can include in these correlations the identified parameters, along with the evaporator and condenser temperatures. The correlations are derived using multiple regression techniques available in the Statgraphics program [31]. The correlation for the COP can have one of the following forms:

$$COP_1 = F_1(UA_{ev}, UA_{cd}, A_l, \dot{V}_s, \alpha, \dot{W}_{lo}, T_{w_{ev2}}, T_{w_{cd1}}) \qquad (6\text{-}8)$$

and

$$COP_2 = F_2(UA_{ev}, UA_{cd}, A_l, \dot{V}_s, \dot{W}_{total-losses}, T_{w_{ev2}}, T_{w_{cd1}}) \qquad (6\text{-}9)$$

In the second form, the two parameters α and $\dot{W}_{lo}$ are replaced by the total losses $\dot{W}_{total-losses}$. Two correlations are also considered for the compressor electric input:

$$\dot{W}_1 = F_3(UA_{ev}, UA_{cd}, A_f, \dot{V}_s, \alpha, \dot{W}_{lo}, T_{w_{ev2}}, T_{w_{cd1}}) \tag{6-10}$$

and

$$\dot{W}_2 = F_4(UA_{ev}, UA_{cd}, A_f, \dot{V}_s, \dot{W}_{total-losses}, T_{w_{ev2}}, T_{w_{cd1}}) \tag{6-11}$$

The generic form of functions F_1 to F_4 is as follows:

$$aUA_{ev} + bUA_{cd} + cA_f + d\dot{V}_s + e\alpha + f\dot{W}_{lo} + g\dot{W}_{total-losses} + hT_{w_{ev2}} + iT_{w_{cd1}} + j \tag{6-12}$$

The coefficients "a" to "j" were evaluated through the multiple regression techniques (Table 6-6).

Table 6-6 Regression coefficients for functions F and f

	a	b	c	d	e	f	g	h	I	j
COP_1	0.0000896788	-0.0000705979	-7314.69	3.79217	-3.64344	-0.0000509149	0	0.0921444	-0.123637	7.48914
COP_2	-0.000165873	0.000137675	-13802.5	9.70095	0	0	-0.0000242834	0.0967529	-0.119931	6.33738
$\dot{W}_1$	-1.40463	1.25165	-184740000	423300	50580.9	0.935412	0	298.448	1616.74	-63537.3
$\dot{W}_2$	-0.709588	0.786514	-251540000	303877	0	0	1.40161	31.6693	1402.15	-42902.7

Statistical information

	SE	MAE	C.V.(%)	R^2(%)
COP_1	0.0737028	0.0575817	1.96	98.63
COP_2	0.0818857	0.0620075	1.83	98.30
$\dot{W}_1$	1990.07	1537.63	2.46	98.87
$\dot{W}_2$	1659.56	1361.69	2.07	99.32

Statistical indices indicate that the four correlations fit well the relevant data. As an example, for model 076 at $T_{w_{ev1}} = 5°C$ and $T_{w_{cd1}} = 35°C$ using table 6-1 for the identified parameters, COP=2.88 (3.7%error) and $\dot{W} = 62196.4$ W (4.9% error) are calculated from equations (6-8) and (6-10) respectively.

These correlations can be used by the facility mangers to compare the measured values of electric input or COP with those predicted by the above correlations. If a large difference is noticed, the building manager is warned about the abnormal operating conditions.

6.8 Identification and correlations-based models for another manufacturer

Another screw-compressor chiller with the same range of cooling capacity (less than 540 kW) from a different manufacturer was obtained later through the web. The new selected chiller is the KRS manufactured by KUO YU Company from Taipei Taiwan China, using the refrigerant R-22. (Table B-4 in appendix B). The four subroutines explained in chapter five (identification and simulation at full load and part load regime) have been used to identify the physical parameters and calculate the COP at different working points. Table 6-7 shows the identified parameters. Tables F-3 and F-4 in appendix F. contain all the results of full and part load regime.

Table 6-7 Identified parameters of KUO YU KRS/R-22 chiller at full load regime

Model	$\dot{Q}_{ev}$ Nom. (W)	$\dot{W}$ (W)	AU_{ev} (W/K)	AU_{cd} (W/K)	$\dot{W}_{lo}$ (kW)	α	$\dot{V}_s$ (m^3/s)	A_l (m^2)	$\dot{W}_m$ (W)
G40	141000	34500	20000	23000	229.7	0.315365	0.05635	-0.0000479	23427.1
G50	176000	43000	25000	29000	-727.1	0.357266	0.06978	-0.0000585	28934.2
G60	211000	51400	30000	35000	-875.5	0.361391	0.08333	-0.0000697	34518.6
G75	264000	64500	37000	44000	-1116.0	0.360143	0.10494	-0.0001239	61928.5
G80	281000	69000	40000	48000	-1240.5	0.367620	0.11212	-0.0000941	46188.9
G100	352000	85900	50000	60000	-1532.1	0.370501	0.13927	-0.0001167	57326.9
G120	422000	102800	60000	72000	-1757.7	0.371783	0.16649	-0.0001395	68465.8
G150	528000	129000	75000	98000	15555.2	0.207152	0.19181	-0.0001216	86120.9

* The values are for the standard condition. To see the values of internal power in other conditions refer to Table D-3 in Appendix D.

Figure 6-8 shows the comparison of the overall heat transfer coefficient of evaporator and condenser. The difference between the two manufacturers appears to be influenced by the type of refrigerant used: R-134a by CARRIER, and R-22 by KUO YU.

Figures 6-8 to 6-12 show the comparisons of the identified parameters of screw chillers from two manufacturers: CARRIER and KUO YU.

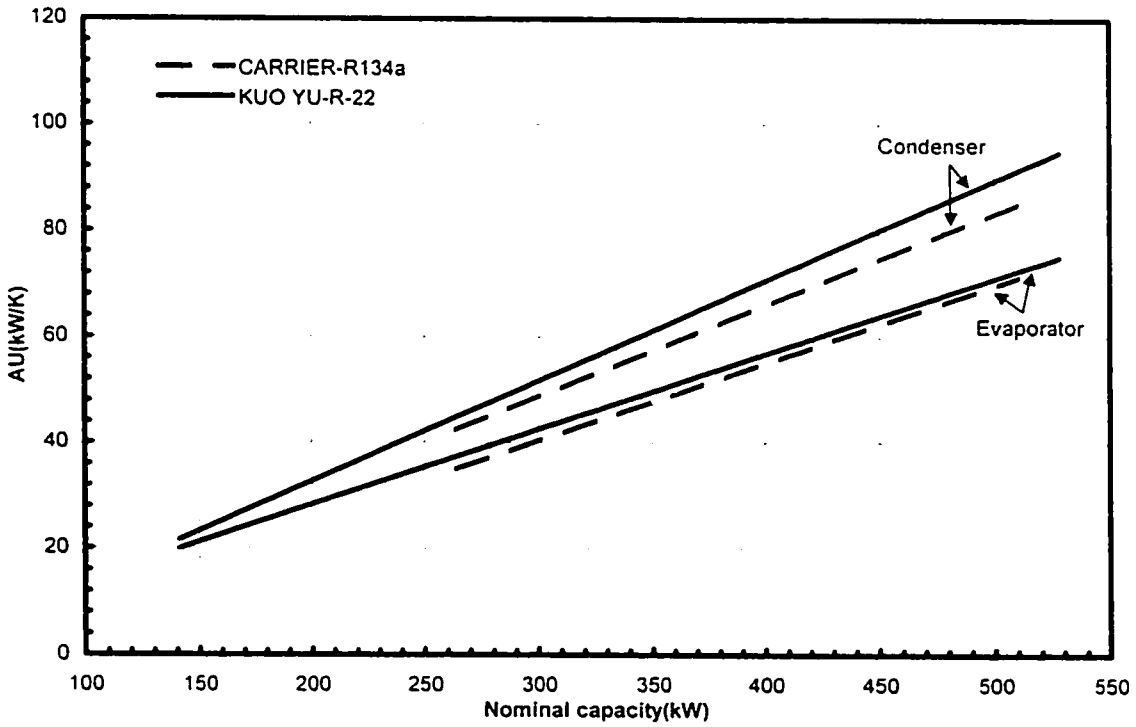

Figure 6-8 Variation of overall heat transfer coefficients with nominal capacity for two chillers from different manufacturers

The KUO YU chiller requires less refrigerant flow rate than the CARRIER chiller at the same nominal capacity (Figure 6-9). For instance, at a nominal capacity of 300 kW the difference between the volumetric flow rates is about 27%.

Figure 6-10 shows a remarkable difference between the two chillers, with respect to the leakage area. For instance, at a nominal capacity of 300 kW, the difference is about 43%.

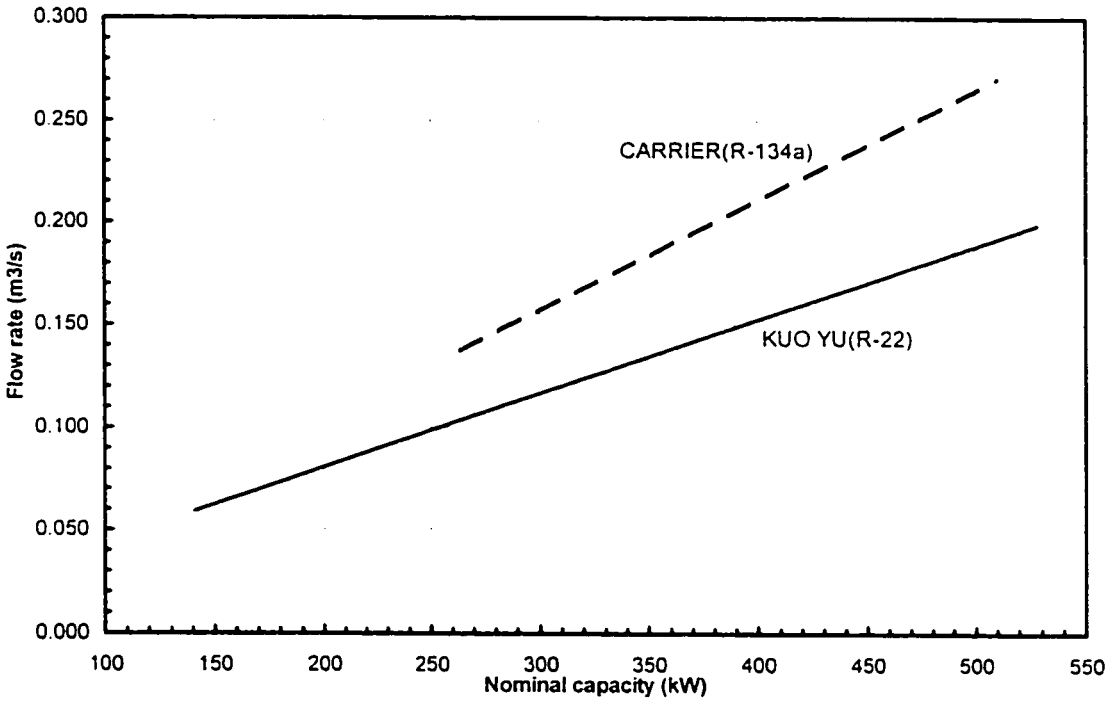

Figure 6-9 Variation of refrigerant volumetric flow rate with nominal capacity for two chillers from different manufacturers

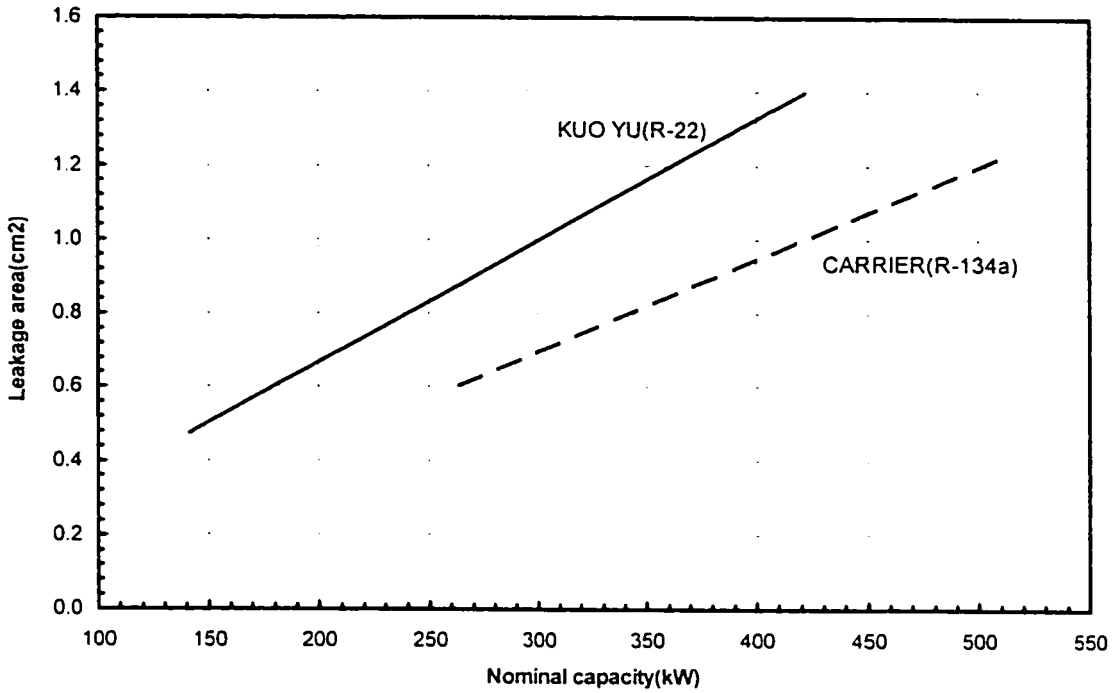

Figure 6-10 Variation of leakage area with nominal capacity for two chillers from different manufacturers

Figure 6-11 shows the electricity demand of the KUO YU chiller is higher than that of the CARRIER chiller, although the former has a lower refrigerant flow rate.

The CARRIER chiller has less electromechanical losses than the KUO YU chiller, so the former requires higher input energy at the same nominal capacity (Figure 6-12).

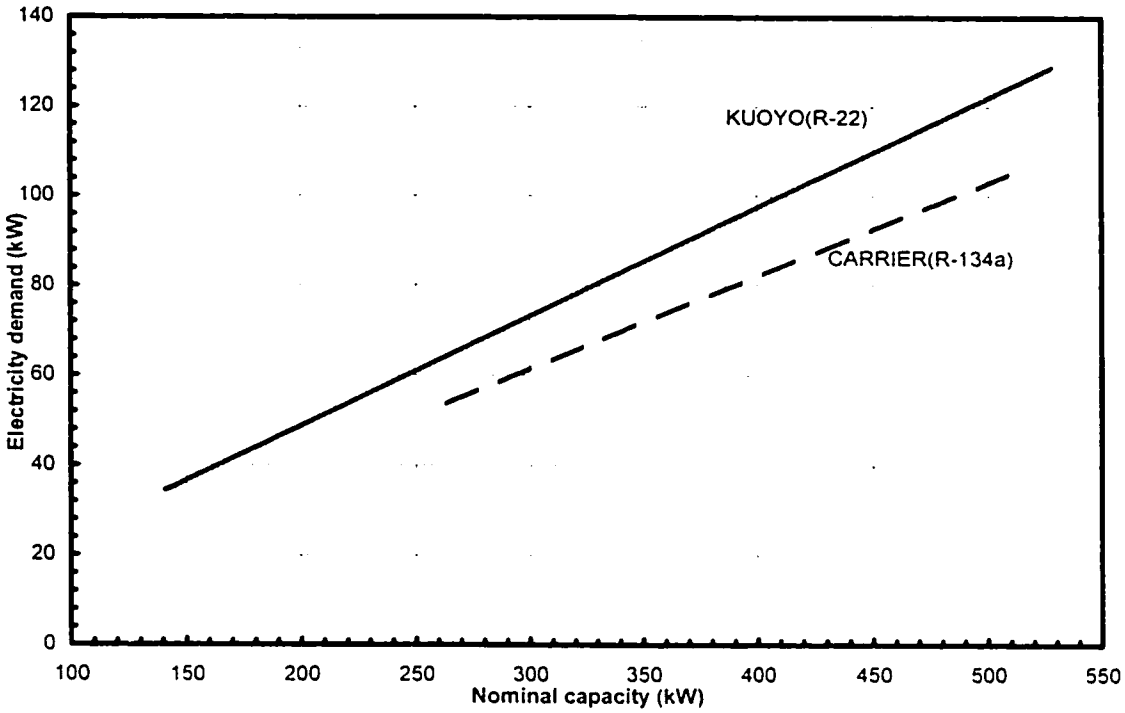

Figure 6-11 Variation of chiller power input with nominal capacity for two chillers from different manufacturers

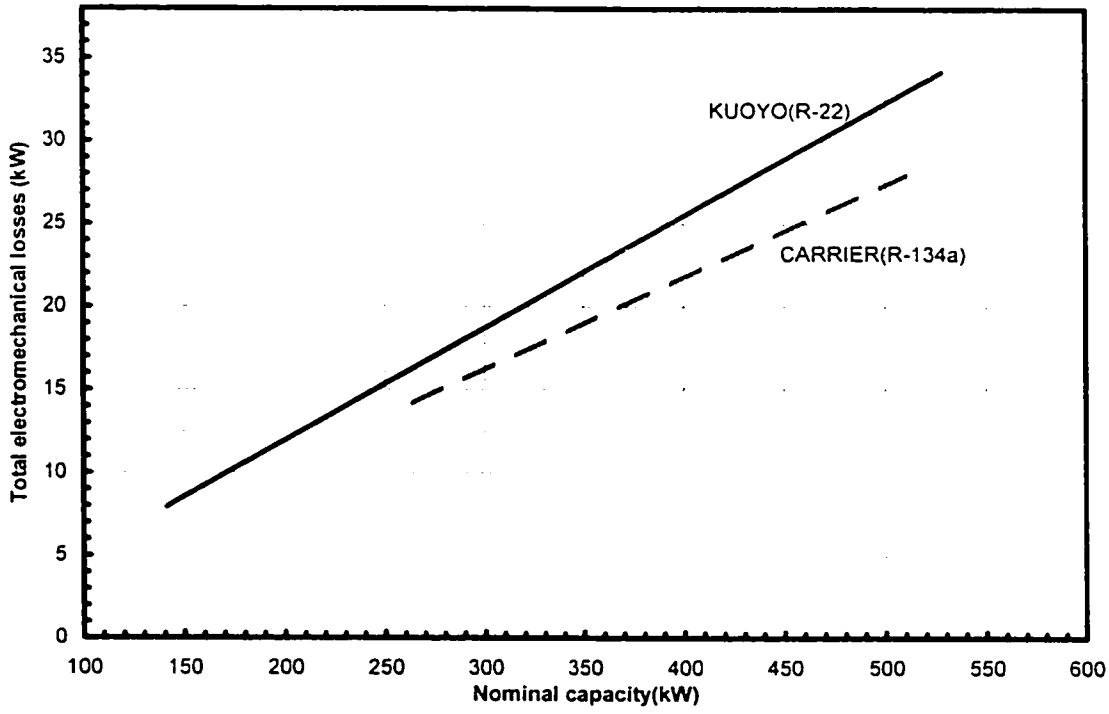

Figure 6-12 Variation of chiller total electromechanical losses with nominal capacity for two chillers from different manufacturers

The correlations for COP were developed using the approach described in section 6.5 that is based on the full load identification, the full load simulation, the part load identification and simulation. Once the correlations for COP were determined, then the correlations for F_1, F_2 and F_3 were derived. The corresponding correlations are shown in Table 6-8.

Table 6-8 Coefficients F_1, F_2 and F_3 for the KUO YU, KRS/R-22 screw compressor chillers

$$F_i = a + b*T_{w_{cd1}}^{\ 2} + c*T_{w_{cd1}} + d*T_{w_{ev2}}^{\ 2} + e*T_{w_{ev2}} + f*T_{w_{cd1}}*T_{w_{ev2}} + g*PLR^2 + h*PLR$$

	a	b	c	d	e	f	g	h
F_1	0.34477	-0.000020235	0.0266426	0.00000249208	-0.0184831	0.000065109	0	0
F_2	2.86098	0	0	0	0	0	3.52293	-5.38391
F_3	0.932318	-0.000089129	-0.00264954	0.000216542	-0.000382859	0.932318	0	0

Statistical information

	SE	MAE	C.V.(%)	R^2(%)
F_1	0.00230904	0.00188132	0.20	99.98
F_2	0.191728	0.131006	14.40	65.75
F_3	0.00566305	0.0048222	0.55	99.82

Figure 6-13 shows the variation of F_1 with condenser entering water temperature for the two chillers. At full load and off-design conditions with higher condenser entering water temperature, the increase of electric demand for CARRIER chiller is more than that of KUO YU chillers.

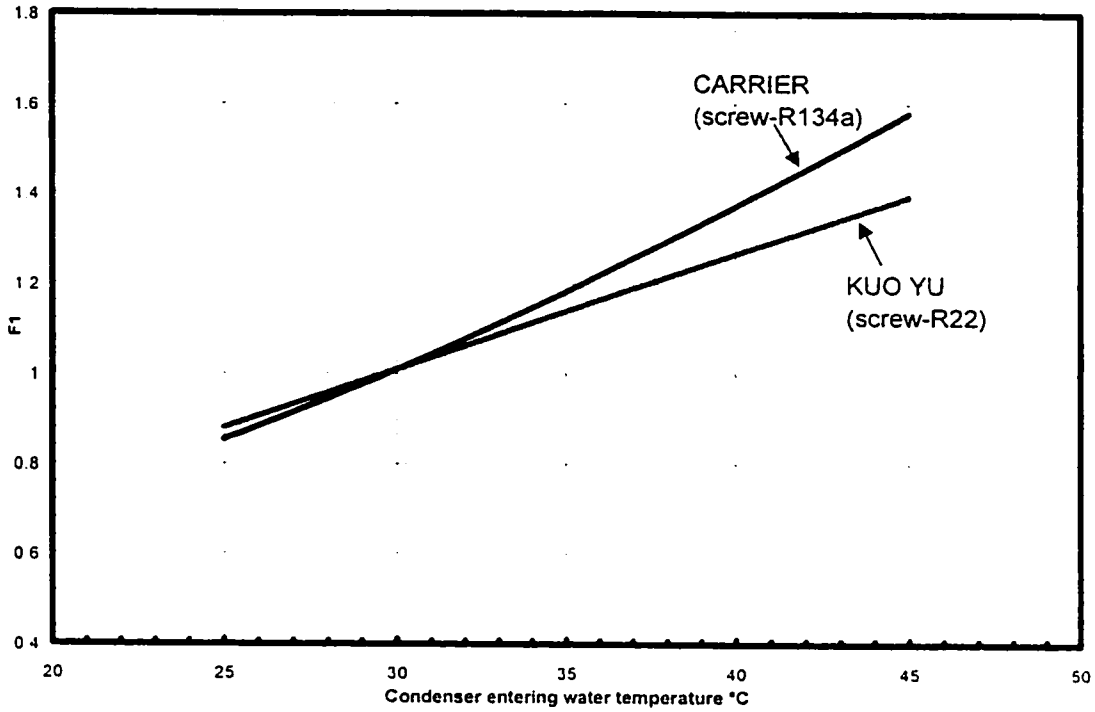

Figure 6-13 Variation of F_1 with condenser entering water temperature at chilled water leaving temperature=7°C for two different manufacturers

The variation of F_2 with part load ratio for the two screw compressor chillers is shown in Figure 6-14. The KUO YU screw chillers require a significant higher electric input than the CARRIER chillers when both are working under part load ratios less than 0.6, while KUO YU chillers show better performance than CARRIER for part load ratios higher than 0.6.

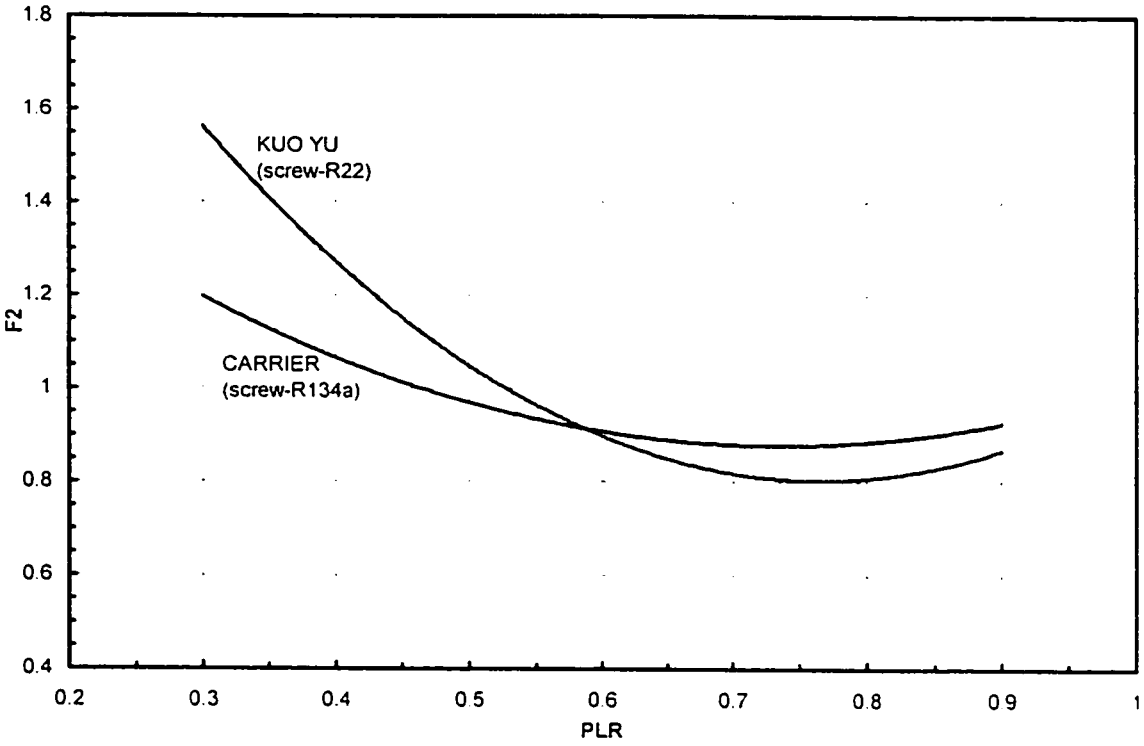

Figure 6-14 Variation of F_2 with part load ratio PLR for two chillers from different manufacturers

Figure 6-15 shows the variation of F3 of the two screw chillers with the condenser entering water temperature. One can notice that the KUO YU chiller has a higher F_3, which indicates that the cooling capacity has a smaller decrease when the condenser temperature is higher, than the CARRIER chiller.

The correction factors F_1, F_2 and F_3 were developed for another manufacturer for comparison purposes. As discussed, Figures 6-13, 6-14 and 6-15 show a significant difference between the correction factors of the two manufacturers which indicates that the coefficients derived are not unique for all screw compressor chillers.

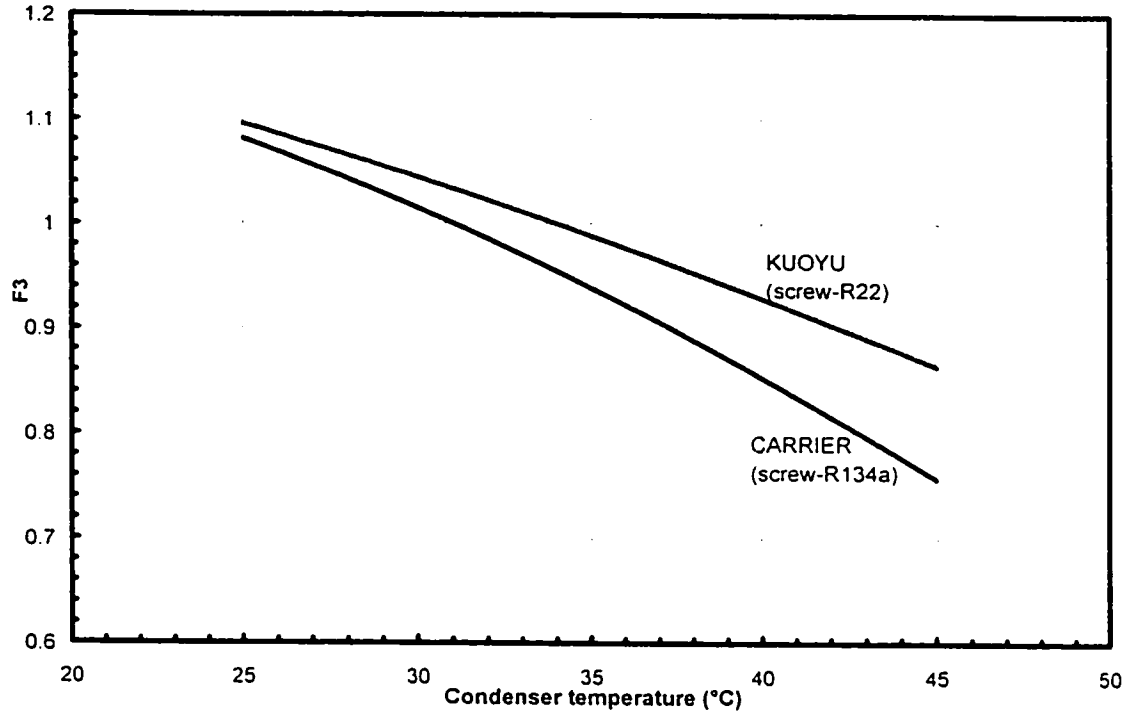

Figure 6-15 Variation of F_3 with condenser entering temperature, at chilled water leaving temperature=7°C, for two chillers from different manufacturers

As an example a chiller with nominal capacity of around 500 kW is selected:

-Model 30HXC-146 CARRIER screw compressor, R-134a

-Model KRS-G150 KOU YU, screw compressor, R-22

-Model WSC-063 McQUAY, centrifugal compressor, R-134a

At design conditions ($T_{w,e2} = 7°C$ and $T_{w,c1} = 30°C$) correction factors F_1=F_3=1 and F_2 is determined based on the corresponding correlation derived for screw compressor chillers; in the case of centrifugal chiller, the DOE-2 default correlation is used. Figure 6-16 shows the electricity demand for the three chillers as a function of part load ratio. It can be seen that the electricity demand for the screw compressor chiller in low part load ratios increases so much that it exceeds the electricity demand at full load.

At part load ratios the efficiency of screw chillers drops so much that makes them inappropriate to be used where cooling load fluctuates remarkably.

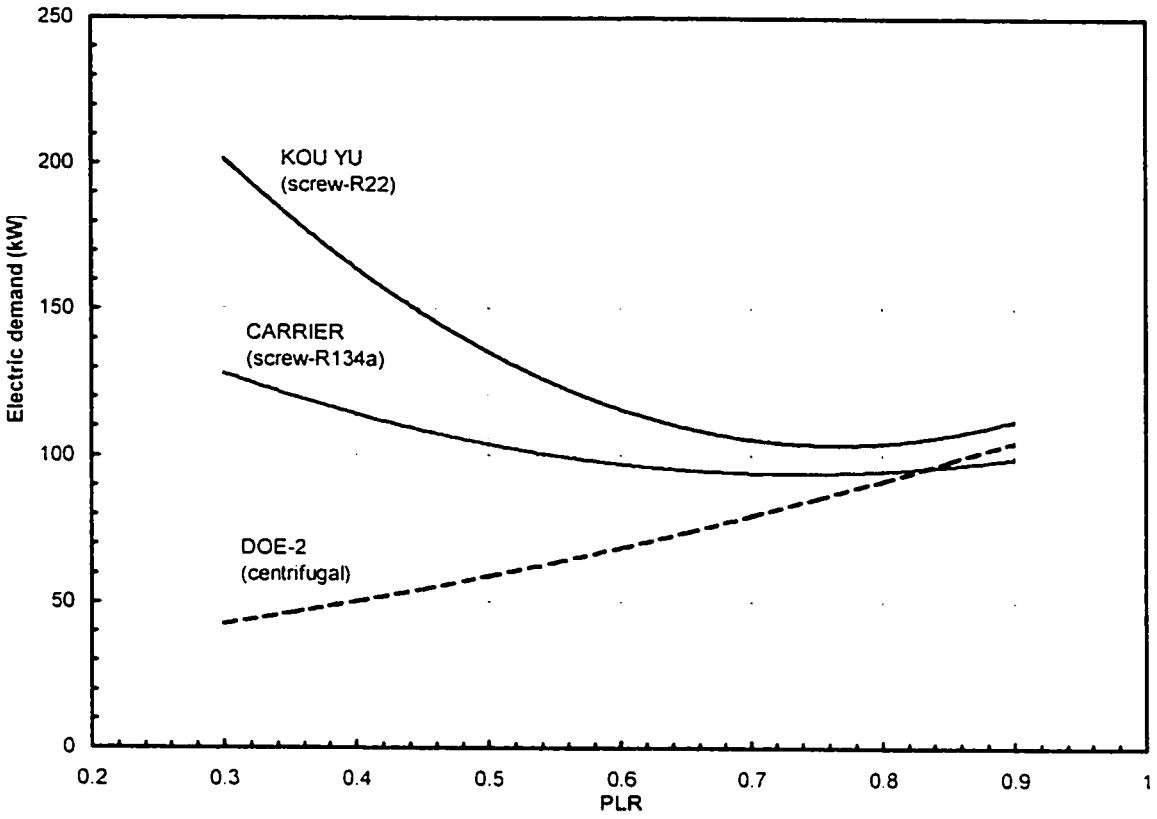

Figure 6-16 Variation of electric demand with part load ratio (PLR) at design conditions (7°C chilled water leaving temperature and 30°C condenser leaving water temperature). Comparison of three correlation-based models for nominal capacity of 500 kW.

6.9 Summary

In this chapter several correlation-based models have been developed to evaluate the energy performance of screw chillers. Data from two manufacturers have been used, in comparison with the correlation-based model of centrifugal chillers presented by DOE-2. The difference between the performances of the two types of chillers was also discussed, however one single correlation was not found due to different performance of screw chillers in part load. Although applying only two manufacturers' product data does not seem to be sufficient to generalize the idea, but the energy performance correlation (equation (6-1)) derived for screw chillers could be used in DOE-2 simulation, which does not contain the corresponding correlations for the screw compressor chillers. The performance correlations derived for screw chillers in this chapter are collected in Table 6-9. To see the corresponding coefficient of the other types of chiller presented by DOE-2 refer to table G-1 in Appendix G.

Table 6-9 Summary of the correlation-based models developed in this chapter

$a+b*X^2+c*X+d*Y^2+e*Y+f*X*Y+g*z^2+h*z$

	Dependent variables	Independent variables			Coefficients							
		X	Y	Z	a	b	c	d	e	f	g	h
CARRIER	$COP_{x_{FL}}$	$T_{w_{cd1}}$	$T_{w_{ev2}}$	PLR	8.02711	0.002688890	-0.250483	0.000367989	0.203902	-0.003963540	0.00000	0.00000
	$COP_{x_{FL}}$	G_2	—	—	-28.23500	0.000000000	34.397000	0.000000000	0.000000	0.000000000	0.00000	0.00000
	$COP_{x_{PL}}$	$T_{w_{cd1}}$	$T_{w_{ev2}}$	PLR	7.81922	0.005304120	-0.455848	-0.009266930	0.450384	-0.004571200	-7.96205	11.88610
	F_1	$T_{w_{ev2}}$	$T_{w_{cd1}}$	—	0.42071	0.000340978	0.160138	0.000444553	-0.016213	-0.000507389	0.00000	0.00000
	F_2	—	—	PLR	1.79173	0.000000000	0.000000	0.000000000	0.000000	0.000000000	1.70263	-2.49436
	F_3	$T_{w_{ev2}}$	$T_{w_{cd1}}$	—	0.85714	-0.000199504	-0.001343	-0.002059180	0.0723178	-0.000129739	0.00000	0.00000
	G_1	G_2	G_3	—	-50.40830	-72.858600000	121.602000	-1.706390000	-20.438200	25.326200000	0.00000	0.00000
KUO YU	$COP_{x_{FL}}$	$T_{w_{cd1}}$	$T_{w_{ev2}}$	—	10.20700	0.002432260	-0.260623	0.000842876	0.160820	-0.003038820	0.00000	0.00000
	$COP_{x_{FL}}$	G_2	—	—	-24.65300	0.000000000	93.018000	0.000000000	0.000000	0.000000000	0.00000	0.00000
	$COP_{x_{PL}}$	$T_{w_{cd1}}$	$T_{w_{ev2}}$	PLR	6.22500	0.002945950	-0.304805	-0.000316648	0.320345	-0.004789100	-5.71633	9.38955
	F_1	$T_{w_{cd1}}$	$T_{w_{ev2}}$	—	0.34477	-0.000020235	0.026643	0.000002492	-0.018483	0.000065109	0.00000	0.00000
	F_2	—	—	PLR	3.11617	0.000000000	0.000000	0.000000000	0.000000	0.000000000	3.52293	-5.38391
	F_3	$T_{w_{cd1}}$	$T_{w_{ev2}}$	—	0.99905	0.000013527	-0.010767	-0.000178959	0.046806	-0.000255378	0.00000	0.00000
	G_1	G_2	G_3	—	-22.52580	-35.023000000	57.163800	-0.868965000	-13.278000	15.943200000	0.00000	0.00000

$$G_1 = \frac{COP_x}{COP_d} \quad , \quad G_2 = \frac{T_{w_{ev2}}}{T_{w_{cd1}}} \quad , \quad G_3 = \frac{\dot{Q}_{ev}}{CAP_d}$$

Chapter 7

Evaluation of thermal loads of a typical office building in different cities in North America

An existing office building in Montreal, built in 1972, has been considered as a typical commercial building in North America and the simulation is done for different cities in that region. The objective is to see the behavior of an office building in terms of energy consumption and compare it in different cities with different climates.

The analysis of energy performance of a building can be done in different ways. There are some factors such as type or complexity of the building or even the objective of energy evaluation, that lead the designer to choose the appropriate way to evaluate the energy consumption of a building. In some cases where there is not enough detailed information on the proposed design, the estimation might be done using simplified analysis like calculating the space loads (steady state) based on only the inside and outside temperatures (e.g. degree-day) or even considering solar radiation (e.g. bin method), internal heat gain and air infiltration.

Another method uses the estimation of instantaneous space load, which is usually calculated with a one-hour interval, followed by calculation of energy consumption according to the type of HVAC system, and the plant equipment. The energy required to maintain the space at the desired condition is calculated by adding up the hourly energy

requirements. However, the accuracy of the energy estimation is based on the assumptions made and absolutely accurate energy prediction is not possible [32].

To analyze the building energy demand and consumptions, most building energy analysis programs use three major steps: (i) thermal load calculations, (ii) system simulation and (iii) central plant simulation; some programs go one step further by including the economic analysis. Therefore these programs include four main analyses: LOADS, SYSTEMS, PLANT and ECONOMIC (LSPE). The differences between different programs are basically in their mathematical models chosen for simulation and the degree of accuracy of their assumptions in comparison to the real situation.

The LOADS subprogram deals with hourly heating and cooling load calculations. The SYSTEMS subprogram takes the output of LOADS subprogram and determines the heat extraction and addition rate required by the secondary system. The PLANT subprogram takes the output of the SYSTEMS subprograms and calculates the fuel and electrical requirements of the primary system equipment. The ECONOMIC subprogram uses the energy consumption and demand data from the PLANT subprogram, and calculates the life cycle cost.

The program, which is used for energy simulation of the office building, is DOE-2. The DOE-2 is a building energy use and cost simulation program developed by the Simulation Research Group at Lawrence Berkeley Laboratory (1979), that and was financially supported mostly by the U.S. Department of Energy [8].

This program estimates the hourly heating and cooling energy used in a building as well as the whole building energy performance, for given hourly weather data, description of building characteristics and HVAC equipments, and profile of operation. Figure 7-1 shows DOE-2 information flow diagram.

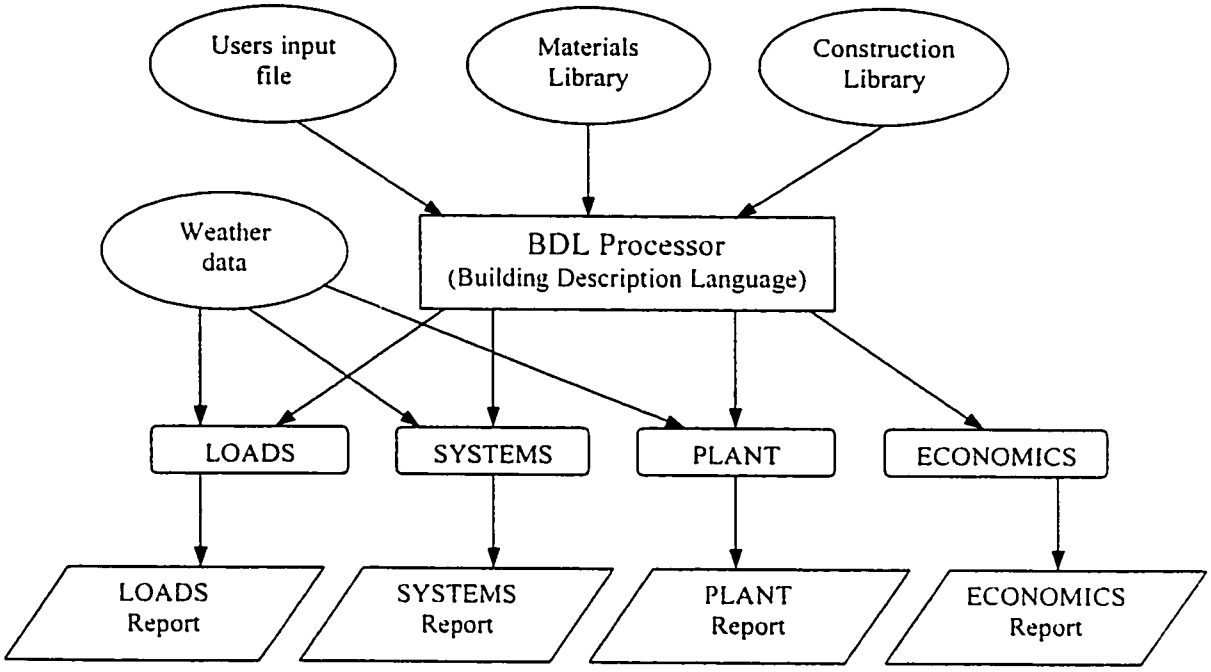

Figure 7-1 Information flow diagram of the DOE-2 program [33]

7.1 Simulation approach used by the DOE-2 program

There are two main methods of estimation of the space thermal loads:

1) Heat balance method

2) Weighting factor method

The DOE-2 program uses the weighting factor method. In this method, the cooling or heating load at constant space temperature is calculated by considering the cooling or heating load history, the instantaneous heat gain/loss through each construction element

and the internal loads [34]. The heat storage in the room elements is taken into account, which causes a delay between the moment the heat flux reaches the internal surface of a building element and the moment the corresponding heat becomes cooling/heating load. Cooling load at the time t is calculated as:

$$Q_t = \upsilon_0 q_t + \upsilon_1 q_{t-1} + \ldots - \omega_1 Q_{t-1} - \omega_2 Q_{t-2} \ldots. \qquad (7\text{-}1)$$

where:

Q_t : cooling load at time t

Q_{t-1}: cooling load at time t-1

.

.

q_t : instantaneous heat gain at time t

q_{t-1} : heat gain at time t-1

.

.

$\upsilon_0, \upsilon_1, \ldots, \omega_1, \omega_2, \ldots$: weighting factors for different configurations of rooms, materials, air circulation and furnishing.

The weighting factors υ_t specify how much the energy stored is released in later times [34].

The instantaneous heat gain q_i through a construction element such as exterior wall is calculated using the conduction transfer functions. For an exterior element i with outside surface temperature T_{os} or one side and inside surface temperature T_{is} or the other side, the instantaneous heat gain at time t is determined as:

$$q_{i,t} = \sum_{j=0}^{n} X_i T_{is,t-j} - \sum_{j=0}^{n} Y_i T_{os,t-j} - c q_{i,t-1} \qquad (7\text{-}2)$$

where X_i, Y_i and c are the transfer function coefficients calculated in terms of materials and their sequence in the exterior wall.

In this method two assumptions are made. First the heat gains are determined individually and the superposition principle is used to get the total results. This approach assumes that the processes can be considered to be linear. Second the room properties are considered to be constant and do not vary with time. The inside surface heat transfer integrates both radiative and convective terms. This coefficient is calculated once at the beginning of the simulation and that value is used throughout the entire simulation.

The system load consists of two portions; the space load and outside air load. The minimum amount of outside air is determined based on the number of the people occupying the space and the minimum outside air required per person according to the standards. To calculate the cooling coil load, the program uses the bypass factor method. In this method the coil load $\dot{Q}_{cc}$ is calculated by the following equation:

$$\dot{Q}_{cc} = \rho_a \dot{V}_a (h_{ma} - h_{adp})(1 - BF) \qquad (7\text{-}3)$$

where:

h_{ma} : enthalpy of mixed air (J/kg), that is, the mixing of return air and outside air, at given proportions, according to the minimum requirements and the control strategy.

h_{adp} :enthalpy of the air at apparatus dew point (J/kg)

ρ_a : air density (kg/m^3)

$\dot{V}_a$:volumetric air flow rate (m^3/s)

BF : bypass factor

Bypass factor BF is the ratio of the airflow rate passing through the coil completely unaltered to the total airflow rate, and it is a function of physical and operational characteristics of the conditioning apparatus [5]. Figure 7-2 shows the air process through the coil from "ma" to "le", in the room (from "le" to "ma"), and in the mixing box of air-handling unit (oa+ rm → ma).

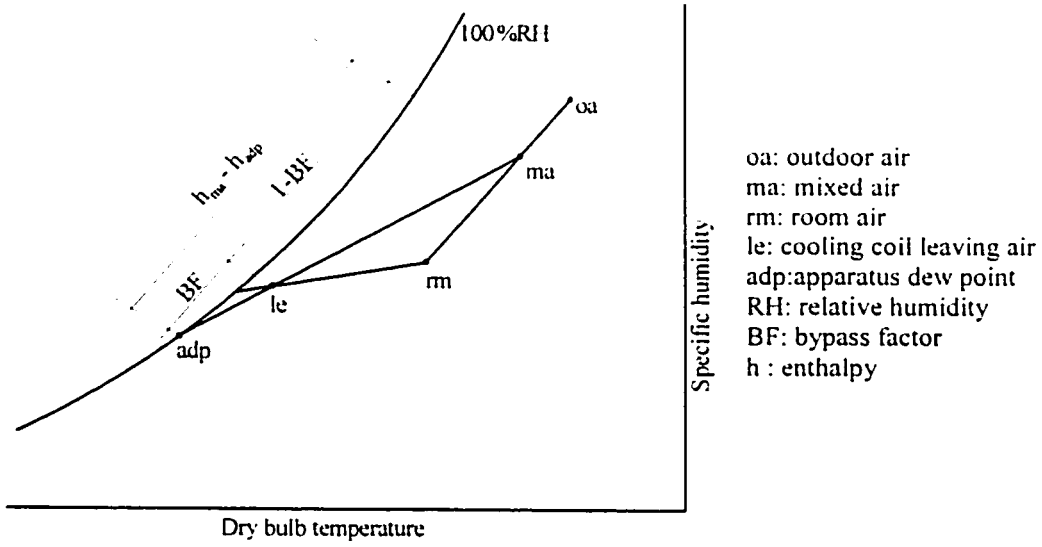

Figure 7-2 Room and cooling coil air process on the psychrometric chart

To describe part load performance of the plant equipment, the DOE-2 program uses polynomial equation. The typical performance data are built into the mathematical model

for each type of equipment. In the DOE-2 program, chillers are modeled by curve fitting the manufacturer's data.

7.2 Climate conditions

Four cities in Canada and three cities in the United States have been selected for comparing the energy performance of the typical office building. The cities are selected in such a way to consider different climate conditions. The weather design data for these cities are summarized in Table 7-1 [34].

Table 7-1 Weather data

	Latitude	Longitude	Elevation (m)	Winter			Summer				
				Design Dry-Bulb Temp. (°C)		HDD	Design Dry-Bulb & Wet-Bulb Temp. (°C)			CDD	Mean Daily Range (°C)
				99%	97.50%		1%	2.50%	5%		
Montreal	45° 28' N	73° 45' W	30	-29	-27	4652	31/23	29/22	28/22	316	9
Toronto	43° 41' N	79° 38' W	176	-21	-18	4344	32/33	31/22	29/22	342	11
Edmonton	53° 34' N	113° 31' W	677	-34	-32	6015	29/19	28/18	26/17	129	13
Vancouver	49° 11' N	123° 10' W	5	-9	-7	3150	26/19	25/19	23/18	70	9
New York	40° 39' N	73° 47' W	4	-11	-9	2790	32/23	31/22	29/22	463	9
Phoenix	33° 26' N	112° 01' W	339	-1	1	1021	43/22	42/22	41/22	2026	15
Chicago	41° 47' N	87° 45' W	185	-21	-18	3417	34/23	33/23	31/22	564	11

In the above table, HDD is the heating degree-days with reference to base temperature of 18°C. This is the cumulated difference between the base temperature and mean daily temperature for every day throughout the year, when the mean daily temperature is less than the base temperature. The CDD is the cooling degree-days with reference to the same base temperature of 18°C. This is defined as the difference between the mean daily temperature and the base temperature for every day of the year, when the mean daily temperature is higher than the base temperature.

It should be noted that due to some provincial regulations, the outside design conditions may be different from those recommended by ASHRAE publications (Table 7-1). For example in Montreal, based on the Regulation for Respecting Energy Conservation in Buildings issued in 1992 by the government of Quebec, the outside design temperature in winter is -23°C and not (-27°C) or (-29°C).

Figure 7-3 shows the difference between the Heating Degree Days (HDD) and the Cooling Degree Days (CDD), used as indicators of climate severity, for each of the cities presented above.

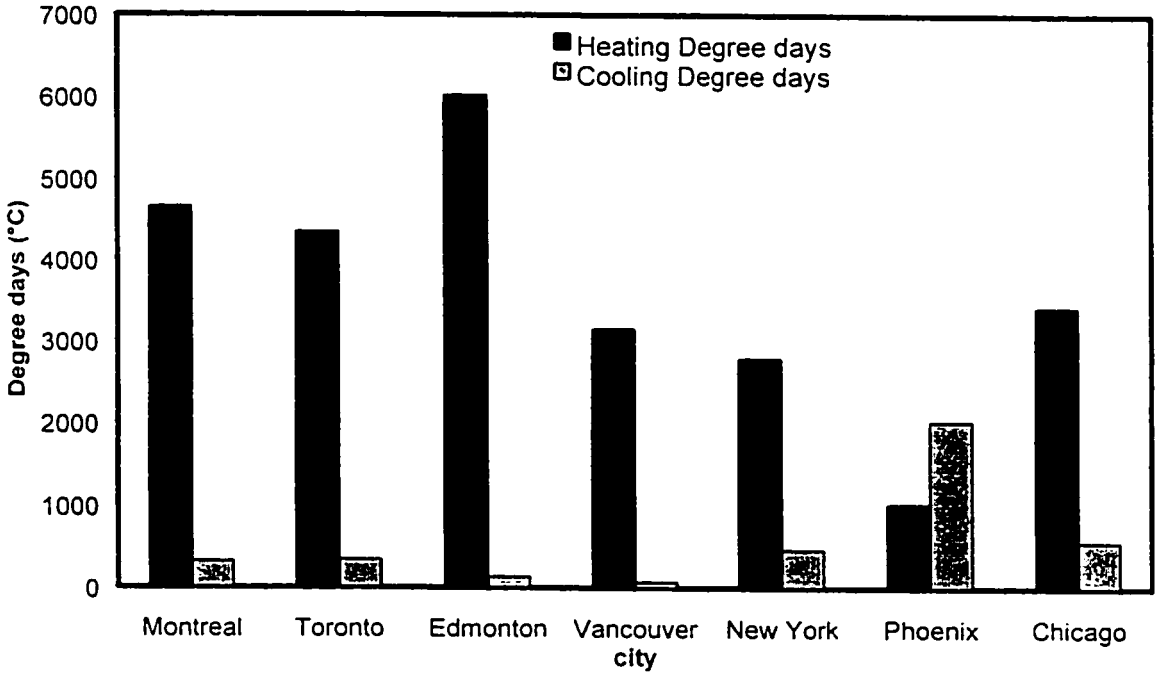

Figure 7-3 Cooling and heating degree-days for seven cities in North America

Temperature distribution throughout the year can also be another indication of climate severity. Figure 7-4 shows the frequency of outdoor air temperature in Montreal

in one year. The number of hours that the temperature is above 18°C is about 1849 hours or 21% of the year. Hence, the buildings are supposed to be operated under the heating mode much longer. However due to the large internal gain of the office building, the balance temperature is below 18°C, and therefore the cooling mode is predominant even under the northern climate.

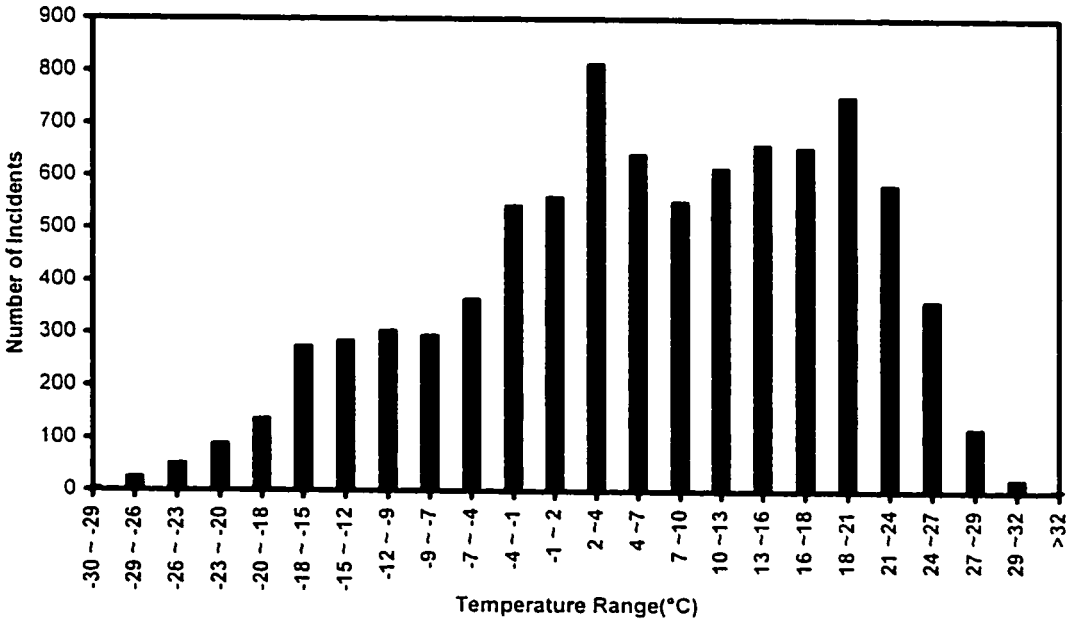

Figure 7-4 Annual temperature distribution in Montreal

7.3 Design requirements based on Model National Energy Code of Canada

The Model National Energy Code of Canada for buildings (MNECCB) [35] contains the specific design conditions of commercial and institutional buildings, which will lead if they are implemented to energy-efficient buildings.

The simulations are performed on the four cities in Canada (Montreal, Toronto, Edmonton, Vancouver). The following sub-sections present the design conditions from

MNECCB for those cities. The typical building is modified for each city to comply with the code requirements. The prescriptions indicated in the code, have been developed using the life cycle cost approach for each province. Therefore, the climate does not have a direct impact on the space cooling and heating loads, which is proportional to the indicators of climate severity such as heating-degree days.

The minimum thermal performance of building envelope is presented in Tables 7-2 and 7-3.

Table 7-2 Minimum effective thermal resistance (m^2 °C/W) (MNECCB)

	Montreal	Toronto	Edmonton	Vancouver
Walls In contact with the ground	2.4	2.4	2.7	1.7

Table 7-3 Maximum U-value of the above ground building assemblies (W/m^2. °C) (MNECCB)

	Montreal	Toronto	Edmonton	Vancouver
Roofs Concrete decks with rigid insulation	0.29	0.29	0.29	0.41
Walls	0.33	0.33	0.30	0.45
Floors Concrete slabs with rigid insulation	0.29	0.29	0.29	0.41
Fenestration Fixed glazing without sash, 0.4<Fenestration-to-wall ratio<0.5	1.90	1.80	1.90	2.90
Doors Swinging, full glazing	2.7	2.7	2.7	2.7

For the compliance check with MNECCB, the air infiltration rate for each perimeter thermal block is considered to be equal to 0.25 L/s per square meter of gross wall area. The recommended internal loads (lighting, people, equipment) for an office building are presented in Table 7-4.

Table 7-4 Recommended internal loads (lighting, people, equipment) for an office building (MNECCB)

Occupant Density (m^2/person)	**Receptacle Power** (W/m^2)	**Lighting Power Density** (W/m^2)
25	7.5	16.9

The default operating schedule is shown in Table 7-5. For instance, on weekdays at 11:00 am, the lighting power density in operation is equal to 90% of the maximum installed (16.9 W/m^2), or $0.9 \times 16.9 = 15.2$ W/m^2.

Table 7-5 Operating schedules (MNECCB)

	Occupants			Lighting			Receptacle			Fans			Cooling			Heating		
	Mon-Fri	Sat	Sun	Mon-Fri	Sat	Sun	Mon-Fri	Sat	Sun	Mon-Fri	Sat	Sun	Mon-Fri	Sat	Sun	Mon-Fri	Sat	Sun
1am	0	0	0	0.5	0.05	0.05	0.2	0.2	0.2	off	off	off	off	off	off	18	18	18
2am	0	0	0	0.5	0.05	0.05	0.2	0.2	0.2	off	off	off	off	off	off	18	18	18
3am	0	0	0	0.5	0.05	0.05	0.2	0.2	0.2	off	off	off	off	off	off	18	18	18
4am	0	0	0	0.5	0.05	0.05	0.2	0.2	0.2	off	off	off	off	off	off	18	18	18
5am	0	0	0	0.5	0.05	0.05	0.2	0.2	0.2	off	off	off	off	off	off	18	18	18
6am	0	0	0	0.5	0.05	0.05	0.2	0.2	0.2	on	off	off	24	off	off	20	18	18
7am	0.1	0	0	0.3	0.05	0.05	0.3	0.2	0.2	on	off	off	24	off	off	22	18	18
8am	0.7	0	0	0.8	0.05	0.05	0.8	0.2	0.2	on	off	off	24	off	off	22	18	18
9am	0.9	0	0	0.9	0.05	0.05	0.9	0.2	0.2	on	off	off	24	off	off	22	18	18
10am	0.9	0	0	0.9	0.05	0.05	0.9	0.2	0.2	on	off	off	24	off	off	22	18	18
11am	0.9	0	0	0.9	0.05	0.05	0.9	0.2	0.2	on	off	off	24	off	off	22	18	18
12am	0.5	0	0	0.9	0.05	0.05	0.9	0.2	0.2	on	off	off	24	off	off	22	18	18
1pm	0.5	0	0	0.9	0.05	0.05	0.9	0.2	0.2	on	off	off	24	off	off	22	18	18
2pm	0.9	0	0	0.9	0.05	0.05	0.9	0.2	0.2	on	off	off	24	off	off	22	18	18
3pm	0.9	0	0	0.9	0.05	0.05	0.9	0.2	0.2	on	off	off	24	off	off	22	18	18
4pm	0.9	0	0	0.9	0.05	0.05	0.9	0.2	0.2	on	off	off	24	off	off	22	18	18
5pm	0.7	0	0	0.8	0.05	0.05	0.9	0.2	0.2	on	off	off	24	off	off	22	18	18
6pm	0.3	0	0	0.5	0.05	0.05	0.5	0.2	0.2	on	off	off	24	off	off	22	18	18
7pm	0.1	0	0	0.3	0.05	0.05	0.3	0.2	0.2	on	off	off	24	off	off	22	18	18
8pm	0.1	0	0	0.3	0.05	0.05	0.2	0.2	0.2	on	off	off	24	off	off	22	18	18
9pm	0.1	0	0	0.1	0.05	0.05	0.2	0.2	0.2	off	off	off	off	off	off	18	18	18
10pm	0.1	0	0	0.1	0.05	0.05	0.2	0.2	0.2	off	off	off	off	off	off	18	18	18
11pm	0	0	0	0.05	0.05	0.05	0.2	0.2	0.2	off	off	off	off	off	off	18	18	18
12pm	0	0	0	0.05	0.05	0.05	0.2	0.2	0.2	off	off	off	off	off	off	18	18	18

The specifications for the HVAC system are presented below [36]:

- Minimum outdoor air = 0.4 L/s per m^2
- For each thermal zone the calculated design airflow rate is the larger value of:
  a) The minimum outdoor requirement.
  b) The design airflow rate of heating determined based on supply air temperature of 43°C.
  c) The design airflow rate of cooling determined based on supply air temperature of 13°C.
- Maximum heating sizing factor R_H is equal to 1.3
- Maximum cooling sizing factor R_C is equal to 1.3
- Minimum performance of the refrigeration equipment is shown in Table 7-6.

Table 7-6 Minimum performance of refrigeration equipment (MNECCB)

Equipment Type	Standard	Minimum Performance
Packaged Terminal Air-Conditioners	CSA C744 Joint Standard with ARI 310/380	In Standard
Air-Cooled Condenser Capacity > 73 kW	ARI 365	EER = 9.9 IPLV = 11.0

- Air distribution system [36]

  The regulations on the air distribution system are shown in Table 7-7.

Table 7-7 Specifications of the air distribution system (MNECCB)

System type	VAV + Direct Expansion Cooling
Max fan power, W per L/s	2.65
Minimum supply air flow rate, L/s per m^2	2
Supply air temperature from secondary system to terminal units	13 °C
Supply Fan Static pressure/Efficiency	750 Pa/ 45%
Return Fan Static pressure/Efficiency	150 Pa / 25 %

The air distribution system should be capable of supplying 100% outdoor air, using enthalpy economizer control free cooling strategy. The fan power versus flow rate characteristic curve shall be as given in Figure 7-5, depending on the design fan power determined from equation (7-4).

$$W_F = (0.001.\ F.\ sp) / eff. \qquad (7\text{-}4)$$

Where:

F : The system design airflow rate in L/s

sp : The design static pressure across the fan in Pa

eff. : The combined fan-drive-motor efficiency expressed as the decimal fraction.

If W_F is less than 7.5 kW then curve "a" is applicable.

If W_F is greater than 7.5 kW but less than 25 kW curve "b" is applicable.

If W_F is greater than 25 kW then curve "c" is applicable.

Fans					
If P < D then F = E otherwise F = A + B • P + C • P • P					
Fan Type\Coefficient	A	B	C	D	E
(a)	0.227143	1.178929	-0.41071	0.47	0.68
(b)	0.584345	-0.57917	0.970238	0.35	0.5
(c)	0.339619	-0.84814	1.495671	0.25	0.22

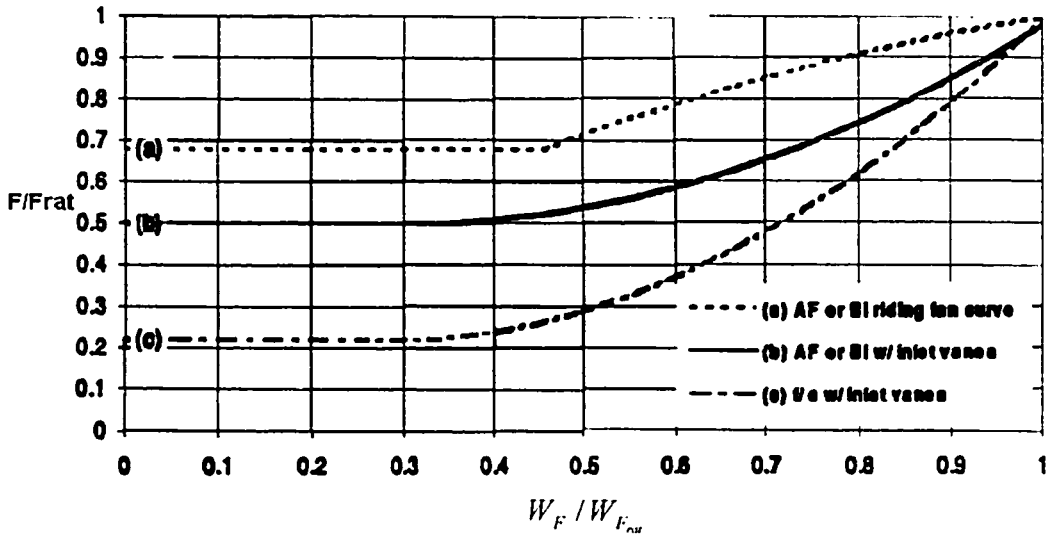

Figure 7-5 Fan part load curve [36]

7.4 Design requirements based on ASHRAE Standard 90.1

The energy simulations are also performed on three cities in the United States (Phoenix, New York, Chicago). The typical building was modified to comply with the requirements of ASHRAE standard 90.1-1985 [3].

The required characteristics of the building envelope were obtained from the following tables of ASHRAE Standard, and are summarized in Table 7-8.

Table 8A-18 (ASHRAE Standard 90.1) for Phoenix.

Table 8A-25 (ASHRAE Standard 90.1) for New York.

Table 8A-26 (ASHRAE Standard 90.1) for Chicago.

Table 7-8 Building envelope specifications (ASHRAE Standard 90.1)

City	Maximum allowable fenestration (%)	Opaque wall U_{max} W/m^2 °C	Roof U_{max} W/m^2 °C
Phoenix	57	1.36	0.26
New York	41	0.51	0.33
Chicago	37	0.46	0.30

When the HVAC system is on, no infiltration shall be assumed to occur. When the HVAC system is off, the infiltration rate for buildings with or without operable windows shall be assumed to be 0.19 L/s per square meter of gross wall area.

For an office building the internal loads (lighting, people, equipment) are presented in Table 7-9.

Table 7-9 Recommended internal loads (lighting, people, equipment) for an office building (ASHRAE Standard 90.1)

Occupant Density (m^2/person)	Receptacle Power W/m^2	Lighting Power Density W/m^2
25	8.06	16.9

The operation schedule is shown in Table 7-10. As an example, on weekdays at 11:00 am, the lighting power density is 90% of the maximum installed (16.9 W/m^2), or 0.9× 16.9=15.2 W/m^2.

Table 7-10 Operating schedules (ASHRAE standard 90.1)

	Occupants			Lighting			Receptacle			HVAC		
	Mon-Fri	Sat	Sun	Mon-Fri	Sat	Sun	Mon-Fri	Sat	Sun	Mon-Fri	Sat	Sun
1am	0	0	0	0	0	0	0	0	0	off	off	off
2am	0	0	0	0	0	0	0	0	0	off	off	off
3am	0	0	0	0	0	0	0	0	0	off	off	off
4am	0	0	0	0	0	0	0	0	0	off	off	off
5am	0	0	0	0	0	0	0	0	0	off	off	off
6am	0	0	0	0	0	0	0	0	0	off	off	off
7am	0	0	0	0.1	0	0	0.1	0	0	on	on	off
8am	0.1	0.1	0	0.3	0.1	0	0.3	0.1	0	on	on	off
9am	0.2	0.1	0	0.9	0.1	0	0.9	0.1	0	on	on	off
10am	0.95	0.3	0	0.9	0.3	0	0.9	0.3	0	on	on	off
11am	0.95	0.3	0	0.9	0.3	0	0.9	0.3	0	on	on	off
12am	0.45	0.3	0	0.9	0.3	0	0.9	0.3	0	on	on	off
1pm	0.45	0.3	0	0.8	0.3	0	0.8	0.3	0	on	on	off
2pm	0.95	0.1	0	0.9	0.15	0	0.9	0.15	0	on	on	off
3pm	0.95	0.1	0	0.9	0.15	0	0.9	0.15	0	on	on	off
4pm	0.95	0.1	0	0.9	0.15	0	0.9	0.15	0	on	on	off
5pm	0.95	0.1	0	0.9	0.15	0	0.9	0.15	0	on	on	off
6pm	0.95	0.1	0	0.5	0.15	0	0.5	0.15	0	on	on	off
7pm	0.3	0	0	0.3	0	0	0.3	0	0	on	on	off
8pm	0.1	0	0	0.3	0	0	0.3	0	0	on	off	off
9pm	0.1	0	0	0.2	0	0	0.2	0	0	on	off	off
10pm	0.1	0	0	0.2	0	0	0.2	0	0	off	off	off
11pm	0	0	0	0	0	0	0	0	0	off	off	off
12pm	0	0	0	0	0	0	0	0	0	off	off	off

The specifications for the HVAC system are presented below:

- Minimum outdoor air = 0.4 L/s/m^2 (0.08 cfm/ft^2)
- Minimum performance of the refrigeration equipment is shown in Table 7-11

Table 7-11 Minimum performance of refrigeration equipment (ASHRAE standard 90.1)

	Reference Standard	Minimum Performance	January 1, 1992
Packaged Terminal Air-Conditioners Standard Rating (95 °F bd)	ARI 310-87	EER = 10.0 – (0.19 x Cap. (Btu/hr/1000)	EER = 10.0 – (0.16 x Cap. (Btu/hr/1000)

➢ Air distribution system

The regulations on the air distribution system are shown in Table 7-12.

Table 7-12 Specifications of the air distribution system (ASHRAE standard 90.1)

System type	VAV + Direct Expansion Cooling
Max fan power, W per L/s	2.65
Minimum ventilation Air Flow Rate,L/s per person	10
Supply air-to-room-air temperature difference	11°C*
Supply fan static pressure/efficiency	750 Pa/ 45%
Return fan static pressure/efficiency	150 Pa / 25 %

* A higher supply air temperature may be used if required to maintain a minimum circulation rate of 4.5 air changers per hour or 7 L/s per person to each zone served by the system

7.5 Building description

The office building, built in Montreal in 1972, has a total floor area of 10,410 m^2 spread over a seven floor office tower, a restaurant and office spaces [37]. There is a central Variable Air Volume system, which provides cooling in the summer and ventilation all year to the office spaces from 7:30 am to 11:00 pm, from Monday to Friday. The supply fan has a capacity of 38,000 L/s and a motor of 93 kW, and the return fan has 35,000 L/s and 56 kW. The cooling setpoint temperature is 23-24°C. Direct expansion cooling coils are connected to four condensing units, each equipped with two compressors with the refrigeration capacity of about 90 kW. The supply air temperature is controlled in terms of outdoor air temperature; it has a minimum value of 14°C when outside temperature is 9°C or higher, and a maximum value of 16°C when outside temperature is –20°C or lower. The proportion of outdoor air varies between 5 and 100%, and is controlled by two parameters in the following order of priority: (1) the supply air temperature, and (2) the concentration of CO_2 in the return air duct. In the winter, the CO_2 level of 1000-2000 ppm is sometimes exceeded since the supply air temperature has

highest priority in the control of outdoor air rate. The system is also equipped with a dry-bulb temperature economizer system, which closes the dampers to a minimum position when the outdoor temperature is too high. The heating for the most of the building is provided by electric baseboard heaters with a total capacity of about 118 W/m^2 of floor area. The heating setpoint is about 20-21°C. However, since there is no central control system, the occupants can modify this value. The restaurant is equipped with a constant volume rooftop unit with the refrigeration capacity of about 27kW, which operates continuously. The unit provides cooling only and is equipped with an enthalpy economizer, which carries the proportion of fresh air from 10 to 100%. The bank is equipped with a constant volume rooftop unit, which provides heating in the winter and operated only during the business hours. The refrigeration capacity is about 55 kW. The operation outdoor air is kept constant at 15%. The garage is heated by two unit heaters to 18-19°C in the winter. There are two exhaust fans in the garage, which work in series and are activated by a sensor of carbon monoxide. Electricity is the only source of energy in this building.

The computer model of the existing building was modified to comply with MNECCB for the Canadian cities, and ASHRAE Standard for the American cities.

7.6 Pattern of energy performance of the existing building

The simulation gives the hourly heating and cooling coil load together with the corresponding wet and dry bulb temperatures.

Figures 7-6 and 7-7 show the variation of cooling and heating loads of the building located in Montreal versus the daily average outside dry bulb temperature through the

year. It can be seen that although there is a remarkable change in temperature, the cooling and heating loads change slightly. This is due to the fact that, in the large office building the internal loads (people and lighting) have a major effect on the cooling load of a building, and the weather conditions have almost a negligible impact.

The other thing that can be seen in those two graphs is that within some periods of the year (intermediate seasons) it happens that the heating and cooling loads are zero. At these times there is no need to use energy to cool or heat the building. This approach uses the economizer system and therefore there is a reduction in energy consumption for refrigeration or heating.

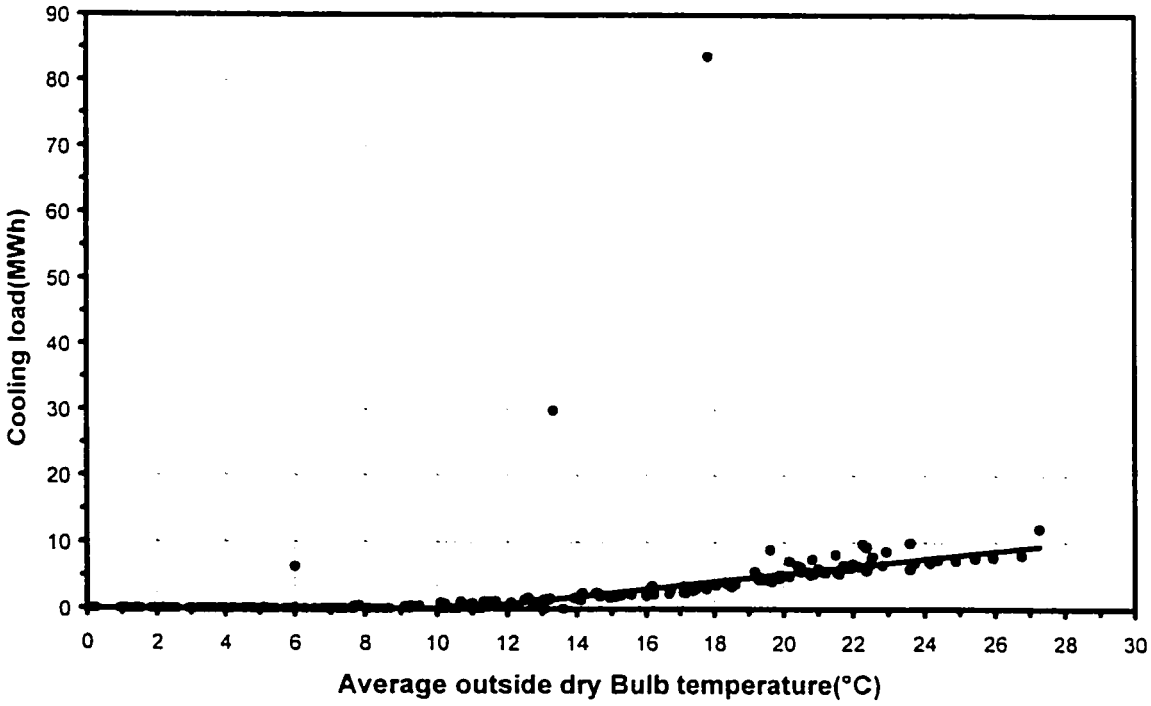

Figure 7-6 Daily cooling coil load versus daily average dry bulb temperature.

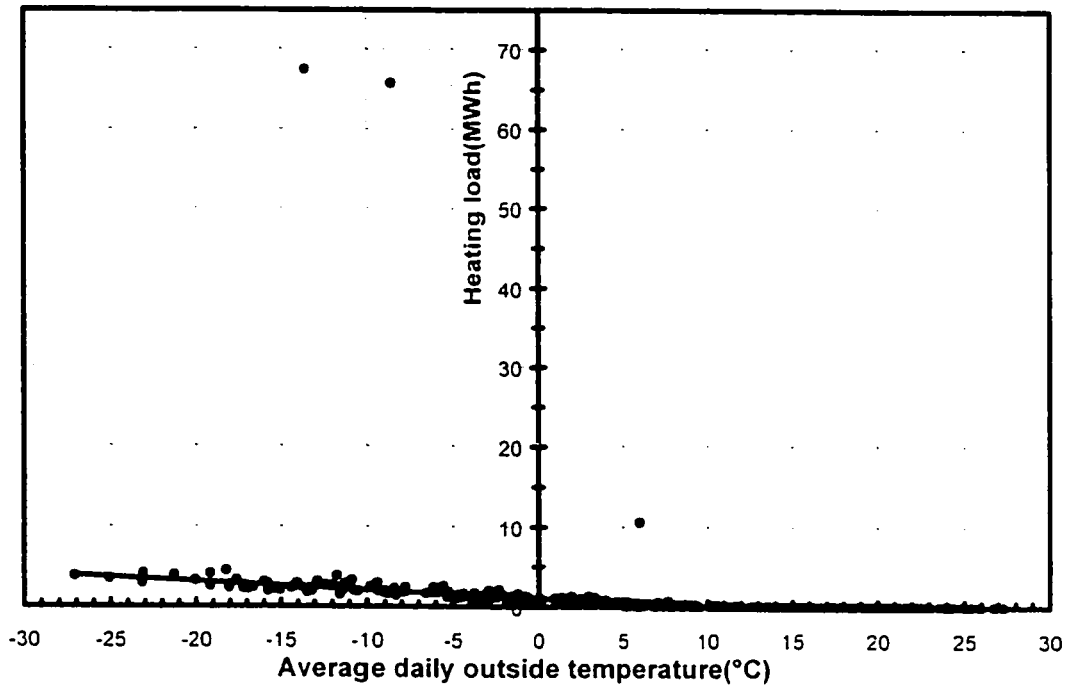

Figure 7-7 Daily heating load versus daily average dry bulb temperature

As an example, Figures 7-8 and 7-9 show the load variation versus time of day, for the days when the peak cooling coil and heating load were estimated in Montreal.

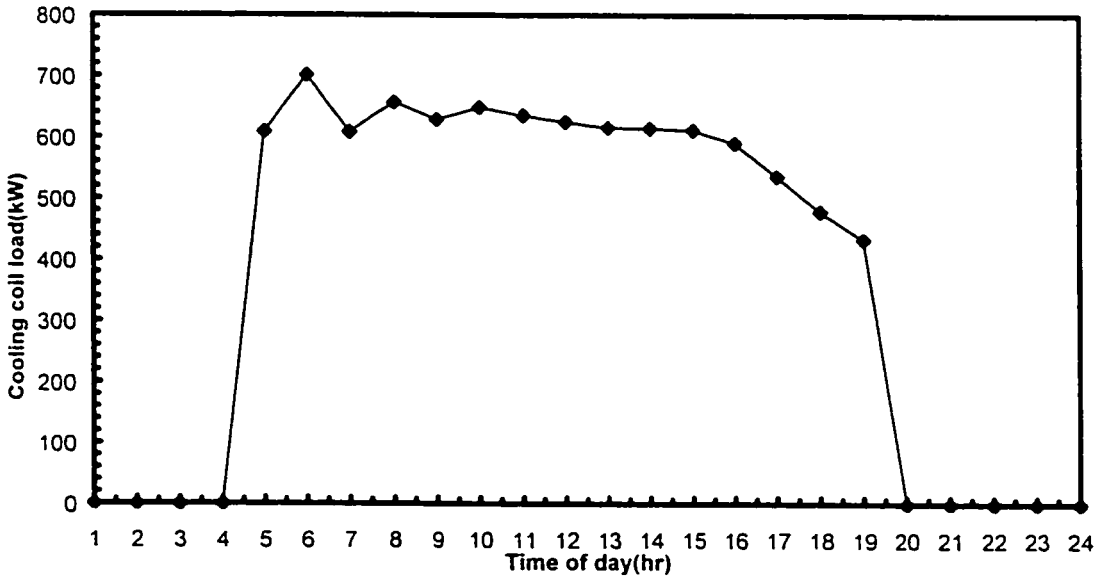

Figure 7-8 Hourly variation of the cooling coil load with time of day, on 6th of July (Montreal)

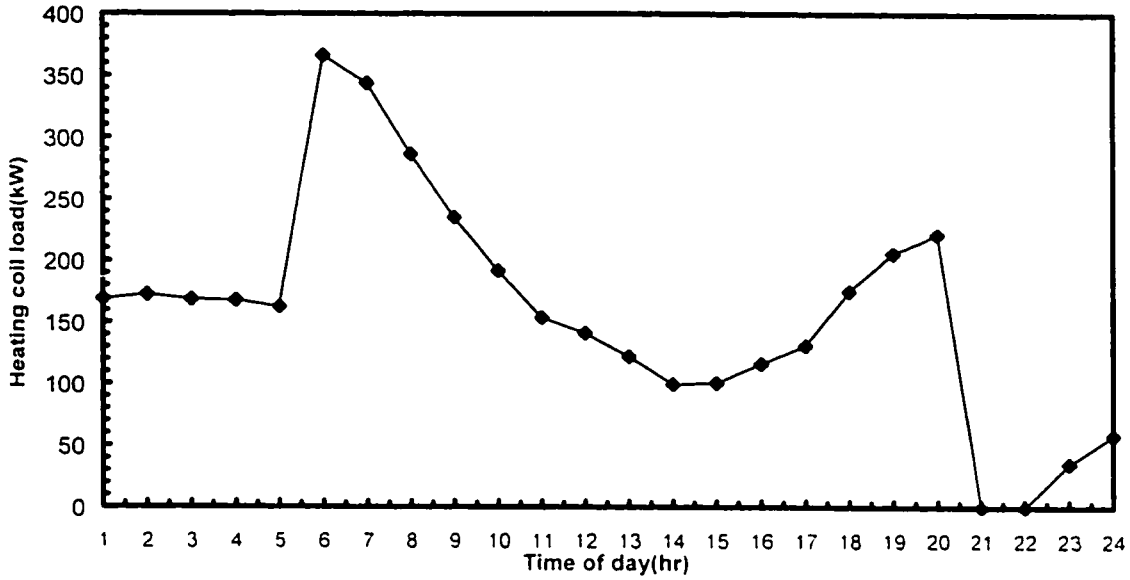

Figure 7-9 Hourly variation of the heating load with time of day, on 27th of December (Montreal)

Figure 7-8 shows that cooling coil load does not fluctuate remarkably from the maximum value, which occurs at the beginning of the operation of HVAC system. This result indicates that the refrigeration system works at an almost constant part load ratio. This information is significant for the selection of chillers. Unlike the cooling coil load, heating load variation is completely distinctive. The minimum heating load occurs around 2:00 pm, when the transmission loads are minimum, and the peak heating load occur early in the morning before people arrive in the building, due to the transmission heating loads. When people start occupying the space, the lights and the equipments such as computers are turned on, the internal loads will be added to the space thus reducing the heating loads. Also when people start leaving the building, the internal load reduces so the heating load increases. The heating and cooling coil load variation for one day of each month in Montreal has been illustrated in Figure 7-10. Cooling loads appear by the end of May. The peak transmission load in summer normally occurs around 4:00 pm, but from the graphs we can see that the peak cooling load occurs early in the morning when the

cooling system starts up. That is due to the fact that, the cooling system does not operate during the night. So the temperature within the space would increase and the heat stored in the masonry during the day will be released to the building. Hence, the cooling coil load during the start up period would be at the peak value, except in July when the transmission load will have greater effect than the start up load on the cooling coil load. In October it can be seen that heating and cooling systems operate at the same day. Before noon the building requires heating and in the afternoon, cooling is required.

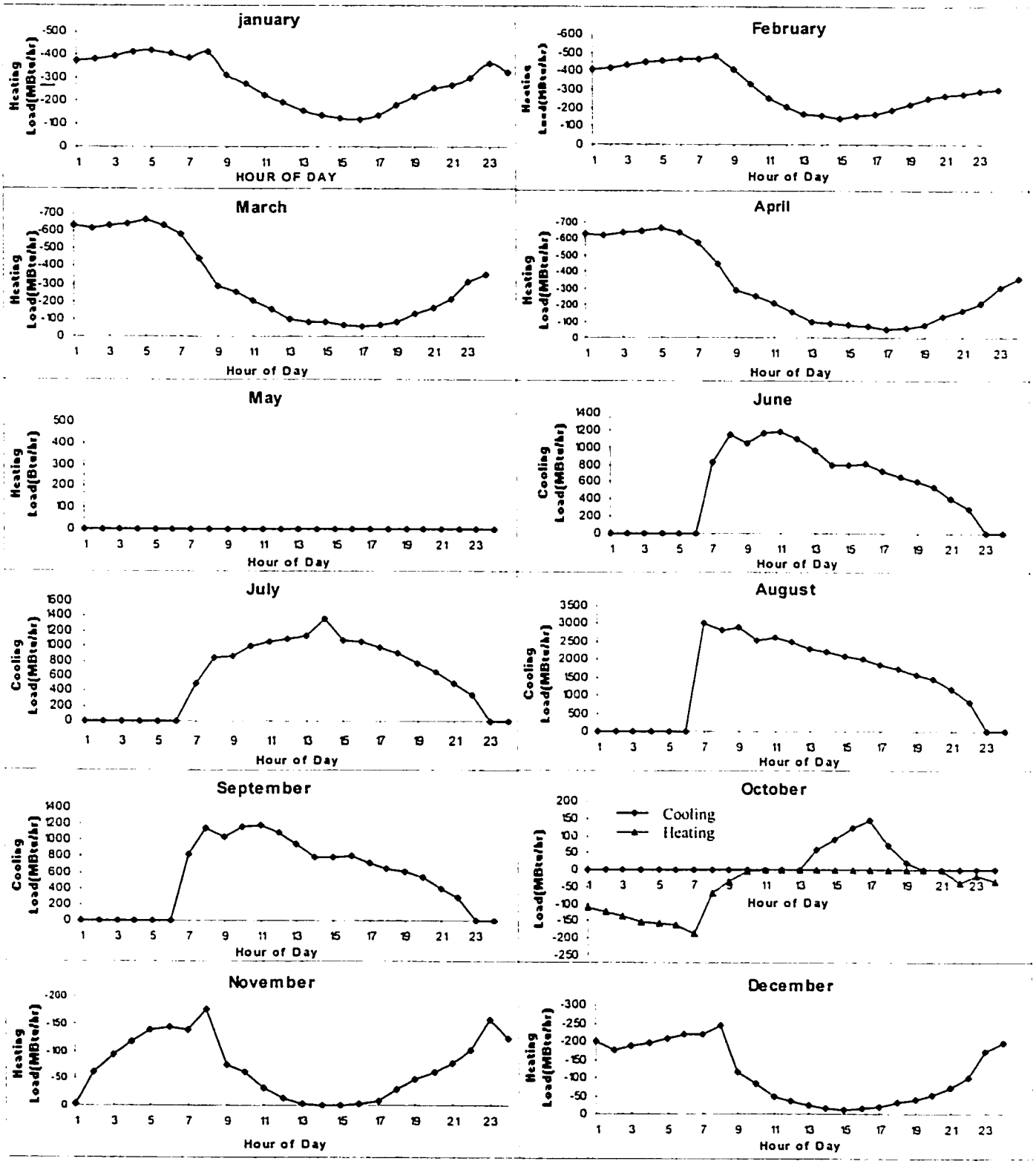

Figure 7-10 Hourly variation of the heating load on 15th of each month (Montreal)

7.7 Results

Table 7-13 shows the maximum, average and total annual system cooling and heating loads with the corresponding dry bulb temperature for the seven selected cities.

Table 7-13 Maximum, average and total system cooling and heating loads of the reference building in seven cities in North America

	summer				winter			
	Max. Cooling coil load (kW)	Average Load(kW)	Dry/Wet bulb Temp. (°C)	Total cooling coil load (MWh)	Max. Heating load (kW)	Average Load(kW)	Dry/ bulb Temp. (°C)	Total heating load(MWh)
Montreal	676.9	51.6	27.2/21.7	445	454.5	78.2	-30	679
Toronto	698.8	50.3	18.9/18.9	441	399.3	63.1	-21.1	553
Edmonton	503.6	27.9	22.8/18.3	244	424.5	81.1	-21.1	711
Vancouver	490.4	35.5	22.8/17.8	311	38.2	0.27	7.2	2
New York	596.4	74.0	21.1/20.6	648	353.4	52.8	-3.9	462
Phoenix	643.2	104.9	30.6/19.4	919	314.8	13.7	-0.6	120
Chicago	564.6	65.9	21.7/20.0	577	495.3	56.3	-17.2	493

Figure 7-11 shows the total system cooling and heating load for the different cities. It can be seen that the maximum system heating load occurs in Chicago which has about the same winter outdoor design temperature as Toronto (-17.2°C versus –21.1°C). This could be due to the lower U value of the walls for Toronto. Also it should be noted that based on the operating schedules of ASHRAE Standard, the HVAC system in the U.S. operates on Saturday too while in Canada it is off for the whole week-end. This might affect the system heating load for the beginning of the week (warm-up period). The other thing that can be recognized in Figure 7-11 is that although Edmonton is colder than Montreal (based on the weather data, Table 7-1), the maximum system heating load in Montreal is slightly higher than Edmonton. This is due to the higher insulation level of wall in Edmonton.

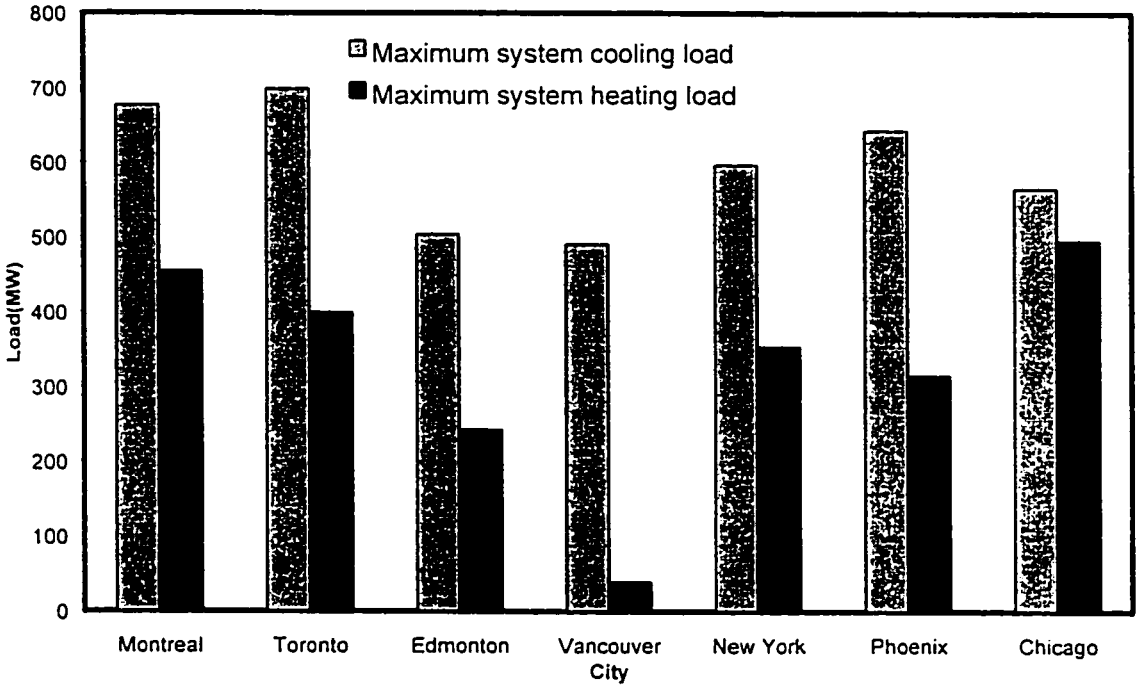

Figure 7-11 Maximum system cooling and heating loads for seven cities in North America

Figure 7-12 shows the total annual system loads for heating and cooling. It can be seen for the Canadian cities, that although the maximum cooling loads are much higher those of heating loads, their total heating energy consumptions are much higher than total cooling energy consumption. This is due to the period of operation and duration of heating season.

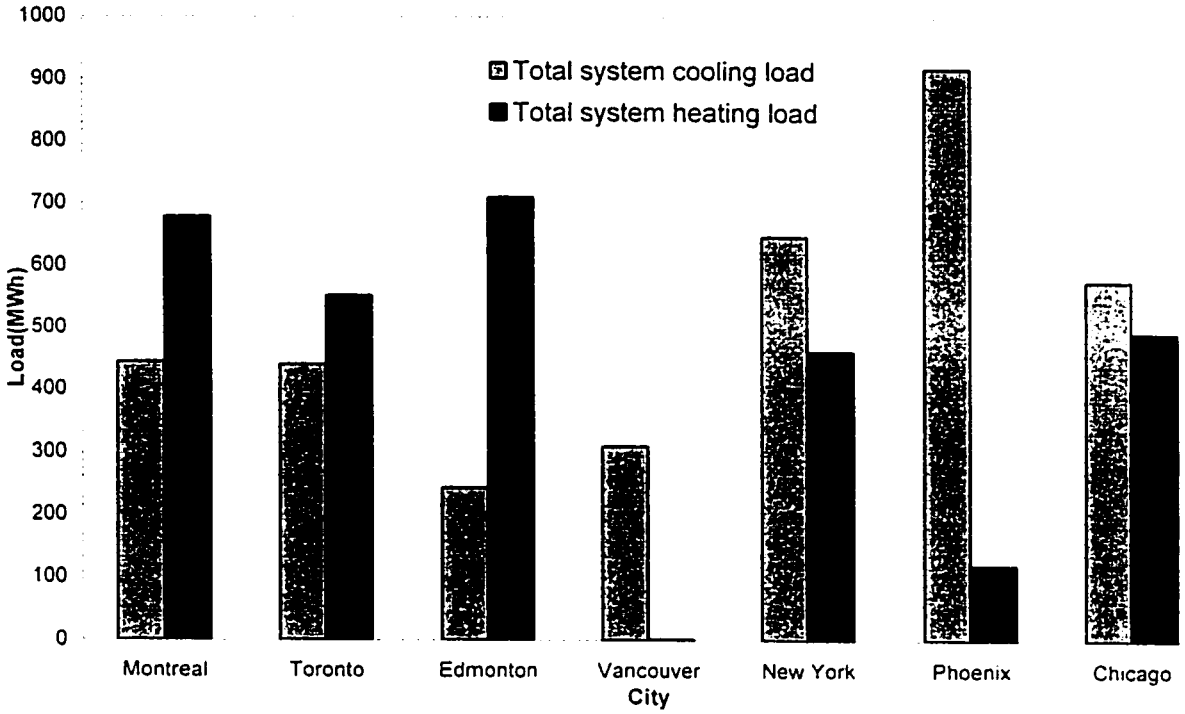

Figure 7-12 Total system cooling and heating load for seven cities in North America

In order to satisfy the system cooling loads, two design alternatives are considered: (i) a screw chiller, and (ii) a centrifugal chiller. The energy performance of centrifugal and screw chillers were evaluated for this building located in Montreal. The correlation and the corresponding coefficients in Table 6-5 are used to evaluate the performance of the screw chiller; the DOE-2 default coefficients are used for the centrifugal chiller, (Table G-1 Appendix G). Figure 7-13 shows the hourly electric demand of screw and centrifugal chillers for April 29th and July 21st. It can be seen that the screw chiller requires larger electric input than the centrifugal chiller. The difference between the electric demands of the two chillers can be explained by the different performance at part load regime (Figure 6-3).

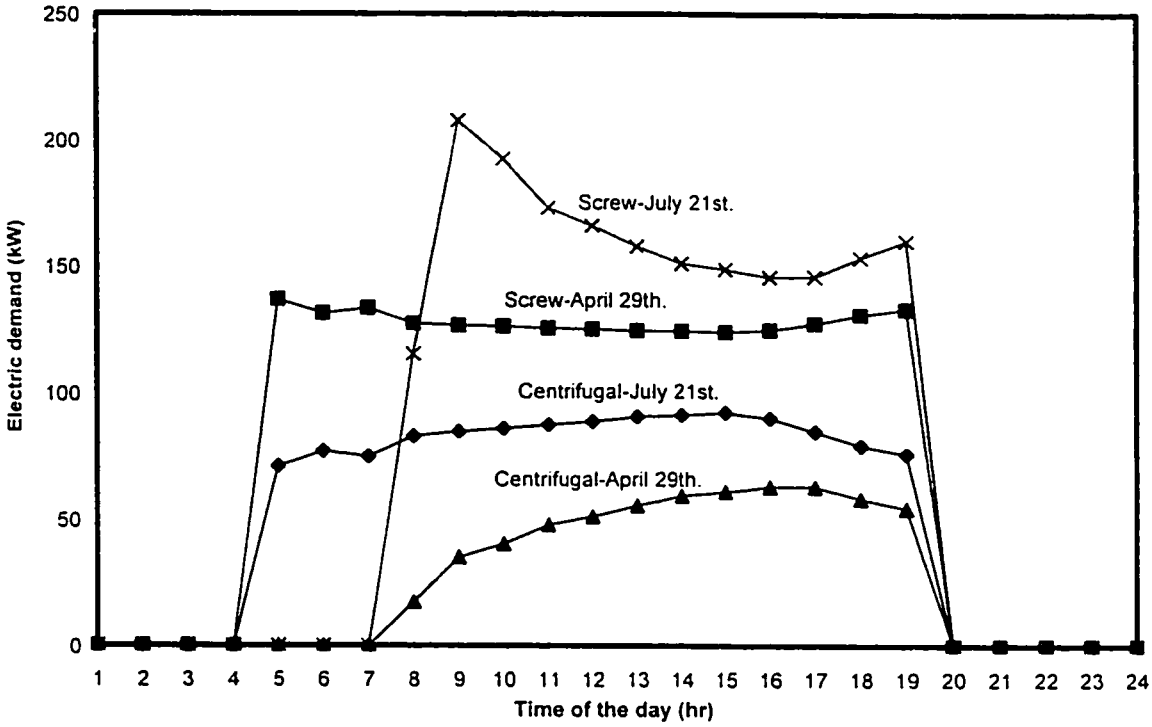

Figure 7-13 Comparison of hourly variation of electric demand of screw and centrifugal chillers for an office building in Montreal

According to the part load performance of the centrifugal chiller, the higher the part load ratio, the higher the energy demand, while for the screw chiller, the highest COP is at part load ratio equal to 0.7 and decreases for the other part load ratios.

The impact of part load performance is also noticed in the monthly peak electric demand (Figure 7-14).

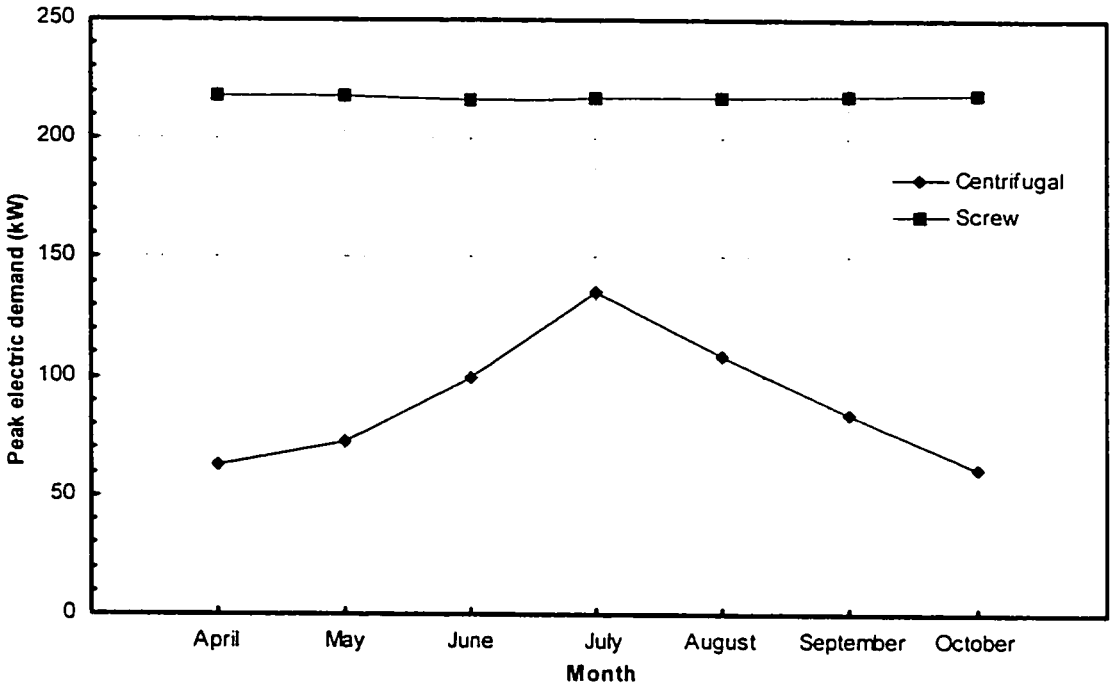

Figure 7-14 Comparison of monthly variation of peak electric demand of screw and centrifugal chillers for an office building in Montreal

The variation of monthly electricity consumption is shown in figure 7-15. The electricity consumption of screw chiller is much higher than that of the centrifugal for the same system cooling load. One can conclude that due to its part load performance the screw chiller is not an appropriate selection when system cooling load varies significantly below the peak load. Normally, the chiller should be selected to satisfy, at least the maximum system load. However, in the case of screw chiller, based on the interpretation of the results, it appears to be more economical to select the chiller in such a way that 70% of chiller capacity satisfies the most frequent system cooling load.

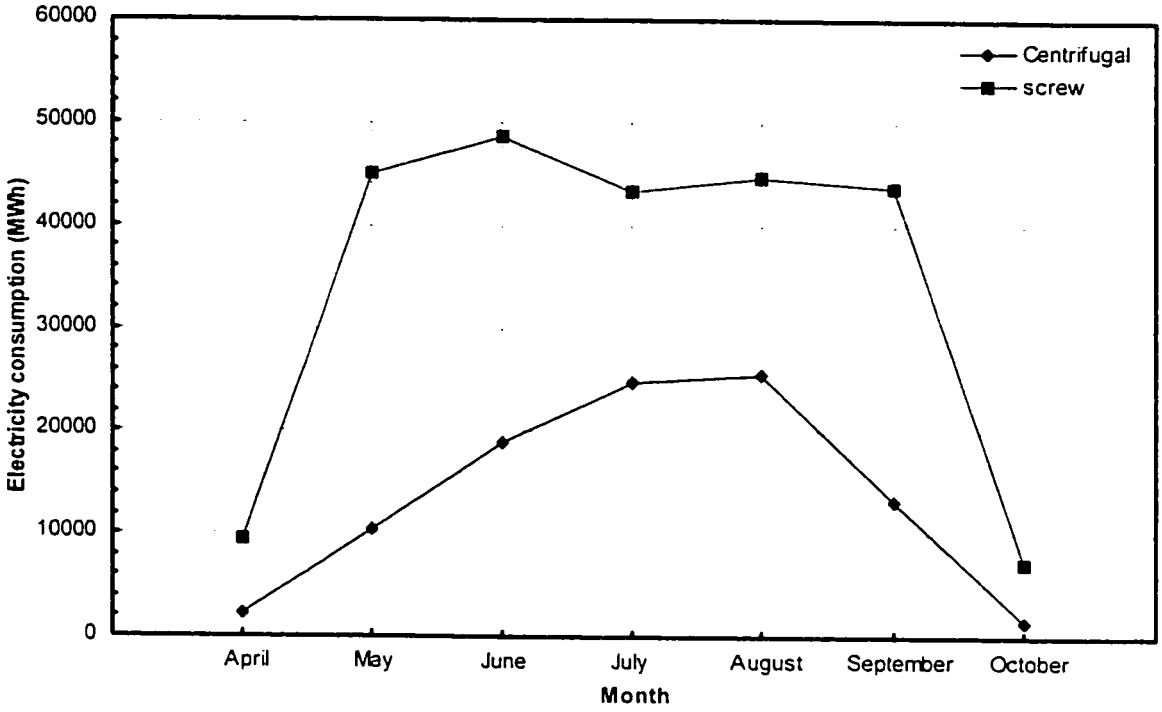

Figure 7-15 Comparison of monthly variation of electricity consumption of screw and centrifugal chillers for an office building in Montreal

Chapter 8

Conclusions

8.1 Conclusions

Energy performance of chillers as one of the important primary equipments in mechanical systems, directly affects the energy consumption of a building. Several thermodynamic and computer models were found presenting the energy performance of different type of chillers, however the screw compressor chillers have not been researched as much as the other type of chillers. The only model found was in ASHRAE toolkit-I.

Based on the thermodynamic model presented in ASHRAE Toolkit-I, the compressor electromechanical losses are sensitive to input data including: cooling capacity, compressor input power, evaporator and condenser water flow rate and temperature. This sensitivity affects the outputs of the model such as COP, which is the main parameter used in this study. Therefore the accuracy of the manufacturer's data plays a great role on the outputs and consequently the correlations derived for energy performance of screw compressor chillers in this study.

For calculating the electric demand of the compressor at part load regime, the model relies on the empirical binomial correlation. The correlations presenting the part load performance of the chiller are satisfactory because they are based on actual measurement data. However care must be taken using an empirical correlation because

the accuracy of such correlations is usually limited to the experimental range and the particular equipment under experiment and extrapolation may cause a remarkable error.

The building energy simulation showed that daily system cooling load does not fluctuate remarkably according to outdoor temperature swing during the day and it mainly varies due to internal loads. But in winter the system heating load is directly affected by outdoor condition during the day. The maximum occurring system heating and cooling load for the same building in different cities in North America follows the degree-days variation. Long winters and humidity directly affects the energy consumptions in cold seasons.

Using the energy performance correlations of screw chillers derived in this study together with the corresponding correlations of the centrifugal chiller presented in the DOE-2 program, the screw compressor chillers present a completely different part load performance. The maximum COP occurs at part load ratio about 0.7. Deviating from this ratio causes a decrease in COP. Because of this part load performance, the screw compressor chillers have almost the same peak monthly electric demand over a year.

Although trying two manufacturers' product does not seem to be sufficient to conclude a general idea on their energy performance, based on ASHRAE Toolkit-I, screw chillers perform in a higher energy consumption level than centrifugal chillers.

The significant contribution of this study is as follows: DOE-2 program, which is one of the most used program in North America, was applied for energy simulation of an office building in seven cities in that region. The building specification such as envelope and HVAC systems were modified to comply the MNECCB which itself was developed based on DOE-2. Since DOE-2 does not contain the correlation-based model for energy performance of screw chillers, the corresponding correlations were developed using ASHRAE Toolkit-I and manufacturers' data based on DOE-2 generic format. Finally the energy performance of screw chiller was compared with centrifugal chiller using the derived correlations in DOE-2 program.

8.2 Topics for future studies

The modified program of energy performance for screw compressor chiller is a program, which receives the input data for different working points through the input files. The input files are all accessible by any editor, however using external editor and different multiple input files with a few changes make the simulation time consuming and distractive. It is worthwhile putting some effort to improve the user-friendliness of the program such as using windows features. Adding an option of graphical presentation could be a good guidance for the user to see the variables in visual format or to recognize a probable mistake.

As was mentioned in literature review, the lack of thermodynamic-based model for part load performance of screw compressor chillers is felt. As a future research, developing a thermodynamic-base model for part load performance of chillers is recommended. Experimental research in this direction is of important significance.

References

1. Natural Gas Technologies Center. 1995. Double-effect technology for the air-conditioning of the buildings-An improved and wholly reliable technology that eliminates the need for environment damaging refrigerants. Energy Forum, Vol. 10, No.1, pp.6-7.
2. ASHRAE. 1995. Application Guide for Absorption Cooling/Refrigeration using recovered heat, Atlanta: American Society of Heating, Refrigeration, and Air-Conditioning Engineers, Inc.
3. ASHRAE/IES. 1989. *ASHRAE Standard 90.1-1989*, Energy efficiency design of new buildings except new low rise residential buildings, Atlanta: American Society of Heating, Refrigeration, and Air-Conditioning Engineers, Inc.
4. Porges, F. 1991. HVAC Engineer's Handbook, Great Britain: Butterworth-Heinemann Ltd.
5. Carrier. 1965. Handbook of Air Conditioning System Design, U.S.A.: McGraw-Hill, Inc.
6. Grimm, N.R.; and R.C. Rosaler. 1990. Handbook of HVAC Design, U.S.A.: McGraw-Hill, Inc.
7. Hittle, D.C. 1977. The building loads analysis and system thermodynamics program (BLAST). Champaign, IL: U.S. Army Construction Engineering Research Laboratory (CERL).
8. LBL. 1979 DOE-2: Vol. I, user's guide; vol. 2, Reference manual; vol. 3, program manual. Berkeley Laboratory.

9. Grossman, G.; and E. Michelson. 1985. A modular computer simulation of absorption systems. ASHRAE Transactions, Vol. 91, part 2B, pp.1808-1827.

10. Grossman, G.; K. Gommed; and D. Gadoth. 1987. A computer model for simulation of absorption systems in flexible and modular form. ASHRAE Transactions, Vol. 93, part 2, pp.2389-2428.

11. Gommed, K.; and G. Grossman. 1990. Performance analysis of staged absorption heat pumps:water-lithium bromide systems. ASHRAE Transactions, Vol. 96, part 1, pp.1590-1598.

12. Grossman, G.; M. Wilk; and R.C. DeVault. 1994. Simulation and performance analysis of triple-effect absorption cycles. ASHRAE Transactions, Vol. 100, part 1, pp.452-462.

13. Seewald, J.S.; and H. Perez-Blanco. 1994. A simple model for calculating the performance of the lithium bromide/water coil absorber. ASHRAE Transactions, Vol. 100, part 2, pp.318-328.

14. Hellmann, H.M.; and F.F. Ziegler. 1999. Simple absorption heat pump modules for system simulation programs. ASHRAE Transactions, Vol. 105, part 1, pp.780-787.

15. Priedeman, D.K.; and R.N. Christensen. 1999. GAX absorption cycle design process. ASHRAE Transactions, Vol. 105, part 1, pp.769-779.

16. Grossman, G.; K. Gommed; and D. Gadoth. 1991. A computer model for simulation of absorption systems in flexible and modular form. Final Report for Oak National Laboratory, Subcontract 90-89673.

17. Cecchini, C.; and D. Marchal. 1991. Simulation model of refrigerating and air conditioning equipment based on experimental data. ASHRAE Transactions, Vol. 97, part 2, pp.388-393.

18. Bourdouxhe, J.P.H.; M. Grodent; J.J. Lebrun; C. Saavedra; and K.L. Silva. 1994. A toolkit for primary HVAC system energy calculation-part 2: Reciprocating chiller model. ASHRAE Transactions, Vol. 100, part 2, pp.774-786.

19. ASHRAE Toolkit-I. A toolkit for primary HVAC system energy calculations. Proposed for ASHRAE, T.C. 4.7 Energy Calculations, by J.P. Bourdouxhe, M. Grodeut and J, Lebrun. January 1994.

20. Strand, R.K.; C.O. Pederson; and G.N. Coleman. 1994. Development of direct and indirect ice-storage models for energy analysis calculations. ASHRAE Transactions, Vol. 100, part 1, pp.1230-1244.

21. Jacobson, D.I. 1982. Simulation and optimization of the operation of an ice storage system. M.S. thesis. Urbana: Department of Mechanical and Industrial Engineering, University of Illinois at Urbana-Champaign.

22. Gordon, J.M.; and K.C. Ng. 1994. Thermodynamic modeling for reciprocating chillers. Journal of Applied physics 75(6): 2769-2774.

23. Phelan, J.; M.J. Brandemuehl; and M. Krarti. 1997. In-situ performance testing of chillers for energy analysis. ASHRAE Transactions, Vol. 103, part 1, pp.290-302

24. Figueroa, I.E.; M.A. Madina; M. Cathey; and D.W. Nutre. 1998. Modification and validation of a universal thermodynamic chiller model used to evaluate the performance of water-cooled centrifugal chillers. The eleventh symposium on improving building systems in hot and humid climates. Fort Worth, Texas, pp.57-65.

25. Jähing, D.I.; D.T. Reindl; and S.A. Klein. 2000. A semi-empirical method for representing domestic refrigerator/freezer compressor calorimeter test data. ASHRAE Transactions, Vol. 106, part 2, pp.122-130.

26. ARI. 1991. ARI Standard 540, A method for presentation of compressor performance data. Air-conditioning and Refrigeration Institute.

27. McIntosh, I.B.D.; J.W. Mitchell; and A. Beckman. 2000. Fault detection and diagnosis in chillers part I: Model development and application. ASHRAE Transaction, Vol. 106, part 2, pp.268-282.

28. McAdams, W.H. 1954. Heat transmission, 3rd ed. New York: McGraw-Hill.

29. Stoecker, W.S.; and J.W.Jones. 1982, Refrigeration and Air Conditioning, McGraw-Hill, U.S.A.

30. Ayres, J.M.; and E. Stamper. 1995. Historical development of building energy calculations. ASHRAE Transactions, Vol. 101, part 1, pp.841-849.

31. Statgraphics Plus 5. 2000. Statgraphics corporation, Manugistics, Inc. USA.

32. Waltz J.P. 1992. Practical experience in achieving high levels of accuracy in energy simulations for existing buildings. ASHRAE Transaction, Vol. 98, part 1, pp.606-617.

33. MICRO-DOE2.1E. User's Guide. ACROSOFT International, Inc. Golden, CO, 1993.

34. ASHRAE. 1997. 1997 ASHRAE Handbook--Fundamentals, Atlanta: American Society of Heating, Refrigeration, and Air-Conditioning Engineers, Inc. Chapter 28.

35. NRC-CNRC. 1997. Model National Energy Code of Canada for Buildings. Ottawa: National Research Council of Canada.

36. NRC. 1998. Performance compliance for buildings-Specification for calculation procedures for demonstrating compliance to the Model National Energy Code for Buildings using whole performance. Ottawa: National Research Council of Canada.

37. Zmeureanu R.; L. Pasqualetto; and F. Bilas. 1995. Comparison of cost and energy savings in an existing large building as predicted by three simulation programs. Building Simulation '95 Conference, Madison.

Appendix A

Computer program for calculation of the standard refrigeration cycle

```
/*************************************************************************
 *                    STANDARD IDEAL THERMODYNAMIC MODEL                 *
 *                       VAPOR-COMPRESSION CYCLE                         *
 *                           Refrigerant R134a                           *
 *                                                                       *
 *                           WRITTEN IN C++                              *
 *                                BY                                     *
 *                           BABAK SOLATI                                *
 *                            WINTER 2001                                *
 *************************************************************************/

#include <fstream.h>
#include <iostream.h>

/************************** Interpolation function definition ***********************/

double interpolation(double a1,double a2,double a3,double b1,double b2) ;
bool check=true;
double interpolation(double a1,double a2,double a3,double b1,double b2)
{
 double b3 = b1 + ((a3-a1)*(b2-b1))/(a2-a1) ;
          return b3 ;
}
/****************************** Main Program ********************************/
void main()
{

/*
  Input variables

  Tcond : condensing temperature (°C)
  Tevap : evaporation temperature (°C)
  Wact  : Actual compressor required work (kW)
  Qevap : Desired coolind capacity (kW)

  Internal variables

  H1   : Enthalpy before compressor (kJ/kg)
  H2   : Enthropy before condenser (kJ/kg)
  H3   : Enthalpy after condenser (kJ/kg)
  H4   : Enthalpy after expansion valve (kJ/kg)
  T2   : Refrigerant temperature after copression process (°C)
  S1   : Entropy before compressor (kJ/kg.K)
  P3   : Condenser pressure (Mpa)
  hs[] : Enthalpy of superheated steam (kJ/kg)
  ss[] : Entropy of superheated steam (kJ/kg.K)

  Output variables

   flow      : Flow rate of refrigerant (kg/s)
  Qcond      : Ideal heat rejected in the condenser (kW)
  Wideal     : Ideal compressor required work (kW)
  copAct     : Actual coefficient of performance
  copCarnot : Carnot coefficient of performance
  copIdeal   : Ideal coefficient of performance
  effw       : Compressor Isentropic efficiency
```

```
*/

 ifstream finR134a ;
 ofstream foutR134a ;

// R134a.dat is the file that thermodynamic properties of refigerant R134a are read from
// and R134a.out is the file that the outputs are saved in.

 finR134a.open("R134a.dat") ;
 foutR134a.open("R134a.out") ;

// Variables declaration

 double Qevap,Qcond,flow,copIdeal,Wideal,Wact,T2,S1 ;
 double H1,H2,H3,H4,P3,Tcond,Tevap;
 int   i,j,k,l,m,n,r,Tc,Te,Pc ;
 double h[60], s[60] ,p[60];
 double hs[60][90], ss[60][90] ;
 double h2[90], s2[90] ;
 char answer;
 double copAct,effw,copCarnot ;

// Reading thermodynamic data from R14a.dat

          for (i=4 ; i<=16 ; i++)
          {
                    finR134a>>h[i]>>s[i] ;
          }

    for (r=24 ; r<=50 ; r++)
          {
                    finR134a>>p[r]>>h[r]>>s[r] ;
          }

          for (j=6 ; j<=14 ; j++)
          {
                    for (k=22 ; k<=50 ; k++)
                    {
               finR134a>>hs[j][k]>>ss[j][k] ;

                    }
          }

while (check)
 {

//        Asking for input data from user

cout<<"Enter evaporator temperature(4-16°C)  " ;
cin>>Tevap ;
cout<<"Enter condenser temperature(25-50°C)  " ;
cin>>Tcond ;
cout<<"Enter desired load(kW)  " ;
cin>>Qevap ;
cout<<"Enter required work(kW)  " ;
```

```
cin>>Wact ;

// Thermodynamic properties determination of points 1,2,3 and 4 in the cycle

 Tc = int(Tcond) ;
 Te = int(Tevap) ;

if ((Tevap - Te) == 0)
{
        H1 = h[Te] ;
        S1 = s[Te] ;
}
else
{
        H1 = interpolation(Te,Te+1,Tevap,h[Te],h[Te+1]) ;
//      cout<<H1<<endl;
        S1 = interpolation(Te,Te+1,Tevap,s[Te],s[Te+1]) ;
//      cout<<S1<<endl;
}

if ((Tcond - Tc) == 0)
{
// cout<<Tc<<endl;
        H3 = h[Tc] ;
        P3=p[Tc] ;
        H4 = H3 ;
}
else
{
        H3 = interpolation(Tc,Tc+1,Tcond,h[Tc],h[Tc+1]) ;
  H4 = H3 ;
        P3 = interpolation(Tc,Tc+1,Tcond,p[Tc],p[Tc+1]) ;
}

double Pcond = P3*10 ;
Pc = int(Pcond) ;

if ((Pcond -Pc) == 0)
{
  for (l=22 ; l<=50 ; l++)
  {
   if ( S1 < ss[Pc][l] )
        {
                H2 = interpolation(ss[Pc][l],ss[Pc][l-1],S1,hs[Pc][l],hs[Pc][l-1]) ;
                T2 = interpolation(ss[Pc][l],ss[Pc][l-1],S1,l,l-1) ;
                break ;
        }
        else if (S1 == ss[Pc][l])
        {
                H2 = hs[Pc][l] ;
                T2 = l ;
        }
        else
                 continue ;
  }
}
```

```
else
{

        for (m=22 ; m<=50 ; m++)
        {
                h2[m] = interpolation(Pc,Pc+1,Pcond,hs[Pc][m],hs[Pc+1][m]) ;
                s2[m] = interpolation(Pc,Pc+1,Pcond,ss[Pc][m],ss[Pc+1][m]) ;
        }


        for (n=22 ; n<=50 ; n++)
        {
                if (S1 < s2[n])
                {
                        H2 = interpolation(s2[n],s2[n-1],S1,h2[n],h2[n-1]) ;
                   T2 = interpolation(s2[n],s2[n-1],S1,n,n-1) ;
                }
          else if (S1 == s2[n])
                {
                        H2 = h2[n] ;
                        T2 = n ;
                }
        }

}

// Output variable calculation

flow = (Qevap)/(H1-H4) ;
Wideal = flow * (H2-H1) ;
copIdeal = (H1-H4)/(H2-H1) ;
Qcond = flow * (H2-H3) ;
copAct = (Qevap)/Wact ;
effw = (Wideal/Wact)*100 ;
copCarnot = (Tevap+273.16)/(Tcond-Tevap) ;


// Writing the outputs into the file R134a.out


foutR134a<<"Tev="<<Tevap<<" °C"<<endl ;
foutR134a<<"Tcd="<<Tcond<<" °C"<<endl ;
foutR134a<<"Wactual="<<Wact<<" kW"<<endl;
foutR134a<<"Wideal="<<Wideal<<" kW"<<endl;
foutR134a<<"Qev="<<Qevap<<" kW"<<endl;
foutR134a<<"Qcd="<<Qcond<<" kW"<<endl;
foutR134a<<"Ref. flow="<<flow<<" kg/s"<<endl;
foutR134a<<"copIdeal="<<copIdeal<<endl;
foutR134a<<"copActual="<<copAct<<endl;
foutR134a<<"copCarnot="<<copCarnot<<endl;
foutR134a<<"Isen. eff.="<<effw<<"%"<<endl;

// Writing the outputs on the screen

cout<<"Tev="<<Tevap<<" °C"<<endl ;
cout<<"Tcd="<<Tcond<<" °C"<<endl ;
```

```
cout<<"Wactual="<<Wact<<" kW"<<endl;
cout<<"Wideal="<<Wideal<<" kW"<<endl;
cout<<"Qev="<<Qevap<<" kW"<<endl;
cout<<"Qcd="<<Qcond<<" kW"<<endl;
cout<<"Ref. flow="<<flow<<" kg/s"<<endl;
cout<<"copIdeal="<<copIdeal<<endl;
cout<<"copActual="<<copAct<<endl;
cout<<"copCarnot="<<copCarnot<<endl;
cout<<"Isen. Eff.="<<effw<<"%"<<endl;


cout<<"Do you want to continue? " ;
cin>>answer;
if (answer == 'Y' || answer == 'y')
{
   check = true;
          foutR134a<<"\n\n" ;
}
else if(answer == 'N' || answer == 'n')
   check = false;


}


finR134a.close() ;
foutR134a.close() ;


return ;
        }
```

R134a.dat

401.00 1.7252
401.71 1.7257
. .
. . } Enthalpy kJ/kg and entropy kJ/kg.K, (vapor , $4 \leq T \leq 16$)
. .
407.16 1.7203
407.70 1.7199

0.64566 233.05 1.1149
0.66549 234.48 1.1196
. . .
. . . } Pressure MPa, enthalpy kJ/kg and entropy kJ/kg.K ($24 \leq T \leq 50$)
. . .
1.28520 270.04 1.2326
1.31770 271.59 1.2373

411.1 1.7192
412.2 1.7212
413.3 1.7251
414.4 1.7291
415.3 1.7324
416.2 1.7357 } Enthalpy kJ/kg and entropy kJ/kg.K (superheated vapor, $24 \leq T_{sat} \leq 50$)
417.1 1.7389
. .
. .
. .

Sample output file (R134a.out)

Tev=4 °C

Tcd=25 °C

Wactual=48.2 kW

Wideal=26.7403 kW

Qev=253.3 kW

Qcd=280.04 kW

Ref. flow=1.52114 kg/s

copIdeal=9.4726

copAct=5.25519

copCarnot=13.1981

effw=55.4778%

Tev=7 °C

Tcd=25 °C

Wactual=62.3 kW

Wideal=32.785 kW

Qev=355.7 kW

Qcd=388.485 kW

Ref. flow=2.11437 kg/s

copIdeal=10.8495

copAct=5.70947

copCarnot=15.5644

effw=52.6243%

Tev=10 °C

Tcd=35 °C

Wactual=111.4 kW

Wideal=50.6293 kW

Qev=502.6 kW

Qcd=553.229 kW

Ref. flow=3.23299 kg/s

copIdeal=9.92705

copAct=4.51167

copCarnot=11.3264

effw=45.4482%

Appendix B

Manufacturers' technical data

Table B-1 Technical catalogue data for 30HXC water-cooled screw compressor chiller (Cont.)

30HXC COOLING CAPACITIES (cont)

60 Hz, SI

LCWT (C)	UNIT SIZE 30HXC	CONDENSER ENTERING WATER TEMPERATURE (C)											
		25				30				35			
		Cap.	Input kW	Cooler Flow Rate (L/s)	Cond Flow Rate (L/s)	Cap.	Input kW	Cooler Flow Rate (L/s)	Cond Flow Rate (L/s)	Cap.	Input kW	Cooler Flow Rate (L/s)	Cond Flow Rate (L/s)
4.0	076	253.3	48.2	10.9	12.8	234.3	53.2	10.1	12.2	219.0	58.9	9.4	11.8
	086	279.3	54.2	12.0	14.2	258.8	59.8	11.1	13.6	242.8	66.3	10.4	13.1
	096	315.5	60.1	13.5	16.0	292.4	66.5	12.5	15.3	274.3	73.8	11.8	14.8
	106	350.4	67.5	15.0	17.8	323.9	74.8	13.9	17.0	304.3	83.6	13.1	16.5
	116	380.9	71.7	16.3	19.3	352.8	79.7	15.1	18.4	330.6	88.9	14.2	17.9
	126	412.5	77.8	17.7	20.9	382.6	86.7	16.4	20.0	359.0	96.8	15.4	19.4
	136	457.2	87.4	19.6	23.2	425.0	96.5	18.2	22.2	400.3	107.0	17.2	21.6
	146	489.2	94.6	21.0	24.9	454.2	104.7	19.5	23.8	428.3	116.7	18.4	23.2
	161	516.5	99.2	22.2	26.2	500.1	115.5	21.5	26.2	494.5	135.8	21.2	26.8
	171	547.2	105.5	23.5	27.8	532.8	122.4	22.9	27.9	526.6	142.9	22.6	28.5
	186	584.8	113.6	25.1	29.8	569.1	131.4	24.4	29.8	563.8	153.4	24.2	30.6
	206	697.8	130.3	29.9	35.3	676.3	150.8	29.0	35.2	663.7	175.8	28.5	35.7
	246	819.9	152.7	35.2	41.5	795.2	178.2	34.1	41.5	782.7	208.6	33.6	42.2
	261	848.6	160.3	36.4	43.0	824.6	186.1	35.4	43.0	814.2	217.4	34.9	43.9
	271	882.7	168.4	37.9	44.8	858.2	195.3	36.8	44.9	848.5	228.0	36.4	45.8
5.0	076	264.0	48.6	11.3	13.3	244.2	53.7	10.5	12.7	227.2	59.3	9.8	12.2
	086	291.1	54.7	12.5	14.7	269.7	60.4	11.6	14.1	251.8	66.7	10.8	13.6
	096	328.8	60.6	14.1	16.6	304.8	67.1	13.1	15.8	284.5	74.3	12.2	15.3
	106	365.2	67.9	15.7	18.5	337.9	75.5	14.5	17.6	315.4	84.1	13.5	17.0
	116	396.9	72.2	17.0	20.0	368.2	80.4	15.8	19.1	342.8	89.4	14.7	18.4
	126	429.7	78.5	18.4	21.7	399.0	87.3	17.1	20.7	372.1	97.3	16.0	20.0
	136	476.5	88.0	20.5	24.1	442.8	97.2	19.0	23.0	415.1	107.6	17.8	22.3
	146	509.7	95.3	21.9	25.8	472.9	105.4	20.3	24.6	443.9	117.3	19.1	23.9
	161	534.4	98.8	22.9	27.0	517.4	115.3	22.2	26.9	508.5	135.7	22.1	27.6
	171	565.5	105.2	24.3	28.6	549.6	121.8	23.6	27.8	541.4	142.7	23.4	28.5
	186	604.6	113.2	26.0	30.6	587.8	131.1	25.2	30.6	579.4	153.6	24.9	31.4
	206	721.6	130.2	31.0	36.3	699.3	150.2	30.0	35.2	689.0	174.9	29.5	36.1
	246	847.2	152.7	36.4	42.6	822.6	177.7	35.3	42.6	804.8	207.6	34.5	43.1
	261	877.0	159.8	37.6	44.2	852.1	185.4	36.6	44.2	836.9	216.1	35.9	44.8
	271	912.2	167.9	39.2	46.0	886.5	194.8	38.1	46.1	872.0	226.9	37.4	46.8
6.0	076	274.8	49.3	11.8	13.8	254.6	54.2	10.9	13.2	235.6	59.7	10.1	12.6
	086	303.0	55.3	13.0	15.3	281.0	60.9	12.1	14.6	261.1	67.2	11.2	14.0
	096	342.1	61.5	14.7	17.2	317.5	67.7	13.6	16.4	295.0	74.8	12.7	15.8
	106	380.0	68.6	16.3	19.1	352.4	76.2	15.1	18.3	326.9	86.5	14.0	17.6
	116	413.0	73.0	17.7	20.7	383.9	81.0	16.5	19.8	355.4	90.5	15.3	19.2
	126	447.2	79.1	19.2	22.4	415.9	88.0	17.9	21.5	385.7	98.2	16.6	20.6
	136	495.8	89.2	21.3	24.9	461.3	98.0	19.8	23.8	430.3	108.1	18.5	22.9
	146	530.4	96.2	22.8	26.7	493.0	106.3	21.2	25.5	460.1	117.8	19.8	24.6
	161	551.9	98.9	23.7	27.8	535.3	115.1	23.0	27.7	522.7	134.7	22.5	28.0
	171	584.0	105.3	25.1	29.4	568.2	121.7	24.4	29.4	556.5	141.7	23.9	29.7
	186	624.0	113.3	26.8	31.4	607.0	130.8	26.1	31.4	595.3	152.0	25.6	31.8
	206	745.8	130.4	32.0	37.4	723.5	150.2	31.1	37.3	703.4	174.7	30.2	37.4
	246	874.5	153.0	37.6	43.8	850.6	177.1	36.5	43.8	827.4	207.0	35.5	44.1
	261	904.8	160.3	38.9	45.4	880.4	184.9	37.8	45.4	860.1	215.0	36.9	45.8
	271	940.9	168.5	40.4	47.3	915.5	194.2	39.3	47.3	895.9	225.6	38.5	47.8

LEGEND

Cap. — Capacity, kW
Cond — Condenser
kW — Compressor Motor Input Power at Rated Voltage
LCWT — Leaving Chilled-Water Temperature (C)

Table B-1 Technical catalogue data for 30HXC water-cooled screw compressor chiller (Cont.)

Performance data (cont)

30HXC COOLING CAPACITIES (cont)

60 Hz, SI (cont)

LCWT (C)	UNIT SIZE 30HXC	CONDENSER ENTERING WATER TEMPERATURE (C)											
		25				30				35			
		Cap.	Input kW	Cooler Flow Rate (L/s)	Cond Flow Rate (L/s)	Cap.	Input kW	Cooler Flow Rate (L/s)	Cond Flow Rate (L/s)	Cap.	Input kW	Cooler Flow Rate (L/s)	Cond Flow Rate (L/s)
7.0	076	285.8	50.0	12.3	14.3	265.5	54.7	11.4	13.7	244.7	60.1	10.5	13.0
	086	315.0	56.1	13.5	15.8	292.7	61.5	12.6	15.1	270.7	67.6	11.6	14.4
	096	355.7	62.3	15.3	17.8	330.9	68.3	14.2	17.0	305.9	75.2	13.1	16.2
	106	395.0	69.4	17.0	19.8	367.3	76.8	15.8	18.9	338.8	86.9	14.6	18.1
	116	429.4	73.8	18.5	21.5	400.0	81.5	17.2	20.5	369.2	90.3	15.9	19.6
	126	465.0	80.0	20.0	23.3	433.2	88.5	18.6	22.2	400.9	98.3	17.2	21.3
	136	515.5	90.3	22.2	25.8	480.7	98.8	20.7	24.7	446.1	108.7	19.2	23.6
	146	551.5	97.2	23.7	27.7	514.0	107.1	22.1	26.5	477.0	120.3	20.5	25.4
	161	569.5	99.1	24.5	28.5	553.9	114.9	23.8	28.5	537.3	136.0	23.1	28.7
	171	602.5	105.7	25.9	30.2	587.0	121.7	25.2	30.2	572.7	141.5	24.6	30.4
	186	643.4	113.6	27.7	32.3	627.0	130.5	26.9	32.3	611.5	151.2	26.3	32.5
	206	767.9	130.7	33.0	38.3	748.2	150.1	32.2	38.3	725.6	174.6	31.2	38.4
	246	902.1	153.1	38.8	45.0	879.4	176.5	37.8	45.0	852.2	205.5	36.6	45.1
	261	933.1	160.9	40.1	46.7	910.0	184.8	39.1	46.7	884.3	214.3	38.0	46.8
	271	970.1	168.8	41.7	48.6	946.0	193.8	40.7	48.6	920.3	224.4	39.6	48.8
8.0	076	297.0	50.5	12.8	14.8	276.7	55.1	11.9	14.2	254.9	60.7	11.0	13.5
	086	327.4	56.9	14.1	16.4	305.0	62.0	13.1	15.7	281.6	68.2	12.1	14.9
	096	369.8	63.0	15.9	18.5	344.8	68.8	14.8	17.6	318.5	75.9	13.7	16.8
	106	410.5	70.2	17.7	20.5	382.6	77.3	16.5	19.6	352.2	85.5	15.1	18.7
	116	446.2	74.5	19.2	22.2	416.7	82.0	17.9	21.3	384.6	90.9	16.5	20.3
	126	482.7	80.8	20.8	24.0	451.2	89.0	19.4	23.1	417.2	98.9	17.9	22.0
	136	535.7	91.4	23.0	26.8	500.7	99.4	21.5	25.6	464.2	109.6	20.0	24.5
	146	573.0	98.2	24.6	28.6	535.4	107.7	23.0	27.4	495.5	120.4	21.3	26.3
	161	587.4	99.2	25.3	29.3	572.5	114.5	24.6	29.3	553.3	133.5	23.8	29.3
	171	620.0	106.1	26.7	31.0	606.4	121.7	26.1	31.1	589.7	141.4	25.4	31.2
	186	663.1	113.8	28.5	33.1	647.6	130.1	27.8	33.2	629.4	150.7	27.1	33.3
	206	788.8	130.7	33.9	39.2	773.3	150.4	33.3	39.4	748.2	174.3	32.2	39.3
	246	927.6	152.7	39.9	46.1	908.8	175.7	39.1	46.3	880.2	205.0	37.8	46.3
	261	961.0	161.1	41.3	47.9	940.1	184.3	40.4	48.0	912.6	214.3	39.2	48.1
	271	999.8	168.9	43.0	49.9	977.1	193.0	42.0	49.9	949.1	224.0	40.8	50.0
9.0	076	307.1	50.9	13.2	15.3	288.1	55.6	12.4	14.7	265.4	61.3	11.4	13.9
	086	339.3	57.5	14.6	16.9	317.5	62.5	13.7	16.2	293.1	68.9	12.6	15.4
	096	382.7	63.6	16.5	19.0	358.9	69.3	15.4	18.3	331.5	76.6	14.3	17.4
	106	425.6	70.8	18.3	21.2	398.2	77.7	17.1	20.3	367.1	86.2	15.8	19.3
	116	461.5	74.9	19.9	22.9	433.7	82.6	18.7	22.0	401.0	91.7	17.3	21.0
	126	499.3	81.2	21.5	24.8	469.5	89.7	20.2	23.9	434.6	99.6	18.7	22.8
	136	554.9	92.1	23.9	27.6	521.4	100.0	22.4	26.5	483.1	110.5	20.8	25.3
	146	593.6	99.0	25.5	29.6	557.2	108.4	24.0	28.4	515.4	119.9	22.2	27.1
	161	604.3	99.0	26.0	30.0	591.4	114.0	25.4	30.1	571.9	133.3	24.6	30.1
	171	636.5	105.9	27.4	31.7	625.9	121.6	26.9	31.9	607.9	141.1	26.2	31.9
	186	681.5	113.6	29.3	33.9	668.5	129.6	28.8	34.1	649.4	150.5	27.9	34.1
	206	810.0	130.3	34.8	40.1	798.6	150.5	34.4	40.5	772.8	174.0	33.2	40.4
	246	950.1	151.7	40.9	47.0	937.9	175.5	40.3	47.5	909.5	204.6	39.1	47.5
	261	983.6	160.4	42.3	48.8	970.2	184.0	41.7	49.3	941.7	214.0	40.5	49.3
	271	1023.9	168.1	44.1	50.9	1008.4	192.0	43.4	51.2	979.1	223.6	42.1	51.3

LEGEND

Cap. — Capacity, kW
Cond — Condenser
kW — Compressor Motor Input Power at Rated Voltage
LCWT — Leaving Chilled-Water Temperature (C)

Table B-1 Technical catalogue data for 30HXC water-cooled screw compressor chiller (Cont.)

30HXC COOLING CAPACITIES (cont)

60 Hz, SI (cont)

LCWT (C)	UNIT SIZE 30HXC	CONDENSER ENTERING WATER TEMPERATURE (C)											
		25				30				35			
		Cap.	Input kW	Cooler Flow Rate (L/s)	Cond Flow Rate (L/s)	Cap.	Input kW	Cooler Flow Rate (L/s)	Cond Flow Rate (L/s)	Cap.	Input kW	Cooler Flow Rate (L/s)	Cond Flow Rate (L/s)
10.0	076	316.8	51.2	13.6	15.7	299.5	56.3	12.9	15.2	276.5	61.8	11.9	14.4
	086	350.6	57.9	15.1	17.4	330.2	63.2	14.2	16.8	305.0	69.5	13.1	16.0
	096	394.6	63.9	17.0	19.6	373.1	70.2	16.1	18.9	345.0	77.2	14.8	18.0
	106	439.6	71.1	18.9	21.8	414.1	78.4	17.8	21.0	382.5	87.0	16.5	20.0
	116	476.2	75.1	20.5	23.5	450.9	83.4	19.4	22.9	417.7	92.3	18.0	21.8
	126	515.7	81.5	22.2	25.5	488.1	90.5	21.0	24.7	452.5	100.4	19.5	23.6
	136	572.0	92.6	24.6	28.4	541.9	101.3	23.3	27.5	502.6	111.4	21.6	26.2
	146	613.8	99.6	26.4	30.5	579.2	109.5	24.9	29.4	536.8	120.9	23.1	28.1
	161	618.4	98.4	26.6	30.6	610.2	114.0	26.3	30.9	590.9	133.0	25.4	30.9
	171	652.7	105.5	28.1	32.4	645.5	121.6	27.8	32.7	627.4	140.9	27.0	32.8
	186	697.0	113.0	30.0	34.6	689.2	129.6	29.7	35.0	669.6	150.2	28.8	35.0
	206	830.5	129.5	35.7	41.0	824.3	150.5	35.5	41.6	798.6	173.7	34.4	41.5
	246	971.5	150.3	41.8	47.9	966.9	175.9	41.6	48.8	939.2	204.0	40.4	48.8
	261	1005.3	159.3	43.3	49.7	999.8	184.7	43.0	50.6	971.6	213.5	41.8	50.6
	271	1046.2	166.9	45.0	51.8	1038.9	192.9	44.7	52.6	1009.6	223.0	43.5	52.6
13.0	076	333.2	51.5	14.4	16.4	318.8	57.5	13.7	16.1	295.3	62.7	12.7	15.3
	086	371.6	58.5	16.0	18.4	351.4	64.7	15.1	17.8	322.0	70.4	13.9	16.7
	096	414.1	64.3	17.8	20.4	396.1	71.7	17.1	20.0	367.5	78.3	15.8	19.0
	106	462.7	71.3	19.9	22.8	441.4	80.0	19.0	22.3	404.1	87.9	17.4	21.0
	116	503.0	75.3	21.7	24.7	482.5	85.1	20.8	24.3	444.8	93.3	19.2	23.0
	126	549.3	81.8	23.7	27.0	523.1	92.4	22.5	26.3	486.7	101.6	21.0	25.1
	136	604.3	93.2	25.0	29.8	580.0	103.7	25.0	29.2	540.2	113.0	23.3	27.9
	146	653.5	99.9	28.2	32.2	626.2	111.9	27.0	31.5	577.9	122.6	24.9	29.9
	161	644.6	96.7	27.8	31.7	644.8	114.5	27.8	32.4	627.2	132.5	27.0	32.4
	171	680.9	104.1	29.3	33.5	683.3	122.1	29.4	34.4	666.1	140.3	28.7	34.4
	186	721.9	111.6	31.1	35.6	722.7	130.3	31.1	36.4	704.3	149.7	30.3	36.5
	206	867.6	128.6	37.4	42.6	868.0	150.8	37.4	43.5	840.0	173.0	36.2	43.3
	246	1005.8	148.1	43.3	49.3	1012.4	176.1	43.6	50.8	986.6	203.0	42.5	50.8
	261	1035.5	157.4	44.6	51.0	1040.5	185.1	44.8	52.4	1014.1	212.8	43.7	52.4
	271	1085.7	164.3	46.8	53.4	1092.2	193.4	47.1	54.9	1065.4	222.0	45.9	55.0
16.0	076	330.1	51.4	14.2	16.3	315.2	57.3	13.6	15.9	291.7	62.6	12.6	15.1
	086	368.2	58.4	15.9	18.2	350.8	64.6	15.1	17.7	325.2	70.5	14.0	16.9
	096	414.4	64.3	17.9	20.4	396.5	71.7	17.1	20.0	363.2	78.1	15.7	18.8
	106	461.4	71.3	19.9	22.8	439.8	79.9	19.0	22.2	408.0	88.0	17.6	21.2
	116	503.5	75.2	21.7	24.7	483.2	85.1	20.8	24.3	449.3	93.5	19.4	23.2
	126	649.5	81.7	23.7	27.0	522.1	92.4	22.5	26.3	485.7	101.6	20.9	25.1
	136	604.9	93.2	26.1	29.8	580.7	103.7	25.0	29.2	540.9	113.0	23.3	27.9
	146	653.8	100.0	28.2	32.2	626.6	111.9	27.0	31.5	576.7	122.4	24.9	29.9
	161	644.7	96.7	27.8	31.7	645.0	114.5	27.8	32.4	627.4	132.5	27.1	32.5
	171	680.8	104.2	29.4	33.5	682.8	122.0	29.4	34.4	665.5	140.3	28.7	34.4
	186	725.8	111.4	31.3	35.8	728.0	130.3	31.4	36.7	703.9	149.7	30.4	36.5
	206	861.0	128.7	37.1	42.3	861.3	150.9	37.1	43.2	837.8	173.1	36.1	43.2
	246	1007.7	148.2	43.5	49.4	1014.1	176.0	43.7	50.9	988.3	202.9	42.6	50.9
	261	1041.2	157.0	44.9	51.2	1048.1	185.2	45.2	52.7	1022.1	212.6	44.1	52.7
	271	1083.0	164.5	46.7	53.3	1088.6	193.4	46.9	54.8	1061.6	222.1	45.8	54.8

LEGEND

Cap. — Capacity, kW
Cond — Condenser
kW — Compressor Motor Input Power at Rated Voltage
LCWT — Leaving Chilled-Water Temperature (C)

Table B-2 Technical catalogue data for 30HXA air-cooled screw compressor chiller

COMBINATION RATINGS (cont)

60 Hz, SI

LCWT (C)	UNIT SIZE 30HXA	09DK AIR-COOLED CONDENSER Unit	(Qty)	CONDENSER ENTERING AIR TEMPERATURE (C) 30 Cap.	30 Input kW	30 Cooler Flow Rate (L/s)	35 Cap.	35 Input kW	35 Cooler Flow Rate (L/s)	40 Cap.	40 Input kW	40 Cooler Flow Rate (L/s)	45 Cap.	45 Input kW	45 Cooler Flow Rate (L/s)	50 Cap.	50 Input kW	50 Cooler Flow Rate (L/s)
4	076	084	(1)	231.7	69.2	9.9	216.1	72.9	9.2	198.6	76.7	8.5	181.2	81.9	7.7	166.4	88.5	7.1
	086	084	(1)	254.3	78.4	10.8	236.2	82.6	10.1	217.3	87.5	9.3	198.8	93.6	8.5	182.0	100.5	7.8
	096	094	(1)	284.3	89.1	12.1	264.7	93.6	11.3	243.5	99.6	10.4	223.3	106.5	9.5	204.7	114.1	8.7
	106	074 (1) and 044	(1)	326.4	98.8	13.9	304.5	103.9	13.0	281.1	109.9	12.0	258.4	117.4	11.0	237.3	126.2	10.1
	116	074 (1) and 044	(1)	350.2	107.1	14.9	326.4	112.7	13.9	301.7	119.4	12.8	277.4	127.9	11.8	254.4	137.0	10.8
	126	074	(2)	386.0	114.9	16.4	360.7	121.2	15.4	333.7	128.2	14.2	307.5	137.1	13.1	282.6	147.2	12.0
	136	074	(2)	418.9	130.0	17.8	391.3	136.5	16.7	362.0	144.8	15.4	334.2	154.9	14.2	307.2	165.9	13.1
	146	084	(2)	466.3	137.5	19.9	436.6	144.4	18.6	405.3	152.1	17.3	373.9	162.7	15.9	345.0	174.5	14.7
	161	084	(2)	485.5	146.3	20.7	465.8	158.5	19.8	444.4	171.7	18.9	424.1	187.5	18.1	402.9	206.8	17.2
	171	084	(2)	521.1	161.4	22.2	498.8	174.5	21.2	476.3	189.0	20.3	454.6	206.6	19.4	432.3	228.5	18.4
	186	084	(2)	564.4	182.9	24.0	536.9	197.1	22.9	514.8	213.2	21.9	490.5	233.9	20.9	465.6	258.3	19.8
	206	084 (2) and 094	(1)	665.3	190.3	28.3	641.2	206.8	27.3	613.6	224.2	26.1	583.6	244.7	24.9	555.1	268.7	23.6
	246	094	(3)	772.8	226.4	32.9	743.9	245.0	31.7	707.4	265.1	30.1	676.2	288.4	28.8	643.0	317.4	27.4
	261	094	(3)	810.1	242.7	34.5	777.0	262.6	33.1	740.5	283.8	31.5	707.8	309.5	30.1	673.0	340.6	28.7
	271	094	(3)	851.7	260.9	36.3	812.7	282.1	34.6	777.3	304.2	33.1	742.6	333.0	31.6	705.9	365.4	30.1
5	076	084	(1)	240.0	70.5	10.2	224.4	74.2	9.6	206.6	78.2	8.8	188.7	83.1	8.0	172.7	89.4	7.4
	086	084	(1)	263.1	79.9	11.2	245.1	84.1	10.4	225.6	89.0	9.6	206.4	94.9	8.8	188.7	101.7	8.0
	096	094	(1)	294.6	90.7	12.6	274.0	95.5	11.7	252.7	101.2	10.8	232.1	107.9	9.9	212.1	115.6	9.0
	106	074 (1) and 044	(1)	337.9	100.6	14.4	315.8	105.8	13.5	292.1	111.5	12.5	268.2	119.0	11.4	246.2	127.7	10.5
	116	074 (1) and 054	(1)	362.3	109.1	15.4	338.4	114.8	14.4	313.1	121.2	13.3	287.7	129.6	12.3	264.2	138.6	11.3
	126	074	(2)	399.2	117.1	17.0	373.8	123.4	15.9	346.8	129.9	14.8	318.8	138.9	13.6	293.0	149.0	12.5
	136	074	(2)	433.6	132.3	18.5	405.4	138.8	17.3	375.4	147.0	16.0	346.6	157.0	14.8	318.5	168.0	13.6
	146	084	(2)	482.3	140.0	20.6	453.2	146.9	19.3	420.8	154.3	17.9	387.9	164.7	16.5	357.9	176.6	15.3
	161	084	(2)	500.7	148.2	21.3	480.3	160.8	20.5	458.9	174.0	19.6	437.5	189.8	18.6	415.5	208.6	17.7
	171	084	(2)	537.5	163.6	22.9	515.1	176.9	22.0	491.5	191.4	20.9	469.0	208.9	20.0	445.7	230.1	19.0
	186	084	(2)	583.3	185.5	24.9	553.9	200.3	23.6	531.2	215.9	22.6	506.4	236.8	21.6	480.2	260.1	20.5
	206	084 (2) and 094	(1)	685.0	193.1	29.2	661.5	209.5	28.2	634.3	227.3	27.0	602.6	247.8	25.7	573.0	270.7	24.4
	246	094	(3)	795.7	229.6	33.9	768.7	248.3	32.8	730.8	268.9	31.1	697.8	291.8	29.7	663.6	320.5	28.3
	261	094	(3)	834.1	246.1	35.5	803.7	266.1	34.3	763.9	288.0	32.6	730.3	312.9	31.1	694.4	344.2	29.6
	271	094	(3)	876.6	265.1	37.4	840.2	286.1	35.8	801.4	309.0	34.2	766.4	336.7	32.7	728.4	369.5	31.0
6	076	084	(1)	248.7	71.8	10.6	232.3	75.7	9.9	214.3	79.7	9.1	196.1	84.3	8.4	179.0	90.4	7.6
	086	084	(1)	272.2	81.5	11.6	253.8	85.8	10.8	234.3	90.4	10.0	214.5	96.1	9.1	196.0	102.7	8.4
	096	094	(1)	304.7	92.6	13.0	283.9	97.4	12.1	262.2	103.0	11.2	240.4	109.5	10.3	219.7	117.0	9.4
	106	074 (1) and 044	(1)	349.7	102.5	14.9	327.3	107.9	14.0	302.8	113.5	12.9	278.2	120.6	11.9	255.4	129.1	10.9
	116	074 (1) and 054	(1)	374.6	111.2	16.0	350.9	116.9	15.0	324.9	122.9	13.9	298.2	131.2	12.7	273.9	140.3	11.7
	126	074	(2)	413.1	119.2	17.6	387.7	125.6	16.5	359.6	132.0	15.3	330.6	140.8	14.1	303.9	150.8	13.0
	136	074	(2)	448.7	134.7	19.1	419.9	141.4	17.9	389.2	149.5	16.6	359.2	159.1	15.3	330.0	170.2	14.1
	146	084	(2)	499.0	142.5	21.3	469.4	149.5	20.0	436.3	156.9	18.6	402.3	167.0	17.2	371.1	178.7	15.8
	161	084	(2)	515.5	150.5	22.0	495.6	163.1	21.1	473.6	176.7	20.2	451.2	192.3	19.2	428.7	210.7	18.3
	171	084	(2)	554.1	165.8	23.6	531.9	179.6	22.7	506.7	194.4	21.6	483.4	211.4	20.6	459.2	232.3	19.6
	186	084	(2)	601.2	188.5	25.6	572.4	203.5	24.4	547.4	219.6	23.3	522.4	239.9	22.3	495.6	262.9	21.1
	206	084 (2) and 094	(1)	705.3	195.7	30.1	682.2	212.3	29.1	655.5	230.4	28.0	621.8	251.0	26.6	591.4	273.4	25.2
	246	094	(3)	818.3	232.9	34.9	792.6	251.9	33.8	755.2	272.8	32.2	719.8	295.8	30.7	684.8	324.0	29.2
	261	094	(3)	858.6	249.6	36.6	830.9	269.6	35.4	788.3	292.3	33.6	753.2	316.6	32.1	716.4	347.9	30.6
	271	094	(3)	902.4	269.1	38.5	868.5	290.2	37.0	825.8	313.8	35.2	790.1	340.6	33.7	751.3	374.1	32.0

LEGEND

Cap. — Capacity, kW
kW — Compressor Motor Input Power at Rated Voltages
LCWT — Leaving Chilled-Water Temperature (C)

Performance data (cont)

Carrier

COMBINATION RATINGS (cont)

60 Hz, SI (cont)

LCWT (C)	UNIT SIZE 30HXA	09DK AIR-COOLED CONDENSER Unit	(Qty)	CONDENSER ENTERING AIR TEMPERATURE (C) 30 Cap.	30 Input kW	30 Cooler Flow Rate (L/s)	35 Cap.	35 Input kW	35 Cooler Flow Rate (L/s)	40 Cap.	40 Input kW	40 Cooler Flow Rate (L/s)	45 Cap.	45 Input kW	45 Cooler Flow Rate (L/s)	50 Cap.	50 Input kW	50 Cooler Flow Rate (L/s)
7	076	084	(1)	257.3	73.4	11.0	240.4	77.3	10.3	222.6	81.2	9.5	204.0	85.5	8.7	185.3	91.3	7.9
	086	084	(1)	281.2	83.2	12.0	262.8	87.5	11.2	243.1	91.9	10.4	222.5	97.4	9.5	202.9	103.9	8.7
	096	094	(1)	314.9	94.5	13.4	293.7	99.3	12.5	272.3	104.6	11.6	249.7	110.9	10.7	227.8	118.3	9.7
	106	074 (1) and 044	(1)	361.6	104.5	15.4	338.7	109.9	14.5	314.4	115.4	13.4	288.8	122.4	12.3	264.7	130.6	11.3
	116	074 (1) and 054	(1)	387.5	113.2	16.5	363.4	119.1	15.5	336.6	125.2	14.4	309.3	133.2	13.2	283.7	142.1	12.1
	126	074	(2)	427.4	121.3	18.2	401.3	127.9	17.1	372.7	134.6	15.9	343.2	142.8	14.6	315.1	152.6	13.4
	136	074	(2)	464.0	137.4	19.8	434.3	144.2	18.5	403.5	152.0	17.2	372.3	161.3	15.9	341.9	172.3	14.6
	146	084	(2)	516.2	144.9	22.0	485.8	152.3	20.7	452.5	159.8	19.3	417.7	169.3	17.8	384.5	180.9	16.4
	161	084	(2)	530.3	152.9	22.6	511.1	165.5	21.8	488.9	179.2	20.9	465.0	195.0	19.8	433.5	211.2	18.5
	171	084	(2)	569.9	168.3	24.3	548.7	182.4	23.4	522.9	197.5	22.3	498.1	214.6	21.3	473.4	234.9	20.2
	186	084	(2)	618.9	191.7	26.4	591.2	206.9	25.2	564.0	223.1	24.1	538.3	243.0	23.0	498.3	263.3	21.3
	206	084 (2) and 094	(1)	725.9	198.3	31.0	703.4	214.9	30.0	676.6	233.5	28.9	642.4	254.0	27.4	610.2	276.6	26.0
	246	094	(3)	842.4	236.1	35.9	816.8	255.5	34.9	780.1	276.7	33.3	742.3	299.7	31.7	706.3	327.5	30.1
	261	094	(3)	883.5	253.1	37.7	856.0	273.8	36.5	814.0	296.9	34.7	776.4	321.1	33.1	738.8	351.8	31.5
	271	094	(3)	928.9	273.1	39.6	897.4	294.3	38.3	850.9	318.6	36.3	814.4	344.5	34.8	774.3	378.9	33.0
8	076	084	(1)	266.1	74.9	11.4	249.0	78.7	10.6	231.1	82.6	9.9	211.8	86.7	9.0	192.3	92.4	8.2
	086	084	(1)	290.7	84.8	12.4	272.2	89.1	11.6	251.7	93.6	10.7	230.7	98.9	9.8	210.1	105.3	9.0
	096	094	(1)	325.4	96.4	13.9	304.2	101.2	13.0	281.9	106.3	12.0	258.6	112.7	11.0	236.2	119.9	10.1
	106	074 (1) and 044	(1)	373.6	106.6	16.0	350.5	112.0	15.0	325.7	117.6	13.9	299.8	124.2	12.8	274.2	132.3	11.7
	116	074 (1) and 054	(1)	400.4	115.3	17.1	375.8	121.3	16.0	348.8	127.5	14.9	321.1	135.0	13.7	294.2	143.8	12.6
	126	074	(2)	441.4	123.7	18.8	415.2	130.2	17.7	386.4	137.0	16.5	356.3	144.8	15.2	326.5	154.4	13.9
	136	074	(2)	479.9	140.2	20.5	449.4	147.0	19.2	417.9	154.5	17.8	385.3	163.6	16.5	350.2	173.8	14.9
	146	084	(2)	533.4	147.7	22.8	502.7	155.0	21.5	468.9	162.7	20.0	433.4	171.7	18.5	398.3	183.1	17.0
	161	084	(2)	545.7	155.2	23.3	526.7	167.9	22.5	504.1	181.9	21.5	479.4	197.3	20.5	442.7	212.7	18.9
	171	084	(2)	586.2	171.0	25.0	565.6	185.1	24.1	539.3	200.6	23.0	513.6	217.4	21.9	479.5	235.7	20.5
	186	084	(2)	636.2	194.8	27.2	610.4	210.1	26.1	580.6	226.9	24.8	554.6	246.0	23.7	505.2	264.9	21.6
	206	084 (2) and 094	(1)	747.2	200.8	31.9	724.7	217.9	30.9	696.5	236.9	29.7	663.6	257.1	28.3	629.3	280.3	26.9
	246	094	(3)	866.5	239.4	37.0	841.8	258.9	35.9	805.9	280.4	34.4	765.1	303.8	32.7	728.3	330.9	31.1
	261	094	(3)	908.4	256.8	38.8	881.8	277.8	37.6	840.6	301.3	35.9	800.1	325.9	34.2	761.5	355.8	32.5
	271	094	(3)	955.8	277.1	40.8	926.2	298.3	39.5	878.7	323.6	37.5	839.2	349.4	35.8	798.3	383.3	34.1
9	076	084	(1)	275.1	76.5	11.7	257.6	80.2	11.0	239.9	84.1	10.2	219.8	88.3	9.4	199.6	93.9	8.5
	086	084	(1)	300.5	86.5	12.8	281.4	90.8	12.0	260.8	95.3	11.1	239.2	100.4	10.2	217.9	106.7	9.3
	096	094	(1)	335.9	98.4	14.3	314.5	103.1	13.4	291.8	108.2	12.5	267.8	114.5	11.4	239.6	120.5	10.2
	106	074 (1) and 044	(1)	386.0	108.6	16.5	362.6	114.1	15.5	337.6	119.8	14.4	310.8	126.2	13.3	284.1	134.1	12.1
	116	074 (1) and 054	(1)	431.7	117.4	17.7	388.2	123.8	16.6	361.0	130.0	15.4	332.7	136.9	14.2	304.2	145.7	13.0
	126	074	(2)	456.1	126.1	19.5	429.0	132.7	18.3	400.3	139.5	17.1	369.4	146.8	15.8	338.3	156.4	14.5
	136	074	(2)	494.5	143.1	21.1	464.7	149.8	19.8	432.5	157.1	18.5	399.1	165.9	17.0	355.2	174.5	15.2
	146	084	(2)	551.0	150.4	23.5	519.5	157.9	22.2	485.5	165.7	20.7	449.4	174.1	19.2	412.8	185.5	17.6
	161	084	(2)	561.1	157.4	24.0	542.7	170.2	23.2	519.4	184.5	22.2	494.3	199.8	21.1	447.6	213.5	19.1
	171	084	(2)	602.7	173.7	25.7	582.3	188.0	24.9	556.0	203.6	23.7	528.9	220.3	22.6	489.7	237.6	20.9
	186	084	(2)	654.2	198.0	27.9	629.7	213.4	26.9	597.5	230.8	25.5	571.1	248.8	24.4	503.8	264.6	21.5
	206	084 (2) and 094	(1)	768.8	203.3	32.8	746.5	220.8	31.9	717.4	240.3	30.6	685.2	260.6	29.3	648.6	283.8	27.7
	246	094	(3)	890.8	242.6	38.0	866.2	262.6	37.0	832.1	284.4	35.5	788.5	308.4	33.7	750.2	334.7	32.0
	261	094	(3)	933.8	260.5	39.9	907.2	282.0	38.7	868.2	305.7	37.1	824.0	331.0	35.2	784.1	359.5	33.5
	271	094	(3)	982.8	281.0	42.0	952.7	303.3	40.7	907.4	328.6	38.8	863.9	355.2	36.9	821.9	387.3	35.1

LEGEND

Cap. — Capacity, kW
kW — Compressor Motor Input Power at Rated Voltages
LCWT — Leaving Chilled-Water Temperature (C)

Table B-2 Technical catalogue data for 30HXA air-cooled screw compressor chiller (Cont.)

COMBINATION RATINGS (cont)

60 Hz, SI (cont)

LCWT (C)	UNIT SIZE 30HXA	09DK AIR-COOLED CONDENSER Unit (Qty)	CONDENSER ENTERING AIR TEMPERATURE (C)													
			30			35			40			45			50		
			Cap.	Input kW	Cooler Flow Rate (L/s)	Cap.	Input kW	Cooler Flow Rate (L/s)	Cap.	Input kW	Cooler Flow Rate (L/s)	Cap.	Input kW	Cooler Flow Rate (L/s)	Cap.	Input kW	Cooler Flow Rate (L/s)
10	076	084 (1)	284.2	78.1	12.1	266.5	81.7	11.4	248.0	85.7	10.6	227.8	90.0	9.7	207.6	95.1	8.9
	086	084 (1)	310.3	88.2	13.3	290.6	92.6	12.4	269.7	97.2	11.5	248.1	101.9	10.6	225.6	108.1	9.6
	096	094 (1)	346.9	100.3	14.8	325.0	105.1	13.9	301.7	110.3	12.9	277.7	116.4	11.9	243.2	121.0	10.4
	106	074 (1) and 044 (1)	398.6	110.7	17.0	374.6	116.3	16.0	349.0	122.2	14.9	322.0	128.2	13.8	294.5	135.9	12.6
	116	074 (1) and 054 (1)	426.7	119.8	18.2	401.1	126.1	17.1	373.7	132.4	16.0	344.7	138.8	14.7	315.0	147.5	13.5
	126	074 (2)	470.7	128.6	20.1	443.3	135.2	18.9	414.1	142.1	17.7	382.6	149.2	16.3	350.5	158.5	15.0
	136	074 (2)	510.4	145.9	21.8	479.9	152.7	20.5	447.3	159.8	19.1	413.0	168.8	17.6	363.9	176.1	15.6
	146	084 (2)	568.7	153.5	24.3	536.8	160.8	22.9	502.6	168.7	21.5	465.4	176.9	19.9	427.5	188.0	18.3
	161	084 (2)	576.7	159.8	24.6	558.7	172.7	23.9	534.3	187.5	22.8	509.3	202.8	21.8	452.6	214.5	19.3
	171	084 (2)	619.3	176.5	26.5	599.3	190.9	25.6	572.6	206.9	24.5	544.3	223.4	23.3	496.1	238.4	21.2
	186	084 (2)	672.1	201.3	28.7	649.3	216.8	27.7	615.1	234.6	26.3	587.5	252.8	25.1	502.1	264.2	21.5
	206	084 (2) and 094 (1)	790.8	206.1	33.8	767.5	224.1	32.8	738.9	243.5	31.6	707.1	264.3	30.2	668.2	287.4	28.6
	246	094 (3)	915.2	245.7	39.1	890.5	266.4	38.1	857.3	288.7	36.6	813.3	313.2	34.8	772.5	339.3	33.0
	261	094 (3)	959.2	264.2	41.0	932.5	286.4	39.8	895.9	310.3	38.3	848.2	336.1	36.2	807.4	363.4	34.5
	271	094 (3)	1008.9	285.2	43.1	979.6	308.3	41.9	936.4	333.6	40.0	889.2	361.0	38.0	846.1	391.7	36.2
13	076	084 (1)	299.4	80.6	12.8	281.1	84.2	12.0	259.5	88.0	11.1	237.1	91.7	10.1	216.0	96.5	9.2
	086	084 (1)	323.6	90.6	13.8	303.6	94.9	13.0	282.4	99.6	12.1	259.8	104.2	11.1	237.0	110.1	10.1
	096	094 (1)	364.2	103.4	15.6	341.7	108.5	14.6	318.0	113.6	13.6	290.2	118.8	12.4	249.7	122.1	10.7
	106	074 (1) and 044 (1)	415.6	113.9	17.8	391.0	119.3	16.7	365.1	125.3	15.6	337.3	131.1	14.4	308.7	138.6	13.2
	116	074 (1) and 054 (1)	448.0	123.8	19.2	421.5	129.9	18.0	393.7	136.3	16.8	363.7	142.5	15.6	332.9	150.8	14.2
	126	074 (2)	498.9	133.3	21.3	470.1	139.8	20.1	440.1	147.0	18.8	404.0	153.1	17.3	370.4	161.8	15.8
	136	074 (2)	540.0	150.9	23.1	508.5	157.9	21.8	474.5	165.3	20.3	439.8	173.9	18.8	373.2	177.4	16.0
	146	084 (2)	607.6	159.7	26.0	569.3	166.2	24.4	534.3	174.4	22.9	496.5	182.7	21.2	452.0	191.9	19.3
	161	084 (2)	602.0	163.2	25.8	583.5	176.8	25.0	559.2	191.6	23.9	534.0	207.4	22.8	461.6	216.1	19.7
	171	084 (2)	652.2	181.8	27.9	632.3	196.8	27.0	606.9	213.3	26.0	575.2	230.6	24.6	503.4	240.1	21.6
	186	084 (2)	702.1	206.4	30.0	679.4	222.8	29.1	646.0	241.0	27.6	614.6	259.8	26.3	501.8	264.1	21.5
	206	084 (2) and 094 (1)	830.4	211.1	35.5	799.3	229.4	34.2	766.7	247.9	32.8	733.9	269.3	31.4	688.8	291.1	29.5
	246	094 (3)	953.4	250.6	40.8	928.3	272.6	39.7	896.6	295.3	38.4	852.3	320.3	36.5	798.6	344.8	34.2
	261	094 (3)	994.1	268.9	42.5	967.6	291.9	41.4	933.4	316.3	39.9	883.4	343.1	37.8	834.6	369.6	35.7
	271	094 (3)	1054.9	292.0	45.1	1016.3	315.0	43.5	976.4	340.4	41.8	923.8	368.7	39.5	866.1	395.5	37.0
16	076	084 (1)	296.7	80.1	12.7	278.3	83.7	11.9	259.3	87.9	11.1	239.2	92.1	10.2	217.9	96.9	9.3
	086	084 (1)	326.1	91.0	14.0	305.8	95.4	13.1	282.0	99.5	12.1	259.5	104.2	11.1	236.8	109.9	10.1
	096	094 (1)	360.9	102.8	15.5	338.7	107.8	14.5	315.0	112.9	13.5	290.4	118.8	12.4	249.6	121.9	10.7
	106	074 (1) and 044 (1)	419.2	114.4	17.9	394.1	119.9	16.9	368.4	125.8	15.8	333.8	130.4	14.3	305.7	137.9	13.1
	116	074 (1) and 054 (1)	451.6	124.4	19.3	420.8	129.6	18.0	392.6	136.1	16.8	362.5	142.3	15.5	331.9	150.6	14.2
	126	074 (2)	498.3	133.1	21.3	469.5	139.6	20.1	439.4	146.8	18.8	407.2	153.9	17.4	373.7	162.4	16.0
	136	074 (2)	535.3	150.1	22.9	503.9	156.9	21.6	470.3	164.3	20.1	435.1	173.1	18.6	376.2	178.0	16.1
	146	084 (2)	602.2	158.7	25.8	568.5	166.1	24.3	533.4	174.3	22.8	495.7	182.5	21.2	456.0	192.5	19.5
	161	084 (2)	605.9	163.9	25.9	587.4	177.6	25.2	558.1	191.2	23.9	532.9	207.2	22.8	465.0	216.8	19.9
	171	084 (2)	647.1	181.0	27.7	627.5	195.8	26.9	601.7	212.3	25.8	570.0	229.7	24.4	503.0	240.1	21.6
	186	084 (2)	701.7	206.4	30.0	679.4	222.5	29.1	646.1	240.7	27.7	609.4	258.7	26.1	501.3	264.1	21.5
	206	084 (2) and 094 (1)	823.5	210.4	35.3	799.7	229.2	34.2	772.2	248.6	33.1	739.4	270.0	31.7	689.3	291.2	29.5
	246	094 (3)	954.7	250.5	40.9	920.9	271.4	39.4	888.8	294.2	38.1	844.4	319.0	36.2	791.6	343.3	33.9
	261	094 (3)	1000.6	269.7	42.8	973.9	293.1	41.7	939.9	317.5	40.2	890.2	344.2	38.1	827.6	367.9	35.4
	271	094 (3)	1051.8	291.5	45.0	1023.1	316.2	43.8	983.7	341.6	42.1	930.1	370.1	39.8	867.7	396.1	37.2

LEGEND

Cap. — Capacity, kW
kW — Compressor Motor Input Power at Rated Voltages
LCWT — Leaving Chilled-Water Temperature (C)

Table B-3 Technical catalogue data for 19DK water-cooled centrifugal compressor chiller

Carrier
HEATING & COOLING

19DK
Hermetic Centrifugal Liquid Chiller

Selection tables — SI

19DK44 UNISHELL (450 NOMINAL kW)

ADJ LVG COND WATER TEMP (C)		ADJ LVG CHILLED WATER TEMP (C)		
		5	6	7
33	kW	475	496	510
	IKW	107	109	110
	CR	124	124	124
35	kW	457	450	492
	IKW	109	101	110
	CR	125	124	124
38	kW	411	433	443
	IKW	110	109	110
	CR	127	126	126

19DK55 UNISHELL (700 NOMINAL kW)

ADJ LVG COND WATER TEMP (C)		ADJ LVG CHILLED WATER TEMP (C)		
		5	6	7
33	kW	714	732	753
	IKW	147	147	148
	CR	174	174	174
35	kW	682	700	728
	IKW	147	146	149
	CR	174	174	174
38	kW	622	651	665
	IKW	149	146	147
	CR	176	175	175

19DK63 UNISHELL (1000 NOMINAL kW)

ADJ LVG COND WATER TEMP (C)		ADJ LVG CHILLED WATER TEMP (C)		
		5	6	7
33	kW	1041	1062	1094
	IKW	208	207	208
	CR	284	284	284
35	kW	978	1000	1052
	IKW	209	202	208
	CR	285	284	284
38	kW	872	911	935
	IKW	209	207	208
	CR	287	286	286

19DK73 UNISHELL (1400 NOMINAL kW)

ADJ LVG COND WATER TEMP (C)		ADJ LVG CHILLED WATER TEMP (C)		
		5	6	7
33	kW	1386	1456	1526
	IKW	271	280	290
	CR	354	354	354
35	kW	1358	1400	1484
	IKW	285	288	292
	CR	355	355	354
38	kW	1308	1358	1414
	IKW	301	307	303
	CR	356	356	355

19DK78 UNISHELL (1600 NOMINAL kW)

ADJ LVG COND WATER TEMP (C)		ADJ LVG CHILLED WATER TEMP (C)		
		5	6	7
33	kW	1572	1656	1727
	IKW	317	329	339
	CR	405	405	405
35	kW	1544	1600	1685
	IKW	335	328	341
	CR	406	405	405
38	kW	1445	1512	1586
	IKW	330	340	338
	CR	406	406	405

kW — Cooling Capacity (Kilowatts)
IKW — Motor Input Power (Kilowatts)
CR — Compressor Model

Table B-4 Technical catalogue data for KRS-KUO YU water-cooled screw compressor chiller

KRS-G40, Screw Water Chilling Unit Capacity Rating						3470RPM R22
Cond.Temp.& Gauge Pressure	Ice Water Outlet ℃	Ice Water Outlet/ InletTemp.Differential Deg.℃	Cooling Capacity Kcal/Hr.	RT	Input KW	Chiller Ice water quantity
30℃ 11.2kg/cm² (160 PSI)	12.5	5.84	154,560	51.1	31.2	(1) Design Ref.Value. (about) 26.6M³/HR Water Pressure Max.3kg/cm² (2) This ice water of the Outlet/ Inlet differential temperature can be calculated, according to the design ref. value of the cooling capacity of this data
	10.0	5.30	141,970	46.9	30.8	
	7.5	4.72	129,580	42.9	30.3	
	5.0	4.28	117,190	38.8	30.2	
35℃ 12.9kg/cm² (184 PSI)	12.5	5.46	145,630	48.2	35.6	
	10.0	5.00	133,440	44.1	35.1	
	7.5	4.56	121,250	40.1	34.5	
	5.0	4.12	109,680	36.3	34.4	
40℃ 14.7kg/cm² (210 PSI)	12.5	5.20	138,520	45.8	38.2	
	10.0	4.73	126,940	42.0	37.8	
	7.5	4.28	115,770	38.3	37.4	
	5.0	3.87	105,010	34.7	37.3	
45℃ 16.7kg/cm² (239 PSI)	12.5	4.94	128,570	42.5	42.5	
	10.0	4.48	117,390	38.8	42.0	
	7.5	4.05	106,430	35.2	41.4	
	5.0	3.66	96,270	31.8	41.3	

Table B-4 Technical catalogue data for KRS-KUO YU water-cooled screw compressor chiller (Cont.)

KRS-G50, Screw Water Chilling Unit Capacity Rating						3470RPM R22
Cond.Temp.& Gauge Pressure	Ice Water Outlet ℃	Ice Water Outlet/InletTemp.Differential Deg.℃	Cooling Capacity Kcal/Hr.	RT	Input KW	Chiller Ice water quantity
30℃ 11.kg/cm² (160 PSI)	12.5	5.84	192,340	63.6	38.9	(1) Design Ref.Value. (about) 33.3M/³HR Water Pressure Max.3kg/cm² (2) This ice water of the Outlet/ Inlet differential temperature can be calculated, according to the design ref value of the cooling capacity of this data
	10.0	5.30	176,670	58.4	38.3	
	7.5	4.72	161,260	53.3	37.7	
	5.0	4.28	145,840	48.2	37.6	
35℃ 12.9kg/cm² (184 PSI)	12.5	5.46	181,220	59.9	44.3	
	10.0	5.00	166,060	54.9	43.6	
	7.5	4.56	150,890	49.9	43.0	
	5.0	4.12	136,490	45.1	42.8	
40℃ 14.7kg/cm² (210 PSI)	12.5	5.20	172,380	57.0	47.6	
	10.0	4.73	157,970	52.2	47.1	
	7.5	4.28	144,070	47.6	46.6	
	5.0	3.87	130,670	43.2	46.5	
45℃ 16.7kg/cm² (239 PSI)	12.5	4.94	159,990	52.9	52.9	
	10.0	4.48	146,090	48.3	52.2	
	7.5	4.05	132,440	43.8	51.6	
	5.0	3.66	119,800	39.6	51.4	

Table B-4 Technical catalogue data for KRS-KUO YU water-cooled screw compressor chiller (Cont.)

KRS-G60, Screw Water Chilling Unit Capacity Rating						3470RPM R22
Cond.Temp.& Gauge Pressure	Ice Water Outlet ℃	Ice Water Outlet/ InletTemp.Differential Deg.℃	Cooling Capacity Kcal/Hr.	RT	Input KW	Chiller Ice water quantity
30℃ 11.2kg/cm² (160 PSI)	12.5	5.84	230,130	76.1	46.5	(1) Design Ref.Value. (about) 39.9M³/HR Water Pressure Max.3kg/cm² (2) This ice water of the Outlet Inlet differential temperature can be calculated, according to the design ref. value of the cooling capacity of this data
	10.0	5.30	211,380	69.9	45.8	
	7.5	4.72	192,930	63.8	45.1	
	5.0	4.28	174,480	57.7	45.0	
35℃ 12.9kg/cm² (184 PSI)	12.5	5.46	216,820	71.7	53.0	
	10.0	5.00	198,680	65.7	52.2	
	7.5	4.56	180,530	59.7	51.4	
	5.0	4.12	163,300	54.0	51.2	
40℃ 14.7kg/cm² (210 PSI)	12.5	5.20	206,240	68.2	56.9	
	10.0	4.73	189,000	62.5	56.3	
	7.5	4.28	172,370	57.0	55.7	
	5.0	3.87	156,340	51.7	55.6	
45℃ 16.7kg/cm² (239 PSI)	12.5	4.94	191,420	63.3	63.3	
	10.0	4.48	174,790	57.8	62.5	
	7.5	4.05	158,460	52.4	61.7	
	5.0	3.66	143,340	47.4	61.5	

Table B-4 Technical catalogue data for KRS-KUO YU water-cooled screw compressor chiller (Cont.)

KRS-G75, Screw Water Chilling Unit Capacity Rating						3470RPM R22
Cond.Temp.& Gauge Pressure	Ice Water Outlet ℃	Ice Water Outlet/ InletTemp.Differential Deg.℃	Cooling Capacity Kcal/Hr.	RT	Input KW	Chiller Ice water quantity
30℃ 11.2kg/cm² (160 PSI)	12.5	5.84	288,510	95.4	58.4	(1) Design Ref.Value. (about) 53.2M³/HR Water Pressure Max.3kg/cm² (2) This ice water of the Outlet/ Inlet differential temperature can be calculated, according to the design ref. value of the cooling capacity of this data
	10.0	5.30	265.000	87.6	57.5	
	7.5	4.72	241.890	80.0	56.6	
	5.0	4.28	218.760	72.3	56.4	
35℃ 12.9kg/cm² (184 PSI)	12.5	5.46	271.830	89.9	66.5	
	10.0	5.00	249.090	82.4	65.4	
	7.5	4.56	226.330	74.8	64.5	
	5.0	4.12	204.730	67.7	64.2	
40℃ 14.7kg/cm² (210 PSI)	12.5	5.20	258.570	85.5	71.4	
	10.0	4.73	236.950	78.4	70.7	
	7.5	4.28	216.100	71.5	69.9	
	5.0	3.87	196.000	64.8	69.8	
45℃ 16.7kg/cm² (239 PSI)	12.5	4.94	239.980	79.4	79.4	
	10.0	4.48	219.130	72.5	78.3	
	7.5	4.05	198.660	65.7	77.4	
	5.0	3.66	179.700	59.4	77.1	

Table B-4 Technical catalogue data for KRS-KUO YU water-cooled screw compressor chiller (Cont.)

2KRS-G80, Screw Water Chilling Unit Capacity Rating						3470RPM R22
Cond.Temp.& Gauge Pressure	Ice Water Outlet ℃	Ice Water Outlet/ InletTemp.Differential Deg.℃	Cooling Capacity Kcal/Hr.	RT	Input KW	Chiller Ice water quantity
30℃ 11.2kg/cm² (160 PSI)	12.5	5.84	309.130	102.2	62.5	(1) Design Ref.Value. (about) 53.2M³/HR Water Pressure Max.3kg/cm² (2) This ice water of the Outlet/ Inlet differential temperature can be calculated, according to the design ref. value of the cooling capacity of this data
	10.0	5.30	283.940	93.9	61.5	
	7.5	4.72	259.160	85.7	60.6	
	5.0	4.28	234.380	77.5	60.4	
35℃ 12.9kg/cm² (184 PSI)	12.5	5.46	291.250	96.3	71.2	
	10.0	5.00	266.880	88.3	70.1	
	7.5	4.56	242.510	80.2	69.0	
	5.0	4.12	219.350	72.5	68.8	
40℃ 14.7kg/cm² (210 PSI)	12.5	5.20	277.030	91.6	76.4	
	10.0	4.73	253.880	84.0	75.6	
	7.5	4.28	231.540	76.6	74.8	
	5.0	3.87	210.010	69.4	74.7	
45℃ 16.7kg/cm² (239 PSI)	12.5	4.94	257.130	85.0	85.0	
	10.0	4.48	234.790	77.6	84.0	
	7.5	4.05	212.850	70.4	82.9	
	5.0	3.66	192.540	63.7	82.6	

Table B-4 Technical catalogue data for KRS-KUO YU water-cooled screw compressor chiller (Cont.)

2KRS-G100, Screw Water Chilling Unit Capacity Rating						3470RPM R22
Cond.Temp.& Gauge Pressure	Ice Water OIutlet ℃	Ice Water Outlet/ InletTemp.Differential Deg.℃	Cooling Capacity Kcal/Hr.	RT	Input KW	Chiller Ice water quantity
30℃ 11.2kg/cm² (160 PSI)	12.5	5.84	384.690	127.2	77.7	(1) Design Ref.Value. (about) 66.6M/³HR Water Pressure Max.3kg/cm² (2) This ice water of the Outlet/ Inlet differential temperature can be calculated. according to the design ref. value of the cooling capacity of this data
	10.0	5.30	353.350	116.8	76.6	
	7.5	4.72	322.510	106.7	75.4	
	5.0	4.28	291.680	96.5	75.2	
35℃ 12.9kg/cm² (184 PSI)	12.5	5.46	362.450	119.9	88.6	
	10.0	5.00	332.120	109.8	87.3	
	7.5	4.56	301.790	99.8	85.9	
	5.0	4.12	272.970	90.3	85.6	
40℃ 14.7kg/cm² (210 PSI)	12.5	5.20	344.750	114.0	95.1	
	10.0	4.73	315.940	104.5	94.1	
	7.5	4.28	288.140	95.3	93.1	
	5.0	3.87	261.350	86.4	92.9	
45℃ 16.7kg/cm² (239 PSI)	12.5	4.94	319.980	105.8	105.8	
	10.0	4.48	292.180	96.6	104.5	
	7.5	4.05	264.880	87.6	103.1	
	5.0	3.66	239.610	79.2	102.8	

Table B-4 Technical catalogue data for KRS-KUO YU water-cooled screw compressor chiller (Cont.)

2KRS-G120, Screw Water Chilling Unit Capacity Rating						3470RPM R22
Cond.Temp.& Gauge Pressure	Ice Water Outlet ℃	Ice Water Outlet/ InletTemp.Differential Deg.℃	Cooling Capacity Kcal/Hr.	RT	Input KW	Chiller Ice water quantity
30℃ 11.2kg/cm² (160 PSI)	12.5	5.84	460.250	152.2	93.0	(1) Design Ref.Value. (about) 79.8M³/HR Water Pressure Max.3kg/cm² (2) This ice water of the Outlet/ Inlet differential temperature can be calculated. according to the design ref. value of the cooling capacity of this data
	10.0	5.30	422.760	139.8	91.6	
	7.5	4.72	385.860	127.6	90.2	
	5.0	4.28	348.970	115.4	90.0	
35℃ 12.9kg/cm² (184 PSI)	12.5	5.46	433.640	143.4	106.0	
	10.0	5.00	397.350	131.4	104.4	
	7.5	4.56	361.070	119.4	102.8	
	5.0	4.12	326.590	108.0	102.4	
40℃ 14.7kg/cm² (210 PSI)	12.5	5.20	412.470	136.4	113.8	
	10.0	4.73	378.000	125.0	112.6	
	7.5	4.28	344.740	114.0	111.4	
	5.0	3.87	312.680	103.4	111.2	
45℃ 16.7kg/cm² (239 PSI)	12.5	4.94	382.840	126.6	126.6	
	10.0	4.48	349.570	115.6	125.0	
	7.5	4.05	316.920	104.8	123.4	
	5.0	3.66	286.680	94.8	123.0	

Table B-4 Technical catalogue data for KRS-KUO YU water-cooled screw compressor chiller (Cont.)

2KRS-G150, Screw Water Chilling Unit Capacity Rating						3470RPM R22
Cond.Temp.& Gauge Pressure	Ice Water Outlet ℃	Ice Water Outlet/InletTemp. Differential Deg.℃	Cooling Capacity Kcal/Hr.	RT	Input KW	Chiller Ice water quantity
30℃ 11.2kg/cm² (160 PSI)	12.5	5.84	577,020	190.8	116.7	(1) Design Ref.Value. (about) 106.4M³/HR Water Pressure Max.3kg/cm² (2) This ice water of the Outlet/ Inlet differential temperature can be calculated. according to the design ref. value of the cooling capacity of this data
	10.0	5.30	530,000	175.3	114.9	
	7.5	4.72	483,780	160.0	113.1	
	5.0	4.28	437,520	144.7	112.8	
35℃ 12.9kg/cm² (184 PSI)	12.5	5.46	543,660	179.8	132.9	
	10.0	5.00	488,180	164.7	130.8	
	7.5	4.56	452,660	149.7	129.0	
	5.0	4.12	409,460	135.4	128.4	
40℃ 14.7kg/cm² (210 PSI)	12.5	5.20	517,140	171.0	142.8	
	10.0	4.73	473,900	156.7	141.3	
	7.5	4.28	432,200	142.9	139.8	
	5.0	3.87	392,000	129.6	139.5	
45℃ 16.7kg/cm² (239 PSI)	12.5	4.94	479,960	158.7	158.7	
	10.0	4.48	438,260	144.9	156.6	
	7.5	4.05	397,320	131.4	154.8	
	5.0	3.66	359,400	118.8	154.2	

Appendix C

Isentropic efficiency and COP values

Table C-1 Water-cooled screw compressor chiller 30HXC carrier/R-134a

T_{cd} (°C)	T_{ev} (°C)	$\dot{Q}_{ev}$ (kW)	$\dot{W}_{ideal}$ (kW)	$\dot{W}_{actual}$ (kW)	η_{is}	COP_{carnot}	$COP_{standard}$	COP_{actual}
30	4	253.3	27.6	48.2	57.2	10.7	9.2	5.3
30	4	279.3	30.4	54.2	56.1	10.7	9.2	5.2
30	4	315.5	34.4	60.1	57.2	10.7	9.2	5.2
30	4	350.4	38.2	67.5	56.5	10.7	9.2	5.2
30	4	380.9	41.5	71.1	58.3	10.7	9.2	5.4
30	4	412.5	44.9	77.8	57.7	10.7	9.2	5.3
30	4	457.2	49.8	87.4	57.0	10.7	9.2	5.2
30	4	489.2	53.3	94.6	56.3	10.7	9.2	5.2
30	4	516.5	56.3	99.2	56.7	10.7	9.2	5.2
30	4	547.2	59.6	105.5	56.5	10.7	9.2	5.2
30	4	584.8	63.7	113.6	56.1	10.7	9.2	5.1
30	4	697.8	76.0	130.3	58.3	10.7	9.2	5.4
30	4	819.9	89.3	152.7	58.5	10.7	9.2	5.4
30	4	848.6	92.4	152.7	60.5	10.7	9.2	5.6
30	4	882.7	96.1	168.4	57.1	10.7	9.2	5.2
35	4	234.3	30.7	53.2	57.8	8.9	7.6	4.4
35	4	258.8	33.9	59.8	56.8	8.9	7.6	4.3
35	4	282.4	37.0	66.5	55.7	8.9	7.6	4.2
35	4	323.9	42.5	74.8	56.8	8.9	7.6	4.3
35	4	352.8	46.3	79.7	58.1	8.9	7.6	4.4
35	4	382.6	50.2	86.7	57.9	8.9	7.6	4.4
35	4	425.0	55.7	96.5	57.8	8.9	7.6	4.4
35	4	454.2	59.6	104.7	56.9	8.9	7.6	4.3
35	4	500.1	65.6	115.5	56.8	8.9	7.6	4.3
35	4	532.8	69.9	122.4	57.1	8.9	7.6	4.4
35	4	569.1	74.7	131.4	56.8	8.9	7.6	4.3
35	4	676.3	88.7	150.8	58 8	8.9	7.6	4.5
35	4	795.2	104.3	178.2	58.5	8.9	7.6	4.5
35	4	824.6	108.2	186.1	58.1	8.9	7.6	4.4
35	4	858.2	112.6	195.3	57.6	8.9	7.6	4.4
40	4	219.0	34.7	58.9	58.9	7.7	6.3	3.7
40	4	242.8	38.5	66.3	58.0	7.7	6.3	3.7
40	4	274.3	43.5	73.8	58.9	7.7	6.3	3.7
40	4	304.3	48.2	83.6	57.7	7.7	6.3	3.6
40	4	330.6	52.4	88.9	58.9	7.7	6.3	3.7
40	4	359.0	56.9	96.8	58.8	7.7	6.3	3.7
40	4	400.3	63.4	107.0	59.3	7.7	6.3	3.7
40	4	428.3	67.9	116.7	58.1	7.7	6.3	3.7
40	4	494.5	78.3	135.8	57.7	7.7	6.3	3.6
40	4	526.6	83.4	142.9	58.4	7.7	6.3	3.7
40	4	563.8	89.3	153.4	58.2	7.7	6.3	3.7
40	4	663.7	105.2	175.8	59.8	7.7	6.3	3.8
40	4	782.7	124.0	208.6	59.4	7.7	6.3	3.8
40	4	814.2	129.0	217.4	59.3	7.7	6.3	3.7
40	4	848.5	134.4	228.0	59.0	7.7	6.3	3.7

Table C-1 Water-cooled screw compressor chiller 30HXC carrier/R-134a (Cont.)

T_{cd} (°C)	T_{ev} (°C)	$\dot{Q}_{ev}$ (kW)	$\dot{W}_{ideal}$ (kW)	$\dot{W}_{actual}$ (kW)	η_{is}	COP_{carnot}	$COP_{standard}$	COP_{actual}
30	5	264.0	27.7	48.6	57.0	11.1	9.5	5.4
30	5	291.1	30.6	54.7	55.9	11.1	9.5	5.3
30	5	328.8	34.5	60.6	56.9	11.1	9.5	5.4
30	5	365.2	38.3	67.9	56.4	11.1	9.5	5.4
30	5	396.9	41.7	72.2	57.7	11.1	9.5	5.5
30	5	429.7	45.1	78.5	57.5	11.1	9.5	5.5
30	5	476.5	50.0	88.0	56.8	11.1	9.5	5.4
30	5	509.7	53.5	95.3	56.1	11.1	9.5	5.3
30	5	534.4	56.1	98.8	56.8	11.1	9.5	5.4
30	5	565.5	59.4	105.2	56.4	11.1	9.5	5.4
30	5	604.6	63.5	113.2	56.1	11.1	9.5	5.3
30	5	721.6	75.7	130.2	58.2	11.1	9.5	5.5
30	5	847.2	88.9	152.7	58.2	11.1	9.5	5.5
30	5	877.0	92.0	159.8	57.6	11.1	9.5	5.5
30	5	912.2	95.7	167.9	57.0	11.1	9.5	5.4
35	5	244.2	31.0	53.7	57.7	9.3	7.9	4.5
35	5	269.7	34.2	60.4	56.7	9.3	7.9	4.5
35	5	304.8	38.7	67.1	57.7	9.3	7.9	4.5
35	5	337.9	42.9	75.5	56.8	9.3	7.9	4.5
35	5	368.2	46.7	80.4	58.1	9.3	7.9	4.6
35	5	399.0	50.7	87.3	58.0	9.3	7.9	4.6
35	5	442.8	56.2	97.2	57.8	9.3	7.9	4.6
35	5	472.9	60.0	105.4	57.0	9.3	7.9	4.5
35	5	517.4	65.7	115.3	57.0	9.3	7.9	4.5
35	5	549.8	69.8	121.8	57.3	9.3	7.9	4.5
35	5	587.8	74.6	131.1	56.9	9.3	7.9	4.5
35	5	699.3	88.8	150.2	59.1	9.3	7.9	4.7
35	5	822.6	104.4	177.7	58.8	9.3	7.9	4.6
35	5	852.1	108.2	185.4	58.3	9.3	7.9	4.6
35	5	886.5	112.5	194.8	57.8	9.3	7.9	4.6
40	5	227.2	35.0	59.3	59.0	7.9	6.5	3.8
40	5	251.8	38.7	66.7	58.1	7.9	6.5	3.8
40	5	284.5	43.8	74.3	58.9	7.9	6.5	3.8
40	5	315.4	48.5	84.1	57.7	7.9	6.5	3.8
40	5	342.8	52.7	89.4	59.0	7.9	6.5	3.8
40	5	372.1	57.3	97.3	58.8	7.9	6.5	3.8
40	5	415.1	63.9	107.6	59.4	7.9	6.5	3.9
40	5	443.9	68.3	117.3	58.2	7.9	6.5	3.8
40	5	508.5	78.2	135.2	57.9	7.9	6.5	3.8
40	5	541.4	83.3	142.1	58.6	7.9	6.5	3.8
40	5	579.4	89.2	152.8	58.3	7.9	6.5	3.8
40	5	683.0	105.1	174.9	60.1	7.9	6.5	3.9
40	5	804.8	123.8	207.6	59.6	7.9	6.5	3.9
40	5	836.9	128.8	216.1	59.6	7.9	6.5	3.9
40	5	872.0	134.2	226.9	59.1	7.9	6.5	3.8

Table C-1 Water-cooled screw compressor chiller 30HXC carrier/R-134a (Cont.)

T_{cd} (°C)	T_{ev} (°C)	$\dot{Q}_{ev}$ (kW)	$\dot{W}_{ideal}$ (kW)	$\dot{W}_{actual}$ (kW)	η_{is}	COP_{carnot}	$COP_{standard}$	COP_{actual}
30	6	274.8	27.2	49.3	55.2	11.6	10.1	5.6
30	6	303.0	30.0	55.3	54.3	11.6	10.1	5.5
30	6	342.1	33.9	61.5	55.1	11.6	10.1	5.6
30	6	380.0	37.7	68.6	54.9	11.6	10.1	5.5
30	6	413.0	40.9	73.0	56.1	11.6	10.1	5.7
30	6	447.2	44.3	79.1	56.0	11.6	10.1	5.7
30	6	495.8	49.1	89.2	55.1	11.6	10.1	5.6
30	6	530.4	52.6	96.2	54.6	11.6	10.1	5.5
30	6	551.9	54.7	98.9	55.3	11.6	10.1	5.6
30	6	584.0	57.9	105.3	55.0	11.6	10.1	5.5
30	6	624.0	61.8	113.3	54.6	11.6	10.1	5.5
30	6	745.8	73.9	130.4	56.7	11.6	10.1	5.7
30	6	874.5	86.7	153.0	56.6	11.6	10.1	5.7
30	6	904.8	89.7	160.3	55.9	11.6	10.1	5.6
30	6	940.9	93.3	168.5	55.3	11.6	10.1	5.6
35	6	254.6	30.7	54.2	56.7	9.6	8.3	4.7
35	6	281.0	33.9	60.9	55.7	9.6	8.3	4.6
35	6	317.5	38.3	67.7	56.6	9.6	8.3	4.7
35	6	352.4	42.5	76.2	55.8	9.6	8.3	4.6
35	6	383.9	46.3	81.0	57.2	9.6	8.3	4.7
35	6	415.9	50.2	88.0	57.0	9.6	8.3	4.7
35	6	461.3	55.7	98.0	56.8	9.6	8.3	4.7
35	6	493.0	59.5	106.3	56.0	9.6	8.3	4.6
35	6	535.3	64.6	115.1	56.1	9.6	8.3	4.7
35	6	568.2	68.6	121.7	56.3	9.6	8.3	4.7
35	6	607.0	73.3	130.8	56.0	9.6	8.3	4.6
35	6	723.5	87.3	150.2	58.1	9.6	8.3	4.8
35	6	850.6	102.7	177.1	58.0	9.6	8.3	4.8
35	6	880.4	106.3	184.9	57.5	9.6	8.3	4.8
35	6	915.5	110.5	194.2	56.9	9.6	8.3	4.7
40	6	235.6	34.7	59.7	58.1	8.2	6.8	3.9
40	6	261.1	38.4	67.2	57.2	8.2	6.8	3.9
40	6	295.0	43.4	74.8	58.1	8.2	6.8	3.9
40	6	326.9	48.1	86.5	55.6	8.2	6.8	3.8
40	6	355.4	52.3	90.5	57.8	8.2	6.8	3.9
40	6	385.7	56.8	98.2	57.8	8.2	6.8	3.9
40	6	430.3	63.3	108.1	58.6	8.2	6.8	4.0
40	6	460.1	67.7	117.8	57.5	8.2	6.8	3.9
40	6	522.7	76.9	134.7	57.1	8.2	6.8	3.9
40	6	556.5	81.9	141.7	57.8	8.2	6.8	3.9
40	6	595.3	87.6	152.0	57.7	8.2	6.8	3.9
40	6	703.4	103.5	174.7	59.3	8.2	6.8	4.0
40	6	827.4	121.8	207.0	58.8	8.2	6.8	4.0
40	6	860.1	126.6	215.0	58.9	8.2	6.8	4.0
40	6	895.9	131.9	225.6	58.5	8.2	6.8	4.0

Table C-1 Water-cooled screw compressor chiller 30HXC carrier/R-134a (Cont.)

T_{cd} (°C)	T_{ev} (°C)	$\dot{Q}_{ev}$ (kW)	$\dot{W}_{ideal}$ (kW)	$\dot{W}_{actual}$ (kW)	η_{is}	COP_{carnot}	$COP_{standard}$	COP_{actual}
30	7	285.8	27.0	50.0	54.0	12.2	10.6	5.7
30	7	315.0	29.8	56.1	53.0	12.2	10.6	5.6
30	7	355.7	33.6	62.3	53.9	12.2	10.6	5.7
30	7	395.0	37.3	69.4	53.8	12.2	10.6	5.7
30	7	429.4	40.6	73.8	55.0	12.2	10.6	5.8
30	7	465.0	43.9	80.0	54.9	12.2	10.6	5.8
30	7	515.5	48.7	90.3	53.9	12.2	10.6	5.7
30	7	551.5	52.1	97.2	53.6	12.2	10.6	5.7
30	7	569.5	53.8	99.1	54.3	12.2	10.6	5.7
30	7	602.5	56.9	105.7	53.8	12.2	10.6	5.7
30	7	643.4	60.8	113.6	53.5	12.2	10.6	5.7
30	7	767.9	72.5	130.7	55.5	12.2	10.6	5.9
30	7	902.1	85.2	153.1	55.7	12.2	10.6	5.9
30	7	933.4	88.2	160.9	54.8	12.2	10.6	5.8
30	7	970.1	91.6	168.8	54.3	12.2	10.6	5.7
35	7	265.5	30.7	54.7	56.2	10.0	8.6	4.9
35	7	292.7	33.9	61.5	55.1	10.0	8.6	4.8
35	7	330.9	38.3	68.3	56.1	10.0	8.6	4.8
35	7	367.3	42.5	76.8	55.3	10.0	8.6	4.8
35	7	400.0	46.3	81.5	56.8	10.0	8.6	4.9
35	7	433.2	50.1	88.5	56.6	10.0	8.6	4.9
35	7	480.7	55.6	98.8	56.3	10.0	8.6	4.9
35	7	514.0	59.5	107.1	55.5	10.0	8.6	4.8
35	7	553.9	64.1	114.9	55.8	10.0	8.6	4.8
35	7	587.0	67.9	121.7	55.8	10.0	8.6	4.8
35	7	627.0	72.6	130.5	55.6	10.0	8.6	4.8
35	7	748.2	86.6	150.1	57.7	10.0	8.6	5.0
35	7	897.4	103.8	176.5	58.8	10.0	8.6	5.1
35	7	910.0	105.3	184.8	57.0	10.0	8.6	4.9
35	7	946.0	109.5	193.8	56.5	10.0	8.6	4.9
40	7	244.7	34.7	60.1	57.8	8.5	7.0	4.1
40	7	270.7	38.4	67.6	56.8	8.5	7.0	4.0
40	7	305.9	43.4	75.2	57.7	8.5	7.0	4.1
40	7	338.8	48.1	86.9	55.3	8.5	7.0	3.9
40	7	369.2	52.4	90.3	58.0	8.5	7.0	4.1
40	7	400.9	56.9	98.3	57.9	8.5	7.0	4.1
40	7	446.1	63.3	108.7	58.2	8.5	7.0	4.1
40	7	477.0	67.7	120.3	56.3	8.5	7.0	4.0
40	7	537.3	76.2	136.0	56.0	8.5	7.0	4.0
40	7	572.7	81.2	141.5	57.4	8.5	7.0	4.0
40	7	611.5	86.8	151.2	57.4	8.5	7.0	4.0
40	7	725.6	102.9	174.6	59.0	8.5	7.0	4.2
40	7	852.2	120.9	205.5	58.8	8.5	7.0	4.1
40	7	884.3	125.5	214.3	58.5	8.5	7.0	4.1
40	7	920.3	130.6	224.4	58.2	8.5	7.0	4.1

Table C-1 Water-cooled screw compressor chiller 30HXC carrier/R-134a (Cont.)

T_{cd} (°C)	T_{ev} (°C)	$\dot{Q}_{ev}$ (kW)	$\dot{W}_{ideal}$ (kW)	$\dot{W}_{actual}$ (kW)	η_{is}	COP_{carnot}	$COP_{standard}$	COP_{actual}
30	8	297.0	26.6	50.5	52.8	12.8	11.1	5.9
30	8	327.4	29.4	56.9	51.6	12.8	11.1	5.8
30	8	369.8	33.2	63.0	52.7	12.8	11.1	5.9
30	8	410.5	36.8	70.2	52.5	12.8	11.1	5.8
30	8	446.2	40.0	74.5	53.7	12.8	11.1	6.0
30	8	482.7	43.3	80.8	53.6	12.8	11.1	6.0
30	8	535.7	48.1	91.4	52.6	12.8	11.1	5.9
30	8	573.0	51.4	98.2	52.3	12.8	11.1	5.8
30	8	587.4	52.7	99.2	53.1	12.8	11.1	5.9
30	8	620.0	55.6	106.1	52.4	12.8	11.1	5.8
30	8	663.1	59.5	113.8	52.3	12.8	11.1	5.8
30	8	788.8	70.8	130.7	54.1	12.8	11.1	6.0
30	8	927.6	83.2	152.7	54.5	12.8	11.1	6.1
30	8	961.0	86.2	161.1	53.5	12.8	11.1	6.0
30	8	999.8	89.7	168.9	53.1	12.8	11.1	5.9
35	8	276.7	30.6	55.1	55.6	10.4	9.0	5.0
35	8	305.0	33.7	62.0	54.4	10.4	9.0	4.9
35	8	344.8	38.1	68.8	55.4	10.4	9.0	5.0
35	8	382.6	42.3	77.3	54.8	10.4	9.0	4.9
35	8	416.7	46.1	82.0	56.2	10.4	9.0	5.1
35	8	451.2	49.9	89.0	56.1	10.4	9.0	5.1
35	8	500.7	55.4	99.4	55.7	10.4	9.0	5.0
35	8	535.4	59.2	107.7	55.0	10.4	9.0	5.0
35	8	572.5	63.3	114.5	55.3	10.4	9.0	5.0
35	8	606.4	67.1	121.7	55.1	10.4	9.0	5.0
35	8	647.6	71.7	130.1	55.1	10.4	9.0	5.0
35	8	773.3	85.6	150.4	56.9	10.4	9.0	5.1
35	8	908.8	100.6	175.7	57.2	10.4	9.0	5.2
35	8	940.1	104.0	184.3	56.4	10.4	9.0	5.1
35	8	977.1	108.1	193.0	56.0	10.4	9.0	5.1
40	8	254.9	34.8	60.7	57.3	8.8	7.3	4.2
40	8	281.6	38.4	68.2	56.3	8.8	7.3	4.1
40	8	318.5	43.5	75.9	57.3	8.8	7.3	4.2
40	8	352.2	48.1	85.5	56.2	8.8	7.3	4.1
40	8	384.6	52.5	90.9	57.7	8.8	7.3	4.2
40	8	417.2	56.9	98.9	57.6	8.8	7.3	4.2
40	8	464.2	63.3	109.6	57.8	8.8	7.3	4.2
40	8	495.5	67.6	120.4	56.2	8.8	7.3	4.1
40	8	553.3	75.5	133.5	56.5	8.8	7.3	4.1
40	8	589.7	80.5	141.4	56.9	8.8	7.3	4.2
40	8	629.4	85.9	150.7	57.0	8.8	7.3	4.2
40	8	748.2	102.1	174.3	58.6	8.8	7.3	4.3
40	8	880.2	120.1	205.0	58.6	8.8	7.3	4.3
40	8	912.6	124.5	214.3	58.1	8.8	7.3	4.3
40	8	949.1	129.5	224.0	57.8	8.8	7.3	4.2

Table C-1 Water-cooled screw compressor chiller 30HXC carrier/R-134a (Cont.)

T_{cd} (°C)	T_{ev} (°C)	$\dot{Q}_{ev}$ (kW)	$\dot{W}_{ideal}$ (kW)	$\dot{W}_{actual}$ (kW)	η_{is}	COP_{carnot}	$COP_{standard}$	COP_{actual}
30	9	307.1	25.6	50.9	50.3	13.4	12.0	6.0
30	9	339.3	28.3	57.5	49.2	13.4	12.0	5.9
30	9	382.7	31.9	63.6	50.2	13.4	12.0	6.0
30	9	425.6	35.5	70.8	50.1	13.4	12.0	6.0
30	9	461.5	38.5	74.9	51.4	13.4	12.0	6 2
30	9	499.3	41.6	81.2	51.3	13.4	12.0	6.1
30	9	554.9	46.3	92.1	50.3	13.4	12.0	6.0
30	9	593.6	49.5	99.0	50.0	13.4	12.0	6.0
30	9	604.3	50.4	99.0	50.9	13.4	12.0	6.1
30	9	636.5	53.1	105.9	50.1	13.4	12.0	6.0
30	9	681.5	56.8	113.6	50.0	13.4	12.0	6.0
30	9	810.0	67.6	130.3	51.8	13.4	12.0	6.2
30	9	950.1	79.2	151.7	52.2	13.4	12.0	6.3
30	9	983.6	82.0	160.4	51.1	13.4	12.0	6.1
30	9	1023.9	85.4	168.1	50.8	13.4	12.0	6.1
35	9	288.1	29.9	55.6	53.8	10.9	9.6	5.2
35	9	317.5	33.0	62.5	52.8	10.9	9.6	5.1
35	9	358.9	37.3	69.3	53.8	10.9	9.6	5.2
35	9	398.2	41.4	77.7	53.2	10.9	9.6	5.1
35	9	433.7	45.1	82.6	54.6	10.9	9.6	5.3
35	9	469.5	48.8	89.7	54.4	10.9	9.6	5.2
35	9	521.4	54.2	100.0	54.2	10.9	9.6	5.2
35	9	557.2	57.9	108.4	53.4	10.9	9.6	5.1
35	9	591.4	61.4	114.0	53.9	10.9	9.6	5.2
35	9	625.9	65.0	121.6	53.5	10.9	9.6	5.1
35	9	668.5	69.5	129.6	53.6	10.9	9.6	5.2
35	9	798.6	83.0	150.5	55.1	10.9	9.6	5.3
35	9	937.9	97.4	175.5	55.5	10.9	9.6	5.3
35	9	970.2	100.8	184.0	54.8	10.9	9.6	5.3
35	9	1008.4	104.8	192.0	54.6	10.9	9.6	5.3
40	9	265.4	34.3	61.3	56.0	9.1	7.7	4.3
40	9	293.1	37.9	68.9	55.0	9.1	7.7	4.3
40	9	331.5	42.8	76.6	55.9	9.1	7.7	4.3
40	9	367.1	47.4	86.2	55.0	9.1	7.7	4.3
40	9	401.0	51.8	91.7	56.5	9.1	7.7	4.4
40	9	434.6	56.2	99.6	56.4	9.1	7.7	4.4
40	9	483.1	62.4	110.5	56.5	9.1	7.7	4.4
40	9	515.4	66.6	119.9	55.6	9.1	7.7	4.3
40	9	571.9	73.9	133.3	55.5	9.1	7.7	4.3
40	9	607.9	78.6	141.1	55.7	9.1	7.7	4.3
40	9	649.4	83.9	150.5	55.8	9.1	7.7	4.3
40	9	772.8	99.9	174.0	57.4	9.1	7.7	4.4
40	9	909.5	117.6	204.6	57.5	9.1	7.7	4.4
40	9	941.7	121.7	214.0	56.9	9.1	7.7	4.4
40	9	979.1	126.6	223.6	56.6	9.1	7.7	4.4

Table C-1 Water-cooled screw compressor chiller 30HXC carrier/R-134a (Cont.)

T_{cd} (°C)	T_{ev} (°C)	$\dot{Q}_{ev}$ (kW)	$\dot{W}_{ideal}$ (kW)	$\dot{W}_{actual}$ (kW)	η_{is}	COP_{carnot}	$COP_{standard}$	COP_{actual}
30	10	316.8	25.5	51.2	49.8	14.2	12.4	6.2
30	10	350.6	28.2	57.9	48.7	14.2	12.4	6.1
30	10	394.6	31.7	63.9	49.7	14.2	12.4	6.2
30	10	439.6	35.4	71.1	49.7	14.2	12.4	6.2
30	10	476.2	38.3	75.1	51.0	14.2	12.4	6.3
30	10	515.7	41.5	81.5	50.9	14.2	12.4	6.3
30	10	572.0	46.0	92.6	49.7	14.2	12.4	6.2
30	10	613.8	49.4	99.6	49.6	14.2	12.4	6.2
30	10	618.4	49.7	98.4	50.6	14.2	12.4	6.3
30	10	652.7	52.5	105.5	49.8	14.2	12.4	6.2
30	10	697.0	56.1	113.0	49.6	14.2	12.4	6.2
30	10	830.5	66.8	129.5	51.6	14.2	12.4	6.4
30	10	971.5	78.1	150.3	52.0	14.2	12.4	6.5
30	10	1005.3	80.9	159.3	50.8	14.2	12.4	6.3
30	10	1046.2	84.2	166.9	50.4	14.2	12.4	6.3
35	10	299.5	30.2	56.3	53.6	11.3	9.9	5.3
35	10	330.2	33.3	63.2	52.6	11.3	9.9	5.2
35	10	373.1	37.6	70.2	53.5	11.3	9.9	5.3
35	10	414.1	41.7	78.4	53.2	11.3	9.9	5.3
35	10	450.9	45.4	83.4	54.5	11.3	9.9	5.4
35	10	488.1	49.2	90.5	54.3	11.3	9.9	5.4
35	10	541.9	54.6	101.3	53.9	11.3	9.9	5.3
35	10	579.2	58.3	109.5	53.3	11.3	9.9	5.3
35	10	610.2	61.5	114.0	53.9	11.3	9.9	5.4
35	10	645.5	65.0	121.6	53.5	11.3	9.9	5.3
35	10	689.2	69.4	129.6	53.6	11.3	9.9	5.3
35	10	824.3	83.0	150.5	55.2	11.3	9.9	5.5
35	10	966.9	97.4	175.9	55.4	11.3	9.9	5.5
35	10	999.8	100.7	184.7	54.5	11.3	9.9	5.4
35	10	1038.9	104.7	192.9	54.3	11.3	9.9	5.4
40	10	276.5	34.8	61.8	56.3	9.4	7.9	4.5
40	10	305.0	38.4	69.5	55.2	9.4	7.9	4.4
40	10	345.0	43.4	77.2	56.2	9.4	7.9	4.5
40	10	382.5	48.1	87.0	55.3	9.4	7.9	4.4
40	10	417.7	52.6	92.3	56.9	9.4	7.9	4.5
40	10	452.5	56.9	100.4	56.7	9.4	7.9	4.5
40	10	502.6	63.2	111.4	56.8	9.4	7.9	4.5
40	10	536.8	67.5	120.9	55.9	9.4	7.9	4.4
40	10	590.9	74.4	133.0	55.9	9.4	7.9	4.4
40	10	627.4	79.0	140.9	56.0	9.4	7.9	4.5
40	10	669.6	84.3	150.2	56.1	9.4	7.9	4.5
40	10	798.6	100.5	173.7	57.9	9.4	7.9	4.6
40	10	939.2	118.2	204.0	57.9	9.4	7.9	4.6
40	10	971.6	122.3	213.5	57.3	9.4	7.9	4.6
40	10	1009.6	127.0	223.0	57.0	9.4	7.9	4.5

Table C-1 Water-cooled screw compressor chiller 30HXC carrier/R-134a (Cont.)

T_{cd} (°C)	T_{ev} (°C)	$\dot{Q}_{ev}$ (kW)	$\dot{W}_{ideal}$ (kW)	$\dot{W}_{actual}$ (kW)	η_{is}	COP_{carnot}	$COP_{standard}$	COP_{actual}
30	13	333.2	22.3	51.5	43.2	16.8	15.0	6.5
30	13	371.6	24.8	58.5	42.5	16.8	15.0	6.4
30	13	414.1	27.7	64.3	43.0	16.8	15.0	6.4
30	13	462.7	30.9	71.3	43.4	16.8	15.0	6.5
30	13	503.0	33.6	75.3	44.6	16.8	15.0	6.7
30	13	549.3	36.7	81.8	44.9	16.8	15.0	6.7
30	13	604.3	40.4	93.2	43.3	16.8	15.0	6.5
30	13	653.5	43.7	99.9	43.7	16.8	15.0	6.5
30	13	644.6	43.1	96.7	44.5	16.8	15.0	6.7
30	13	680.9	45.5	104.1	43.7	16.8	15.0	6.5
30	13	721.9	48.2	111.6	43.2	16.8	15.0	6.5
30	13	867.6	58.0	128.6	45.1	16.8	15.0	6.7
30	13	1005.8	67.2	148.1	45.4	16.8	15.0	6.8
30	13	1035.5	69.2	157.4	44.0	16.8	15.0	6.6
30	13	1085.7	72.6	164.3	44.2	16.8	15.0	6.6
35	13	318.8	27.5	57.5	47.8	13.0	11.6	5.5
35	13	351.4	30.3	64.7	46.8	13.0	11.6	5.4
35	13	396.1	34.1	71.7	47.6	13.0	11.6	5.5
35	13	441.4	38.1	80.0	47.6	13.0	11.6	5.5
35	13	482.5	41.6	85.1	48.9	13.0	11.6	5.7
35	13	523.1	45.1	92.4	48.8	13.0	11.6	5.7
35	13	580.0	50.0	103.7	48.2	13.0	11.6	5.6
35	13	626.2	54.0	111.9	48.2	13.0	11.6	5.6
35	13	644.8	55.6	114.5	48.5	13.0	11.6	5.6
35	13	683.3	58.9	122.1	48.2	13.0	11.6	5.6
35	13	722.7	62.3	130.3	47.8	13.0	11.6	5.5
35	13	868.0	74.8	150.8	49.6	13.0	11.6	5.8
35	13	1012.4	87.3	176.1	49.6	13.0	11.6	5.7
35	13	1040.5	89.7	185.1	48.5	13.0	11.6	5.6
35	13	1092.2	94.2	193.4	48.7	13.0	11.6	5.6
40	13	295.3	32.6	62.7	52.0	10.6	9.1	4.7
40	13	322.0	35.5	70.4	50.5	10.6	9.1	4.6
40	13	367.5	40.5	78.3	51.8	10.6	9.1	4.7
40	13	404.1	44.6	87.9	50.7	10.6	9.1	4.6
40	13	444.8	49.1	93.3	52.6	10.6	9.1	4.8
40	13	486.7	53.7	101.6	52.8	10.6	9.1	4.8
40	13	540.2	59.6	113.0	52.7	10.6	9.1	4.8
40	13	577.9	63.7	122.5	52.0	10.6	9.1	4.7
40	13	627.2	69.2	132.5	52.2	10.6	9.1	4.7
40	13	666.1	73.5	140.3	52.4	10.6	9.1	4.7
40	13	704.3	77.7	149.7	51.9	10.6	9.1	4.7
40	13	840.0	92.7	173.0	53.6	10.6	9.1	4.9
40	13	986.6	108.8	203.0	53.6	10.6	9.1	4.9
40	13	1014.1	111.9	212.8	52.6	10.6	9.1	4.8
40	13	1065.4	117.5	222.0	52.9	10.6	9.1	4.8

Table C-1 Water-cooled screw compressor chiller 30HXC carrier/R-134a (Cont.)

T_{cd} (°C)	T_{ev} (°C)	$\dot{Q}_{ev}$ (kW)	$\dot{W}_{ideal}$ (kW)	$\dot{W}_{actual}$ (kW)	η_{is}	COP_{carnot}	$COP_{standard}$	COP_{actual}
30	16	330.1	17.9	51.4	34.9	20.7	18.4	6.4
30	16	368.2	20.0	58.4	34.2	20.7	18.4	6.3
30	16	414.4	22.5	64.3	35.0	20.7	18.4	6.4
30	16	461.4	25.1	71.3	35.2	20.7	18.4	6.5
30	16	503.5	27.4	75.2	36.4	20.7	18.4	6.7
30	16	549.5	29.8	81.7	36.5	20.7	18.4	6.7
30	16	604.9	32.9	93.2	35.3	20.7	18.4	6.5
30	16	653.8	35.5	100.0	35.5	20.7	18.4	6.5
30	16	644.7	35.0	96.7	36.2	20.7	18.4	6.7
30	16	680.8	37.0	104.2	35.5	20.7	18.4	6.5
30	16	725.8	39.4	111.4	35.4	20.7	18.4	6.5
30	16	861.0	46.8	128.7	36.3	20.7	18.4	6.7
30	16	1007.7	54.7	148.2	36.9	20.7	18.4	6.8
30	16	1041.2	56.6	157.0	36.0	20.7	18.4	6.6
30	16	1083.0	58.8	164.5	35.8	20.7	18.4	6.6
35	16	315.2	23.0	57.3	40.1	15.2	13.7	5.5
35	16	350.8	25.6	64.6	39.6	15.2	13.7	5.4
35	16	396.5	28.9	71.7	40.3	15.2	13.7	5.5
35	16	439.8	32.0	79.9	40.1	15.2	13.7	5.5
35	16	483.2	35.2	85.1	41.4	15.2	13.7	5.7
35	16	522.1	38.0	92.4	41.2	15.2	13.7	5.7
35	16	580.7	42.3	103.7	40.8	15.2	13.7	5.6
35	16	626.6	45.7	111.9	40.8	15.2	13.7	5.6
35	16	645.0	47.0	114.5	41.0	15.2	13.7	5.6
35	16	682.8	49.8	122.0	40.8	15.2	13.7	5.6
35	16	728.0	53.0	130.3	40.7	15.2	13.7	5.6
35	16	861.3	62.8	150.9	41.6	15.2	13.7	5.7
35	16	1014.1	73.9	176.0	42.0	15.2	13.7	5.8
35	16	1048.1	76.4	185.5	41.2	15.2	13.7	5.7
35	16	1088.6	79.3	193.4	41.0	15.2	13.7	5.6
40	16	291.7	28.0	62.6	44.8	12.0	10.4	4.7
40	16	325.2	31.2	70.5	44.3	12.0	10.4	4.6
40	16	363.2	34.9	78.1	44.7	12.0	10.4	4.7
40	16	408.0	39.2	88.0	44.5	12.0	10.4	4.6
40	16	449.3	43.2	93.5	46.2	12.0	10.4	4.8
40	16	485.7	46.7	101.6	45.9	12.0	10.4	4.8
40	16	540.9	52.0	113.0	46.0	12.0	10.4	4.8
40	16	576.7	55.4	122.4	45.3	12.0	10.4	4.7
40	16	627.4	60.3	132.5	45.5	12.0	10.4	4.7
40	16	665.5	63.9	140.3	45.6	12.0	10.4	4.7
40	16	703.9	67.6	149.7	45.2	12.0	10.4	4.7
40	16	837.8	80.5	173.1	46.5	12.0	10.4	4.8
40	16	988.3	94.9	202.9	46.8	12.0	10.4	4.9
40	16	1022.1	98.2	212.6	46.2	12.0	10.4	4.8
40	16	1061.6	102.0	222.1	45.9	12.0	10.4	4.8

Table C-2 Air-cooled screw compressor chiller 30HXA carrier/R-134a

T_{cd} (°C)	T_{ev} (°C)	$\dot{Q}_{ev}$ (kW)	$\dot{W}_{ideal}$ (kW)	$\dot{W}_{actual}$ (kW)	η_{is}	COP_{carnot}	$COP_{standard}$	COP_{actual}
35	4	231.7	30.4	69.2	43.9	8.9	7.6	3.3
35	4	254.3	33.4	78.4	42.5	8.9	7.6	3.2
35	4	284.3	37.3	89.1	41.9	8.9	7.6	3.2
35	4	326.4	42.8	98.8	43.3	8.9	7.6	3.3
35	4	350.2	45.9	107.1	42.9	8.9	7.6	3.3
35	4	386.0	50.6	114.9	44.1	8.9	7.6	3.4
35	4	418.9	54.9	130.0	42.3	8.9	7.6	3.2
35	4	466.3	61.2	137.5	44.5	8.9	7.6	3.4
35	4	485.5	63.7	146.3	43.5	8.9	7.6	3.3
35	4	521.1	68.4	161.4	42.4	8.9	7.6	3.2
35	4	564.4	74.0	182.9	40.5	8.9	7.6	3.1
35	4	665.3	87.3	190.3	45.9	8.9	7.6	3.5
35	4	772.8	101.4	226.4	44.8	8.9	7.6	3.4
35	4	810.1	106.3	242.7	43.8	8.9	7.6	3.3
35	4	851.7	111.7	260.9	42.8	8.9	7.6	3.3
40	4	216.1	34.2	72.9	47.0	7.7	6.3	3.0
40	4	236.2	37.4	82.6	45.3	7.7	6.3	2.9
40	4	264.7	41.9	93.6	44.8	7.7	6.3	2.8
40	4	304.4	48.2	103.9	46.4	7.7	6.3	2.9
40	4	326.4	51.7	112.7	45.9	7.7	6.3	2.9
40	4	360.7	57.1	121.2	47.2	7.7	6.3	3.0
40	4	391.3	62.0	136.5	45.4	7.7	6.3	2.9
40	4	436.6	69.2	144.4	47.9	7.7	6.3	3.0
40	4	465.8	73.8	158.5	46.6	7.7	6.3	2.9
40	4	498.8	79.0	174.5	45.3	7.7	6.3	2.9
40	4	536.9	85.1	197.1	43.2	7.7	6.3	2.7
40	4	641.2	101.6	206.8	49.1	7.7	6.3	3.1
40	4	734.9	116.4	245.0	47.5	7.7	6.3	3.0
40	4	777.0	123.1	262.6	46.9	7.7	6.3	3.0
40	4	812.7	128.8	282.1	45.6	7.7	6.3	2.9
45	4	198.6	37.1	76.7	48.4	6.8	5.3	2.6
45	4	217.3	40.6	87.5	46.4	6.8	5.3	2.5
45	4	243.5	45.5	99.6	45.7	6.8	5.3	2.4
45	4	281.1	52.6	109.9	47.8	6.8	5.3	2.6
45	4	301.7	56.4	119.4	47.2	6.8	5.3	2.5
45	4	333.7	62.4	128.2	48.7	6.8	5.3	2.6
45	4	362.0	67.7	144.8	46.7	6.8	5.3	2.5
45	4	405.3	75.8	152.1	49.8	6.8	5.3	2.7
45	4	444.4	83.1	171.7	48.4	6.8	5.3	2.6
45	4	476.3	89.1	189.0	47.1	6.8	5.3	2.5
45	4	514.8	96.3	213.2	45.1	6.8	5.3	2.4
45	4	613.6	114.7	224.2	51.2	6.8	5.3	2.7
45	4	707.4	132.3	265.1	49.9	6.8	5.3	2.7
45	4	740.5	138.5	283.8	48.8	6.8	5.3	2.6
45	4	777.3	145.3	304.2	47.8	6.8	5.3	2.6

Table C-2 Air-cooled screw compressor chiller 30HXA carrier/R-134a (Cont.)

T_{cd} (°C)	T_{ev} (°C)	$\dot{Q}_{ev}$ (kW)	$\dot{W}_{ideal}$ (kW)	$\dot{W}_{actual}$ (kW)	η_{is}	COP_{carnot}	$COP_{standard}$	COP_{actual}
35	5	240.0	30.5	70.5	43.2	9.3	7.9	3.4
35	5	263.1	33.4	79.9	41.8	9.3	7.9	3.3
35	5	294.6	37.4	90.7	41.2	9.3	7.9	3.2
35	5	337.9	42.9	100.6	42.6	9.3	7.9	3.4
35	5	362.3	46.0	109.1	42.2	9.3	7.9	3.3
35	5	399.2	50.7	117.1	43.3	9.3	7.9	3.4
35	5	433.6	55.0	132.3	41.6	9.3	7.9	3.3
35	5	482.3	61.2	140.0	43.7	9.3	7.9	3.4
35	5	500.7	63.6	148.2	42.9	9.3	7.9	3.4
35	5	537.5	68.2	163.6	41.7	9.3	7.9	3.3
35	5	583.3	74.1	185.5	39.9	9.3	7.9	3.1
35	5	685.0	87.0	193.1	45.0	9.3	7.9	3.5
35	5	795.7	101.0	229.6	44.0	9.3	7.9	3.5
35	5	834.1	105.9	246.1	43.0	9.3	7.9	3.4
35	5	876.6	111.3	265.1	42.0	9.3	7.9	3.3
40	5	224.4	34.5	74.2	46.5	7.9	6.5	3.0
40	5	245.1	37.7	84.1	44.8	7.9	6.5	2.9
40	5	274.0	42.2	95.5	44.1	7.9	6.5	2.9
40	5	315.0	48.5	105.8	45.8	7.9	6.5	3.0
40	5	338.4	52.1	114.8	45.4	7.9	6.5	2.9
40	5	373.8	57.5	123.4	46.6	7.9	6.5	3.0
40	5	405.4	62.4	138.8	44.9	7.9	6.5	2.9
40	5	453.2	69.7	146.9	47.5	7.9	6.5	3.1
40	5	480.3	73.9	160.8	46.0	7.9	6.5	3.0
40	5	515.1	79.3	176.9	44.8	7.9	6.5	2.9
40	5	553.9	85.2	200.3	42.5	7.9	6.5	2.8
40	5	661.5	101.8	209.5	48.6	7.9	6.5	3.2
40	5	768.7	118.3	248.3	47.6	7.9	6.5	3.1
40	5	803.7	123.7	266.1	46.5	7.9	6.5	3.0
40	5	840.2	129.3	286.1	45.2	7.9	6.5	2.9
45	5	206.6	37.6	78.2	48.1	7.0	5.5	2.6
45	5	225.6	41.0	89.0	46.1	7.0	5.5	2.5
45	5	252.7	46.0	101.2	45.4	7.0	5.5	2.5
45	5	292.1	53.1	111.5	47.7	7.0	5.5	2.6
45	5	313.1	57.0	121.2	47.0	7.0	5.5	2.6
45	5	346.8	63.1	129.9	48.6	7.0	5.5	2.7
45	5	375.4	68.3	147.0	46.5	7.0	5.5	2.6
45	5	420.8	76.6	154.3	49.6	7.0	5.5	2.7
45	5	458.9	83.5	174.0	48.0	7.0	5.5	2.6
45	5	491.5	89.4	191.4	46.7	7.0	5.5	2.6
45	5	531.2	96.6	215.9	44.8	7.0	5.5	2.5
45	5	634.3	115.4	227.3	50.8	7.0	5.5	2.8
45	5	730.8	133.0	268.9	49.4	7.0	5.5	2.7
45	5	763.9	139.0	288.0	48.3	7.0	5.5	2.7
45	5	801.4	145.8	309.0	47.2	7.0	5.5	2.6

Table C-2 Air-cooled screw compressor chiller 30HXA carrier/R-134a (Cont.)

T_{cd} (°C)	T_{ev} (°C)	$\dot{Q}_{ev}$ (kW)	$\dot{W}_{ideal}$ (kW)	$\dot{W}_{actual}$ (kW)	η_{is}	COP_{carnot}	$COP_{standard}$	COP_{actual}
35	6	248.7	30.0	71.8	41.8	9.6	8.3	3.5
35	6	272.2	32.9	81.5	40.3	9.6	8.3	3.3
35	6	304.7	36.8	92.6	39.7	9.6	8.3	3.3
35	6	349.7	42.2	102.5	41.2	9.6	8.3	3.4
35	6	374.6	45.2	111.2	40.7	9.6	8.3	3.4
35	6	413.1	49.9	119.2	41.8	9.6	8.3	3.5
35	6	448.7	54.2	134.7	40.2	9.6	8.3	3.3
35	6	499.0	60.2	142.5	42.3	9.6	8.3	3.5
35	6	515.5	62.2	150.5	41.3	9.6	8.3	3.4
35	6	554.1	66.9	165.8	40.3	9.6	8.3	3.3
35	6	601.2	72.6	188.5	38.5	9.6	8.3	3.2
35	6	705.3	85.1	195.7	43.5	9.6	8.3	3.6
35	6	818.3	98.8	232.9	42.4	9.6	8.3	3.5
35	6	858.6	103.6	249.6	41.5	9.6	8.3	3.4
35	6	902.4	108.9	269.1	40.5	9.6	8.3	3.4
40	6	232.3	34.2	75.7	45.2	8.2	6.8	3.1
40	6	253.8	37.4	85.8	43.5	8.2	6.8	3.0
40	6	283.9	41.8	97.4	42.9	8.2	6.8	2.9
40	6	327.3	48.2	107.9	44.7	8.2	6.8	3.0
40	6	350.9	51.7	116.9	44.2	8.2	6.8	3.0
40	6	387.7	57.1	125.6	45.4	8.2	6.8	3.1
40	6	419.9	61.8	141.4	43.7	8.2	6.8	3.0
40	6	469.4	69.1	149.5	46.2	8.2	6.8	3.1
40	6	495.6	73.0	163.1	44.7	8.2	6.8	3.0
40	6	531.9	78.3	179.6	43.6	8.2	6.8	3.0
40	6	572.4	84.3	203.5	41.4	8.2	6.8	2.8
40	6	682.2	100.4	212.3	47.3	8.2	6.8	3.2
40	6	792.6	116.7	251.9	46.3	8.2	6.8	3.1
40	6	830.9	122.3	269.6	45.4	8.2	6.8	3.1
40	6	868.5	127.8	290.2	44.1	8.2	6.8	3.0
45	6	214.3	37.5	79.7	47.1	7.2	5.7	2.7
45	6	234.3	41.0	90.4	45.4	7.2	5.7	2.6
45	6	262.2	45.9	103.0	44.6	7.2	5.7	2.5
45	6	302.8	53.0	113.5	46.7	7.2	5.7	2.7
45	6	324.9	56.9	122.9	46.3	7.2	5.7	2.6
45	6	359.6	62.9	132.0	47.7	7.2	5.7	2.7
45	6	389.2	68.1	149.5	45.6	7.2	5.7	2.6
45	6	436.3	76.4	156.9	48.7	7.2	5.7	2.8
45	6	473.6	82.9	176.7	46.9	7.2	5.7	2.7
45	6	506.7	88.7	194.4	45.6	7.2	5.7	2.6
45	6	547.4	95.8	219.6	43.6	7.2	5.7	2.5
45	6	655.5	114.7	230.4	49.8	7.2	5.7	2.8
45	6	755.2	132.2	272.8	48.5	7.2	5.7	2.8
45	6	788.3	138.0	292.3	47.2	7.2	5.7	2.7
45	6	825.8	144.5	313.8	46.1	7.2	5.7	2.6

Table C-2 Air-cooled screw compressor chiller 30HXA carrier/R-134a (Cont.)

T_{cd} (°C)	T_{ev} (°C)	$\dot{Q}_{ev}$ (kW)	$\dot{W}_{ideal}$ (kW)	$\dot{W}_{actual}$ (kW)	η_{is}	COP_{carnot}	$COP_{standard}$	COP_{actual}
35	7	257.3	29.8	73.4	40.6	10.0	8.6	3.5
35	7	281.2	32.5	83.2	39.1	10.0	8.6	3.4
35	7	314.9	36.4	94.5	38.6	10.0	8.6	3.3
35	7	361.6	41.8	104.5	40.0	10.0	8.6	3.5
35	7	387.5	44.8	113.2	39.6	10.0	8.6	3.4
35	7	427.4	49.5	121.3	40.8	10.0	8.6	3.5
35	7	464.0	53.7	137.4	39.1	10.0	8.6	3.4
35	7	516.2	59.7	144.9	41.2	10.0	8.6	3.6
35	7	530.3	61.4	152.9	40.1	10.0	8.6	3.5
35	7	569.9	65.9	168.3	39.2	10.0	8.6	3.4
35	7	618.9	71.6	191.7	37.4	10.0	8.6	3.2
35	7	725.9	84.0	198.3	42.4	10.0	8.6	3.7
35	7	842.4	97.5	236.1	41.3	10.0	8.6	3.6
35	7	883.5	102.2	253.1	40.4	10.0	8.6	3.5
35	7	928.9	107.5	273.1	39.4	10.0	8.6	3.4
40	7	240.4	34.1	77.3	44.1	8.5	7.0	3.1
40	7	262.8	37.3	87.5	42.6	8.5	7.0	3.0
40	7	293.7	41.7	99.3	42.0	8.5	7.0	3.0
40	7	338.7	48.1	109.9	43.7	8.5	7.0	3.1
40	7	363.4	51.6	119.1	43.3	8.5	7.0	3.1
40	7	401.3	56.9	127.9	44.5	8.5	7.0	3.1
40	7	434.3	61.6	144.2	42.7	8.5	7.0	3.0
40	7	485.8	68.9	152.3	45.3	8.5	7.0	3.2
40	7	511.1	72.5	165.5	43.8	8.5	7.0	3.1
40	7	548.7	77.8	182.4	42.7	8.5	7.0	3.0
40	7	591.2	83.9	206.9	40.5	8.5	7.0	2.9
40	7	703.4	99.8	214.9	46.4	8.5	7.0	3.3
40	7	816.8	115.9	255.5	45.4	8.5	7.0	3.2
40	7	856.0	121.4	273.8	44.4	8.5	7.0	3.1
40	7	897.4	127.3	294.3	43.3	8.5	7.0	3.0
45	7	222.6	37.7	81.2	46.4	7.4	5.9	2.7
45	7	243.1	41.2	91.9	44.8	7.4	5.9	2.6
45	7	272.3	46.1	104.6	44.1	7.4	5.9	2.6
45	7	314.4	53.2	115.4	46.1	7.4	5.9	2.7
45	7	336.6	57.0	125.2	45.5	7.4	5.9	2.7
45	7	372.7	63.1	134.6	46.9	7.4	5.9	2.8
45	7	403.5	68.3	152.0	45.0	7.4	5.9	2.7
45	7	452.5	76.6	159.8	48.0	7.4	5.9	2.8
45	7	488.9	82.8	179.2	46.2	7.4	5.9	2.7
45	7	522.9	88.6	197.5	44.8	7.4	5.9	2.6
45	7	564.0	95.5	223.1	42.8	7.4	5.9	2.5
45	7	676.6	114.6	233.5	49.1	7.4	5.9	2.9
45	7	780.1	132.1	276.7	47.7	7.4	5.9	2.8
45	7	814.0	137.9	296.9	46.4	7.4	5.9	2.7
45	7	850.0	144.0	318.6	45.2	7.4	5.9	2.7

Table C-2 Air-cooled screw compressor chiller 30HXA carrier/R-134a (Cont.)

T_{cd} (°C)	T_{ev} (°C)	$\dot{Q}_{ev}$ (kW)	$\dot{W}_{ideal}$ (kW)	$\dot{W}_{actual}$ (kW)	η_{is}	COP_{carnot}	$COP_{standard}$	COP_{actual}
35	8	266.1	29.4	74.9	39.3	10.4	9.0	3.6
35	8	290.7	32.2	84.8	37.9	10.4	9.0	3.4
35	8	325.4	36.0	96.4	37.3	10.4	9.0	3.4
35	8	373.6	41.3	106.6	38.8	10.4	9.0	3.5
35	8	400.4	44.3	115.3	38.4	10.4	9.0	3.5
35	8	441.4	48.8	123.7	39.5	10.4	9.0	3.6
35	8	479.9	53.1	140.2	37.9	10.4	9.0	3.4
35	8	533.4	59.0	147.7	40.0	10.4	9.0	3.6
35	8	545.7	60.4	155.2	38.9	10.4	9.0	3.5
35	8	586.2	64.9	171.0	37.9	10.4	9.0	3.4
35	8	636.2	70.4	194.8	36.1	10.4	9.0	3.3
35	8	747.2	82.7	200.8	41.2	10.4	9.0	3.7
35	8	866.5	95.9	239.4	40.0	10.4	9.0	3.6
35	8	908.4	100.5	256.8	39.1	10.4	9.0	3.5
35	8	955.8	105.8	277.1	38.2	10.4	9.0	3.4
40	8	249.0	34.0	78.7	43.2	8.8	7.3	3.2
40	8	272.2	37.1	89.1	41.7	8.8	7.3	3.1
40	8	304.2	41.5	101.2	41.0	8.8	7.3	3.0
40	8	350.5	47.8	112.0	42.7	8.8	7.3	3.1
40	8	375.8	51.3	121.3	42.3	8.8	7.3	3.1
40	8	415.2	56.6	130.2	43.5	8.8	7.3	3.2
40	8	449.4	61.3	147.0	41.7	8.8	7.3	3.1
40	8	502.7	68.6	155.0	44.3	8.8	7.3	3.2
40	8	526.7	71.9	167.9	42.8	8.8	7.3	3.1
40	8	565.6	77.2	185.1	41.7	8.8	7.3	3.1
40	8	610.4	83.3	210.1	39.6	8.8	7.3	2.9
40	8	724.7	98.9	217.9	45.4	8.8	7.3	3.3
40	8	841.8	114.9	258.9	44.4	8.8	7.3	3.3
40	8	881.8	120.3	277.8	43.3	8.8	7.3	3.2
40	8	926.2	126.4	298.3	42.4	8.8	7.3	3.1
45	8	231.1	37.8	82.6	45.8	7.6	6.1	2.8
45	8	251.7	41.2	93.6	44.0	7.6	6.1	2.7
45	8	281.9	46.1	106.3	43.4	7.6	6.1	2.7
45	8	325.7	53.3	117.6	45.3	7.6	6.1	2.8
45	8	348.8	57.1	127.8	44.6	7.6	6.1	2.7
45	8	386.4	63.2	137.0	46.1	7.6	6.1	2.8
45	8	417.9	68.4	154.5	44.2	7.6	6.1	2.7
45	8	468.9	76.7	162.7	47.1	7.6	6.1	2.9
45	8	504.1	82.5	181.9	45.3	7.6	6.1	2.8
45	8	539.3	88.2	200.6	44.0	7.6	6.1	2.7
45	8	580.6	95.0	226.9	41.9	7.6	6.1	2.6
45	8	696.5	113.9	236.9	48.1	7.6	6.1	2.9
45	8	805.9	131.8	280.4	47.0	7.6	6.1	2.9
45	8	840.6	137.5	301.3	45.6	7.6	6.1	2.8
45	8	878.7	143.8	323.6	44.4	7.6	6.1	2.7

Table C-2 Air-cooled screw compressor chiller 30HXA carrier/R-134a (Cont.)

T_{cd} (°C)	T_{ev} (°C)	$\dot{Q}_{ev}$ (kW)	$\dot{W}_{ideal}$ (kW)	$\dot{W}_{actual}$ (kW)	η_{is}	COP_{carnot}	$COP_{standard}$	COP_{actual}
35	9	275.1	28.6	76.5	37.4	10.9	9.6	3.6
35	9	300.5	31.2	86.5	36.1	10.9	9.6	3.5
35	9	335.9	34.9	98.4	35.5	10.9	9.6	3.4
35	9	386.0	40.1	108.6	36.9	10.9	9.6	3.6
35	9	431.7	44.9	117.4	38.2	10.9	9.6	3.7
35	9	456.1	47.4	126.1	37.6	10.9	9.6	3.6
35	9	494.5	51.4	143.1	35.9	10.9	9.6	3.5
35	9	551.0	57.2	150.4	38.1	10.9	9.6	3.7
35	9	561.1	58.3	157.4	37.0	10.9	9.6	3.6
35	9	602.7	62.6	173.7	36.0	10.9	9.6	3.5
35	9	654.2	68.0	198.0	34.3	10.9	9.6	3.3
35	9	768.8	79.9	203.3	39.3	10.9	9.6	3.8
35	9	890.8	92.6	242.6	38.1	10.9	9.6	3.7
35	9	933.8	97.0	260.5	37.2	10.9	9.6	3.6
35	9	982.8	102.1	281.0	36.3	10.9	9.6	3.5
40	9	257.6	33.3	80.2	41.5	9.1	7.7	3.2
40	9	281.4	36.4	90.8	40.1	9.1	7.7	3.1
40	9	314.5	40.7	103.1	39.4	9.1	7.7	3.1
40	9	362.6	46.9	114.1	41.1	9.1	7.7	3.2
40	9	388.2	50.2	123.8	40.5	9.1	7.7	3.1
40	9	429.0	55.4	132.7	41.8	9.1	7.7	3.2
40	9	464.7	60.1	149.8	40.1	9.1	7.7	3.1
40	9	519.5	67.1	157.9	42.5	9.1	7.7	3.3
40	9	542.7	70.1	170.2	41.2	9.1	7.7	3.2
40	9	582.3	75.3	188.0	40.0	9.1	7.7	3.1
40	9	629.7	81.4	213.4	38.1	9.1	7.7	3.0
40	9	746.5	96.5	220.8	43.7	9.1	7.7	3.4
40	9	866.2	112.0	262.6	42.6	9.1	7.7	3.3
40	9	907.2	117.3	282.0	41.6	9.1	7.7	3.2
40	9	952.7	123.1	303.3	40.6	9.1	7.7	3.1
45	9	239.9	37.4	84.1	44.5	7.8	6.4	2.9
45	9	260.8	40.7	95.3	42.7	7.8	6.4	2.7
45	9	291.8	45.6	108.2	42.1	7.8	6.4	2.7
45	9	337.6	52.7	119.8	44.0	7.8	6.4	2.8
45	9	361.0	56.4	130.0	43.3	7.8	6.4	2.8
45	9	400.3	62.5	193.5	32.3	7.8	6.4	2.1
45	9	432.5	67.5	157.1	43.0	7.8	6.4	2.8
45	9	485.5	75.8	165.7	45.7	7.8	6.4	2.9
45	9	519.4	81.1	184.5	43.9	7.8	6.4	2.8
45	9	556.0	86.8	203.6	42.6	7.8	6.4	2.7
45	9	597.5	93.3	230.8	40.4	7.8	6.4	2.6
45	9	717.4	112.0	240.3	46.6	7.8	6.4	3.0
45	9	832.1	129.9	284.4	45.7	7.8	6.4	2.9
45	9	868.2	135.5	305.7	44.3	7.8	6.4	2.8
45	9	907.4	141.6	328.6	43.1	7.8	6.4	2.8

Table C-2 Air-cooled screw compressor chiller 30HXA carrier/R-134a (Cont.)

T_{cd} (°C)	T_{ev} (°C)	$\dot{Q}_{ev}$ (kW)	$\dot{W}_{ideal}$ (kW)	$\dot{W}_{actual}$ (kW)	η_{is}	COP_{carnot}	$COP_{standard}$	COP_{actual}
35	10	284.2	28.6	78.1	36.7	11.3	9.9	3.6
35	10	310.3	31.3	88.2	35.4	11.3	9.9	3.5
35	10	346.9	34.9	100.3	34.8	11.3	9.9	3.5
35	10	398.6	40.2	110.7	36.3	11.3	9.9	3.6
35	10	426.7	43.0	119.8	35.9	11.3	9.9	3.6
35	10	470.7	47.4	128.6	36.9	11.3	9.9	3.7
35	10	510.4	51.4	145.9	35.2	11.3	9.9	3.5
35	10	568.7	57.3	153.5	37.3	11.3	9.9	3.7
35	10	576.7	58.1	159.8	36.4	11.3	9.9	3.6
35	10	619.3	62.4	176.5	35.3	11.3	9.9	3.5
35	10	672.1	67.7	201.3	33.6	11.3	9.9	3.3
35	10	790.8	79.7	206.1	38.7	11.3	9.9	3.8
35	10	915.2	92.2	245.7	37.5	11.3	9.9	3.7
35	10	959.2	96.6	264.2	36.6	11.3	9.9	3.6
35	10	1008.9	101.6	285.2	35.6	11.3	9.9	3.5
40	10	266.5	33.5	81.7	41.0	9.4	7.9	3.3
40	10	290.6	36.6	92.6	39.5	9.4	7.9	3.1
40	10	325.0	40.9	105.1	38.9	9.4	7.9	3.1
40	10	374.6	47.1	116.3	40.5	9.4	7.9	3.2
40	10	404.1	50.9	126.1	40.3	9.4	7.9	3.2
40	10	443.3	55.8	135.2	41.3	9.4	7.9	3.3
40	10	479.9	60.4	152.7	39.5	9.4	7.9	3.1
40	10	536.8	67.5	160.8	42.0	9.4	7.9	3.3
40	10	558.7	70.3	172.7	40.7	9.4	7.9	3.2
40	10	599.3	75.4	190.9	39.5	9.4	7.9	3.1
40	10	649.3	81.7	216.8	37.7	9.4	7.9	3.0
40	10	767.5	96.6	224.1	43.1	9.4	7.9	3.4
40	10	890.5	112.1	266.4	42.1	9.4	7.9	3.3
40	10	932.5	117.3	286.4	41.0	9.4	7.9	3.3
40	10	979.6	123.3	308.3	40.0	9.4	7.9	3.2
45	10	248.0	37.8	85.7	44.1	8.1	6.6	2.9
45	10	269.7	41.1	97.2	42.3	8.1	6.6	2.8
45	10	301.7	46.0	110.3	41.7	8.1	6.6	2.7
45	10	349.0	53.2	122.2	43.5	8.1	6.6	2.9
45	10	373.7	56.9	132.4	43.0	8.1	6.6	2.8
45	10	414.1	63.1	142.1	44.4	8.1	6.6	2.9
45	10	447.3	68.1	159.8	42.6	8.1	6.6	2.8
45	10	502.6	76.6	168.7	45.4	8.1	6.6	3.0
45	10	534.3	81.4	187.5	43.4	8.1	6.6	2.8
45	10	572.6	87.2	206.9	42.2	8.1	6.6	2.8
45	10	615.1	93.7	234.6	39.9	8.1	6.6	2.6
45	10	738.9	112.6	243.5	46.2	8.1	6.6	3.0
45	10	857.3	130.6	288.7	45.2	8.1	6.6	3.0
45	10	895.9	136.5	310.3	44.0	8.1	6.6	2.9
45	10	936.4	142.6	333.6	42.8	8.1	6.6	2.8

Table C-2 Air-cooled screw compressor chiller 30HXA carrier/R-134a (Cont.)

T_{cd} (°C)	T_{ev} (°C)	$\dot{Q}_{ev}$ (kW)	$\dot{W}_{ideal}$ (kW)	$\dot{W}_{actual}$ (kW)	η_{is}	COP_{carnot}	$COP_{standard}$	COP_{actual}
35	13	299.4	25.8	80.6	32.0	13.0	11.6	3.7
35	13	323.6	27.9	90.6	30.8	13.0	11.6	3.6
35	13	364.2	31.4	103.4	30.4	13.0	11.6	3.5
35	13	415.6	35.8	113.9	31.5	13.0	11.6	3.6
35	13	448.0	38.6	123.8	31.2	13.0	11.6	3.6
35	13	498.9	43.0	133.3	32.3	13.0	11.6	3.7
35	13	540.0	46.6	150.9	30.9	13.0	11.6	3.6
35	13	607.6	52.4	159.7	32.8	13.0	11.6	3.8
35	13	602.0	51.9	163.2	31.8	13.0	11.6	3.7
35	13	652.2	56.2	181.8	30.9	13.0	11.6	3.6
35	13	702.1	60.5	206.4	29.3	13.0	11.6	3.4
35	13	830.4	71.6	211.1	33.9	13.0	11.6	3.9
35	13	953.4	82.2	250.6	32.8	13.0	11.6	3.8
35	13	994.1	85.7	268.9	31.9	13.0	11.6	3.7
35	13	1054.9	90.9	292.0	31.1	13.0	11.6	3.6
40	13	281.1	31.0	84.2	36.8	10.6	9.1	3.3
40	13	303.6	33.5	94.9	35.3	10.6	9.1	3.2
40	13	341.7	37.7	108.5	34.7	10.6	9.1	3.1
40	13	391.0	43.1	119.3	36.2	10.6	9.1	3.3
40	13	421.5	46.5	129.9	35.8	10.6	9.1	3.2
40	13	470.1	51.9	139.8	37.1	10.6	9.1	3.4
40	13	508.5	56.1	157.9	35.5	10.6	9.1	3.2
40	13	569.3	62.8	166.2	37.8	10.6	9.1	3.4
40	13	583.5	64.4	176.8	36.4	10.6	9.1	3.3
40	13	632.3	69.7	196.8	35.4	10.6	9.1	3.2
40	13	679.4	74.9	222.8	33.6	10.6	9.1	3.0
40	13	799.3	88.2	229.4	38.4	10.6	9.1	3.5
40	13	928.3	102.4	272.6	37.6	10.6	9.1	3.4
40	13	967.6	106.7	291.9	36.6	10.6	9.1	3.3
40	13	1016.3	112.1	315.0	35.6	10.6	9.1	3.2
45	13	259.5	35.3	88.0	40.1	8.9	7.4	2.9
45	13	282.4	38.4	99.6	38.5	8.9	7.4	2.8
45	13	318.0	43.2	113.6	38.0	8.9	7.4	2.8
45	13	356.1	48.4	125.3	38.6	8.9	7.4	2.8
45	13	393.7	53.5	136.3	39.2	8.9	7.4	2.9
45	13	440.1	59.8	147.0	40.7	8.9	7.4	3.0
45	13	474.5	64.5	165.3	39.0	8.9	7.4	2.9
45	13	534.3	72.6	174.4	41.6	8.9	7.4	3.1
45	13	559.2	76.0	191.6	39.6	8.9	7.4	2.9
45	13	606.9	82.4	213.3	38.7	8.9	7.4	2.8
45	13	646.0	87.8	241.0	36.4	8.9	7.4	2.7
45	13	766.7	104.2	247.9	42.0	8.9	7.4	3.1
45	13	896.6	121.8	295.3	41.2	8.9	7.4	3.0
45	13	933.4	126.8	316.3	40.1	8.9	7.4	3.0
45	13	976.4	132.6	340.4	39.0	8.9	7.4	2.9

Table C-2 Air-cooled screw compressor chiller 30HXA carrier/R-134a (Cont.)

T_{cd} (°C)	T_{ev} (°C)	$\dot{Q}_{ev}$ (kW)	$\dot{W}_{ideal}$ (kW)	$\dot{W}_{actual}$ (kW)	η_{is}	COP_{carnot}	$COP_{standard}$	COP_{actual}
35	16	296.7	21.6	80.1	27.0	15.2	13.7	3.7
35	16	326.1	23.8	91.0	26.1	15.2	13.7	3.6
35	16	360.9	26.3	102.8	25.6	15.2	13.7	3.5
35	16	419.2	30.5	114.4	26.7	15.2	13.7	3.7
35	16	451.6	32.9	124.4	26.5	15.2	13.7	3.6
35	16	498.3	36.3	133.1	27.3	15.2	13.7	3.7
35	16	535.3	39.0	150.1	26.0	15.2	13.7	3.6
35	16	602.2	43.9	158.7	27.7	15.2	13.7	3.8
35	16	605.9	44.2	163.9	26.9	15.2	13.7	3.7
35	16	647.1	47.2	181.0	26.1	15.2	13.7	3.6
35	16	701.7	51.1	206.4	24.8	15.2	13.7	3.4
35	16	823.5	60.0	210.4	28.5	15.2	13.7	3.9
35	16	954.7	69.6	250.5	27.8	15.2	13.7	3.8
35	16	1000.6	72.9	269.7	27.0	15.2	13.7	3.7
35	16	1051.8	76.6	291.5	26.3	15.2	13.7	3.6
40	16	278.3	26.7	83.7	31.9	12.0	10.4	3.3
40	16	305.8	29.4	95.4	30.8	12.0	10.4	3.2
40	16	338.7	32.5	107.8	30.2	12.0	10.4	3.1
40	16	394.1	37.9	119.9	31.6	12.0	10.4	3.3
40	16	420.8	40.4	129.6	31.2	12.0	10.4	3.2
40	16	469.5	45.1	139.6	32.3	12.0	10.4	3.4
40	16	503.9	48.4	156.9	30.8	12.0	10.4	3.2
40	16	568.5	54.6	166.1	32.9	12.0	10.4	3.4
40	16	587.4	56.4	177.6	31.8	12.0	10.4	3.3
40	16	627.5	60.3	195.8	30.8	12.0	10.4	3.2
40	16	679.4	65.3	222.5	29.3	12.0	10.4	3.1
40	16	799.7	76.8	229.2	33.5	12.0	10.4	3.5
40	16	920.9	88.5	271.4	32.6	12.0	10.4	3.4
40	16	973.9	93.5	293.1	31.9	12.0	10.4	3.3
40	16	1023.1	98.3	316.2	31.1	12.0	10.4	3.2
45	16	259.3	31.3	87.9	35.6	10.0	8.3	2.9
45	16	282.0	34.0	99.5	34.2	10.0	8.3	2.8
45	16	315.0	38.0	112.9	33.7	10.0	8.3	2.8
45	16	368.4	44.5	125.8	35.4	10.0	8.3	2.9
45	16	392.6	47.4	136.1	34.8	10.0	8.3	2.9
45	16	439.4	53.1	146.8	36.1	10.0	8.3	3.0
45	16	470.3	56.8	164.3	34.6	10.0	8.3	2.9
45	16	533.4	64.4	174.3	36.9	10.0	8.3	3.1
45	16	558.1	67.4	191.2	35.2	10.0	8.3	2.9
45	16	601.7	72.6	212.3	34.2	10.0	8.3	2.8
45	16	646.1	78.0	240.7	32.4	10.0	8.3	2.7
45	16	772.2	93.2	248.6	37.5	10.0	8.3	3.1
45	16	888.8	107.3	294.2	36.5	10.0	8.3	3.0
45	16	939.9	113.5	317.5	35.7	10.0	8.3	3.0
45	16	983.7	118.8	341.6	34.8	10.0	8.3	2.9

Table C-3 Water-cooled centrifugal compressor chiller 19DK carrier /R-11

T_{cd} (°C)	T_{ev} (°C)	$\dot{Q}_{ev}$ (kW)	$\dot{W}_{ideal}$ (kW)	$\dot{W}_{actual}$ (kW)	η_{is}	COP_{carnot}	$COP_{standard}$	COP_{actual}
33	5	475	46.12	107.00	43.11	9.93	10.30	4.44
35	5	457	49.36	109.00	45.29	9.27	9.26	4.19
38	5	411	50.04	110.00	45.49	8.43	8.21	3.74
33	5	714	69.33	147.00	47.16	9.93	10.30	4.86
35	5	682	73.66	147.00	50.11	9.27	9.26	4.64
38	5	622	75.73	149.00	50.83	8.43	8.21	4.17
33	5	1041	101.08	208.00	48.60	9.93	10.30	5.00
35	5	978	105.64	209.00	50.54	9.27	9.26	4.68
38	5	872	106.17	209.00	50.80	8.43	8.21	4.17
33	5	1386	134.58	271.00	49.66	9.93	10.30	5.11
35	5	1358	146.68	285.00	51.47	9.27	9.26	4.76
38	5	1308	159.26	301.00	52.91	8.43	8.21	4.35
33	5	1572	152.64	317.00	48.15	9.93	10.30	4.96
35	5	1544	166.77	335.00	49.78	9.27	9.26	4.61
38	5	1445	175.94	330.00	53.31	8.43	8.21	4.38
33	6	495	45.74	109.00	41.96	10.34	10.82	4.54
35	6	450	46.45	101.00	45.99	9.63	9.69	4.46
38	6	433	50.59	109.00	46.41	8.72	8.56	3.97
33	6	732	67.63	147.00	46.01	10.34	10.82	4.98
35	6	700	72.25	146.00	49.49	9.63	9.69	4.79
38	6	651	76.06	148.00	51.39	8.72	8.56	4.40
33	6	1062	98.13	207.00	47.40	10.34	10.82	5.13
35	6	1000	103.22	202.00	51.10	9.63	9.69	4.95
38	6	911	106.44	207.00	51.42	8.72	8.56	4.40
33	6	1456	134.53	280.00	48.05	10.34	10.82	5.20
35	6	1400	144.51	288.00	50.18	9.63	9.69	4.86
38	6	1358	158.67	307.00	51.68	8.72	8.56	4.42
33	6	1656	153.01	329.00	46.51	10.34	10.82	5.03
35	6	1600	165.15	328.00	50.35	9.63	9.69	4.88
38	6	1512	176.66	340.00	51.96	8.72	8.56	4.45
33	7	510	44.77	110.00	40.70	10.78	11.39	4.64
35	7	492	48.47	110.00	44.07	10.01	10.15	4.47
38	7	443	49.63	110.00	45.12	9.04	8.93	4.03
33	7	753	66.10	148.00	44.66	10.78	11.39	5.09
35	7	728	71.73	149.00	48.14	10.01	10.15	4.89
38	7	665	74.50	147.00	50.68	9.04	8.93	4.52
33	7	1094	96.04	208.00	46.17	10.78	11.39	5.26
35	7	1052	103.65	208.00	49.83	10.01	10.15	5.06
38	7	935	104.74	208.00	50.36	9.04	8.93	4.50
33	7	1526	133.96	290.00	46.19	10.78	11.39	5.26
35	7	1484	146.21	292.00	50.07	10.01	10.15	5.08
38	7	1414	158.40	303.00	52.28	9.04	8.93	4.67
33	7	1727	151.61	339.00	44.72	10.78	11.39	5.09
35	7	1685	166.01	341.00	48.68	10.01	10.15	4.94
38	7	1586	177.67	338.00	52.57	9.04	8.93	4.69

Appendix D

Compressor internal power values

Table D-1 CARRIER-30HXC/R134a compressor internal power, $\dot{W}_{in}$ (kW) for different working points before modification

		Model number														
$T_{w_{evi}}$ (°c)	$T_{w_{cnd1}}$ (°c)	076	086	096	106	116	126	136	146	161	171	186	206	246	261	271
4	25	48.99	54.95	60.87	67.53	74.11	80.07	87.42	95.15	64.63	66.06	69.75	85.37	98.98	99.62	103.89
5	25	49.85	55.93	61.98	68.69	75.39	81.39	88.94	96.74	65.75	67.19	71.03	86.94	100.72	101.44	105.77
6	25	50.75	56.86	63.09	69.85	76.67	82.77	90.48	98.31	66.78	68.30	72.17	88.46	102.33	103.12	107.43
7	25	51.66	57.84	64.20	71.00	77.93	84.10	92.01	99.86	72.96	69.36	73.23	89.52	103.85	104.72	109.03
8	25	52.54	58.85	65.32	72.20	79.22	85.41	93.49	101.45	68.71	70.13	74.24	90.19	104.78	106.08	110.56
9	25	53.08	59.68	66.18	73.19	80.06	86.26	94.72	102.68	69.34	70.58	74.88	90.76	105.00	106.28	110.85
10	25	53.52	60.30	66.63	73.87	80.68	87.03	95.32	103.75	69.33	70.87	74.86	91.07	111.97	106.16	110.63
13	25	51.72	58.87	64.20	71.35	78.30	85.41	92.54	101.74	66.09	67.72	70.67	87.29	98.83	99.26	104.77
16	25	45.59	52.02	57.50	63.49	70.08	76.38	82.81	91.00	58.39	59.78	62.92	76.03	87.47	88.34	91.97
4	30	53.58	60.29	66.65	73.91	81.41	88.12	96.18	104.89	70.92	72.64	76.43	93.38	108.28	108.54	113.41
5	30	54.47	61.31	67.88	75.26	82.90	89.64	97.76	106.47	72.33	73.87	77.91	95.23	110.59	110.88	115.71
6	30	55.44	62.37	69.04	76.60	84.38	91.20	99.45	108.33	73.82	75.35	79.41	97.28	112.85	113.16	117.96
7	30	56.52	63.49	70.36	78.06	85.87	92.77	101.26	110.25	75.33	76.82	80.94	99.23	115.16	115.59	120.41
8	30	57.61	64.65	71.72	79.48	87.39	94.36	103.07	112.19	76.74	78.33	82.49	101.33	117.40	117.94	122.77
9	30	58.73	65.89	73.04	80.86	89.02	96.05	105.00	114.15	78.10	79.75	84.02	103.24	119.49	120.16	125.01
10	30	59.83	67.08	74.46	82.34	90.59	97.75	106.87	116.10	79.43	81.12	85.43	105.11	121.49	122.24	127.10
13	30	59.11	66.26	73.35	81.42	90.05	97.32	106.33	116.86	78.47	80.45	83.48	103.30	118.29	117.93	124.76
16	30	52.78	59.96	66.57	73.41	81.77	87.95	96.46	105.97	70.46	72.04	75.76	91.44	106.32	107.00	111.11
4	35	59.00	66.84	73.70	82.07	90.14	97.78	106.80	116.99	79.43	80.73	85.07	102.83	119.66	119.92	125.55
5	35	59.69	67.52	74.52	82.89	91.11	98.76	107.93	118.15	80.41	81.78	86.20	104.29	121.25	121.59	127.26
6	35	60.34	68.30	75.40	84.07	92.20	99.87	109.17	119.36	81.38	82.89	87.30	105.97	122.88	123.25	128.92
7	35	61.18	69.09	76.33	85.02	93.32	101.15	110.44	120.97	82.53	84.16	88.35	107.97	124.80	125.07	130.56
8	35	62.27	70.20	77.67	85.91	94.87	102.75	112.22	122.47	83.52	85.53	89.74	109.93	127.42	127.73	133.14
9	35	63.42	71.43	79.07	87.57	96.73	104.57	114.17	124.24	85.27	87.08	91.54	112.18	130.22	130.42	135.83
10	35	64.64	72.65	80.49	89.26	98.48	106.47	116.15	126.46	87.00	88.81	93.27	114.63	132.91	133.10	138.48
13	35	64.17	71.21	79.74	87.40	97.41	106.52	116.18	126.59	87.05	89.05	92.15	113.12	130.94	129.93	137.63
16	35	57.87	65.85	71.94	80.83	90.21	97.17	106.42	115.49	78.95	80.52	83.33	102.01	118.88	119.01	123.78

Table D-2 CARRIER-30HXC/R134a compressor internal power, $\dot{W}_{in}$ (kW) for different working points after modification

		Model number														
$T_{w_{ev2}}$ (°c)	$T_{w_{cnd1}}$ (°c)	076	086	096	106	116	126	136	146	161	171	186	206	246	261	271
4	25	36.51	39.88	45.73	50.27	54.10	58.44	65.63	69.13	98.12	105.79	113.96	133.48	157.65	166.21	172.73
5	25	37.47	40.98	46.96	51.59	55.54	59.96	67.34	70.94	98.78	106.38	114.67	134.44	158.63	167.13	173.71
6	25	38.46	42.03	48.18	52.88	56.97	61.50	69.05	72.72	99.37	106.98	115.23	135.34	159.48	167.95	174.45
7	25	39.46	43.11	49.40	54.16	58.39	63.01	70.74	74.49	105.97	107.53	115.70	135.76	160.23	168.69	175.14
8	25	40.42	44.22	50.62	55.49	59.82	64.47	72.39	76.27	100.46	107.77	116.15	135.73	160.31	169.18	175.76
9	25	41.08	45.16	51.59	56.62	60.84	65.53	73.80	77.74	100.63	107.62	116.15	135.60	159.59	168.30	174.95
10	25	41.64	45.90	52.21	57.46	61.66	66.51	74.64	79.04	100.07	107.30	115.39	135.15	167.09	167.05	173.54
13	25	40.49	45.20	50.58	55.85	60.30	65.90	72.97	78.24	94.75	101.72	108.34	128.47	148.57	155.64	163.27
16	25	35.45	39.65	45.11	49.44	53.72	58.65	65.02	69.65	84.30	90.51	97.05	113.09	132.45	139.42	144.72
4	30	38.04	41.53	47.81	52.41	56.45	61.13	68.98	72.39	113.59	123.36	132.86	154.66	183.08	193.54	201.21
5	30	39.07	42.71	49.17	53.92	58.14	62.87	70.80	74.26	114.48	123.93	133.64	155.76	184.52	194.73	202.43
6	30	40.16	43.91	50.49	55.45	59.81	64.65	72.70	76.37	115.49	124.82	134.48	157.12	185.90	196.00	203.62
7	30	41.35	45.15	51.93	57.04	61.48	66.41	74.71	78.54	116.55	125.73	135.34	158.32	187.37	197.51	205.08
8	30	42.54	46.44	53.41	58.61	63.19	68.22	76.72	80.71	117.48	126.67	136.26	159.88	188.76	198.92	206.45
9	30	43.74	47.77	54.84	60.14	64.96	70.08	78.82	82.89	118.38	127.55	137.16	161.16	190.06	200.22	207.71
10	30	44.92	49.08	56.35	61.74	66.68	71.93	80.86	85.05	119.27	128.40	137.96	162.40	191.27	201.41	208.86
13	30	44.83	49.01	56.03	61.69	67.09	72.52	81.35	86.89	116.35	125.41	133.24	157.68	184.31	192.64	202.30
16	30	39.70	44.06	50.59	55.28	60.59	65.13	73.43	78.36	105.29	113.35	121.67	141.23	167.04	175.94	182.24
4	35	39.82	43.64	50.40	55.43	59.29	64.36	73.12	76.70	133.33	144.72	156.33	179.98	213.98	226.97	236.33
5	35	40.69	44.56	51.46	56.52	60.55	65.69	74.61	78.27	133.62	144.96	156.55	180.46	214.35	227.29	236.62
6	35	41.54	45.55	52.55	57.90	61.92	67.11	76.14	79.87	133.93	145.29	156.77	181.24	214.81	227.60	236.87
7	35	42.53	46.54	53.68	59.09	63.33	68.69	77.73	81.78	134.51	145.83	156.91	182.41	215.62	228.15	237.14
8	35	43.76	47.81	55.18	60.29	65.12	70.55	79.77	83.67	134.79	146.49	157.48	183.57	217.27	229.71	238.56
9	35	45.01	49.19	56.72	62.09	67.15	72.60	81.94	85.76	136.02	147.39	158.57	185.05	219.17	231.36	240.13
10	35	46.35	50.56	58.28	63.93	69.10	74.70	84.14	88.24	137.26	148.47	159.58	186.80	220.96	232.99	241.67
13	35	46.59	50.05	58.40	63.19	69.18	75.88	85.34	89.75	135.16	146.19	155.39	181.96	214.87	224.92	236.16
16	35	41.60	65.85	52.19	58.23	63.84	68.72	77.72	81.27	123.69	133.65	142.13	165.96	196.98	207.62	215.31

Table D-3 KUO YU-KRS/R22 compressor internal power, $\dot{W}_{in}$ (kW) for different working points

		Model number							
$T_{w_{evp}}$ ($^{\circ}c$)	$T_{w_{cnd}}$ ($^{\circ}c$)	G40	G50	G60	G75	G80	G100	G120	G150
12.5	30	36.51	39.88	45.73	50.27	54.10	58.44	65.63	69.13
10	30	37.47	40.98	46.96	51.59	55.54	59.96	67.34	70.94
7.5	30	38.46	42.03	48.18	52.88	56.97	61.50	69.05	72.72
5	30	39.46	43.11	49.40	54.16	58.39	63.01	70.74	74.49
12.5	35	38.04	41.53	47.81	52.41	56.45	61.13	68.98	72.39
10	35	39.07	42.71	49.17	53.92	58.14	62.87	70.80	74.26
7.5	35	40.16	43.91	50.49	55.45	59.81	64.65	72.70	76.37
5	35	41.35	45.15	51.93	57.04	61.48	66.41	74.71	78.54
12.5	40	39.82	43.64	50.40	55.43	59.29	64.36	73.12	76.70
10	40	40.69	44.56	51.46	56.52	60.55	65.69	74.61	78.27
7.5	40	41.54	45.55	52.55	57.90	61.92	67.11	76.14	79.87
5	40	42.53	46.54	53.68	59.09	63.33	68.69	77.73	81.78
12.5	45	43.76	47.81	55.18	60.29	65.12	70.55	79.77	83.67
10	45	45.01	49.19	56.72	62.09	67.15	72.60	81.94	85.76
7.5	45	46.35	50.56	58.28	63.93	69.10	74.70	84.14	88.24
5	45	46.59	50.05	58.40	63.19	69.18	75.88	85.34	89.75

Appendix E

Computer program of the modified model for the identification of screw chiller

```
/*************************************************************************
*                                ASHRAE TOOLKIT-I                       *
*                            IDENTIFICATION PROGRAM                     *
*                                                                       *
*                                                                       *
*                           SCREW COMPRESSOR CHILLER                    *
*                                                                       *
*                                                                       *
*                                                                       *
*                                                                       *
*                                WRIITTEN IN C++                        *
*                                AND MODIFIED                           *
*                                    BY                                 *
*                                BABAK SOLATI                           *
*                                WINTER 2001                            *
*************************************************************************/


/****************************** Main Program ******************************/


/*
  Input variables

  Qevap[]    : Evaporator capacity (W)
  Wcomp[]    : Compressor input power (W)
  Mflwev[]   : Evaporator water flow rate (l/s)
  Mflwcd[]   : Condenser water flow rate (l/s)
  Twev       : Evaporator exhaust water temperature (K)
  Twcd       : Condenser supply water temperature (K)
  N          : Number of working points

  Internal variables

  Qev[]      : Evaporator Capacity (W)
  Qcd[]      : Condenser heat rejection (W)
  Mwev       : Evaporator water flow rate (l/s)
  Mwcd       : Condenser water flow rate (l/s)
  Qev_avg    : Average evaporator capacity (W)
  Qcd_avg    : Average condenser heat rejection (W)
  Mwev_avg   : Average evaporator water flow rate (l/s)
  Mwcd_avg   : Average condenser water flow rate (l/s)
  Effev      : Average evaporator effectiveness
  Effcd      : Average condenser effectiveness
  EffevMean  : Mean evaporator effectiveness
  EffcdMean  : Mean condenser effectiveness
  Tev[]      : Evaporating temperature (K)
  Tcd[]      : Condensing temperature (K)

  Thermodynamic parameters

  Gamma   : Isentropic coefficient
  AC1     : First coefficient in Clausius-Clapeyron equation
  BC1     : Second coefficient in Clausius-Clapeyron equation
  CPwat   : water specific heat (J/kg/K)
  hfo     : Enthalpy of saturated liquid at reference temperature (J/kg)
```

```
 hfgo     : Enthalpy of vaporization at the reference temperature (J/kg)
 cpvap    : Mean specific heat at constant pressure in superheated vapor state (J/kg/K)
 r        : Gas constant (J/kg/K)
 cpliq    : Mean specific heat in saturated liquid state (J/kg/K)
 Zetta    : Mean compressibility factor
 To       : Reference temperature (273.15 K)
 Pevap    : Evaporating pressure (pa)
 Pcond    : Condensing pressure (pa)
 h1       : Enthalpy of refrigerant leaving the evaporator (J/kg/K)
 h3       : Enthalpy of the refrigerant leaving the condenser (J/kg/K)
 Mfrref   : Mass flow rate of the refrigerant (kg/s)
 Pratio   : External pressure ratio
 T1p      : Temperature of the refrigerant after heating up (K)
 V1p      : Specific volume of the refrigerant after heating up (m3/kg)
 X[]      : leaking refrigerant speed (m/s)
 Y[]      : Volumetric flow rate of the refrigerant before compression (m3/s)

 Outputs

 UAev     : Evaporator overall heat transfer coefficient (W/K)
 UAcd     : Condenser overall heat transfer coefficient (W/K)
 Win[]    : Internal power (W)
 Alld     : Leakage area (m2)
 VsFl     : Volumetric flow rate of the refrigerant (m3/s)
 Alphald  : Coefficient of variable electro-mechanical losses
 Lossld   : Constant of electro-mechanical losses (W)

*/


//****************************** Main Program ********************************

#include <iostream.h>
#include <fstream.h>
#include <math.h>

void main()
{

 ifstream fin;
 ofstream fout;

// Variable declaration

 double Qevap[100],Qcond[100],Wcomp[100],Mflwev[100],Mflwcd[100],Twev[100];
 double Twcd[100],Tev[100],Tcd[100],Qev,Qcd,Mwev,Mwcd;
 double CPwat,Qev_avg,Qcd_avg,Mwev_avg,Mwcd_avg,Gamma;
 double EffevMean,EffcdMean,Effev,Effcd,AUev,AUcd,Ac1,Bc1,Pevap,Pcond;
 double T1,T3,To,h1,h3;
 double hfo,hfgo,cpvap,r,cpliq,Zetta,MfrRef,Pratio,T1p,T1pp,Err,Err1 ;
 double Alid, Alp,X[100],Y[100],Win[100],VsFl,V1p ;
 double sum1,sum2,sum3,sum4,sum5,sum6,sum7,sum8,Iter1,Iter2 ;
 double Alphald,Lossld ;
 int   N,i,j ;
```

```
// Thermodynamic properties of R134a

Gamma = 1.072 ;
Acl = 15.489 ;
Bcl = -2681.99 ;
CPwat = 4187 ;
hfo = 200000 ;
hfgo = 197900 ;
cpvap = 892.5 ;
r = 81.4899 ;
cpliq = 1265 ;
To = 273.15 ;
Zetta = 0.9411 ;

// tool-076.inp is the input file that contains the data of all working points.
// tool-076.txt is the output file that all the output will be saved in.

fin.open("tool-076.inp");
fout.open("tool-076.txt");

// Reading the inputs from the input file

fin>>N ;
cout<<N<<endl;

for (i=1 ; i<=N ; i++)
{
fin>>Qevap[i]>>Wcomp[i];
// cout<<Qevap[i]<<"  "<<Wcomp[i]<<endl;
// fout<<Qevap[i]<<"  "<<Wcomp[i]<<endl;
}

for (j=1 ; j<=N ; j++)
{
fin>>Mflwev[j]>>Mflwcd[j]>>Twev[j]>>Twcd[j];
// cout<<Mflwev[j]<<"  "<<Mflwcd[j]<<endl<<Twev[j]<<"  "<<Twcd[j]<<endl;
// fout<<Mflwev[j]<<"  "<<Mflwcd[j]<<endl<<Twev[j]<<"  "<<Twcd[j]<<endl;
}

// Initializing the variables

Alid = 0.000001 ;
Qev=0 ;
Qcd=0 ;
Mwev=0 ;
Mwcd=0 ;

// Calculating the average value of the evaporator capacity, condenser heat rejection,
// evaporator and condenser water flow rate.

for (i=1 ; i<=N ; i++)
{
        Qev = Qev + Qevap[i] ;
        Qcond[i] = Qevap[i] + Wcomp[i] ;
        Qcd = Qcd + Qevap[i] + Wcomp[i] ;
        Mwev = Mwev + Mflwev[i] ;
```

```
        Mwcd = Mwcd + Mflwcd[i] ;
}


Qev_avg = Qev/N ;
Qcd_avg = Qcd/N ;
Mwev_avg = Mwev/N ;
Mwcd_avg = Mwcd/N ;

// Calculating the mean condenser and evaporator effectiveness

EffevMean = 1/(1+CPwat*Mwev_avg*5/Qev_avg) ;
EffcdMean = 1/(1+CPwat*Mwcd_avg*5/Qcd_avg) ;

// Calculating the evaporator and consdenser overall heat transfer coefficient
// based on their mean effectivenesses.

AUev = 1000*(int(-CPwat*Mwev_avg*log(1-EffevMean)/1000)) ;
AUcd = 1000*(int(-CPwat*Mwcd_avg*log(1-EffcdMean)/1000)) ;

// Sending the overall heat transfer coefficients into the output file

fout<<"AUev = "<<AUev<<"  ";
fout<<"AUcd = "<<AUcd<<endl ;

// Calculating the condenser and evaporator effectiveness for each working point

for (i=1 ; i<=N ; i++)
{
        Effev = 1 - exp(-AUev/(CPwat*Mflwev[i])) ;
        Effcd = 1 - exp(-AUcd/(CPwat*Mflwcd[i])) ;

/*
 Calculatin the evaporating and condensing temperature

 Equations to be used when the supply water temperature is known for both
 evaporator and condenser

        Tev[i] = Twev[i]-Qevap[i]/(Effev*CPwat*Mflwev[i]) ;
        Tcd[i] = Twcd[i]+Qcond[i]/(Effcd*CPwat*Mflwcd[i]) ;

 Equations to be used when the water temperature is known at the evaporator
 supply and at the condenser exhaust

   Tev[i] = Twev[i]-Qevap[i]/(Effev*CPwat*Mflwev[i]) ;
   Tcd[i] = Twcd[i]+Qcond[i]*(1/Effcd-1)/(CPwat*Mflwcd[i]) ;

 Equations to be used when the exhaust water temperature is known for both
 evaporator and condenser

   Tev[i] = Twev[i]+Qevap[i]*(1-1/Effev)/(CPwat*Mflwev[i]) ;
   Tcd[i] = Twcd[i]+Qcond[i]*(1/Effcd-1)/(CPwat*Mflwcd[i]) ;

 Equations to be used when the water temperature is known at the evaporator exhaust
 and at the condenser supply.
*/
```

```
   Tev[i] = Twev[i]+Qevap[i]*(1-1/Effev)/(CPwat*Mflwev[i]) ;
   Tcd[i] = Twcd[i]+Qcond[i]/(Effcd*CPwat*Mflwcd[i]) ;
}

double Gm1G = (Gamma-1)/Gamma ;

// Starting the iteration to calculate Alid

Iter1 = 0 ;
do
{
Iter1 = Iter1 + 1 ;
sum1=0 ;
sum2=0 ;
sum3=0 ;
sum4=0 ;
sum5=0 ;
sum6=0 ;
sum7=0 ;
sum8=0 ;

// Calculating the required thermodynamic properties of the refrigerant

for (i=1 ; i<=N ; i++ )
{
        Pevap = 1000*exp(Ac1+Bc1/Tev[i]) ;
        Pcond = 1000*exp(Ac1+Bc1/Tcd[i]) ;

        T1 = Tev[i] ;
        T3 = Tcd[i] ;

        h1 = hfo + hfgo + cpvap*(T1-To) ;
        h3 = hfo + cpliq*(T3 - To) ;

        MfrRef = Qevap[i]/(h1-h3) ;
        Pratio = Pcond/Pevap ;

// Starting the iteration to calculate T1p

        T1p = T1 ;
   Iter2=0 ;
   Err = 1 ;

        while (Err>0.0001 && Iter2<100)
        {
        V1p = Zetta*r*T1p/Pevap ;
        Y[i] = MfrRef*V1p ;
        double A = Pevap*V1p ;
        double B = (Gamma+1)/(2*Gamma) ;
        double C = 2/(Gamma+1) ;
        double D = (Gamma+1)/(Gamma-1) ;
        double E = Gamma*pow(C,D) ;
        X[i] = sqrt(Pevap*V1p)*pow(Pratio,B)*sqrt(E) ;
        VsFl = Y[i] + Alid * X[i] ;
        Win[i] = Pevap*VsFl*(pow(Pratio,Gm1G)-1)/Gm1G ;
        T1pp=T1p ;
```

```
        T1p = T1 + (Wcomp[i]-Win[i])/(MfrRef*cpvap) ;
        Err = ((T1p-T1pp)/T1pp) ;
        if(Err<0)
                Err=-Err ;
  Iter2 = Iter2 + 1 ;
        }

// Statistical calcualtion to identifiy Alid, VsFl, Alphald and Lossld

sum1 = sum1 + X[i] ;
sum2 = sum2 + Y[i] ;
sum3 = sum3 + pow(X[i],2) ;
sum4 = sum4 + X[i]*Y[i] ;
sum5 = sum5 + Wcomp[i] ;
sum6 = sum6 + Win[i] ;
sum7 = sum7 + pow(Win[i],2) ;
sum8 = sum8 + Wcomp[i]*Win[i] ;

}

Alp = Alid ;
VsFl =(sum1*sum4-sum2*sum3)/(pow(sum1,2)-N*sum3) ;
Alid = -(N*sum4-sum2*sum1)/(pow(sum1,2)-N*sum3) ;
Alphald = (sum5*sum6-N*sum8)/(pow(sum6,2)-N*sum7)-1 ;
Lossld = (sum5-(1+Alphald)*sum6)/N ;

Err1 = ((Alid-Alp)/Alp) ;
     if(Err1<0)
                Err1=-Err1 ;
}

while (Err1>0.0001 && Iter1<100) ;
for (i=1 ; i<=N ; i++)
{
fout<<"Win"<<i<<"="<<Win[i]<<"    Wcomp="<<Wcomp[i]<<endl ;
cout<<"Win"<<i<<"="<<Win[i]<<"    Wcomp="<<Wcomp[i]<<endl ;
}

fout<<"Lossld="<<Lossld<<endl;
fout<<"Alphald="<<Alphald<<endl;
fout<<"VsFl="<<VsFl<<endl;
fout<<"Alld="<<Alp<<endl ;

return ;
}
```

Appendix F

Full load and part load simulation results

Table F-1 30HXC/R-134a carrier screw-compressor full load simulation results

Model	$\dot{Q}_{ev}$ (kW)	$T_{w_{ev1}}$ (°C)	$T_{w_{cd1}}$ (°C)	COP (toolkit)	COP (actual)	Identified Parameters						
						$\dot{Q}_{ev}$ Nom. kW)	UA_{ev} (kW/K)	UA_{cd} (kW/K)	$\dot{W}_{lo}$ (kW)	α	$\dot{V}_s$ (m^3/s)	A_l (cm^2)
076	253.3	4	25	3.95	5.26	264	36	44	8.25	0.143929	0.14043	0. 611
	264.0	5	25	4.06	5.43							
	274.8	6	25	4.17	5.57							
	285.8	7	25	4.28	5.72							
	297.0	8	25	4.40	5.88							
	307.1	9	25	4.51	6.03							
	316.8	10	25	4.63	6.19							
	333.2	13	25	4.98	6.47							
	330.1	16	25	5.34	6.42							
	234.3	4	30	3.38	4.40							
	244.2	5	30	3.47	4.58							
	254.6	6	30	3.57	4.70							
	265.5	7	30	3.66	4.85							
	276.7	8	30	3.75	5.02							
	288.1	9	30	3.81	5.18							
	299.5	10	30	3.94	5.32							
	318.8	13	30	4.23	5.54							
	315.2	16	30	4.51	5.50							
	219.0	4	35	2.92	3.72							
	227.2	5	35	2.99	3.83							
	235.6	6	35	3.08	3.95							
	244.7	7	35	3.14	4.07							
	254.9	8	35	3.22	4.20							
	265.4	9	35	3.30	4.33							
	276.5	10	35	3.38	4.47							
	295.3	13	35	3.38	4.75							
	291.7	16	35	3.85	4.66							
086	279.3	4	25	3.76	5.15	300	40	48	6.88	0.228645	0.15718	0.732
	291.1	5	25	3.86	5.32							
	303.0	6	25	3.97	5.48							
	315.0	7	25	4.08	5.61							
	327.4	8	25	4.18	5.75							
	339.3	9	25	4.29	5.90							
	350.6	10	25	4.40	6.06							
	371.6	13	25	4.74	6.35							
	368.2	16	25	5.08	6.21							
	258.8	4	30	3.20	4.33							
	269.7	5	30	3.28	4.47							
	281.0	6	30	3.37	4.61							
	292.7	7	30	3.46	4.76							
	305.0	8	30	3.54	4.92							
	317.5	9	30	3.63	5.08							
	330.2	10	30	3.72	5.22							
	351.4	13	30	4.00	5.43							
	350.8	16	30	4.26	5.43							
	242.8	4	35	2.74	3.66							
	251.8	5	35	2.81	3.78							
	261.1	6	35	2.88	3.89							
	270.7	7	35	2.95	4.00							
	281.6	8	35	3.03	4.13							
	293.1	9	35	3.10	4.25							
	305.0	10	35	3.18	4.39							
	322.0	13	35	3.39	4.57							
	291.7	16	35	3.61	4.61							

Table F-1 30HXC/134a carrier screw-compressor full load simulation results (Cont.)

Model	$\dot{Q}_{ev}$ (kW)	$T_{w_{ev1}}$ (°C)	$T_{w_{cd1}}$ (°C)	COP (toolkit)	COP (actual)	Identified Parameters						
						$\dot{Q}_{ev}$ Nom.(kW)	UA_{ev} (kW/K)	UA_{cd} (kW/K)	$\dot{W}_{lo}$ (kW)	α	$\dot{V}_s$ (m^3/s)	A_l (cm^2)
096	315.5	4	25	3.95	5.25	335	45	54	6.87	0.202624	0.17452	0.738
	328.8	5	25	4.06	5.42							
	342.1	6	25	4.17	5.56							
	355.7	7	25	4.28	5.71							
	369.8	8	25	4.39	5.87							
	382.7	9	25	4.50	6.02							
	394.6	10	25	4.62	6.18							
	414.1	13	25	4.96	6.44							
	414.4	16	25	5.31	6.44							
	292.4	4	30	3.37	4.40							
	304.8	5	30	3.45	4.54							
	317.5	6	30	3.54	4.69							
	330.9	7	30	3.63	4.84							
	344.8	8	30	3.72	5.01							
	359.9	9	30	3.81	5.19							
	373.1	10	30	3.90	5.31							
	396.1	13	30	4.18	5.52							
	396.5	16	30	4.46	5.53							
	274.3	4	35	2.89	3.72							
	284.5	5	35	2.96	3.83							
	295.0	6	35	3.03	3.94							
	305.9	7	35	3.11	4.07							
	318.5	8	35	3.18	4.20							
	331.5	9	35	3.26	4.33							
	345.0	10	35	3.33	4.47							
	367.5	13	35	3.56	4.69							
	363.2	16	35	3.78	4.65							
106	350.4	4	25	3.83	5.19	370	51	61	3.18	0.310862	0.19372	0.847
	365.2	5	25	3.94	5.38							
	380.0	6	25	4.04	5.54							
	395.0	7	25	4.15	5.69							
	410.5	8	25	4.26	5.85							
	425.6	9	25	4.37	6.01							
	439.6	10	25	4.48	6.18							
	462.7	13	25	4.82	6.49							
	461.4	16	25	5.16	6.47							
	323.9	4	30	3.23	4.33							
	337.9	5	30	3.31	4.48							
	352.4	6	30	3.40	4.62							
	367.3	7	30	3.48	4.78							
	382.6	8	30	3.57	4.95							
	398.2	9	30	3.66	5.12							
	414.1	10	30	3.75	5.28							
	441.4	13	30	4.02	5.52							
	439.8	16	30	4.29	5.50							
	304.3	4	35	2.75	3.64							
	315.4	5	35	2.82	3.78							
	326.9	6	35	2.89	3.78							
	338.8	7	35	2.96	3.90							
	352.2	8	35	3.03	4.12							
	367.1	9	35	3.10	4.26							
	382.5	10	35	3.18	4.40							
	404.1	13	35	3.40	4.60							
	408.0	16	35	3.61	4.64							

Table F-1 30HXC carrier screw-compressor full load simulation results (Cont.)

Model	$\dot{Q}_{ev}$ (kW)	$T_{w_{ev2}}$ (°C)	$T_{w_{cd1}}$ (°C)	COP (toolkit)	COP (actual)	Identified Parameters						
						$\dot{Q}_{ev}$ Nom. (kW)	UA_{ev} (kW/K)	UA_{cd} (kW/K)	$\dot{W}_{lo}$ (kW)	α	$\dot{V}_s$ (m^3/s)	A_l (cm^2)
116	380.9	4	25	3.84	5.31	405	55	66	5 39	0.254628	0 21284	0 980
	396.9	5	25	3.94	5.50							
	413.0	6	25	4.05	5.66							
	429.4	7	25	4.16	5.82							
	410.5	8	25	4.26	5.99							
	461.5	9	25	4.38	6.16							
	476.2	10	25	4.49	6.34							
	503.0	13	25	4.83	6.68							
	503.5	16	25	5.18	6.70							
	352.8	4	30	3.25	4.43							
	368.2	5	30	3.34	4.58							
	383.9	6	30	3.42	4.74							
	400.0	7	30	3.51	4.91							
	416.7	8	30	3.60	5.08							
	433.7	9	30	3.69	5.25							
	450.9	10	30	3.78	5.41							
	482.5	13	30	4.06	5.67							
	483.2	16	30	4.33	5.68							
	330.6	4	35	2.78	3.72							
	342.8	5	35	2.85	3.83							
	355.4	6	35	2.92	3.93							
	369.2	7	35	3.00	4.09							
	384.6	8	35	3.06	4.23							
	401.0	9	35	3.14	4.37							
	417.7	10	35	3.21	4.53							
	444.8	13	35	3.44	4.77							
	449.3	16	35	3.66	4.81							
126	412.5	4	25	3.87	5.30	440	60	72	4 91	0 274017	0 23039	1 062
	429.7	5	25	3.98	5.42							
	447.2	6	25	4.08	5.65							
	465.0	7	25	4.19	5.81							
	482.7	8	25	4.30	5.97							
	499.3	9	25	4.41	6.15							
	515.7	10	25	4.53	6.33							
	549.3	13	25	4.87	6.72							
	549.5	16	25	5.22	6.72							
	382.6	4	30	3.27	4.41							
	399.0	5	30	3.35	4.57							
	415.9	6	30	3.44	4.73							
	433.2	7	30	3.53	4.89							
	451.2	8	30	3.62	5.07							
	469.5	9	30	3.71	5.23							
	488.1	10	30	3.80	5.99							
	523.1	13	30	4.08	6.39							
	522.1	16	30	4.35	6.39							
	359.0	4	35	2.79	3.71							
	372.1	5	35	2.86	3.82							
	385.7	6	35	2.93	3.93							
	400.9	7	35	3.00	4.08							
	417.2	8	35	3.07	4.22							
	434.6	9	35	3.15	4.36							
	452.5	10	35	3.22	4.51							
	486.7	13	35	3.45	4.79							
	485.7	16	35	3.67	4.78							

Table F-1 30HXC carrier screw-compressor full load simulation results (Cont.)

Model	$\dot{Q}_{ev}$ (kW)	$T_{w_{ev1}}$ (°C)	$T_{w_{cd1}}$ (°C)	COP (toolkit)	COP (actual)	Identified Parameters						
						$\dot{Q}_{ev}$ Nom. (kW)	UA_{ev} (kW/K)	UA_{cd} (kW/K)	$\dot{W}_{in}$ (kW)	α	$\dot{V}_s$ (m^3/s)	A_l (cm^2)
136	457.2	4	25	3.98	5.23	475	67	80	9.56	0.210964	0.25230	1.073
	476.5	5	25	4.09	5.41							
	495.8	6	25	4.19	5.56							
	515.5	7	25	4.31	5.74							
	535.7	8	25	4.42	5.86							
	554.9	9	25	4.54	6.02							
	572.0	10	25	4.66	6.18							
	604.3	13	25	5.01	6.48							
	604.9	16	25	5.37	6.49							
	425.0	4	30	3.38	4.40							
	442.8	5	30	3.48	4.56							
	461.3	6	30	3.56	4.71							
	480.7	7	30	3.65	4.87							
	500.7	8	30	3.74	5.04							
	521.4	9	30	3.84	5.21							
	541.9	10	30	3.93	5.35							
	580.0	13	30	4.22	5.59							
	580.7	16	30	4.50	5.60							
	400.3	4	35	2.90	3.74							
	415.1	5	35	2.97	3.86							
	430.3	6	35	3.04	3.98							
	480.7	7	35	3.12	4.10							
	464.2	8	35	3.20	4.24							
	483.1	9	35	3.27	4.37							
	502.6	10	35	3.35	4.51							
	540.2	13	35	3.59	4.78							
	540.9	16	35	3.82	4.79							
146	489.2	4	25	3.79	5.17	510	72	86	7.87	0.276929	0.27425	1.279
	509.7	5	25	3.90	5.35							
	530.4	6	25	4.00	5.51							
	551.5	7	25	4.11	5.67							
	573	8	25	4.22	5.84							
	593.6	9	25	4.33	6.00							
	613.8	10	25	4.44	6.16							
	653.5	13	25	4.79	6.54							
	653.8	16	25	5.13	6.54							
	454.2	4	30	3.21	4.34							
	472.9	5	30	3.29	4.49							
	493	6	30	3.38	4.64							
	514	7	30	3.46	4.80							
	500.7	8	30	3.55	4.97							
	557.2	9	30	3.64	5.14							
	579.2	10	30	3.73	5.29							
	626.2	13	30	4.01	5.60							
	626.6	16	30	4.28	5.60							
	428.3	4	35	2.74	3.67							
	443.9	5	35	2.81	3.78							
	460.1	6	35	2.88	3.91							
	477	7	35	2.95	3.97							
	495.5	8	35	3.02	4.12							
	515.4	9	35	3.09	4.30							
	536.8	10	35	3.17	4.44							
	577.9	13	35	3.39	4.72							
	576.7	16	35	3.61	4.71							

Table F-2 30HXC/R-134a carrier screw-compressor part load simulation results

$T_{w_{cd1}}$ (°C)	$T_{w_{ev2}}$ (°C)	PLR	COP_{PL}							
			076	086	096	106	116	126	136	146
25	4	0.3	3.74	3.64	3.78	3.73	3.77	3.76	3.75	3.65
25	4	0.4	4.50	4.39	4.53	4.49	4.55	4.54	4.50	4.41
25	4	0.5	4.96	4.86	4.99	4.95	5.03	5.03	4.96	4.88
25	4	0.6	5.23	5.13	5.25	5.21	5.31	5.30	5.22	5.15
25	4	0.8	5.38	5.28	5.39	5.34	5.45	5.44	5.36	5.30
25	4	0.9	5.34	5.24	5.34	5.29	5.41	5.40	5.32	5.26
30	4	0.3	2.99	2.90	3.01	2.96	2.98	2.97	3.01	2.91
30	4	0.4	3.61	3.53	3.64	3.58	3.62	3.61	3.63	3.54
30	4	0.5	4.02	3.94	4.04	3.98	4.04	4.03	4.04	3.95
30	4	0.6	4.26	4.19	4.28	4.22	4.30	4.28	4.28	4.20
30	4	0.8	4.45	4.37	4.45	4.39	4.48	4.46	4.46	4.38
30	4	0.9	4.44	4.37	4.44	4.38	4.47	4.46	4.45	4.38
35	4	0.3	2.43	2.36	2.50	2.39	2.40	2.40	2.46	2.37
35	4	0.4	2.95	2.89	3.28	2.91	2.94	2.94	2.99	2.90
35	4	0.5	3.31	3.25	3.85	3.26	3.30	3.25	3.34	3.26
35	4	0.6	3.53	3.47	4.23	3.47	3.53	3.52	3.56	3.48
35	4	0.8	3.72	4.30	4.61	3.65	3.73	3.72	3.75	3.68
35	4	0.9	3.74	3.68	4.67	3.66	3.74	3.73	3.76	3.69
25	5	0.3	3.82	3.81	3.97	3.93	3.96	3.95	3.94	3.83
25	5	0.4	4.57	4.60	4.75	4.72	4.77	4.75	4.72	4.62
25	5	0.5	5.04	5.08	5.22	5.20	5.27	5.25	5.19	5.11
25	5	0.6	5.30	5.35	5.48	5.46	5.34	5.52	5.46	5.38
25	5	0.8	5.45	5.48	5.59	5.56	5.67	5.64	5.58	5.51
25	5	0.9	5.41	5.42	5.53	5.49	5.61	5.58	5.52	5.46
30	5	0.3	3.27	3.03	3.15	3.10	3.13	3.12	3.15	3.05
30	5	0.4	3.94	3.68	3.80	3.74	3.80	3.79	3.80	3.70
30	5	0.5	4.37	4.10	4.21	4.15	4.22	4.22	4.21	4.13
30	5	0.6	4.62	4.36	4.46	4.40	4.48	4.47	4.46	4.38
30	5	0.8	4.78	4.63	4.62	4.56	4.65	4.64	4.63	4.56
30	5	0.9	4.76	4.52	4.60	4.54	4.64	4.63	4.61	4.54
35	5	0.3	2.53	2.45	2.62	2.48	2.50	2.50	2.56	2.47
35	5	0.4	3.07	3.00	3.44	3.02	3.06	3.05	3.11	3.02
35	5	0.5	3.43	3.37	4.03	3.38	3.43	3.42	3.47	3.38
35	5	0.6	3.66	3.60	4.42	3.60	3.66	3.65	3.70	3.61
35	5	0.8	3.84	3.79	4.80	3.77	3.85	3.84	3.88	3.80
35	5	0.9	3.86	3.80	4.86	3.78	3.86	3.85	3.89	3.81
25	6	0.3	4.10	3.99	4.13	4.12	4.15	4.14	4.11	4.02
25	6	0.4	4.90	4.80	4.93	4.93	4.99	4.98	4.91	4.83
25	6	0.5	5.36	5.29	5.41	5.42	5.49	5.49	5.39	5.33
25	6	0.6	5.65	5.56	5.67	5.68	5.77	5.77	5.65	5.60
25	6	0.8	5.75	5.66	5.76	5.75	5.86	5.86	5.75	5.70
25	6	0.9	5.68	5.59	5.68	5.67	5.78	5.78	5.68	5.63
30	6	0.3	3.13	3.18	3.30	3.25	3.28	3.27	3.30	3.20
30	6	0.4	3.77	3.85	3.97	3.92	3.98	3.97	3.98	3.88
30	6	0.5	4.19	4.28	4.39	4.34	4.42	4.41	4.40	4.31
30	6	0.6	4.44	4.54	4.64	4.58	4.68	4.66	4.65	4.56
30	6	0.8	4.61	4.70	4.79	4.73	4.84	4.82	4.80	4.73
30	6	0.9	4.60	4.68	4.76	4.70	4.81	4.80	4.77	4.70
35	6	0.3	2.63	2.74	2.76	2.53	2.59	2.59	2.68	2.57
35	6	0.4	3.19	3.35	3.61	3.07	3.16	3.17	3.24	3.14
35	6	0.5	3.56	3.75	4.22	3.43	3.54	3.54	3.61	3.52
35	6	0.6	3.79	4.00	4.63	3.65	3.77	3.78	3.84	3.75
35	6	0.8	3.97	4.20	5.00	3.81	3.96	3.96	4.02	3.94
35	6	0.9	3.98	4.20	5.04	3.82	3.96	3.93	4.02	3.94

Table F-2 30HXC/R-134a carrier screw-compressor part load simulation results (Cont.)

$T_{w_{cd1}}$ (°C)	$T_{w_{ev2}}$ (°C)	PLR	COP_{PL}							
			076	086	096	106	116	126	136	146
25	7	0.3	4.27	4.15	4.31	4.30	4.34	4.33	4.29	4.20
25	7	0.4	5.09	5.99	5.14	5.14	5.20	5.20	5.11	5.05
25	7	0.5	5.58	5.49	5.62	5.64	5.72	5.72	5.61	5.55
25	7	0.6	5.84	5.75	5.88	5.89	5.99	5.98	5.86	5.82
25	7	0.8	5.92	5.83	5.94	5.93	6.05	6.05	5.93	5.89
25	7	0.9	5.84	5.74	5.84	5.84	5.96	5.95	5.84	5.81
30	7	0.3	3.43	3.32	3.46	3.41	3.45	3.44	3.46	3.36
30	7	0.4	4.12	4.02	4.16	4.11	4.18	4.16	4.16	4.07
30	7	0.5	4.56	4.47	4.59	4.54	4.63	4.62	4.60	4.51
30	7	0.6	4.81	4.72	4.83	4.78	4.88	4.87	4.84	4.76
30	7	0.8	4.96	4.87	4.96	4.91	5.03	5.02	4.98	4.91
30	7	0.9	4.93	4.84	4.93	4.87	4.99	4.98	4.94	4.88
35	7	0.3	2.74	2.66	2.94	2.64	2.73	2.72	2.79	3.64
35	7	0.4	3.32	3.25	3.80	3.20	3.33	3.32	3.37	3.22
35	7	0.5	3.70	3.63	4.43	3.57	3.72	3.71	3.75	3.60
35	7	0.6	3.93	3.87	4.84	3.79	3.96	3.95	3.98	3.83
35	7	0.8	4.11	4.04	5.22	3.95	4.13	4.12	4.15	4.00
35	7	0.9	4.11	4.04	5.25	3.94	4.13	4.12	4.15	4.00
25	8	0.3	4.47	4.33	4.51	4.50	4.54	4.53	4.48	4.40
25	8	0.4	5.32	5.19	5.36	5.37	5.44	5.43	5.33	5.27
25	8	0.5	5.82	5.69	5.86	5.87	5.96	5.95	5.82	5.77
25	8	0.6	6.07	5.95	6.10	6.11	6.23	6.21	6.07	6.05
25	8	0.8	6.12	6.00	6.13	6.13	6.26	6.24	6.11	6.09
25	8	0.9	6.02	5.90	6.02	6.01	6.15	6.24	6.01	5.99
30	8	0.3	3.61	3.49	3.64	3.58	3.63	6.13	3.64	3.53
30	8	0.4	4.33	4.22	4.36	4.31	4.38	3.62	4.37	4.27
30	8	0.5	4.77	4.67	4.80	4.75	4.85	4.37	4.81	4.73
30	8	0.6	5.02	4.92	5.04	4.99	5.10	4.84	5.06	4.98
30	8	0.8	5.15	4.32	5.16	5.10	5.23	5.09	5.18	5.11
30	8	0.9	5.11	5.00	5.11	5.05	5.18	5.22	5.13	5.06
35	8	0.3	2.86	2.78	3.08	2.82	2.86	5.16	2.91	2.77
35	8	0.4	3.47	3.39	4.01	3.42	3.48	2.85	3.52	3.38
35	8	0.5	3.85	3.78	4.66	3.81	3.88	3.48	3.91	3.77
35	8	0.6	4.08	4.01	5.09	4.03	4.13	3.88	4.14	4.00
35	8	0.8	4.25	4.18	5.45	4.19	4.29	4.11	4.30	4.17
35	8	0.9	4.25	4.18	5.47	4.17	4.28	4.28	4.29	4.16
25	9	0.3	4.84	4.51	4.70	4.71	4.75	4.27	4.68	4.59
25	9	0.4	5.75	5.40	5.58	5.61	5.68	5.67	5.56	5.50
25	9	0.5	6.26	5.91	6.08	6.11	6.21	6.20	6.06	6.02
25	9	0.6	6.50	6.16	6.31	6.35	6.47	6.46	6.30	6.28
25	9	0.8	6.49	6.18	6.31	6.33	6.47	6.46	6.31	6.29
25	9	0.9	6.36	6.06	6.18	6.19	6.34	6.33	6.19	6.16
30	9	0.3	3.78	3.66	3.82	3.77	3.81	3.80	3.83	3.71
30	9	0.4	4.53	4.42	4.57	4.53	4.60	4.58	4.58	4.48
30	9	0.5	4.98	4.88	5.02	4.98	5.07	5.05	5.04	4.95
30	9	0.6	5.23	5.13	5.26	5.22	5.32	5.31	5.29	5.20
30	9	0.8	5.34	5.24	5.35	5.31	5.43	5.41	5.38	5.31
30	9	0.9	5.28	5.18	5.29	5.24	5.36	5.34	5.32	5.25
35	9	0.3	2.99	2.90	3.26	2.96	3.00	2.99	3.05	2.93
35	9	0.4	3.61	3.53	4.23	3.58	3.65	3.64	3.68	3.57
35	9	0.5	4.01	3.93	4.91	3.98	4.06	4.05	4.07	3.98
35	9	0.6	4.24	4.39	5.34	4.20	4.30	4.29	3.96	4.22
35	9	0.8	4.40	4.33	5.69	4.34	4.45	4.44	4.45	4.38
35	9	0.9	4.38	4.31	5.70	5.32	4.43	4.42	4.43	4.36

Table F-2 30HXC/R-134a carrier screw-compressor part load simulation results (Cont.)

$T_{w_{cd1}}$ (°C)	$T_{w_{ev2}}$ (°C)	PLR	COP_{PL}							
			076	086	096	106	116	126	136	146
25	10	0.3	4.84	4.71	5.70	4.93	4.96	4.96	5.87	4.80
25	10	0.4	5.75	5.63	5.80	5.86	5.93	5.93	5.78	5.74
25	10	0.5	6.26	6.14	6.31	6.37	6.47	6.47	6.29	6.27
25	10	0.6	6.50	6.38	6.54	6.60	6.71	6.72	6.52	6.52
25	10	0.8	6.49	6.37	6.50	6.54	6.68	6.68	6.50	6.49
25	10	0.9	6.36	6.23	6.36	6.38	6.53	6.52	6.36	6.35
30	10	0.3	3.94	3.83	3.98	3.95	3.99	3.98	3.99	3.88
30	10	0.4	4.71	4.61	4.75	4.74	4.80	4.79	4.77	4.67
30	10	0.5	5.13	5.08	5.21	5.20	5.28	5.27	5.23	5.15
30	10	0.6	5.42	5.32	5.45	5.44	5.53	5.52	5.48	5.40
30	10	0.8	5.50	5.41	5.51	5.50	5.61	5.60	5.55	5.48
30	10	0.9	5.43	5.34	5.44	5.41	5.53	5.52	5.47	5.41
35	10	0.3	3.14	3.03	3.45	3.10	3.15	3.14	3.19	3.07
35	10	0.4	3.78	3.68	4.48	3.74	3.82	3.81	3.84	3.74
35	10	0.5	4.19	4.10	5.18	4.15	4.24	4.23	4.25	4.05
35	10	0.6	4.42	4.33	5.62	4.38	4.49	4.47	4.48	4.39
35	10	0.8	4.56	4.48	5.96	4.50	4.63	4.61	4.48	4.54
35	10	0.9	4.54	4.45	5.95	4.47	4.60	4.58	4.61	4.51
25	13	0.3	5.21	5.10	5.25	5.34	5.41	5.47	4.58	5.29
25	13	0.4	6.17	6.07	6.21	6.34	6.45	6.52	6.24	6 31
25	13	0.5	6.69	6.61	6.73	6.86	7.01	7.08	6.76	6.86
25	13	0.6	6.92	6.84	6.94	7.07	7 24	7.30	6.98	7.08
25	13	0.8	6.84	6.75	6.84	6.93	7.12	7.17	6 88	6 97
25	13	0 9	6.68	6.57	6.66	6.73	6.92	6.96	6.70	6.78
30	13	0.3	4 22	4.09	4 25	4 25	4.32	4 31	4.30	4.25
30	13	0 4	5.03	4.91	5.06	5.08	5.18	5.18	5.12	5.11
30	13	0.5	5.50	5.39	5.53	5.56	5.68	5.67	5.60	5.60
30	13	0.6	5.74	5.63	5.76	5.79	5.92	5.92	5.83	5.84
30	13	0.8	5.78	5.67	5.78	5.79	5.94	5.93	5.85	5.86
30	13	0.9	5.68	5.57	5.67	5.67	5.83	5.82	5.74	5.75
35	13	0.3	3.38	3.22	3.77	3.31	3.40	3.43	3.47	3.36
35	13	0.4	4.06	3.91	4.88	3.99	4.11	4.15	4.17	4.07
35	13	0.5	4.49	4.34	5.63	4.41	4.56	4.59	4.59	4.51
35	13	0.6	4.72	4.57	6.09	4.64	4.80	4.83	4.82	4.75
35	13	0.8	4.84	4.69	6.39	4.74	4.72	4.94	4.93	4 86
35	13	0.9	4.79	4.66	6.35	4.69	4.85	4.88	4.87	4.81
25	16	0.3	5.15	5.04	5.27	5.33	5.44	5.49	5.29	5.29
25	16	0.4	6.12	6.03	6.25	6.34	6.50	6.56	6.28	6.33
25	16	0.5	6.65	6.57	6.77	6.87	7.07	7.13	6.81	6.89
25	16	0.6	6.88	6.80	6.98	7.08	7.30	7.35	7.03	7.12
25	16	0.8	6.80	6.70	6.86	6.92	7.15	7.19	6.91	6.98
25	16	0.9	6.63	6.52	6.67	6.72	6.94	6.98	6.72	6.78
30	16	0.3	4.16	4.08	4.26	4.24	4.32	4.30	4.31	4.26
30	16	0.4	4.98	4.92	5.08	5.08	5.02	5.17	5.15	5.12
30	16	0.5	5.46	5.40	5.55	5.56	5.71	5.68	5.63	5.62
30	16	0.6	5.69	5.64	5.78	5.78	5.95	5.92	5.85	5.86
30	16	0.8	5.73	5.68	5.79	5.78	5.96	5.93	5.86	5.87
30	16	0.9	5.64	5.58	5.68	5.66	5.84	5.81	5.79	5.76
35	16	0.3	3.32	3.01	3.68	3.34	3.43	3.41	3.47	3 34
35	16	0.4	4.00	3.65	4.78	4.04	4.16	4.14	4.18	4 06
35	16	0.5	4.43	4.05	5.53	4.47	4.61	4.59	4.61	4.51
35	16	0.6	4.68	4.28	5.98	4.70	4.86	4.83	4.84	4.74
35	16	0.8	4.79	4.43	6.29	4.79	4.96	4.94	4.94	4.86
35	16	0.9	4.74	4.41	6.25	4.73	4.90	4.88	4.88	4.81

Table F-3 KRS KOU YU/R-22 screw-compressor full load simulation results

Model	$\dot{Q}_{ev}$ (kW)	$T_{w_{ev2}}$ (°C)	$T_{w_{cd1}}$ (°C)	COP (toolkit)	COP (actual)	Identified Parameters						
						$\dot{Q}_{ev}$ Nom. (kW)	UA_{ev} (kW/K)	UA_{cd} (kW/K)	$\dot{W}_{to}$ (kW)	α	$\dot{V}_s$ (m^3/s)	A_l (cm^2)
G40	179.8	12.5	30	5.60	5.76	141	20	23	229.7	0.315365	0.05635	0.478
	165.1	10.0	30	5.38	5.36							
	150.7	7.5	30	5.16	4.97							
	136.3	5.0	30	4.98	4.51							
	169.4	12.5	35	4.90	4.76							
	155.2	10.0	35	4.73	4.42							
	141.0	7.5	35	4.57	4.09							
	127.6	5.0	35	4.42	3.71							
	161.1	12.5	40	4.34	4.68							
	147.6	10.0	40	4.21	3.86							
	134.6	7.5	40	4.09	3.56							
	122.1	5.0	40	3.97	3.26							
	149.5	12.5	45	3.91	3.52							
	136.5	10.0	45	3.81	3.25							
	123.8	7.5	45	3.71	2.99							
	112.0	5.0	45	3.61	2.71							
G50	223.7	12.5	30	5.59	5.75	176	25	29	-727.1	0.357266	0.06978	0.585
	205.5	10.0	30	5.35	5.37							
	187.5	7.5	30	5.13	4.97							
	169.6	5.0	30	4.94	4.51							
	210.8	12.5	35	4.85	4.76							
	193.1	10.0	35	4.68	4.43							
	175.5	7.5	35	4.52	4.08							
	158.7	5.0	35	4.36	3.71							
	200.5	12.5	40	4.28	4.21							
	183.7	10.0	40	4.15	3.90							
	167.6	7.5	40	4.02	3.60							
	152.0	5.0	40	3.90	3.27							
	186.1	12.5	45	3.84	3.52							
	169.9	10.0	45	3.73	3.25							
	154.0	7.5	45	3.62	2.98							
	139.3	5.0	45	3.53	2.71							
G60	267.6	12.5	30	5.60	5.75	211	30	35	-875.5	0.361391	0.08333	0.697
	245.8	10.0	30	5.36	5.37							
	224.4	7.5	30	5.14	4.98							
	202.9	5.0	30	4.94	4.51							
	252.2	12.5	35	4.86	4.76							
	231.1	10.0	35	4.68	4.43							
	210.0	7.5	35	4.52	4.09							
	189.9	5.0	35	4.36	3.71							
	239.9	12.5	40	4.28	4.22							
	219.8	10.0	40	4.14	3.90							
	200.5	7.5	40	4.02	3.60							
	181.8	5.0	40	3.89	3.27							
	222.6	12.5	45	3.83	3.52							
	203.3	10.0	45	3.73	3.25							
	184.3	7.5	45	3.62	2.99							
	166.7	5.0	45	3.52	2.71							

Table F-3 KRS KOU YU/R-22 screw-compressor full load simulation results (Cont.)

Model	$\dot{Q}_{ev}$ (kW)	$T_{w_{ev1}}$ (°C)	$T_{w_{cd1}}$ (°C)	COP (toolkit)	COP (actual)	Identified Parameters						
						$\dot{Q}_{ev}$ Nom. (kW)	UA_{ev} (kW/K)	UA_{cd} (kW/K)	$\dot{W}_{in}$ (kW)	α	$\dot{V}_s$ (m^3/s)	A_l (cm^2)
G75	335.0	12.5	30	5.58	5.74	264	37	44	-1116.0	0.360143	0.10494	0.879
	308.2	10.0	30	5.34	5.36							
	281.3	7.5	30	5.12	6.74							
	254.4	5.0	30	4.92	4.51							
	316.1	12.5	35	4.84	4.75							
	289.7	10.0	35	4.67	4.43							
	263.2	7.5	35	4.51	4.08							
	238.1	5.0	35	4.35	3.71							
	300.7	12.5	40	4.28	4.21							
	275.6	10.0	40	4.14	3.90							
	251.3	7.5	40	4.01	3.60							
	228.0	5.0	40	3.89	3.27							
	279.1	12.5	45	3.83	3.52							
	254.9	10.0	45	3.72	3.26							
	231.0	7.5	45	3.62	2.98							
	209.0	5.0	45	3.52	2.71							
G80	359.5	12.5	30	5.60	5.75	281	40	48	-1240.5	0.367620	0.11212	0.941
	330.2	10.0	30	5.36	5.37							
	301.4	7.5	30	5.14	4.97							
	272.6	5.0	30	4.94	4.51							
	338.7	12.5	35	4.86	4.76							
	310.4	10.0	35	4.68	4.43							
	282.0	7.5	35	4.52	4.09							
	255.1	5.0	35	4.36	3.71							
	322.2	12.5	40	4.28	4.22							
	295.3	10.0	40	4.14	3.91							
	269.3	7.5	40	4.01	3.60							
	244.2	5.0	40	3.89	3.27							
	299.0	12.5	45	3.83	3.52							
	273.1	10.0	45	3.72	3.25							
	247.5	7.5	45	3.62	2.99							
	223.9	5.0	45	3.52	2.71							
G100	447.4	12.5	30	5.60	5.76	352	50	60	-1532.1	0.370501	0.13927	1 167
	411.0	10.0	30	5.36	5.37							
	375.1	7.5	30	5.14	4.97							
	339.2	5.0	30	4.94	4.51							
	421.5	12.5	35	4.86	4.76							
	386.3	10.0	35	4.68	4.42							
	351.0	7.5	35	4.51	4.09							
	317.5	5.0	35	4.36	3.71							
	401.0	12.5	40	4.28	4.22							
	367.4	10.0	40	4.14	3.90							
	335.1	7.5	40	4.01	3.60							
	304.0	5.0	40	3.89	3.27							
	372.1	12.5	45	3.83	3.52							
	339.8	10.0	45	3.72	3.25							
	308.1	7.5	45	3.61	2.99							
	278.7	5.0	45	3.51	2.71							

Table F-3 KRS KOU YU/R-22 screw-compressor full load simulation results (Cont.)

Model	$\dot{Q}_{ev}$ (kW)	$T_{w_{ev1}}$ (°C)	$T_{w_{cd1}}$ (°C)	COP (toolkit)	COP (actual)	Identified Parameters						
						$\dot{Q}_{ev}$ Nom. (kW)	UA_{ev} (kW/K)	UA_{cd} (kW/K)	$\dot{W}_{in}$ (kW)	α	$\dot{V}_s$ (m^3/s)	A_l (cm^2)
G120	535.3	12.5	30	5.61	5.76	422	60	72	-1757.7	0.371783	0.16649	1.395
	491.7	10.0	30	5.36	5.37							
	448.8	7.5	30	5.14	4.98							
	405.9	5.0	30	4.93	4.51							
	504.3	12.5	35	4.86	4.76							
	462.1	10.0	35	4.68	4.43							
	419.9	7.5	35	4.51	4.08							
	379.8	5.0	35	4.36	3.71							
	479.9	12.5	40	4.28	4.22							
	439.6	10.0	40	4.14	3.90							
	400.9	7.5	40	4.01	3.60							
	363.7	5.0	40	3.88	3.27							
	445.3	12.5	45	3.83	3.52							
	406.6	10.0	45	3.72	3.25							
	368.6	7.5	45	3.61	2.99							
	333.4	5.0	45	3.51	2.71							

Table F-4 KRS-KOU YU/R-22 screw-compressor part load simulation results

$T_{w,cd1}$ (°C)	$T_{w,ev2}$ (°C)	PLR	COP_{PL}						
			G40	G50	G60	G75	G80	G100	G120
30	5	0.3	2.76	2.78	2.90	2.78	2.78	2.78	2.79
30	5	0.4	3.42	3.43	3.57	3.43	3.44	3.43	3.43
30	5	0.5	3.87	3.88	4.01	3.88	3.88	3.88	3.88
30	5	0.6	4.18	4.18	4.29	4.18	4.18	4.18	4.18
30	5	0.8	4.47	4.47	4.52	4.47	4.47	4.47	4.46
30	5	0.9	4.51	4.51	4.54	4.51	4.51	4.51	4.51
35	5	0.3	2.20	2.21	2.29	2.22	2.22	2.22	2.23
35	5	0.4	2.74	2.74	2.84	2.75	2.75	2.75	2.75
35	5	0.5	3.11	3.12	3.21	3.12	3.12	3.12	3.12
35	5	0.6	3.37	3.37	3.45	3.38	3.37	3.38	3.38
35	5	0.8	3.64	3.64	3.68	3.64	3.64	3.64	3.64
35	5	0.9	3.69	3.69	3.71	3.69	3.69	3.69	3.69
40	5	0.3	1.90	1.91	1.97	1.91	1.92	1.92	1.92
40	5	0.4	2.37	2.38	2.45	2.38	2.38	2.38	2.38
40	5	0.5	2.70	2.71	2.78	2.71	2.71	2.71	2.71
40	5	0.6	2.93	2.94	3.00	2.94	2.94	2.94	2.94
40	5	0.8	3.18	3.19	3.23	3.19	3.19	3.19	3.19
40	5	0.9	3.24	3.25	3.26	3.24	3.25	3.25	3.25
45	5	0.3	1.55	1.55	1.58	1.55	1.56	1.56	1.56
45	5	0.4	1.93	1.93	1.98	1.93	1.93	1.93	1.93
45	5	0.5	2.20	2.21	2.25	2.21	2.21	2.21	2.21
45	5	0.6	2.40	2.40	2.44	2.40	2.40	2.40	2.40
45	5	0.8	2.63	2.63	2.65	2.63	2.63	2.63	2.63
45	5	0.9	2.68	2.68	2.69	2.68	2.68	2.68	2.68
30	7.5	0.3	3.10	3.12	3.29	3.12	3.13	3.13	3.13
30	7.5	0.4	3.84	3.86	4.05	3.86	3.86	3.87	3.87
30	7.5	0.5	4.35	4.36	4.54	4.36	4.36	4.36	4.36
30	7.5	0.6	4.68	4.68	4.83	4.68	4.68	4.68	4.68
30	7.5	0.8	4.96	4.97	5.04	4.96	4.97	4.97	4.97
30	7.5	0.9	4.99	4.99	5.03	4.99	4.99	4.99	4.99
35	7.5	0.3	2.46	2.47	2.58	2.47	2.48	2.48	2.48
35	7.5	0.4	3.06	3.07	3.20	3.07	3.08	3.08	3.08
35	7.5	0.5	3.48	3.48	3.61	3.49	3.49	3.49	3.49
35	7.5	0.6	3.76	3.76	3.86	3.76	3.77	3.77	3.76
35	7.5	0.8	4.04	4.03	4.09	4.03	4.04	4.04	4.04
35	7.5	0.9	4.08	4.08	4.11	4.08	4.08	4.08	4.08
40	7.5	0.3	2.09	2.12	2.20	2.12	2.13	2.14	2.14
40	7.5	0.4	2.61	2.65	2.74	2.65	2.65	2.65	2.65
40	7.5	0.5	2.98	3.02	3.11	3.02	3.02	3.02	3.02
40	7.5	0.6	3.23	3.27	3.35	3.27	3.27	3.27	3.27
40	7.5	0.8	3.49	3.53	3.57	3.53	3.53	3.53	3.53
40	7.5	0.9	3.54	3.58	3.61	3.58	3.58	3.58	3.58
45	7.5	0.3	1.72	1.72	1.77	1.72	2.72	1.73	1.73
45	7.5	0.4	2.14	2.14	2.21	2.14	2.15	2.15	2.15
45	7.5	0.5	2.45	2.45	2.52	2.45	2.46	2.46	2.46
45	7.5	0.6	2.67	2.67	2.73	2.67	2.67	2.67	2.67
45	7.5	0.8	2.91	2.91	2.94	2.91	2.91	2.91	2.91
45	7.5	0.9	2.96	2.96	2.98	2.96	2.96	2.96	2.96

Table F-4 KRS-KOU YU/R-22 screw-compressor part load simulation results (Cont.)

$T_{w_{cd1}}$ (°C)	$T_{w_{cd2}}$ (°C)	PLR	COP_{PL}						
			G40	G50	G60	G75	G80	G100	G120
30	10	0.3	3.38	3.44	3.65	2.73	3.45	3.45	3.45
30	10	0.4	4.19	4.26	4.49	3.40	4.27	4.26	4.25
30	10	0.5	4.73	4.80	5.02	3.85	4.81	4.80	5.78
30	10	0.6	5.06	5.14	5.32	4.14	5.14	5.14	5.11
30	10	0.8	5.34	5.41	5.49	4.41	5.41	5.41	5.37
30	10	0.9	5.34	5.41	5.45	4.44	5.41	5.41	5.36
35	10	0.3	2.70	2.73	2.87	3.44	2.74	3.13	2.74
35	10	0.4	3.37	3.39	3.55	4.26	3.37	3.87	3.40
35	10	0.5	3.83	3.85	3.99	4.80	3.85	4.36	3.85
35	10	0.6	4.13	4.14	3.03	5.14	4.14	4.68	4.14
35	10	0.8	4.40	4.41	4.47	5.40	4.41	4.97	4.41
35	10	0.9	4.43	4.44	4.47	5.41	4.44	4.99	4.44
40	10	0.3	2.30	2.33	2.44	2.33	2.34	2.34	2.35
40	10	0.4	2.87	2.91	3.03	2.91	2.92	2.92	2.92
40	10	0.5	3.28	3.32	3.43	3.32	3.32	3.32	3.32
40	10	0.6	3.55	3.58	3.68	3.58	3.59	3.59	3.59
40	10	0.8	3.81	3.85	3.90	3.85	3.86	3.85	3.85
40	10	0.9	3.86	3.90	3.92	3.90	3.90	3.90	3.90
45	10	0.3	1.88	1.89	1.95	1.89	1.68	1.90	1.90
45	10	0.4	2.36	2.37	2.44	2.37	2.24	2.37	2.37
45	10	0.5	2.70	2.71	2.78	2.71	2.67	2.71	2.71
45	10	0.6	2.93	2.94	3.01	2.94	2.99	2.94	2.94
45	10	0.8	3.18	3.19	3.22	3.19	3.35	3.18	3.18
45	10	0.9	3.23	3.24	3.25	3.24	3.44	3.23	3.23
30	12.5	0.3	3.75	3.75	4.04	3.77	3.78	3.79	3.79
30	12.5	0.4	4.67	4.67	4.97	4.67	4.68	4.69	4.69
30	12.5	0.5	5.26	5.26	5.53	5.26	5.27	5.27	5.27
30	12.5	0.6	5.62	5.62	5.83	5.60	5.61	5.62	5.62
30	12.5	0.8	5.86	5.86	5.96	5.84	5.85	5.86	5.85
30	12.5	0.9	5.84	5.84	5.88	5.81	5.83	5.83	5.83
35	12.5	0.3	2.96	2.96	3.16	2.99	2.99	3.00	3.00
35	12.5	0.4	3.70	3.70	3.92	3.72	3.72	3.72	3.72
35	12.5	0.5	4.20	4.20	4.39	4.21	4.21	4.21	4.21
35	12.5	0.6	4.51	4.51	4.67	4.52	4.52	4.52	4.52
35	12.5	0.8	4.77	4.77	4.85	4.77	4.77	4.77	4.77
35	12.5	0.9	4.79	4.79	4.82	4.78	4.78	4.78	4.78
40	12.5	0.3	2.82	2.82	2.69	2.56	2.57	2.57	2.57
40	12.5	0.4	3.54	3.54	3.35	3.20	3.20	3.21	3.21
40	12.5	0.5	4.04	4.04	3.78	3.64	3.64	3.64	3.64
40	12.5	0.6	4.36	4.36	4.04	3.92	3.93	3.93	3.93
40	12.5	0.8	4.66	4.66	4.25	4.19	4.19	4.26	4.19
40	12.5	0.9	4.70	4.70	4.25	4.22	4.23	4.22	4.22
45	12.5	0.3	2.05	2.05	2.15	2.09	1.87	2.07	2.08
45	12.5	0.4	2.58	2.58	2.69	2.63	2.50	2.60	2.60
45	12.5	0.5	2.95	2.95	3.06	3.00	2.97	2.96	2.96
45	12.5	0.6	3.20	3.20	3.29	3.26	3.31	3.21	3.21
45	12.5	0.8	3.46	3.46	3.50	3.51	3.69	3.46	3.46
45	12.5	0.9	3.51	3.51	3.53	3.56	3.78	3.51	3.51

Appendix G

DOE-2 default coefficients

Table G-1 DOE-2 performance correlations for chillers

Equations are assumed to take the following form: $F = a + bx + cx^2 + dy + ey^2 + fxy$ or $F = a + bx + cx^2 + dx^3$

Keyword	Independent Variables*	a	b	c	d	e	f	Default Curve Name
		Cooling Equipment						
		Absorption Chillers						
ABSOR1-CAP-FT	Tout, Tin	0.723412	0.079006	0.000897	-0.025285	-0.000048	0.000276	ACAPT1
ABSOR1-HIR-FPLR	PLR	0.098585	0.583850	0.560658	-0.243093	-	-	HIRPLR1
ABSOR1-HIR-FT	Tout, Tin	0.652273	0.000000	0.000000	-0.000545	0.000055	0.000000	HIRT1
ABSOR2-CAP-FT	Tout, Tin	-0.816039	-0.038707	0.000450	0.071491	-0.000636	0.000312	ACAPT2
ABSOR2-HIR-FPLR	PLR	0.013994	1.240449	-0.914883	0.660441	-	-	HIRPLR2
ABSOR2-HIR-FT	Tout, Tin	1.658750	0.000000	0.000000	-0.029000	0.000250	0.000000	HIRT2
ABSOR3-CAP-FT	Tout, Tin	*0.723412	0.079006	-0.000897	-0.025285	-0.000048	0.000276	ACAPT3
ABSOR3-CAP-FTS	HW-T	*1.000000	0.000000	0.000000	-	-	-	ACAPTS
ABSOR3-HIR-FPLR	PLR	*0.098585	0.583850	0.560658	0.243093	-	-	HIRPLR3
ABSOR3-HIR-FT	Tout, Tin	*0.652273	0.000000	0.000000	0.000545	0.000055	0.000000	HIRT3
ABSOR3-HIR-FTS	HW-T	*1.000000	0.000000	0.000000	-	-	-	HIRTS
		Compression Chillers						
HERM-CENT-CAP-FT	Tout, Tin	-1.742040	0.029292	-0.000067	0.048054	-0.000291	-0.000106	CCAPT3
HERM-CENT-EIR-FPLR	PLR	0.222903	0.313387	0.463710	-	-	-	EIRPLR3
HERM-CENT-EIR-FT	Tout, Tin	3.117500	-0.109236	0.001389	0.003750	0.000150	0.000375	EIRT3
HERM-REC-CAP-FT	Tout, Tin	-4.161461	0.207050	0.000193	0.004723	-0.000040	-0.000087	CCAPT4
HERM-REC-EIR-FPLR	PLR	0.088065	1.137742	-0.225806	-	-	-	EIRPLR4
HERM-REC-EIR-FT	Tout, Tin	4.720965	-0.187504	0.002192	0.009209	0.000098	-0.000322	EIRT4
OPEN-CENT-CAP-FT	Tout, Tin	-1.742040	0.029292	-0.000067	0.048054	0.000291	-0.000106	CCAPT1
OPEN-CENT-EIR-FPLR	PLR	0.222903	0.313387	0.463710	-	-	-	EIRPLR1
OPEN-CENT-EIR-FT	Tout, Tin	3.117500	-0.109236	0.001389	0.003750	0.000150	0.000375	EIRT1
OPEN-REC-CAP-FT	Tout, Tin	-4.161461	0.207050	-0.001931	0.004723	-0.000040	-0.000087	CCAPT2
OPEN-REC-EIR-FPLR	PLR	0.088065	1.137742	-0.225806	-	-	-	EIRPLR2
OPEN-REC-EIR-FT	Tout, Tin	4.720965	-0.187504	0.002192	0.009209	0.000098	-0.000322	EIRT2
		Double-Bundle Chillers						
DBUN-CAP-FT	Tout, Tin	1.742040	0.029292	0.000067	0.048054	0.000291	-0.000106	DBCAPT
DBUN-CAP-FTRISE	Tdiff	1.000000	-0.005650	-0.000365		-	-	DBCAPREC
DBUN-EIR-FPLR	PLR	0.349032	0.263871	0.387097		-	-	DBEIRPLR
DBUN-EIR-FT	Tout, Tin	3.117500	-0.109236	0.001389	0.003750	0.000150	-0.000375	DBEIRT
DBUN-EIR-FTRISE	Tdiff	0.012250	0.000175	0.000360		-	-	DBEIRREC

*The user is instructed to simulate a solar absorption refrigeration unit with the PLANT EQUIPMENT TYPE = ABSOR1 CHLR unless these coefficients can be defined by the user for his particular chiller.